Decisional Tools for Supply Chain Economics of Cell and Gene Therapy Products

Thesis submitted to University College London for the degree of

Doctor of Engineering (EngD) in Biochemical Engineering

By

Ruxandra-Maria Comisel, BSc, MSc

The Advanced Centre for Biochemical Engineering

Department of Biochemical Engineering

UCL

Torrington Place

London

WC1E 7JE

September 2021

I, Ruxandra-Maria Comisel confirm that the work presented in this thesis is my own. Where information has been derived from other sources, I confirm that this has been indicated in the thesis.

To my loving family

Abstract

Gene therapy products have tremendous therapeutic potential for indications such as cancer and even curative potential for some genetic diseases. Most of today's gene therapy products are viral vector-based, typically relying on plasmid DNA supply for their production, and many are autologous *ex vivo* applications (e.g. chimeric antigen receptor T-cell therapy – CAR T), hence the supply chain of these products is highly complex. Given the relative infancy of the sector, there is a strong drive towards adopting technologies that minimise costs and supply chain complexity. This thesis aims to explore these avenues by developing and applying advanced decisional tools that analyse the gene therapy supply chain systematically whilst capturing multiple stakeholder perspectives.

The decisional tools employed in this thesis included bioprocess economics models tailored to autologous CAR T-cell therapy and viral vector products. From the cost perspective, models were built to compute manufacturing costs, namely cost of goods (COG) and fixed capital investment (FCI), and coupled with brute force optimisation to identify optimal manufacturing strategies. In addition, a cost of drug development model and a cash flow model were built to evaluate the impact of process changes at different stages in the drug development pathway and evaluate the profitability of different manufacturing strategies.

The case studies presented in this thesis explored the autologous supply chains and automation, a range of viral vector manufacturing flowsheets and viral vector process changes. In particular, the autologous supply chain case study provides a feasibility analysis of the optimal number of sites for the decentralised enterprise models and gives new insights into the feasibility of bedside models and impact of quality control (QC) automation. For example, for autologous CAR T cell therapy commercial manufacture,

the tool predicted that bedside models such as "GMP-in-a-box" can be more profitable than the regional model for low demand scenarios and identified the critical demand where the regional model starts to outperform bedside manufacture.

The viral vector manufacture case study offers the first thorough analysis of the COG associated with a range of flowsheets employing different cell culture technologies for multiple gene therapy product type and process performance scenarios. For lentiviral vector manufacture, it was found that suspension culture or adherent cell culture using fixed bed technology can offer cost savings in the order of 95% when compared to traditional manufacturing approaches in multi-layer vessels. Moreover, suspension cell culture was found to be more suitable for supplying large indications due to its high scalability potential.

The process change case study offers a detailed evaluation of the switch from transient transfection to a stable producer cell line for viral vector manufacture by capturing the impact on key financial outputs for both drug development and commercial manufacture, in the case of four topical gene therapy product types. The analysis highlighted that the optimal time to switch was most sensitive to the pDNA requirement and unit cost, the expected delay to market and the titre differences. For example, for products associated with a low pDNA requirement (e.g. CAR T and AAV), switching to stable cell lines post-approval was found to be more attractive than switching early if delays to market were incurred.

This thesis provides an account of how the advanced decisional tools employed can help decision-makers create optimal manufacturing strategies so as to maximise patient accessibility and provides a methodology for building decisional tools for emerging products.

Impact Statement

Decisional tools have been developed historically to support decision-makers find answers to complex questions so as to enable commercial viability of novel products. This thesis describes how decisional tools can be used in the field of gene therapies to analyse trade-offs behind technology selection, process change during drug development pathway and decentralisation of autologous gene therapy manufacture. These tools can be used for gaining product-specific insights on optimal process flowsheets, long-term impact of performing a process change on financial metrics and strategies to simplifying supply chains and increasing patient accessibility. The addition of the herein developed decisional tools to the cell and gene therapy industry's toolbox provides developers with a framework to gain early visibility over the impact of their future process development and manufacturing strategy decisions.

The work described in this thesis has been endorsed by industry experts who took part in sponsoring this research. Bo Kara (ex-GSK; currently VP Process Development a Evox Therapeutics, Oxford, United Kingdom) stated that "*The results from the EngD collaboration between GSK and UCL demonstrated we could save 90% COG by switching from traditional platforms to scalable technologies for lentiviral vectors used in the manufacture of gene-modified cell therapies. Many players have started to invest in scalable technologies and believe this will translate into savings of potentially up to $40M-$100M USD per year when we get to commercialisation of CAR T, TCR and HSC therapies at peak demands".* Furthermore, Fritz Fiesser (Director, Cell & Gene Therapy Engineering & Informatics, GSK, Brentford, United Kingdom), stated that "*The work described in this thesis flagged the high plasmid DNA cost contribution to viral vector production processes relying on transient transfection as ranging between 15%-30% of total batch costs. When moving to stable producer systems, assuming no changes in harvest titre, this already translates into annual savings between $1.5M-$2.5M for viral*

vector needed for ex vivo gene therapies and much higher than that for high dose LV in vivo applications. However, stable producer systems have proven to be much more productive, hence we're likely looking at significantly higher cost savings across all gene therapy product types. The decisional tool developed in collaboration with UCL provides a structured approach to determining impact of these kinds of process changes and their risks of delays to market on the overall project profitability. This can facilitate better decision-making and will hopefully translate into more products with curative potential becoming available to patients".

Acknowledgements

Firstly, I would like to wholeheartedly thank my supervisor Professor Suzanne Farid for the continuous guidance, constructive feedback and trust that she offered me throughout this EngD. I would also like to thank my supervisors from my sponsor company, Fritz Fiesser and Bo Kara, for their guidance, feedback and patience. Your support for this project has helped me immensely to navigate the inherent challenges of doing an EngD, starting a family, having a baby, moving to a new city and going through a pandemic. Furthermore, I'd like to thank the members of my sponsor company, as well as the members of the wider cell and gene therapy community, for taking the time to discuss key cell and gene therapy topics with me.

Moreover, I would like to thank the Biochemical Engineering Department at the University College London for all their support. Gratefully, I would like to acknowledge the financial support from the Engineering and Physical Sciences Research Council (EPSRC) and GSK.

I would also like to thank my family for encouraging me and putting up with me throughout this EngD. I'd like to especially thank my husband, David, for his enthusiasm, support and love, and my son, Joseph, for giving meaning to my existence. Also, I'm forever grateful to my mum and dad for always being there for me and instilling in me the thirst for knowledge. Now I know what you, dad, went through when you were doing a doctorate and I was a young child...

Contents

List of Tables

List of Figures

Abbreviations

aAPC	Artificial antigen presenting cell
AAV	Adeno-associated virus vector
ACT	Adoptive cell therapy
ADA-SCID	Adenosine deaminase deficiency severe combined immunodeficiency
AEX	Anion exchange chromatography
ALL	Acute lymphoblastic leukaemia
Allo	Allogeneic
ATMP	Advanced therapeutic medicinal product
Auto	Autologous
CALD	Cerebral adrenoleukodystrophy
CAR	Chimeric antigen receptor
CDMO	Contract development and manufacturing company
CEX	Cation exchange chromatography
$C_{Development}$	Cost of drug development
CF10	10-layer flask
cGMP	Current good manufacturing practice
CHMD	Congenital haematological monogenic disorders
CIP	Cleaning in place
CMO	Contract manufacturing organisation
CMC	Chemistry Manufacture and Control
CNC	Controlled not classified

COG	Cost of goods
CRS	Cytokine Release Syndrome
CRISPR	Clustered regularly interspaced short palindromic repeats
CTL	Cytotoxic T lymphocytes
ddPCR	Droplet digital polymerase chain reaction
DepthF	Depth filtration
DF	Diafiltration
DLBCL	Diffuse large B cell lymphoma
DSP	Downstream processing
EMA	European Medicines Agency
FACS	Florescence activated cell sorting
FBR	Fixed bed bioreactor
FCI	Fixed capital investment
FDA	Food and drugs agency
FF	Fill finish
FTE	Full-time equivalent
GMPiB	GMP-in-a-box
GvHD	Graft-versus-host disease
g-RV	Gamma-retroviral vector
HF	Hollow fibre
HIC	Hydrophobic interaction chromatography
HSC	haematopoietic stem cells
HSC GT	haematopoietic stem cell gene therapy

HSP	Hospital
HSPC	haematopoietic stem and progenitor cells
HVAC	Heating, ventilation and air conditioning systems
ICER	Institute for Clinical and Economic Review
IND	Investigational New Drug (application to the FDA)
IPC	In process control
IPSC	Induced pluripotent stem cells
LV	Lentiviral vector
mAb	Monoclonal antibody
MCB	Master cell bank
MLD	Metachromatic leukodystrophy
MNC	Mononuclear cells
MOI	Multiplicity of infection
MSC	Mesenchymal stem cells
NFF	Normal flow filtration
NICE	National Institute for Health and Care Excellence
NPV	Net present value
PBMC	Peripheral blood mononuclear cells
pDNA	Plasmid DNA
PLC	Project lifecycle cost
QA	Quality assurance
QC	Quality control
QP	Qualified person

qPCR	Quantitative polymerase chain reaction
r/r	Relapsed or refractory
RCL	Replication competent lentivirus
RCV	Replication competent virus
rNPV	Risk-adjusted net present value
RMmc	Rocking motion bioreactor run with microcarriers
SBTT	Sleeping beauty transposone/transposase
SCD	Sickle cell disease
SF	Sterile filtration
SMA	Spinal muscular atrophy
SPCL	Stable producer cell line
SPCL-Ph1	Switch to SPCL for Phase 1 Clinical Trial
SUB	Single-use stirred tank bioreactor
S&M	Sales and Marketing
SUSAR	Suspected unexpected serious adverse reactions
TAA	Tumour-associated antigen
TCR	T-cell receptor
TFF	Tangential flow filtration
TU	Transducing units
UF/DF	Ultrafiltration/Diafiltration
USP	Upstream processing
VBA	Visual Basic for Applications
VCN	Vector copy number

vg	Viral genomes
VV	Viral vector
WAS	Wiskott Aldrich syndrome
WCB	Working cell bank
X-ALD	X-linked adrenoleukodystrophy
X-SCID	X-linked severe combined immunodeficiency

Chapter 1: Scope and Background

1.1 Cell and gene therapy industry snapshot

1.1.1 Overview

Cell and gene therapies, also known as advanced therapeutic medicinal products (ATMPs) in the EU, are the most complex and expensive of all healthcare products. These have garnered significant momentum since 2017 when therapy types such as Luxturna® (Spark Therapeutics, Philadelphia, Pennsylvania, USA), an *in vivo* gene therapy, and Kymriah® (Novartis, Basel, Switzerland) and Yescarta® (Gilead, Foster City, California, USA), *ex vivo* gene therapies, received marketing approval. Since 2017, the industry has seen the approval of 7 additional products and further approvals of existing products for other indications (ARM 2021). Cell and gene therapy products represent a broad category of healthcare products that span from the delivery of living cells through to the delivery of genes, with gene-modified cell therapies or *ex vivo* gene therapies at the intersection of both product types. In 2020, worldwide, there were 1,220 ongoing clinical trials in cell and gene therapy and regenerative medicine space with 383 at Phase 1, 685 at Phase 2 and 152 at Phase 3 (ARM 2020). The majority of these studies target oncology (550), central nervous system (94), monogenic diseases (87) and infectious diseases (73) (ARM 2020).

This thesis addresses specifically the gene therapy products, both the *ex vivo* and *in vivo* modalities. These are defined more specifically in **Section 1.1.2**. Key products that have been approved to date as well as their key characteristics such as approval year, sponsor company, indication and price are presented in **Table 1.1**.

Table 1.1 Gene therapy products approved since 2016.

Modality	Type	Approval year	Product name	Company	Indication	Territory	Vector type	List price
ex vivo	CD34+	2016	Strimvelis®	GSK/Orchard Therapeutics	ADA-SCID	EU	g-RV	£505,000 [a] ($694,300)
		2019	Zynteglo®	bluebird bio	B-thalassemia	EU	LV	$1.8M [b]
		2021	Libmeldy®	Orchard Therapeutics	Metachromatic leukodystrophy	EU	LV	not confirmed
		2021	Skysona®	bluebird bio	CALD	EU	LV	not confirmed
	Adoptive T-cell therapy (cell-based immune-oncology)*	2017	Kymriah®	Novartis	ALL, r/r large B-cell lymphoma	US, EU	LV	$475,000 [c]
		2017	Yescarta®	Kite/Gilead	r/r large B-cell lymphoma	US, EU	g-RV	$373,000 [c]
		2020	Tecartus®	Kite/Gilead	r/r mantle cell lymphoma	US, EU(conditional)	g-RV	$373,000 [f]
		2021	Abecma®	bluebird bio/BMS	Multiple Myeloma	US	LV	$419,000 [d]
		2021	Breyanzi®	Juno/BMS	r/r large B-cell lymphoma	US	LV	$410,300 [e]
		2022	Carvykti®	Janssen/Legend	r/r Multiple Myeloma	US, EU: pending	LV	$465,000[g]
in vivo	Ophthalmologic	2017	Luxturna®	Spark Therapeutics/Novartis	Retinal dystrophy	US	AAV	$850,000 [b]
	Neurological	2020	Zolgensma®	AveXis/Novartis	SMA-1	US, EU	AAV	£1.79M ($2.46M) [b]

* all adoptive T-cell therapies approved to date represent CAR T-cell therapies. CALD = cerebral adrenoleukodystrophy, r/r = relapsed or refractory, g-RV = gamma-retroviral vector, LV = lentiviral vector, AAV = adeno-associated virus vector, SMA-1= spinal muscular atrophy type 1. References for selling prices: [a] Killi and Chaffman (2020), [b] Nature (2019), [c] Senior (2018), [d] Voelker (2021), [e] Jaklevic (2021), [f] Voelker (2020), [g] Liu (2022). Exchange rate used for the Strimvelis and Zolgensma prices was 1.37 USD per 1 GBP.

While cell therapy products are more complex than biopharmaceuticals due to the delivery of therapeutic effect via packages of biological components versus one defined biochemical entity (e.g. a mAb), gene therapies are associated with an even higher complexity (Seimetz et al. 2019). Gene therapy products involve typically the introduction or alteration of genetic material into patients' cells' nuclei – either *ex vivo* (*in vitro)* or *in vivo*, directly in the patients' bodies. This is achieved using viral vectors (employed to introduce a gene) however efforts are also dedicated on the development of non-viral vectors (typically employed to alter a gene i.e. gene editing) due to their potentially superior safety profiles. In either case, faulty, absent or therapeutic genes can get expressed in patients' cells and thus deliver their therapeutic effect. This thesis will focus on viral vector methodologies only.

1.1.2 Types of gene therapy products

1.1.2.1 *Ex vivo* gene therapies

Ex vivo gene therapies, also known as gene-modified cell therapies, have acquired significant interest over the last decade. They differ in terms of therapeutic indications, targeted cell types for genetic modification (i.e., T-cells or haematopoietic and progenitor stem cells - HSCs), whether they involve viral or non-viral vectors, and whether they are autologous or allogeneic. While some industry players are moving towards non-viral vectors and allogeneic approaches, the majority of these therapies in development and on the market still involve viral vectors and are autologous. The most addressed therapeutic indications in clinical studies are cancers or genetic diseases targeted with therapies which genetically modify patients' T-cells or HSCs, respectively. Other therapeutic areas targeted are Graft-versus-host diseases (GvHD) and HIV. The most common vectors used in genetically modifying (or engineering) both T-cells and HSCs are gamma-retroviral

vectors and lentiviral vectors. This thesis will focus on autologous *ex vivo* gene therapies that employ lentiviral vectors.

Ex vivo gene therapies employing T-cell genetic engineering

The most popular *ex vivo* gene therapy strategy is to genetically engineer T-cells to express a chimeric antigen receptor (CAR) or an enhanced T-cell receptor (TCR) that enables T-cells to target and kill tumour cells based on recognition of tumour-associated antigens (TAAs) such as CD19 and NY-ESO (Rosenberg 2012a; Fesnak et al. 2016b; Hartmann et al. 2017). T-cell based gene-therapy products have been gaining popularity over the past decade peaking with the 2017 FDA approval of Kymriah® (Novartis). CAR T-cell and enhanced TCR therapies target cancers such as haematological malignancies e.g. leukaemias and lymphomas (Porter et al. 2015), myeloma (Rapoport et al. 2015) and solid tumours (Ahmed et al. 2015) by engineering T-cells to target and destroy tumour cells. Extensive accounts of the clinical trials employing such therapies are given in Holzinger et al. (2016), Fesnak et al. (2016b), Fesnak et al. (2016a), Hartmann et al. (2017).

There are 6 CAR T-cell therapy products that achieved approval in the last 5 years i.e. Kymriah®, Abecma®, Breyanzi®, Yescarta®, and Tecartus® (Geethakumari et al. 2021) and Carvykti® (**Table 1.1**).

Biology background

The main therapeutic approaches are the chimeric antigen receptor T-cells (CAR T-cell) and the enhanced T-cell receptor (TCR) therapies and these have been successful particularly in treating relapsed and refractory haematological malignancies and less so in treating solid tumours (Britten et al. 2021). The chimeric antigen receptor (CAR) consists of intracellular signalling domains which are fused to an antigen recognition domain which is a single-chain variable (scFv) fragment of an antibody raised against a

specific antigen. The scFv fragment of the CAR is able to bind specific antigens and, upon binding, it triggers the activation of the T-cell in a similar manner to the endogenous TCR (Levine 2015). The TCR approach implies increasing the affinity of T cell receptors (TCRs) by screening for natural TCRs in healthy population which bind to tumour antigens, cloning the TCR genes and developing an affinity enhanced TCR (Manfredi et al. 2020). The process of building the TCR involves extensive molecular engineering and can take about a year to develop. The difference between this technology and CAR T-cell technology is the fact that the latter uses an engineered extracellular antibody fragment to recognise target cells whilst this type of product is capable of targeting both intracellular as well as extracellular target protein (Zhao et al. 2021).

It is important to note that, although these therapies show promising results, there are severe side effects that were found to be associated with the degree of function of the CAR T-cells. The main side effect is the cytokine release storm (CRS), a type of non-infective fever whereby cytokines are released by the activated T-cells generating leading to high fever (Porter et al. 2015). With all these trials, efforts are being made to understand which would be the best dose size in order to ensure the success of the therapy whilst maintaining the CRS as low as possible. A further side effect is neurotoxicity.

Ex vivo gene therapies employing HSC genetic engineering

There are about 30 million people suffering from rare diseases in Europe, and, amongst the 6,172 different rare diseases, 72% of these are genetic disorders (Wakap et al. 2020). Genetic diseases caused by mainly one genetic mutation (monogenic) could be potentially treated using gene therapy that inserts the correct gene sequence inside patient's faulty genomic DNA. Specifically, treatment of congenital haematological monogenic disorders (CHMD) can be approached using patients' own haematopoietic stem cells (HSCs) that carry the CD34+ marker on their surface which are genetically modified in order to

restore their physiological, correct function. These cells are known as the CD34+ HSCs or the haematopoietic stem and progenitor cells (HSPCs). Once reintroduced in the patient's body, these modified stem cells migrate back to the bone marrow and become the stem source for creating healthy blood cells. For example, ADA-SCID or Adenosine deaminase (ADA) deficiency with severe combined immunodeficiency is a disease whereby adenosine deaminase is not produced by patients' blood cells which leads to immune-compromised patients of "bubble-boy" disease. By inserting the correct ADA gene using a viral vector into patients' blood stem cells and introducing these cells back into the patient, tens of paediatric children have been cured to date. In fact, in May 2016, Strimvelis® (GSK, London, United Kingdom), the first autologous *ex vivo* gene therapy was approved in the EU for the treatment of ADA-SCID. In the meantime, the product was divested to Orchard Therapeutics (London, United Kingdom). This therapy uses a retroviral vector (MoMLV) as means of inserting the gene into the CD34+ cells' genome (Aiuti et al. 2017).

In the context of HSC gene therapy, the lentiviral vector (LV) is employed to insert either absent or mutated genes into CD34+ cells' genomes in order to tackle rare and monogenic disorders (e.g. ADA-SCID, WAS, MLD, X-ALD, X-SCID etc.) and haemoglobinopathies (Aiuti et al. 2013; Aiuti et al. 2009a; Biffi et al. 2013; Cavazzana et al. 2017; Rai and Malik 2016; Ribeil et al. 2017; Rio et al. 2017; Wang and Riviere 2017; Zonari et al. 2017; Cartier et al. 2009; Mamcarz et al. 2019; Greene et al. 2012; Cavazzana-Calvo et al. 2010; Booth et al. 2016).

There have been three approved HSC gene therapies to date i.e. Strimvelis® for ADA-SCID, Zyntelgo® (bluebird bio, Cambridge, Massachusetts, USA) for beta-thalassemia and Libmeldy® (Orchard Therapeutics) for metachromatic leukodystrophy (MLD), as indicated in **Table 1.1** (**Section 1.1.1**). However, Zynteglo® has undergone precautionary

suspension in early 2020 due to two suspected unexpected serious adverse reactions (SUSARs) which occurred to two patients enrolled in a sickle cell disease clinical study using the same lentiviral vector platform (LentiGlobin). The manufacturer's reports suggest that it is 'unlikely' that their LV product caused the adverse events and that it is expected that the suspension will be lifted (Kansteiner 2021).

1.1.2.2 *In vivo* gene therapies

There were 423 ongoing clinical trials testing gene therapy products alone (not accounting for cell-based immune-oncology products), in 2020 according to the Alliance of Regenerative Medicine (ARM 2020). This comprises both viral vector and non-viral vector products, although the landscape is dominated by viral vector approaches. Although there have been numerous clinical trials testing the adenovirus vector and plasmid DNA (non-viral vector), no such gene therapy products have been approved to date in the US or EU.

The key viral vector used for *in vivo* gene therapy products is the adeno-associated virus (AAV) vector. However, lentiviral vectors have also been employed in *in vivo* gene therapy studies. The target tissues for gene delivery for both vectors are typically the eye, brain, and respiratory tissue while motor neurons and skeletal muscles tend to be targeted with AAV only. As *in vivo* gene therapy vectors, LVs are being clinically tested as a treatment for cystic fibrosis, macular degeneration and Parkinson's disease.

Only AAV has been used in *in vivo* products that have gained marketing approval so far. These vectors have gained traction in the last 10 years with the approval of 3 gene therapy products using AAV i.e. Glybera® (Uniqure, Amsterdam, Netherlands), Luxturna® (Sparks Therapeutics, Philadelphia, Pennsylvania) and Zolgensma® (Novartis Gene Therapies, Chicago, Illinois, USA) (Bryant et al. 2013; Keeler and Flotte 2019). Glybera (Uniqure) the first AAV gene therapy to gain regulatory approval in EU in 2012 for

lipoprotein lipase deficiency was commercially short-lived due to low demands and an extremely high selling price (Ylä-Herttuala 2012; Keeler and Flotte 2019; Bulcha et al. 2021). In terms of clinical studies, AAV vector is employed in ~200 trials worldwide with a particular focus on addressing haemophilia and ophthalmologic disorders (Bulcha et al. 2021).

1.1.3 Development journey snapshot

The *ex vivo* gene therapies approved to date have been associated with slightly different development journeys when compared to those associated with biopharma products. These have been abbreviated in some cases and, have followed a two-stage approach (pilot and pivotal) rather than the three-phase approach for clinical trials (Phase 1, 2, 3). The reason behind the two stages is likely be linked to their predominantly autologous nature and the lack of predictive preclinical models, which means that Phase 1 clinical trial which assesses safety can only be performed on patients rather than on healthy volunteers. Consequently, efficacy can be assessed from the onset of the Phase 1 clinical trial of the clinical study program. The reason behind the shortened timeframes could be two-fold. Firstly, this is likely linked to the fact that critically ill patients who underwent 2-3 lines of treatment were the initial participants in these studies. Given the small population size of this group, the developers were able to access regulatory tools (i.e., the orphan or the rare disease designation) to fast-track their journey to achieving marketing approval. Secondly, additional regulatory tools (e.g. the breakthrough designation and PRIME) were accessible given the unmet need and the very promising clinical results achieving up to high overall response rates (Yip and Webster 2018). The regulatory tools used by CAR T-cell therapy developers in both EU and US are described by (Seimetz et al. 2019).

The marketing approval of Strimvelis® for ADA-SCID, Kymriah® for paediatric ALL and Yescarta® for adult Diffuse large B cell lymphoma (DLBCL) in 2016-2017 constitute the long-waited entrance of this therapy type on the commercial stage. In the following year, Kymriah® was further approved for adult DLBCL while in 2020, Yescarta® was also approved for follicular lymphoma. Zynteglo®, a beta-thalassemia *ex vivo* gene therapy product using patients' CD34+ cells, saw conditional marketing approval in the EU in 2019. So far, these therapies had been approved as third line therapies (relapsed/refractory diseases) however, it is expected that innovator companies may get their products approved as 2nd or 1st line therapies within the next 10 years. To support this statement, there appears to be a wealth of clinical trials aimed at assessing the efficacy of these approved therapies in a broad range of other indications and therapeutic lines. For example, Kymriah® is being investigated as a potential treatment for follicular lymphoma in Elara Phase 2 study, for adult ALL in combination with other drugs in Oberon Phase 3 study, and as first line for high risk paediatric ALL patients in Cassiopeia Phase 2 study.

Another mechanism companies can rely on to accelerate the path to market is described by Britten et al. (2021). This is a regulatory mechanism allowing a more streamlined clinical assessment of therapies called the 'Parent-child' IND framework. This allows companies to study the efficacy of closely related CAR T or TCR products more efficiently by enabling the submission of an initial IND ('parent') providing all key product information plus potential enhancements routes for it. For the next generation products, a simplified IND ('child') can be submitted cross-referencing the 'parent' IND, tackling the specific changes brought to the new product.

1.1.4 Supply chain overview

The *ex vivo* gene therapies utilising viral vectors as means of genetic engineering involve the manufacture of the gene-modified cell therapy itself as well as the manufacture of the viral vector. In turn, the manufacture of the viral vector, be it needed for *ex vivo* or *in vivo* modalities, requires the manufacture of plasmid DNA (pDNA) if transient transfection is employed. As such, *ex vivo* gene therapy processes typically involve the manufacture of 3 biological products: the cell therapy, the viral vector and the pDNA all at GMP-grade as shown in **Figure 1.1**.

In the context of autologous *ex vivo* gene therapy employing viral vectors, **Figure 1.1** shows these three processes overlaid onto the circular, patient-centric supply chain characteristic of autologous therapies. As such, the first step is material collection, taking place at an apheresis centre, which is represented by an apheresis procedure, whereby a patient's cells are collected. These are then transported to the manufacturing facility either fresh (2-6°C) or cryopreserved (-180°C). In some cases, they may be transported fresh and cryopreserved once they reach the manufacturing facility. The manufacture of the gene-modified therapy product follows where the cells are typically washed, selected, activated and genetically engineered using the viral vector. The cells may or may not be expanded depending on the starting cell type. The product is then washed, formulated and release testing is performed. Throughout the manufacturing process, in process control (IPC) is performed to ensure product quality. Once the product is released, it is transported to the administration centre either fresh or cryopreserved. Here, the patient, whose cells were collected in the first place, is infused with the therapy.

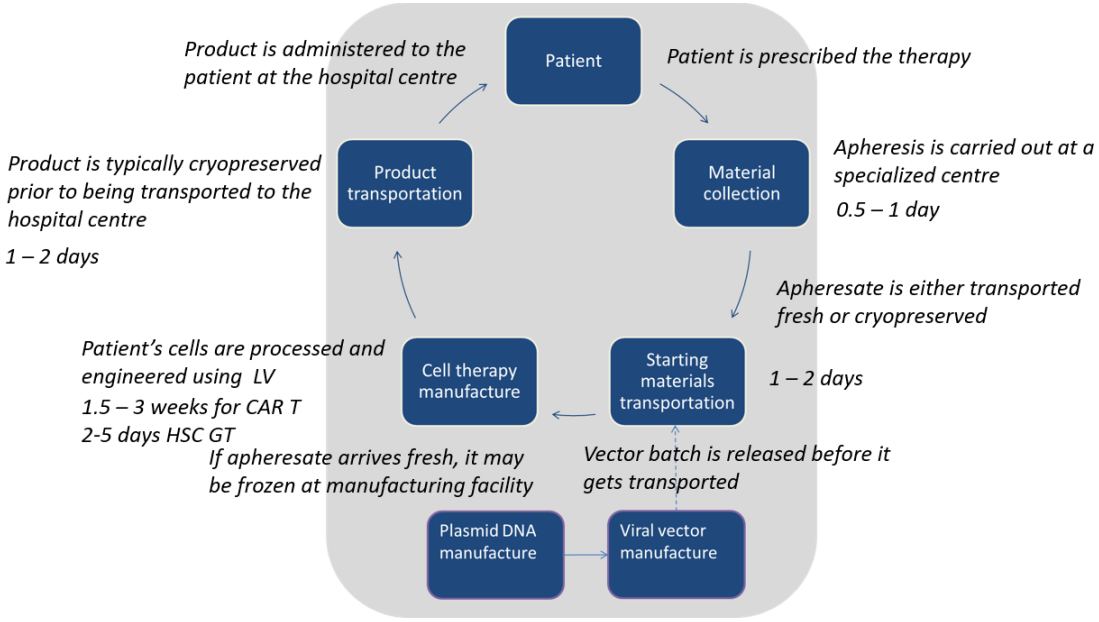

Figure 1.1 Supply chain overview of autologous *ex vivo* gene therapies including viral vector and plasmid DNA processes assuming transient transfection as expression system for the viral vector. HSC GT = haematopoietic stem cell gene therapy.

On the other hand, in the context of the *in vivo* gene therapy, which are 'off-the-shelf', **Figure 1.2** shows the linear supply chain characteristics, typical of biopharma products. Here, the viral vector manufacture requires cGMP-manufactured pDNA as a key raw material input and it outputs the gene therapy products which are then sent to distribution centres. The vector manufacturing process is not dissimilar to protein manufacturing processes. It requires mammalian cell culture for the viral vector or fermentation for the pDNA, recovery and downstream processing involving one or more chromatography steps, concentration and buffer exchange steps.

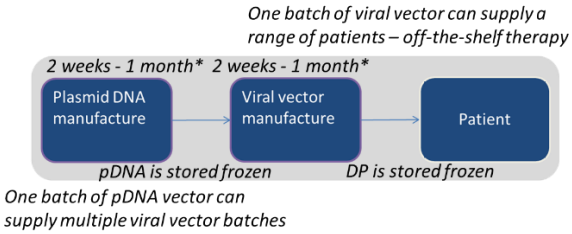

Figure 1.2 Supply chain overview of *in vivo* gene therapies assuming transient transfection as expression system for the viral vector. * Time required to manufacture and release a batch depending on the level of lean operations achieved. pDNA = plasmid DNA, DP = drug product.

The next three sections of this chapter will discuss the commercialisation challenges and key supply chain considerations, and will present an overview of decisional tools developed to address critical questions associated with the cell therapy and the cell and gene therapy sectors.

1.2 Commercialisation challenges

Whilst gene therapies may have incredible therapeutic potential in a range of indications, and assuming that harmful side-effects can be minimised effectively, there are significant challenges that need to be addressed in order to safeguard their commercial success. These challenges can be grouped in the following categories: manufacturing, reimbursement, costs and supply chain challenges.

1.2.1 Manufacturing challenges

The manufacturing challenges associated with gene therapies will be described for gene-modified cell therapies, viral vectors and plasmid DNA vectors. These three biological-based products are associated with different types of processes as described in **Chapter 2**, each presenting specific challenges. However, common manufacturing challenges for all three processes are related to chemistry manufacturing and controls (CMC) strategy. Key manufacturing challenges that developers face are driven by the trade-off between speed to market and, to name a few, choice of manufacturing flowsheets, quality of materials and building product and process understanding. As such, it is not uncommon

for developers to head into early clinical trials with unscalable, manual and open processes utilising raw materials which are not cGMP-grade or that can only be produced by unique suppliers. Furthermore, analytical techniques represent a key concern in the field of cell and gene therapies and these tend to be poorly defined in early studies. Whilst risk assessments and promising data can ensure some level of success in early clinical trials using immature manufacturing processes, it is unlikely that these processes will be fit for purpose for later stage clinical trials or commercial manufacture. Consequently, many developers choose to perform process changes between clinical trial phases so as to make their processes more amenable to scaling up for commercial manufacture. Such changes need to be accompanied by extensive product characterisation studies and comparability studies which are laborious, lengthy and expensive. The risk associated with this route is the inability to prove comparability between the old and the new process which may mean that the clinical study will have to be repeated. The alternative is to adopt a more risk-advert but streamlined strategy by developing GMP-compliant, scalable and closed processes early on, which may require arguably similar times to reach market.

In terms of gene-modified cell therapies, the key manufacturing challenges are related to their predominantly autologous nature as well their manual and open processing, and analytics. Patient-specific manufacture cannot be scaled up but scaled out. Consequently, manufacturing for high demands requires large footprints and personnel numbers driving capital investment and labour costs up. This is aggravated by manual and open processing which poses stringent requirements on facility design such as the use of isolators within Grade C environments or the use of biosafety cabinets within Grade B environments. This is associated with risks of cross-contamination, high process variability as well as high facility running costs. Furthermore, each patient is different in terms of quality of the starting cell collection which, in turn, means that the quality of the final product is

variable. It is not uncommon for CAR T batches to fail because patient's T-cells cannot be expanded to large enough numbers to exert their therapeutic effect. The development of automated and closed equipment for cell processing has most certainly benefited the field of autologous cell therapy enabling increases in throughputs due to minimising risk of cross-contamination. Whilst closing and automating processes can reduce process variability, it cannot tackle the issue of variability coming from the starting cell material. The development of closed, scalable and automated allogeneic gene-modified cell therapies would obviate at least some of these issues, ensuring consistent quality between batches and benefitting from larger scalability and hence economies of scale. Furthermore, the development of novel cryopreservation formulations, conserving functional cell viability post-thaw is also key to enabling global adoption of gene modified cell therapies.

In terms of viral vectors such as LV and AAV vectors, key manufacturing challenges are associated with dependency on adherent cell cultures and transient transfection, low and variable process yields and lack of viral vector-fit analytical assays. Until recently, viral vector manufacture was generally performed in adherent cell culture using multi-layer flasks and employing transient transfection. This method was labour-intensive, prone to errors and unscalable. Nowadays however, production of viral vectors in large scale suspension cultures or large scale adherent cultures using fixed bed bioreactors using transient transfection is widely employed. Whilst the introduction of fixed bed bioreactors has increased the scalability limit of adherent cell cultures from 100L to 500 – 1,000L of harvest volume per batch, the predicted viral vector demand is likely to require higher limits than currently available with such technology. Stirred-tank bioreactor suspension cultures can be scaled up beyond 2,000L and hence represent the ideal candidate flowsheet for meeting the future viral vector demands. However, the majority of large-scale viral vector processes use transient transfection, which is associated with large

quantities of plasmid DNA (pDNA) that drive up operational costs due to the cost of pDNA (manufacture and supply chain) and restricted optimisation potential (Merten et al. 2016; Chen et al. 2020). Further issues associated with transient transfection are the reliance on custom cGMP-manufacture pDNA, which can potentially introduce process variability as well as logistical challenges when implementing above 2,000L scale. Therefore, there is an active interest in switching to stable producer cell line (SPCL) systems to lower viral vector manufacturing costs by eliminating the pDNA component and increase process performance (e.g. titres) to further support the commercialisation of cell and gene therapies. Yet SPCL systems can require lengthier development timelines potentially leading to delays to market. Whilst several accounts of SPCL system development for LV have been published, there are limited accounts of virus-free SPCL systems for AAV due to its inherent reliance on helper viruses.

With regards to the issues surrounding low yields and high process variability are especially acute for LV manufacturing due to the low stability of the LV particles at ambient temperature and its size which make it particularly difficult to purify. Currently, there is no commercial resin or method that enables purification of functional LV particles i.e. fully packed and enveloped. The drive towards developing such method is limited since non-functional LV particles have not yet posed any safety questions. On the other hand, for AAV and pDNA, whilst they do not have the same stability issues as LV, the purification of full AAV capsids and supercoiled pDNA isoform is mandatory and can be challenging. Consequently, multiple chromatography steps need to be developed and optimised to maximise overall process yields whilst minimising impurity levels. The size of LV, AAV particles and pDNA make these unsuitable for conventional resin chromatography which was developed for much smaller biological entities. As such, macro-porous chromatographic media is being developed to enhance dynamic binding capacity and decrease processing times.

Whilst there is a wide agreement that analytical development is critical to the commercial success of cell and gene therapies, analytical development for characterisation and quantification of complex biological entities such as viral vectors has proven to be very challenging. Different titration readings of the same sample are not uncommon in the viral vector sector. Furthermore, process performance comparison between different manufacturers cannot be established since viral vector quantification methods tend to be different from one group to another. The development of a toolbox of orthogonal analytical methods is critical to building an accurate picture of viral vector process performance. **Chapter 2** further discusses the viral vector analytical challenges.

In terms of pDNA, the main manufacturing challenges are the low titres associated with the larger transgene constructs as well as the successful removal of *E*. coli DNA, RNA and non-supercoiled pDNA isoforms. Whilst the latter can be tackled employing and optimising a suite of chromatography steps, the former may be tackled at viral vector DNA sequence design level.

1.2.2 Reimbursement and costs challenges

Gene therapies are associated with very high selling prices ranging from $373,000 (Yescarta®, Tecartus®) to $2.1M (Zolgensma®) (**Table 1.1, Section 1.1.1**). These high selling prices are justified by sponsor companies based on the superior therapeutic benefit they bring to patients in comparison with existing therapies. Secondly, these are justified by the high manufacturing costs mainly driven by high raw materials and labour costs as well as complex supply chains. Authorities such as National Institute for Health and Care Excellence (NICE) and Institute for Clinical and Economic Review (ICER) have the mission of analysing the cost-effectiveness of therapies and informing healthcare authorities as to whether they should reimburse them or not. Provenge (Dendreon) (an autologous cell therapy) and Glybera (Uniqure) (an AAV therapy), amongst the first approved cell and gene therapies, are key examples of products where high manufacturing

costs and logistical hurdles impaired their commercial viability (Harrison et al. 2017). To tackle at least one of the challenges to achieving commercial viability, several reimbursement models have been proposed and a risk-sharing contract (pay-for-performance) was established for therapies such as Luxturna® (Spark Therapeutics) and Zolgensma® (Novartis) (Alhakamy et al. 2021). In a recent example, Zynteglo®, a haematopoietic stem cell gene therapy for beta-thalassemia developed by bluebird bio, was rejected by NICE due to small clinical trial data and insufficient data to justify reimbursement. Furthermore, German health authorities have also recently rejected the price set by bluebird bio, resulting in the company withdrawing its therapy from the German market (Liu 2021).

Other avenues to increasing commercial viability chances are linked to decreasing manufacturing costs. In terms of the cost of goods estimated for autologous CAR T-cell therapies, published accounts quote a range of $60,000 to $110,000 per patient (Spink and Steinsapir 2018; Harrison et al. 2019; Ran et al. 2020; Pereira Chilima 2019; Lopes et al. 2020). Production, QC labour and materials and viral vector costs are typically quoted as the key cost drivers (Nam et al. 2019)

These COGs represent 13-28% of the Yescarta® selling price which fall within the biopharma industry standard range of 15-25% (Basu et al. 2008). According to an analysis performed by Spink and Steinsapir (2018), it is estimated that large scale, maximising capacity utilisation, implementation of automation and lean operations could decrease the cost of goods per therapy down to $20,000. However, when accounting for the industry practice ratio of COG per selling price of 20%, the selling price may still not fall under the $100,000 ballpark which is yet unaffordable if CAR T-cell therapies were developed for large indications. It is concluded that potential route towards increases in affordability is the development of allogeneic therapies. On this topic, Jenkins et al. (2018) provide an

account of cost of goods analysis of allogeneic universal CAR T manufacture. This analysis revealed a COG/dose in the range of $8,000 to $10,000 per therapy enabling a potential selling price ranging between $40,000 and $50,000. On the other hand, another account of allogeneic CAR T cost of goods analysis presented COG/dose in the range of $5,000 (Harrison et al. 2019) which would translate into a selling price ranging between $25,000 - $30,000/dose.

With regards to lentiviral vector manufacturing, multiple accounts flagged the large cost contribution of LV towards the autologous CAR T-cell therapy manufacturing COG. However, these were likely quoting cost values associated with small scale adherent cell culture LV productions.

In terms of AAV cost of goods, Cameau et al. (2019) presents an account of AAV cost of analysis comparing the costs achieved when using multi-layer flasks versus a fixed bed bioreactor versus a suspension cell culture system. This analysis predicted that the COG/dose associated with a 10^{14} vg/dose product decreased from $25,000 as achieved with a multi-layer flask adherent cell culture process down to $8,000 – $12,000 when using large scale technologies such as suspension and fixed bed bioreactors.

In terms of cGMP-grade pDNA costs, the industry is quoting values priced between 50,000 and 100,000 €/g (Cameau et al. 2019; Cesari M. 2017), however even higher prices have been reported (personal communications). Whilst there are no published reports of pDNA cost of goods analyses, it is common knowledge that a batch of microbial culture can be priced in the order of the low digit £100,000s depending on scale. Typically, pDNA costs are larger for early clinical trials due to small scale and un-optimised productions and tend to decrease for late clinical trial and commercial stage as titres and process yields are improved and scale up is performed. The transfer plasmid

carrying the therapeutic gene is typically associated with a larger cost than the helper plasmids, likely due to its larger size (Hitchcock et al. 2010).

In terms of the supply chain challenges, these will be discussed as part of the next section.

1.3 Gene therapy supply chain considerations

An overview of the supply chain of gene therapies is provided in **Section 1.1.4.** This section describes the challenges associated with *in vivo* and *ex vivo* gene therapies and also gives a brief account of the impact of COVID-19 pandemic on the cell and gene therapy sector.

1.3.1 Supply chains of *in vivo* gene therapies

The supply chain of *in vivo* gene therapies is linear and it is not too dissimilar from that of biopharma products. However, it is arguably associated with more acute challenges linked to dependency on plasmid DNA, monopoly of equipment and material suppliers and reliance on highly qualified staff, all driven by slightly higher manufacturing complexities. With the adoption of stable producer cell lines, however, the dependency on pDNA will be removed, alleviating the supply chains of viral vector-based gene therapy products.

1.3.2 Supply chain of *ex vivo* gene therapies

1.3.2.1 Allogeneic *ex vivo* gene therapy supply chains

The level of complexity of supply chains of *ex vivo* gene therapies depends on whether these are allogeneic or autologous. The allogeneic cell therapy supply chain is still linear but has an even higher dependency on biologic-based materials, being complicated by reliance on frequent donor aphereses, availability of viral vector and/or plasmid DNA-derived gene editing tools. This would be simplified significantly by the development of the appropriate induced pluripotent stem cell banks, thus obviating the need for apheresis

donations, which could then be genetically modified to create large batches of allogeneic therapies.

1.3.2.2 Autologous *ex vivo* gene therapy supply chains

The supply chain of autologous gene-modified cell therapies is the most complex of all by far. Its non-linearity incorporating the patient and the healthcare provider poses challenges from logistical, regulatory and cost points of view. Whilst depending on the orchestrated availability of biological-based materials such as apheresis, viral vector or non-viral vectors, it needs to work around the clock to supply therapies to critically ill patients in a timely manner. Efficient coordination between healthcare provider, patient, leukapheresis centre, courier, manufacturer, and treatment centre is paramount. However, perhaps the most debated topic on the supply chain of autologous ATMPs is the centralised versus decentralised manufacturing paradigm. This section will discuss the supply chain considerations linked to supplier availability and the circular supply chain characteristic of autologous *ex vivo* gene therapies.

In terms of material and supplier considerations, gene-modified cell therapies tend to be heavily reliant on unique vendors such as Miltenyi Biotec (Bergisch Gladbach, Germany) which supply media, cell selection solutions, critical equipment and tubing sets as well as on their vector suppliers. In terms of raw materials other than vector and equipment, this is particularly relevant to the integrated end-to-end automated manufacturing processes. Such monopoly poses high risks to manufacturers if this vendor's supply capability is decreased or jeopardised. Furthermore, the lack of supplier competition means that the cell and gene therapy market is prepared to accept high materials and equipment prices, lacking any other options. This in turn, leads to high cost of goods and, to some extent, higher target selling prices. On the other hand, most if not all *ex vivo* gene therapy developers choose to manufacture their vectors using CDMOs rather than in house. Since

each vector is specific to each developer, the relationship with the vector CDMO is critical to the viability of the final product. With regards to all bioprocessing materials used in GMP manufacture, risk assessments need to be performed for each material to confirm GMP status, safety, identity, purity and potency. Supplier auditing and tactful contract negotiations are keys to establishing healthy relationships with supplier partners.

In terms of the supply chain strategy adopted for autologous gene-modified cell therapies, this is a centralised approach, with Novartis and Kite/Gilead reportedly utilising initially one manufacturing facility each to supply the US market (Spink and Steinsapir 2018). This requires the transportation of patients' apheresis product from collection centres to the manufacturing site for processing and the transportation of the product back to the same patient from whom the apheresis was collected. Whilst it provides control and consistency over the core manufacturing activities, this approach is associated with lengthy turnaround times, risk of temperature excursions, interruptions, delays or loss of patients starting material or drug product during long haul flights. This is aggravated further in the case of starting materials or products which are transported "fresh" (refrigerated) at temperatures between 2-6°C between sites since manufacturing or product administration need to start within a predefined time window from arrival. Typically, the leukapheresate as well as the drug product have a shelf life limited to roughly 24 hours (Papathanasiou et al. 2020). The "fresh in, fresh out" option is typically chosen due to limited availability of cryopreservation formulations which conserve functional cell viability to acceptable levels. On the other hand, other therapies adhere to a "frozen in, frozen out" paradigm where both leukapheresis and product are transported in a cryopreserved formulation (-180 °C). Alongside the harmonisation of leukapheresis and product administration procedures across sites, this requires also the harmonisation of the cryopreservation and thaw protocols at the leukapheresis and the product administration site, respectively. A further approach meant to be more amenable to

manufacturing flexibility is cryopreserving the leukapheresate once it reaches the manufacturing site. Whilst it has the same advantage of easing the scheduling of manufacturing slots as the "frozen in, frozen out" paradigm, the manufacturer has full control over the cryopreservation protocol as well as any analytics and storage required. On the other hand, the "frozen in, frozen out" option does not break the dependency cycle completely as patients require complex treatments where timing of medicines administration including that of the gene-modified cell therapy needs to be carefully orchestrated by physicians (Nam et al. 2019; Strachan 2019). Accounts such as Papathanasiou et al. (2020) provide an impact analysis of increased demand in the context of "fresh" and "frozen" paradigms, outlining the risks and potential solutions by employing intermediary sites. Therapies such as Yescarta®, a "fresh in" product and Kymriah®, a "frozen in" product, are associated with a complex cold chain which needs to manage the chain of custody and chain of identity of each product successfully (O'Donnell 2015). Furthermore, partnership with software companies such as TrakCel (Cardiff, United Kingdom) or Vineti (San Francisco, California, USA), supporting with data management platforms for tracking and tracing products have been reported (Nam et al. 2019). These companies provide real time tracking systems typically monitoring the product/intermediates/raw materials flow between manufacturing sites, CDMOs and treatment centres. These data management systems are required for ensuring patient safety, product quality, regulatory compliance, and customer service (Strachan 2019).

With regards to the turnaround times, or the time between the leukapheresis procedure and product administration, also known as vein-to-vein duration ranges between 17 and 22 days (Papathanasiou et al. 2020). These relatively long vein-to-vein times may mean that only certain patients are eligible to receiving this therapy, those who are less critically ill. In the context of treating very ill patients, the lack of flexibility associated with "fresh-in, fresh out" model could mean they could lose their therapy if they are not fit for cell

collection or receiving the therapy on the specific designated dates. Strategies to reduce vein-to-vein durations include product shipping ahead of full return of the release testing results, fast-tracking and optimisation of QC assays or collecting and storing early leukapheresis when patients are less poorly (Nam et al. 2019).

A further downside of the centralised model is represented by the challenge to correctly predict demand at peak sales early enough in order to make the appropriate changes efficiently. As such, it is likely that manufacturers will build overcapacity. This was shown to have a significant impact on COG/dose, especially since many of these processes are still labour intensive, driving costs per therapy up due to poor resource utilisation (Spink and Steinsapir 2018; Lopes et al. 2020).

Decentralised manufacturing paradigm represents the alternative to centralisation of manufacture and has been extensively discussed in the industry (Harrison et al. 2017; Zhu et al. 2018; Harrison et al. 2018c; Harrison et al. 2018b; Lopes et al. 2020). This has the potential to decrease or eliminate starting material or product transportation, thus decreasing vein-to-vein durations, risks and hence logistical costs. Several degrees of decentralisation have been debated by the industry, from establishing regional manufacturing centres to co-locating manufacturing sites to key hospital centres to incorporating manufacturing within key hospital centres.

The manufacturing in hospital model, also referred to as “bedside” or “point of care” manufacture is particularly attractive as it eliminates the transportation burden altogether and would reduce the vein-to-vein duration to a minimum. Furthermore, this would be more convenient to patients as they would only need to travel to one, close-by hospital centre for apheresis, preconditioning and product administration. There are published accounts of clinical trial CAR T-cell therapy manufacture or similar in the clinical setting, under unclassified environment using closed integrated systems (Jackson et al. 2020b;

Schwarze et al. 2021; Zhu et al. 2018). However, there are multiple concerns associated with this approach related to regulatory aspects, and control and oversight. In terms of regulatory aspects, a critical roadblock is the fact that the current regulatory framework requires that each hospital site to be used for core manufacturing needs to obtain a manufacturing license. This is a time-consuming and laborious process, requiring the implementation of a pharmaceutical quality system, qualification and validation of equipment and facilities and staff recruitment and training. Adoption of such rigorous systems is thought to be incompatible with cultures present in typical hospitals, especially those which struggle with insufficient resources. Furthermore, unless adoption of "GMP-in-a-box"-like systems (i.e. fully closed, integrated and automated) is possible, the manufacture of gene-modified cell therapies would be restricted to hospital centres which have cleanroom facilities (Trainor et al. 2014). Additionally, a further roadblock is the limited control and oversight that the sponsor company can realistically exert over hospital sites. The sponsor company would likely need to rely on the hospital's recruitment capabilities of hiring and retaining the appropriately qualified talent to manufacture their product at the required quality standards. Furthermore, the sponsor company would need to organise campaign training to ensure consistent manufacture across sites. With lengthy and labour intensive processes and testing schedules, there is a high degree of nervousness associated with delegating hospital sites to manufacture and test CAR T-like therapies. Moreover, the issue of procedure standardisation becomes even more critical here than in the centralised model since standardisation needs to be implemented also at the core manufacturing level so as to prove comparability across sites.

Industry leaders predict that the adoption of the "bedside manufacturing" paradigm will be brought to reality by the development of automated, integrated and fully-closed processing and testing systems (i.e. true "GMP-in-a-box"). In addition, increase in

product and process understanding, adoption of digitised technology solutions and changes in regulatory frameworks are also deemed to be required (Kaiser 2017; Strachan 2019). With at least two commercially available integrated closed systems (i.e. the CliniMACS Prodigy and the Cocoon), these still require other instruments for final packaging and cryopreservation hence they only come close to the "GMP-in-a-box" idea (Mukherjee et al. 2021). Furthermore, some of the analytics associated with these therapies are still labour intensive requiring machine set-up, sample preparation, load and analysis, hence still far from the true plug-and-play paradigm, although some progress is being made in that direction (National Academies of Sciences and Medicine 2018; Schwarze et al. 2021). Moreover, to enable further development of automated processing and testing solutions as well as to shift the regulatory frameworks towards providing more point-of-care amenable regulations, product and process understanding need to be expanded.

There has been an extensive debate surrounding the definition of the future supply chain model of autologous gene-modified cell therapies. Product manufacturing taking place in academic centres has been the approach for early clinical trials. Whilst the first products were market-launched using a centralised approach, large companies (e.g. Novartis) have since established other sites to de-risk their business, increase manufacturing capacity and ease the logistical hurdles of reaching other markets. As such, there has been an organic move towards a regional model where at minimum two manufacturing sites are established to meet market demand. On the other hand, the "GMP-in-a-box" paradigm is a relatively new concept, discussed over the last 5-7 years. Whilst its adoption may still be scarce, it is very likely that it will gain territory once fully-closed and automated cell processing systems as well as QC systems become available, potentially closely competing with the regional manufacturing approach.

Regardless of the supply paradigm approach adopted, supply chain complexities will remain. These can be grouped into managing stakeholders, standardisation and implementation of digitised technology systems. The relatively high number of stakeholders belonging to diverse disciplines such as apheresis lab technician, manufacturer, nurse practitioners, courier, pharmacist, physician have to coordinate efficiently so as to deliver the therapy to the patient. As such, a relatively large number of carefully orchestrated staff is required to ensure successful delivery of a therapy. Some territories, such as the UK, are actively trying to support the implementation of these transformative therapies by the establishment of advanced therapies treatment centres (ATTCs) which aim to bring together key stakeholders to work towards making adoption of ATMPs a reality. Moreover, sources of process and product variability are linked to supply chain such as the risk of differences in apheresis collection protocols across blood collection site or differences in product preparation and administration protocols. The harmonization of leukapheresis and product preparation and administration protocols could tackle this issue. Implementation of standard operating procedures (SOPs) would facilitate opening new clinical centres, alleviating the need for staff retraining rounds from one company to another. With regards to documentation, the patient-centric nature of these therapies means that one patient equals one batch. As GMP guidance states the requirement of a record for each batch, these representing lengthy documents, the manufacturing of multiple batches concurrently leads to mountains of papers if paper-work systems are adopted. Such burden is difficult to manage even at small scale, hence electronic batch records solutions integrated with electronic pharmaceutical quality systems are mandatory for exerting control over autologous therapy manufacture quality.

1.3.3. COVID-19 pandemic impact

The COVID-19 pandemic has had a significant impact on the biopharma and cell and gene therapy sector. On the one hand, it accelerated the development of mRNA-based

therapeutics and it raised awareness about biotechnology in general, attracting workforce, while on the other hand, it disrupted massively the supply chains of many cell and gene therapy products (Qiu et al. 2021). Since vaccine manufacture using mRNA technology utilises similar unit operations to viral vector manufacture, it has been the case that critical consumables (e.g. flasks, tubing sets, pipette tips, flow paths) secured for viral vector development activities were re-directed to vaccine manufacturers upon very short notice from suppliers. A similar issue was encountered with plasmid DNA availability. This delayed cell and gene therapy clinical programs and put pressure on the industry as a whole. Despite these disruptions, the cell and gene therapy sector has not experienced reductions in investment levels due to the pandemic (ARM 2021).

1.4 Decisional tools

1.4.1 Overview

In order to evaluate the trade-offs associated with different routes to commercialisation, decisional tools have been developed historically to aid the biopharma sector to find cost-effective manufacturing solutions, as well as identify performance targets to help decrease their costs (Farid et al. 2005; Stonier et al. 2013; Lim et al. 2005; Farid et al. 2000; Stamatis 2019; Pollock et al. 2013). Furthermore, decisional tools are software tools able to capture the impact of decisions, uncertainties and limitations on key financial, operational and risk factors whilst predicting cost-effectiveness and robustness metrics (Farid 2012). These are aimed at facilitating decision-making in early drug development by enabling the assessment of alternative strategies of delivering biotech products to the market. Commonly integrated sets of techniques into these tools are process economics, simulation, risk analysis, optimisation, operation research and multivariate analysis which enable analysing product challenges from multiple perspectives. The metrics that these tools calculate include capital investment, manufacturing cost of goods (COG),

throughput, capacity utilisation and these built into assessment of process robustness and ease of implementation maintaining high product quality (Farid 2012).

Decisional tools have been developed to support the biopharma (Stonier et al. 2013; Pollock et al. 2013; Farid et al. 2005; Farid et al. 2000; Stamatis 2019; Lim et al. 2005) and cell and gene therapy (Chilima et al. 2018; Chilima et al. 2020; Jenkins et al. 2016; Jenkins and Farid 2015; Hassan et al. 2015; Comisel et al. 2021; da Silva et al. 2021) sectors to analyse trade-offs associated with various manufacturing options and identify performance targets to aid the sector decrease costs.

In terms of the biopharma sector, decisional tools have been developed for evaluation of alternative flowsheets, impact of process variability, portfolio management, capacity planning, production planning and chromatography sizing optimisation. Alternative flowsheet strategies have been assessed by capturing robustness under uncertainty via Monte Carlo simulation which analysed the reward/risk ratio in the case of perfusion versus fed-batch culture mode for commercial scale supply of antibodies (Pollock et al. 2011). Also, analysis of stainless steel vs single-use facilities for clinical trials had been explored by reconciling multiple conflicting outputs such as cost and capacity utilisation under uncertainty (Farid et al. 2005). Portfolio management, capacity planning (George and Farid 2008) as well as multisite long-term production planning (Lakhdar et al. 2007) and chromatography sizing optimisation in multiproduct facilities (Simaria et al. 2011) have been tackled by exploring large decisional spaces using heuristics methods.

A list of the typical components or computational methods for decisional tools developed for cell and gene therapies developed over the last 7 years is provided in **Table 1.3**. The cost of goods (COG) and project valuation methodologies represent key components of bioprocess economics models. These are built to include the whole bioprocess and are used for comparing different technologies or flowsheets by capturing the trade-offs between the characteristics of each technology or flowsheet analysed, from a cost

perspective. COG models include all the costs required to manufacture a product such as direct and indirect costs. These may capture fixed capital investment (FCI) values if the assumption is that the product is manufactured in house or CDMO charges if manufacture is assumed to be outsourced. Project valuation is typically performed using net present value (NPV) analysis. The risk-adjusted NVP (rNPV) metric captures outgoings such as initial capital investment, manufacturing costs, logistics and sales and marketing costs, taxes and sales whilst accounting for the time-value of money and risks (Bogdan and Villiger 2010). rNPV analysis is useful for evaluating scenarios of process changes occurring at different time points in the drug development journey so as to identify the most attractive points to implement a process change (Hassan et al. 2016). Furthermore, it can be used to inform decisions such as build or buy as well as centralised or decentralised manufacture of autologous CAR T-cell therapies (Pereira Chilima 2019). In terms of the optimisation component, this can include routes to determine target process performance or identify most cost-effective technologies or flowsheets that meet input conditions. This can be implemented using brute force search or heuristics such as genetic algorithms (Jankauskas et al. 2019; Fellows et al. 2012). Whilst the latter strategy sits outside of the scope of this thesis, brute force search can be used to perform screenings of all given possible combinations, check whether they meet input conditions, and record the optimal solution based on the set objective (Sui 2007).

The following sections will describe the advances in the development of decisional tools for allogeneic and autologous cell therapies. **Table 1.3** summarises key information on these tools in terms of references and tool components. A systematic review of the landscape of decisional tools developed for regenerative medicines is also provided by Lam et al. (2018). It is critical to note that no academic peer reviewed accounts have been published so far on the topic of viral vector manufacture other than the work described within this thesis.

Table 1.2 Key recent references of decisional tool development and their components.

Therapy type	Key decisional tool references	Infra-structure	Tool components								
			Cost of goods analysis*	Optimisation algorithms	Sensitivity analyses	Project valuation (rNPV)	Cost of drug development analysis	Uncertainty analysis	MADM analysis	Dynamic modelling	Supply chain analyses
Allogeneic MSC therapies	Simaria et al.(2014)	C#, Microsoft Access	✓	✓	✓						
	Hassan et al. (2015)		✓	✓	✓						
	Hassan et al.(2016)		✓		✓	✓	✓	✓			
	Chilima et al.(2018)	Excel, VBA	✓	✓	✓			✓	✓		
	Harrison et al. (2018a)	Excel, VBA	✓								
	Harrison et al. (2018b)	Excel, VBA	✓								✓
Allogeneic CAR T-cell therapies	Jenkins et al. (2018)	Excel, VBA	✓	✓	✓			✓	✓		✓
	Harrison et al. (2019)	Excel, VBA	✓		✓						
Other allogeneic applications	Jenkins et al. (2016)(hiPSC)	Excel, VBA	✓	✓	✓			✓			
	da Silva et al. (2021) (BAL)	Excel, VBA	✓								
Autologous CAR T –cell therapies	Pereira Chilima (2019)	Excel, VBA	✓	✓	✓	✓					✓
	Lopes et al. (2020)	Biosolve, Orchestrate	✓		✓						✓
	Spink and Steinsapir et al. (2018)	NC	✓		✓						
	Wang et al. (2019)	DES	✓**			✓**		✓		✓	✓
	Lam et al. (2021)	DES	✓					✓		✓	✓

*includes fixed capital investment analyses. ** could be linked with, NC - not communicated, VBA -visual basic for applications, hiHSC – human induced pluripotent stem cells, BAL – bioartificial liver.

1.4.2 Decisional tools for allogeneic cell therapies

A range of decisional tools have been described for allogeneic cell therapies addressing mesenchymal stem cell processes, human induced pluripotent stem cells (iPSCs) used for drug screening, CAR T-cell and bioartificial liver devices (BAL) manufacturing processes.

In terms of mesenchymal stem cells (MSC) manufacturing processes, these provide process flowsheets evaluations, identification of process performance targets, scalability limits, impact of uncertainty, and impact of process change at different time points using COG, robustness and profitability metrics. Simaria et al. (2014) is amongst the first to describe a cell therapy decisional tool looking at comparing different mesenchymal stem cells (MSC) manufacturing platforms from an upstream COG perspective across a range of commercialisation scenarios. Planar and microcarrier-based flowsheets were evaluated, the gaps in technology capabilities as well as the target process performance to support future demands were identified. The key cost differentiating factors between flowsheets were surface area, harvest cell density and resource requirement per technology with demand and dose size dictating technology ranking. Hassan et al. (2015) explored the downstream flowsheets that are used in MSC manufacture and provided an extensive analysis of their COG and ranking. The tool predicted that fluidised bed centrifugation represented the only feasible option for large scale microcarrier productions of MSCs while tangential flow filtration was the most cost-effective option for small scale, planar MSC cultures. Both of these tools included a bioprocess economics model, which is essentially a COG model, an optimisation algorithm based on brute force methodology which searches for the optimal solutions based on input constraints and a data base for inputs and capturing generated outputs. Chilima et al. (2018) evaluated the costs, robustness, operational ease and business feasibility of candidate MSC flowsheets

across different scenarios of scale, demand, reimbursement and dose size scenarios. This work predicted that microcarrier cell cultures are more likely to lead to feasible business models despite the uncertainty associated with their use and flagged future bottlenecks in downstream processing capacity when dealing with large dose size products. The tool used to perform this analysis was built based on the tool described by Simaria et al. (2014) and Hassan et al. (2015) with the addition of a stochastic modelling using Monte Carlo simulation and a multi-attribute decision-making (MADM) model based on the weighted sum method. Further to this, Hassan et al. (2016) described a decisional tool evaluating the impact of process changes from planar to microcarriers-based manufacture during different phases of clinical development on the long-term profitability of an MSC allogeneic cell therapy project. This work predicted that switching to microcarrier-based manufacture early in clinical development is associated with lower total costs compared to sticking to planar technologies. However, despite higher total costs associated with switching post-approval, from a profitability perspective, it was found that this scenario was as profitable as switching early due to minimising the time-to market. The conclusion of the study was that switching early to microcarrier-based cell cultures was the most optimal approach due to lower risks from a budget perspective. The tool used for performing this analysis contained three key models, coupled with stochastic modelling using Monte Carlo simulation. These were a bioprocess economics model assessing the COG, a cost of drug development model computing Chemistry Manufacturing and Controls (CMC) and clinical trials costs and a project valuation model computing the risk-adjusted net present (rNPV). Additionally, Harrison et al. (2018b) described a manufacturing cost model designed to assess the implications of decentralising manufacture of MSC products within the UK. This study explored the differences in labour cost and rent between regions, the impact of centralising QC activities and the impact of product loss during processing and in transit.

In terms of iPSC processes, a decisional tool designed for hiPSCs bioprocessing for drug screening products has also been developed (Jenkins et al. 2016). This tool was applied in a case study determining the most optimal flowsheet to be used for generating a range of numbers of patient-specific neuron cell lines for drug screening studies. This study predicted that the use of automated equipment led to more robust bioprocess when accounting for impact of uncertainty on COG. The tool used in this work consisted of a bioprocess economics model, information database and a brute-force search algorithm, which was used in conjunction with stochastic modelling employing a Monte Carlo simulation method.

In terms of allogeneic CAR T-cell manufacturing process, two accounts have been published so far (Jenkins and Farid 2018; Harrison et al. 2019). Jenkins et al. (2018) present a decisional tool employed to compare a range of flowsheets for manufacturing allogeneic, universal CAR T-cells from a COG perspective. COG values ranging from ~$8,000 to ~$10,000/dose were identified depending on flowsheet. This study predicted that a modular flowsheet including a rocking motion bioreactor was the most attractive from both COG and financial and operational perspectives and that transduction and electroporation efficiency were key process economics factors. The tool used here contained the same types of components as that described in Jenkins et al. (2016) with the addition of a multi-attribute decision-making (MADM) model. On the other hand, Harrison et al. (2019) described an account of COG analysis for an allogeneic CAR T-cell product manufactured in four geographic regions i.e. two sites in USA, Mexico and Argentina for the supply of the US market. The focus of this study was to characterise the cost savings achieved when manufacturing onshore and offshore, driven by reductions in labour, transportation and facility costs. The tool consisted of a process economics model described in Harrison et al. (2018a), developed initially for MSC-based cell therapies to assess the cost-benefit of implementing automated manufacture, which was adapted for

CAR T-cell therapies. Whilst staff cost savings were obvious when moving to offshore manufacturing sites, the overall COG/dose decrease was of only 11% from a value of ~$4,500/dose when manufacturing inshore. Furthermore, this account predicted that consumables and QC activities represented the cost drivers of allogeneic CAR T-cell therapies. The difference in the COG value achieved between these two studies could be attributed to different assumptions linked to dose size, viral vector costs and number of doses that can be produced from one donor leukapheresis.

In terms of bioartificial liver (BAL) device manufacture, da Silva et al. (2021) provides an account of a decisional tool developed to analyse the COG difference between four process flowsheets that could be employed in BAL manufacture. Whilst the use of a microcarrier flowsheet using stainless steel technology was found to be the most optimal, the cost drivers identified were medium volume and cost. The tool consisted of a whole bioprocess economics model linked to a cost and process information database.

Furthermore, Chilima et al.(2020) presents a methodology that allows the calculation of facility capital investment (FCI) and facility footprint for cell therapies that can be fed into COG analyses. The detailed factorial methodology accounting for technology-specific factors was employed to derive cost and area factors that can be used to generate quick and reliable FCI and footprint estimations depending on technology type of choice. Key findings of this study were that, for a greenfield project in a medium-developed country, area factors ranged between ~$700 – $7,000/$m^2$ while cost factors ranged between 2.3 - 8.5. Furthermore, it revealed that facilities for autologous cell therapies are typically 6-fold larger and more expensive than those for allogeneic cell therapies generating the same volume of therapies due to economies of scale achieved when scaling up allogeneic manufacture.

1.4.3 Decisional tools for autologous gene-modified therapies

In terms of decisional tools for autologous gene-modified therapies, there is a limited account of academic peer reviewed publications (Pereira Chilima 2019; Wang et al. 2019; Lam et al. 2021) whilst a handful of accounts are provided by industry peer reviewed publications (Spink and Steinsapir 2018; Lopes et al. 2020; McCoy et al. 2020). These can be grouped in process economics and supply chain accounts, process economics accounts and supply chain accounts.

In terms of process economics and supply chain accounts, Pereira Chilima (2019) described a decisional tool employed to evaluate a range of cell expansion technologies for the manufacture of autologous CAR T-cell therapies and assess the optimal supply chain configuration. This work revealed that for low dose size products in the order of 5M CAR T-cells, the static suspension bag was the optimal technology from a COG perspective, while for dose sizes in the range of 50M CAR T-cells, that changed to the integrated USP/DSP platform. For even larger dose size, the tool predicted that the rocking motion bioreactor would be the most cost-effective. In terms of supply chain considerations, this study predicted that multi-site manufacture employing hospitals as manufacturing sites could be more attractive than the centralised paradigm, depending on the number of manufacturing sites, based on risk-reward profile analyses. The tool employed in this study consisted of a COG model, brute optimisation algorithm, a database and a project valuation model using risk-adjusted net present value methodology. Furthermore, Lopes et al. (2020) described the use of the Biosolve software to compare the COG achieved using manual, semi-automated and automated processing as well as the financial impact of point-of-care manufacture. A key finding of this work is that semi-automated manufacture, following a modular approach as described in **Chapter 2,** may lead to higher throughputs and hence COG/dose due to enhanced flexibility over fully-integrated automated systems. However, this analysis does not

account for the higher risks of cross-contamination and/or processing errors in the case of modular manufacture due to transitioning batches at different processing stages from one module to the other simultaneously. Furthermore, this work predicted that the COG differences between centralised and point-of-care manufacture were small, however the centralised model was deemed to be more at risk of demand fluctuations.

In terms of decisional tools including process economics only accounts, Spink and Steinsapir (2018) describe the use of a decisional tool to compute the COG associated with autologous CAR T-cell therapy products. This study identified labour cost as the key cost driver, followed by materials cost. Further, it evaluated potential avenues to minimising COG/dose by decreasing labour costs via implementation of automation, lean operations and digital technologies, and materials costs via increase in economies of scale and negotiation of discounts. Based on their analyses, this best case scenario could not achieve high enough cost reductions to trigger a significant drop in selling price so as to ensure affordability of these therapies for large demand indications.

Recent literature accounts on autologous supply chain decisional tools have included methodologies such as discrete event simulation to model resource management and risks (Wang et al. 2019; Farsi et al. 2019; Lam et al. 2021). Furthermore, accounts employing mixed-integer linear programming to tackle supply chain optimisation have also been reported as reviewed by Sarkis et al. (2021). Additionally, mathematical models to identify optimal manufacturing and cryopreservation facilities for patients' cells using multi-objective genetic algorithms have been described (Avramescu et al. 2021).

1.5 Aims and organisation of thesis

This chapter has provided a gene therapy industry snapshot by discussing the key types of cell and gene therapies, the differences between them, and drug development considerations. Then, the attention was brought to the complexity of cell and gene therapy

supply chains, especially those associated with the autologous approaches, initially from a biological-based product manufacture perspective. Furthermore, the commercialisation challenges associated with gene therapies were addressed from manufacturing, cost and supply chain perspectives. Discussion on key supply chain considerations with a focus on the logistics of autologous gene-modified cell therapies was provided in the context of centralised and decentralised manufacture. This chapter has also provided an overview of the decisional tools that have been developed so far for cell therapy products to assess the cost-effectiveness of flowsheets, identify the scalability limits and performance targets and capture impact of process changes. Whilst some accounts describe decisional tools used for the supply chain analysis of autologous CAR T-cell therapies, these have not provided a thorough analysis on the impact of the number of decentralised sites from both profitability and operational easiness perspectives. Furthermore, decisional tools have not yet characterised the impact of financial agreements between stakeholders on profitability or captured the impact of analytical automation implementation on cost of goods. On the other hand, there are no academic accounts of decisional tools developed to assess the cost-effectiveness of a range of manufacturing flowsheets for viral vectors. Also, no study has been published so far which assesses the financial implications of switching from manufacturing viral vectors using transient transfection to manufacturing using stable producer cell lines at different stages in the drug development pathway.

The aim of this thesis is to describe how the application of decisional tools in key areas of the supply chain of cell and gene therapies can provide valuable insights towards achieving commercial viability of cell and gene therapy products.

Chapter 2 presents a thorough review of the manufacturing processes associated with cell and gene therapy products. **Chapter 3** provides a description of the advanced integrated bioprocess economics tools which were employed to generate the results

presented in **Chapter 4** to **Chapter 6**. The tool incorporates a cost of goods model, a fixed capital investment model, a cost of drug development model, as well as a project valuation model, all coupled with technology data bases and a brute force optimisation algorithm.

Chapter 4 describes the application of the decisional tool to provide an analysis of the decentralised manufacture configuration options as well as impact of analytical equipment automation in the context of autologous CAR T-cell manufacture.

Chapter 5 focuses on the lentiviral vector component of the supply chain of gene therapies, describing the application of the decisional tool to assess the cost-effectiveness of different cell culture technologies and to identify scale limitations and targets. **Chapter 6** describes the use of the decisional tool to analyse the trade-offs between using transient transfection and switching to stable producer cell lines at different stages in the drug development pathway in the context of three LV products and one AAV product, from a financial perspective. **Chapter 7** provides a summary of the key conclusions and contributions from the case studies described in **Chapter 4** to **Chapter 6.** Furthermore, it discusses further questions and analyses that would be valuable to approach in future work while **Chapter 8** provides an overview of the process validation of gene therapies as well as its key challenges.

Chapter 2: Manufacturing processes and technologies

2.1 Introduction

This section will describe the manufacturing processes associated with *ex vivo* gene therapies as indicated in **Figure 1.1 (Chapter 1**) namely, the gene-modified cell therapy, viral vector and plasmid DNA (pDNA) manufacture. The key gene-modified cell therapy processes will be classified and described in more detail, and the technologies utilised to manufacture these will be discussed. There are no major differences between the manufacturing processes for *ex vivo* viral vectors and *in vivo* viral vectors or for pDNA intended for either modality, hence these will be presented together. It is important to mention that all of these processes apart from pDNA process, which is predominantly using stainless-steel equipment, are associated with single-use operations.

2.2 Gene-modified cell therapy manufacturing processes

Multiple manufacturing approaches for *ex vivo* gene therapies emerged over the last 20 years. Many of these are highly manual and complex, while some others are streamlined and involve certain degrees of automation. This section will first provide a process classification, a picture of a range of manufacturing processes identified in literature and will later on focus on technologies used, with a particular focus on the most recently developed technologies.

Table 2.1 shows a proposed gene-modified cell therapy classification based on indication, starting cell type, vector type used, cell modification type and whether it is autologous or allogeneic. As such, the therapy types can be grouped in 4 therapeutic indications with cancers, graft-versus-host (GvHD) disease and HIV being tackled with the modification of T-cells, while the HIV and genetic diseases being tackled with the modification of the haematopoietic stem cells (HSCs). Two main types of vectors are used i.e. viral vectors such as lentiviral and gamma-retroviral vectors and non-viral

vectors such as plasmid DNA (Sleeping Beauty Transposone/Transposase system), mRNA electroporation and genetic editing tools (CRISPR, TALENs, ZNF). The vectors are mainly used to introduce a gene in the target cell type, or to knock-out a gene in the case of the HIV therapy, or both add a gene and knock-out another gene as in the case of universal CAR T-cell approaches. Whilst the therapies developed for cancer are both autologous and allogeneic, those developed for Graft-versus-host disease are predominantly allogeneic, and those for HIV and genetic diseases are autologous. In the case of allogeneic approaches, a combination of viral vectors and non-viral vectors can be employed. The colour system in the 'Type of vectors' column shows the level of maturity of each of the approaches, with darker green showing the approaches that have been commercialised and lighter green showing the investigated approaches which have not reached market yet. The most advanced therapy types so far are addressing cancer and genetic diseases with products in the market employing autologous approaches and gene additions via viral vectors (e.g. cancers: Kymriah, Yescarta etc.; genetic disease: Strimvelis, Zynteglo, Lipmeldy). Despite reaching conditional marketing approval, the GvHD product, Zalmoxis, manufactured by MolMed has been withdrawn (Elsallab et al. 2020). So far, no other allogeneic *ex vivo* gene therapy has achieved marketing authorisation.

Table 2.1 Classification of gene-modified cell therapies.

Therapeutic indication	Starting cell type	Type of modification	Autologous/Allogeneic	Type of vectors	References
Cancer	T-cells	Gene addition	Autologous	VV (LV or g-RV)	Reviewed in Holzinger et al. (2016) and Fesnak et al. (2016a) for CAR T and TCR products. All currently approved CAR T products (up until June 2021)
				Non-VV (SBTT)	Auto: NCT00968760, NCT01497184, NCT01653717
				Non-VV (transient expression with mRNA electroporation)	NCT01355965
			Allogeneic (Donor-derived)	VV (LV or g-RV) or Non-VV (SBTT)	NCT00924326, NCT00840853; NCT01362452
		Gene addition and receptor knock-out	Allogeneic (Universal)	VV (LV or AAV) and genome editing (TALEN, ZFN etc)	NCT02808442 NCT02746952 NCT03203369 e.g. CTX110, CRISPR Therapeutics
GvHD	T-cells	Gene addition	Allogeneic (Donor-derived)	VV (LV or g-RV)	NCT01494103 NCT00914628 Zalmoxis, MolMed (withdrawn)
HIV	T-cells and/or HSCs	Receptor silencing knock-out (main)	Autologous	VV (LV or g-RV)	NCT00295477
				Genome editing (ZFN)	NCT00842634; NCT02500849
Genetic diseases*	HSCs	Gene addition	Autologous	VV (LV or g-RV)	Reviewed in Scott and DeFrancesco (2016)

GvHD = graft-versus-host disease, HSC = haematopoietic stem cells, VV= viral vector, LV = lentiviral vector, g-RV = gamma-retroviral vector, SBTT = sleeping beauty transposone/transposase, TALEN = Transcription activator-like effector nucleases, ZFN = Zinc-finger nucleases; CRISPR = clustered regularly interspaced short palindromic repeats. * genetic diseases affecting tissues accessible to blood cells.

Process types

The type of *ex vivo* gene therapy impacts the manufacturing process flowsheet. As such, this section describes the process flowsheets of the therapy classes shown in **Table 2.1**. **Table 2.2** shows the sequence of manufacturing steps, process durations, cell doses, transduction efficiency and leading organisations working on each therapy class. The processes associated with the approved products will be discussed first while the processes associated with emerging products will be discussed afterwards.

Table 2.2 Process details associated with key classes of *ex vivo* gene therapy products.

Process steps	Cancer				GvHD (allo e.g. Zalmoxis)	HIV (LV / genome editing) (auto)	HIV (genome editing) (auto)	Genetic disorders (auto)
	Viral vector (auto/allo)	SBTT (auto/allo)	CAR mRNA transcript electroporation (auto)	Viral vector and genome editing (universal)				
Collection	1	1	1	1	1	1	1	1
Enrichment/ Wash	2	2	2	2	2	2	2	2
Selection	3	3. aAPC / ACB	3.ACB	3.ACB		3.NS	3	3
Activation					3.OKT3	4.ACB	4.+L-glutamine	4
Genetic modification	4. LV or g-RV	4. Nucleofector II	6. MaxCyte GTX	4.1.LV, 4.2.TALENs, APD	4.1. g-RV, 4.2. PMS	5. LV / Ad5-ZFN	5.MaxCyte GTX	5. LV or g-RV
Culture	5	5. aAPC, WAVE / G-Rex	4	5.WAVE	5	6.WAVE	6.VueLife bag	
Wash	6	6	5.RB	6.PMS	6	7.RB	7	6
Formulation	7	7	7	7	7	8	8	7
Process duration	11-17 days (Gill, 2015), 3 weeks min. (e.g. Kymriah)	Min. 28 days	10+/- 2 days	18 days	~12 days	Min. 12-14 days	~ 4 days	2-5 days
Dose size	Order of 10^6-10^7 CAR T-cells /kg	Up to 10^8 CAR T-cells/m^2	10^8-10^9/infusion (multiple infusions required)	4-5 x 10^6 CAR19 T cells/kg	0.02 – 5 x 10^6 cells/kg	0.5-1 x 10^{10} cells	Min 5 x 10^6 CD34+ cells/kg	Min. 2 x 10^6 engineered cells/kg
MOI/ Transduction efficiency	MOI<5	56.8-96.5% CAR +ve	>90% transfected cells	NC	NC	5/0.25 – 3.4 VCN per cell / ~20%	Preclinical: 40-60%	MOI = 25-100

Process steps	Cancer				GvHD (allo e.g. Zalmoxis)	HIV (LV / genome editing) (auto)	HIV (genome editing) (auto)	Genetic disorders (auto)
	Viral vector (auto/allo)	**SBTT (auto/allo)**	**CAR mRNA transcript electroporation (auto)**	**Viral vector and genome editing (universal)**				
e.g. Organisations	Novartis, Kite/Gilead, Juno/BMS, Adaptimmune, Baylor College of Medicine, NCI	University of Texas MDACC	University of Pennsylvania	Cellectis/ Pfeizer, Servier	Baylor College of Medicine; MolMed	University of Pennsylvania ViRxSYS (LV) / Sangamo Therapeutics (AdV-ZFN)	Sangamo Biosciences	GSK, Orchard Therapeutics, bluebird bio, Genethon, San Raffaele Scientific Institute
e.g. References	Reviewed in Kochenderfer et al. (2013), Wang and Rivière (2016), Levine (2015); Fesnak et al. (2016a); Gill and June (2015)	Singh et al. (2013); Singh et al. (2014); Kebriaei et al. (2016); Hudecek et al. (2017); Prommersberger et al. (2021)	Beatty et al. (2014)	Torikai et al. (2012); Field and Qasim (2015); Poirot et al. (2015); MacLeod et al. (2017)	Reviewed in Zhou et al. (2015); Di Stasi et al. (2011); Ciceri et al. (2009)	Tebas et al. (2013); Tebas et al. (2014); Peterson et al. (2016)	DiGiusto et al. (2016)	Reviewed in Wang and Rivière (2017); Scott and DeFrancesco (2016); Digiusto and Kiem (2012); Aiuti et al. (2017)

In grey: HSC processes. SBTT = sleeping beauty transposone/transposase system; Allo = allogeneic; Auto = autologous; APD = Agile Pulse Device (BTX-Harvard Apparatus); PMS = post-modification selection; ACB = antibody-coated beads; aAPC = artificial antigen presenting cells; NS = negative selection; RB = remove beads; NCI = National Cancer Institute; NC = not communicated.

2.2.1 Processes associated with approved products

Two types of *ex vivo* gene therapy products have achieved regulatory approval to date: the CAR T products for cancers and the haematopoietic stem cell (HSC) gene therapy products for genetic diseases, both autologous approaches employing viral vectors, listed in **Table 1.1** (**Chapter 1**). These are described in terms of process flowsheet and key information in the first and the last column of **Table 2.2** (above). The autologous TCR therapies investigated in clinical trials follow also the key steps identified in **Table 2.2**, first column. Whilst CAR T and TCR manufacturing processes are virtually the same utilising T-cells as starting material, it was reported that TCR products require slightly larger dose sizes and have a higher potential for treatment of solid tumours when compared to their CAR T counterpart.

Generally, these processes involve the addition of a therapeutic gene into donor's T-cells in the case of the CAR T/TCR products or into donor's CD34+ stem cells in the case of the HSC gene therapy products. The differences between these two product classes in terms of starting material collection, selection and activation, transduction, cell culture and formulation will be described below.

The first key difference between the T-cell-based and HSC-based gene therapies is the starting material collection approach and selection and activation of target cell type driven by the differences in target cell substrates. In terms of collection of starting material, whilst both T-cells and HSCs can be collected using apheresis techniques, the HSCs can also be collected via bone marrow collection. In the case of the T-cell-based therapies, the starting material is collected using the leukapheresis method which separates the peripheral blood mononuclear cells (MNC) which includes lymphocytes, from the donor's whole blood using centrifugation (Fesnak and O'Doherty 2017). This procedure processes between 0.8-7 blood volumes in oncology patients so as to ensure the collection

of a minimum of 0.6×10^9 and a target of 2×10^9 CD3+ cells (Allen et al. 2017). In the case of the HSC gene therapies, the starting material, namely the autologous CD34+ HSC progenitors, can be collected from bone marrow or from mobilised peripheral blood via apheresis techniques (Wang and Rivière 2017). The bone marrow extraction requires surgical intervention via needle insertion into the rear of the hip performed under regional or general anaesthesia. The collection via mobilised peripheral blood requires the release of the HSCs from bone marrow niche into the blood stream via administration of mobilising agents such as granulocyte colony-stimulating factor (G-CSF) and Plerixafor to donors. Up to 5 blood volumes are processed via apheresis techniques in order to collect sufficient numbers of HSCs for gene therapy manufacture for sickle cell disease (Esrick et al. 2018). Examples of apheresis machines that can be used for either therapy type are COBE Spectra and Spectra Optia Apheresis System (Terumo BCT, Lakewood, Colorado, USA) and Amicus Cell Separator (Fenwal Inc/Fresenius Kabi, Bad Homburg, Germany) (Fesnak et al. 2016a). Furthermore, regardless of therapy type, the apheresis packs are then washed to remove red blood cells and platelet contaminates using closed and automated devices such as the Haemonetics Cell Saver 5+ (Soma Tech Intl, Bloomfield, Connecticut, USA), LOVO (Fresenius Kabi) or CliniMACs Prodigy® (Miltenyi Biotec). In the case of the T-cell therapies only, enrichment is a step that is often employed between the apheresis and the wash step. Isolation of lymphocytes from a monocyte-rich fraction can be done based on size and cell density differences using the elutriation principle (Fesnak et al. 2017). As such, the Elutra Cell Separation System (Terumo BCT) and the Elutriation System (Beckman Coulter Systems) were developed (Stroncek et al. 2014). This step is often called an enrichment step. Moreover, the enrichment step may also include the T-cell selection step in some publications (Fesnak et al. 2017).

In terms of selection of target cell type, this can be performed based on immunophenotypic characteristics with the antibody-bead conjugation representing perhaps the most established route in the case of both therapy types. Selection using antibody-bead conjugation can be done using magnetic beads fused with monoclonal antibodies targeting cell markers of the target cell type. In the case of T-cells, magnetic beads conjugated with CD3/CD28 antibodies are most commonly employed to both select and activate T-cells. Activation of T-cells is required in order to trigger their innate immunologic response to antigens. The anti-CD3 mAb is known to trigger T-cell proliferation via the T-cell receptor complex, while the anti-CD28 mAb represents a strong co-stimulatory signal leading to production of high cytokine levels (Levine 2015). Since retroviral vectors are known to be associated with higher transduction efficiency in dividing cells, T-cell activation is also required for the transduction step (Wang and Rivière 2016). Example of technologies specific for T-cell selection and activation are the Dynabeads CD3/28 (Thermo Fisher Scientific, Waltham, Massachusetts, USA), the MACS GMP ExpAct Treg beads and MACS GMP TransAct CD3/28 nanobeads (Miltenyi), and the Expamers technology (Juno Therapeutics, a BMS company, Seattle, Washington, USA) (Wang and Rivière 2016; Vormittag et al. 2018). The TransAct reagent by Miltenyi is a particularly attractive option because the TransAct nanobeads are biodegradable hence do not require elimination prior to formulation (Wang and Rivière 2016). In the case of the HSC-based therapies, the selection of the CD34+ stem cells is performed using the CD34+ reagent by Miltenyi which constitutes of anti-CD34+ monoclonal antibody fused to superparamagnetic iron dextran particles (microbeads) (Wang and Rivière 2017). Activation in the case of HSCs is required in order to re-start the cell cycle i.e. re-start of cell proliferation. To activate CD34+ cells, a cocktail of stem cell factor (SCF), Fms-like tyrosine kinase 3 ligand (Flt3-L), thrombopoietin (TPO) and interleukin 3 (IL-3) (Wang and Rivière 2017).

The second key difference between the T-cell-based and HSC-based gene-modified cell therapies relates to the transduction step. Whilst both T-cells and HSCs cells have been genetically modified with lentiviral and gamma-retroviral vectors, the scientific community learned that gamma-retroviral modification of HSCs can have tragic consequences on patients. HSCs, as opposed to T-cells, which were genetically modified with gamma-retroviral vectors were associated with insertional mutagenesis (Hacein-Bey-Abina et al. 2008; Scholler et al. 2012) causing blood cancers in paediatric clinical trial participants suffering from genetic disorders (Booth et al. 2016). Consequently, with the exception of the approved product, Strimvelis (Orchard Therapeutics), the HSC-based cell therapies typically employ lentiviral vectors nowadays. However, fears that insertional oncogenesis cannot be fully avoided with lentiviral vectors still exist and were recently triggered by safety concerns around the use of Zynteglo® (bluebird bio) (Brennan 2021; Kansteiner 2021). A critical quality attribute which is directly linked to the risk of insertional mutagenesis is the vector copy number (VCN). The VCN needs to be tightly controlled as an increased VCN (or insertions of vector per cell) may increase the risk of insertional mutagenesis. FDA recommends an integrated VCN of less than 5 copies per genome (Zhao et al. 2017).

A further difference between the two therapy types linked to the transduction step is the viral vector dose size required. The viral vector dose size typically employed in T-cell-based gene-modified cell therapies is much lower than that associated with the HSC-based gene-modified cell therapies. In terms of *ex vivo* HSC gene therapies, several publications pointed at likely LV dose sizes in the range of 1-500 x 10^9 TU/dose and a final LV concentration of 1-6 x 10^8 TU/ml **(Table 2.3)**. The justification for these large dose sizes is the very high multiplicity of infection (MOI) values (~100) as well as often the inclusion of a second transduction step due to the lower transducibility of CD34+ HSC cells when compared to T-cells (Sheridan 2011; Aiuti et al. 2013). In terms of CAR

T/TCR, there have been limited accounts available publicly regarding the exact LV dose size used in manufacturing apart from two reported accounts of 2 x 10^8 TU/dose (Blaeschke et al. 2018; Lock et al. 2017).

Table 2.3 Notable clinical trials utilising lentiviral vectors in *ex vivo* gene therapy applications.

Target	Indication	LV dose size range (TU)	Sponsor	Clinical trial no.
T-cells	DLBCL (CAR T)	ND	Novartis	NCT03630159
	ALL (CAR T)		Novartis	NCT03628053
	Solid tumour (CAR T)		Tmunity Therapeutics	NCT04025216
	ALL (TCR)		Fred Hutchinson Cancer Research Center	NCT03326921
	Solid tumours (TCR)		Adaptimmune	NCT03132922
CD34+ cells	Beta-thalassemia LentiGlobin BB305	10^{10} – 5 x10^{11} (Ribeil et al. 2017; Cavazzana-Calvo et al. 2010)	bluebird bio	NCT03207009
	Sickle cell disease LentiGlobin BB305		bluebird bio	NCT02140554
	Wiskott Aldrich syndrome	10^{10} – 10^{11} (Aiuti et al. 2013; Ferrua et al. 2019)	Orchard therapeutics	NCT01515462
	ADA-SCID	ND	Great Ormond Street Hospital for Children NHS Foundation Trust	NCT03765632
	X-SCID	10^9 – 10^{10} (Mamcarz et al. 2019)	St. Jude Children's Research Hospital	NCT01512888

ALL = acute lymphoblastic leukaemia; DLBCL = diffuse large B-cell lymphoma; ND = not disclosed, TU = transducing units.

The final key difference between the T-cell and the HSC-based gene-modified cell therapies relates to the cell culture step. The T-cell processes require the expansion of the T-cells to reach adequate numbers to deliver the therapeutic effect. T-cell expansion is typically performed either in static systems (i.e. G-rex, Wilson Wolf Inc., New Brighton,

Minnesota, USA) or rocking systems (e.g. Wave^{TM}, Cytiva, Marlborough, Massachusetts, USA). In terms of the starting number of T-cells and variable patient weights, the general approach is to always start with the same number of T- cells at the beginning of the core manufacturing process i.e. to perform transduction on a fixed number of T-cells. This has multiple advantages. Firstly, it enables the use of the same material quantity requirements for each batch, it provides a level of consistency across batches and it does not require any changes in expansion durations or DSP process parameters. On the other hand, the HSCs do not undergo an expansion step. Instead transduction can be performed either in culture bags such as the VueLife® (Saint-Gobain, Courbevoie, France) or within the CentriCult chamber of the CliniMACs Prodigy® system. Extended *ex vivo* culture of HSCs was found to be detrimental for the maintenance of stem cell properties which is essential in order to guarantee *in vivo* persistency and engraftment potential (Glimm et al. 2000; Naldini 2011; Wang and Riviere 2017). As a result, HSCs-based processes are much shorter than their correspondent T-cell processes i.e. 2-5 days as opposed to 1.5-3 weeks in case of T-cell processes (Gill and June 2015; Wang and Rivière 2016). Integrated and automated cell processing systems have been developed and employed with both CAR T-cell (Blaeschke et al. 2018) and HSC gene therapy manufacture (Adair et al. 2016). These will be discussed in **Section 2.2.3**.

There are advantages in cryopreserving autologous drug products when marketing a product at a global level. Whilst some approved CAR T products are shipped in a cryopreserved form (e.g. Kymriah ®), others are shipped fresh (e.g. Yescarta ®). In the case of the gene-modified HSCs, cryopreservation appears to be a less likely option since reduction in thawed HSCs engraftment potential had been reported (Watts and Linch 2016; Wang and Rivière 2017).

Given the finite resources companies have, developer companies need to strike the right balance between investing into speed to clinic, maximising reimbursement chances, building a strong CMC file and designing a suitable manufacturing strategy.

Since the cost of materials has been found to be one of the largest cost drivers for autologous CAR T-cell therapy manufacture, a key focus for companies should be decreasing materials cost whilst safeguarding product quality. An example avenue towards achieving this would be outsourcing viral vector produced using scalable processes.

On the other hand, the impact of the autologous nature of CAR T-cell therapies on COG/dose can be alleviated by minimising indirect costs (labour and facility) by decreasing manufacturing duration either by reducing or eliminating the expansion stage.

2.2.2 Processes associated with emerging products

Whilst autologous and viral vector-based *ex vivo* gene therapy products dominate the cell and gene therapy market, there are reimbursement concerns associated with the autologous nature of these products and safety concerns associated with the use of viral vectors. As a result, efforts have been dedicated to developing allogeneic approaches and non-viral vector platforms. However, none of these approaches is currently approved. This section describes key processes employing allogeneic and/or non-viral vector routes targeting cancers and Graft-versus-host-disease, previously mentioned in **Table 2.2** (**Section 2.1**). *Ex vivo* gene therapies for HIV utilising either patient's T-cells or CD34+ cells are described here also as examples of genome editing systems employing the use of a combination of non-viral and viral vectors.

Allogeneic viral vector approaches

Two types of allogeneic approaches of viral vector processes will be described herein i.e. a process for manufacturing allogeneic CAR T-cell therapies and a process for manufacturing allogeneic Graft-versus-Host-disease (GvHD) gene-modified cell therapies.

Firstly, allogeneic approaches have been developed for patients with persisting malignancy post-haematopoietic stem cell transplant (HSCT) whereby HSCT donor T cells (from whom the HSCs were harvested) are engineered to express CARs against tumour cells (Cruz et al. 2013; Kochenderfer et al. 2013; Brentjens and Curran 2012; Brudno et al. 2016). Cruz et al. (2013) describes a process whereby HSCT donor T-cells cultured with special types of donor-derived antigen presenting cells (APCs) that had been infected with Epstein-Barr virus, adenovirus and CMV. This process generates virus-specific T-cells (VSTs) which are then engineered to express an anti-CD19 CAR using a gamma-retroviral vector and expanded. Since Epstein-Barr virus, adenovirus and CMV are viruses which commonly cause severe infections in patients post-allogeneic HSCTs, these CAR-VSTs are theoretically capable to target and kill both virus infected cells and tumour cells presenting the CD19 antigen. However, this manufacturing process is quite lengthy taking minimum 5-6 weeks to complete. Another account of donor-derived anti-CD19 CAR T-cell therapy associated with a shorter process duration is presented by Kochenderfer et al. (2013) and Brudno et al. (2016). The 8 day CAR manufacturing process employed an alternative activation system to those mentioned so far in the thesis i.e. OKT-3 and IL-2 antibodies and used a gamma-retroviral vector.

Furthermore, genetically engineering HSCT donor T-cells with kill switches as a strategy to control GvHD almost reached the European market as Zalmoxis developed by MolMed had received conditional EMA approval in 2016 (de Wilde et al. 2018). Zalmoxis' 10 day

manufacturing process involved genetically engineering HSCT donor T-cells with a gamma-retroviral vector delivering a human herpes simplex virus thymidine kinase type 1 (HSVtk) suicide gene and a truncated form of the low affinity nerve-growth factor receptor (LNGFR) marker. This was administered 21 days post-HSCTs under multiple infusions according to recipient's reaction to these therapeutic cells (Ciceri et al. 2009). The NGFR marker was engineered into the T-cells in order to allow selection of transduced T-cells using magnetic immune-selection representing an example of post-modification selection strategy. If GvHD developed then ganciclovir, which selectively annihilates therapeutic cells, was administered. However, Zalmoxis was withdrawn in 2019 due to unfavourable results obtained in a Phase 3 clinical trial (Elsallab et al. 2020). On the other hand, another strategy was developed whereby T-cells are genetically engineered with a gamma-retroviral vector to express the Cas9 protein linked to a modified human FK-binding protein which can dimerise upon interaction with a small molecule drug (AP1903) (Di Stasi et al. 2011; Zhou et al. 2015). Dimerization of this protein construct leads to activation of the inducible caspase 9 (iCasp9) system which triggers T-cell apoptosis (Di Stasi et al. 2011). Besides, donor T-cells are also engineered to express a truncated CD19 antigen marker to enable CD19 positive cell selection using established magnetic immune-selection systems. According to Zhou et al. (2015), this strategy is superior to Zalmoxis because AP1903 is an otherwise inert small molecule as opposed to gancyclovir which is an antiviral medication and the *iC9* safety switch is less immunogenic than the *HSV-tk*–based suicide switch.

Autologous and Allogeneic non-viral vector approaches

The non-viral vector approaches had emerged as alternatives to the high cost and complexity associated with the production of viral vectors (Waehler et al. 2007). The key non-viral vector platforms developed to date are the transposone/transposase system (e.g.

Sleeping Beauty) and the mRNA electroporation of therapeutic genes (e.g. CARs) or genome editing tools (e.g. Zinc Fingers and CRISPR). A summary table listing all the vector types used in *ex vivo* gene therapy clinical trials as well as their advantages and disadvantages is shown below **(Table 2.4)**.

Table 2.4 Gene therapy vectors: advantages and disadvantages.

Vector	**Advantages**	**Disadvantages**
Lentiviral vector (LV)	• Safer than gamma-RV (at least in HSCs applications)	• Costly manufacturing system; • Risk of insertional mutagenesis; • Risk of replication competent virus generation; • Semi-random integration, variable VCN, heterogenous expression (MacLeod et al. 2017)
Gamma-Retroviral vector **(g-RV)**	• Producer cell lines in place • Less expensive than LV	• Higher risk of insertional mutagenesis than for LV (Hacein-Bey-Abina et al. 2008); • Risk of replication competent virus generation; • Semi-random integration, variable VCN, heterogenous expression (MacLeod et al. 2017)
Sleeping Beauty transposone/transposase (SBTT)	• Cheaper than VV; • No risk of replication competent viruses; • Potentially larger cargos than VV (up to 12kb); • Random genome-wide integration (Hudecek et al. 2017)	• Autointegration risk (Hudecek et al. 2017); remobilisation of the inserted transposon; • Some risk of insertional mutagenesis
mRNA transgene electroporation of therapeutic gene (transient expression)	• Cheaper than VV, short-lived - useful for solid tumour indications; • No obvious risk of insertional mutagenesis	• Hard to tune transgene expression in order to obtain therapeutic benefit
mRNA transgene electroporation of genome editing tools via mRNA electroporation (potentially stable expression)	• Cheaper than VV' • Targeted gene manipulation, • No obvious risk of insertional mutagenesis	• Reliance on error prone endogeneous DNA repair systems

aAPC = artificial antigen presenting cells; VV = viral vector; HSC = haematopoietic and progenitor stem cells.

2.2.3 *Ex vivo* gene therapy analytics & QP considerations

Gene therapy products need to be safe, efficacious (potent), pure and, in order to ensure that they are, their critical quality attributes (CQAs) need to be met. CQAs are derived from the quality target product profile and are met if all the validated analytical assays testing the chemical, biological or microbiological product properties output values within the target pre-established limits, range or distribution.

As such, both in process control and release testing are employed. While the in process control strategy tends to be highly specific for each product (i.e. cell therapy versus viral vector versus pDNA), the release testing strategy tends to be similar. Generally, the suite of release testing includes sterility, mycoplasma, endotoxin, process and product-related impurities, quantification and functional assays. Whilst sterility testing is performed using traditional techniques (e.g. microbial culture), mycoplasma testing is nowadays widely performed using PCR-based assays (De Rooij et al. 2019). Endotoxin testing is performed typically using a Limulus Amebocyte Lysate (LAL) Assay (Lock et al. 2010).

For autologous *ex vivo* gene therapies, in process control (IPC) is particularly critical due to their patient-specific nature. As such, IPC is used to fine-tune the critical process parameters in order to ensure that the quality target product profile is met for each patient's cellular material. The most used measurement is cell counting assessed using flow cytometry (e.g. fluorescent activated cell sorting - FACS analysis).

The release testing of autologous *ex vivo* gene therapies consists of sterility, mycoplasma, endotoxin and purity testing (e.g. FACs-based i.e. % CD3+ T-cells, % CAR T-cells, residual tumour burden, %CD34+, residual beads). For viral vector-based *ex vivo* gene therapies only, the release testing requires the measurements of transgene copy insertions per cell, vector copy number (VCN) and replication competent lentivirus (RCL). Accounts of release testing typically performed for CAR T-cell therapies and HSC gene

therapies are provided in Wang and Rivière (2016) and Mukherjee et al. (2021) and Wang and Rivière (2017), respectively.

Given the complexities associated with the autologous nature of the majority of *ex vivo* gene therapies, described in **Chapter 1**, the product release aspects also require consideration. Currently in the EU and UK, the qualified person (QP) reviews all testing results and the relevant quality data to ensures that the product quality is satisfactory prior to formally releasing it for use in the case of every individual batch, meaning, for every single patient. Each batch is associated with a significant documentation volume which requires reviewing and it can take a QP up to 3-5 days in order to release one batch (the formal release is done in person typically).

Given the large effort required, especially in a commercial setting, and the time contribution to the product turnaround time also referred to as the needle-to-needle time (time from apheresis, to manufacturing, to product release, to patient administration, including transportation), alternative models for product release are needed. A route towards decreasing product release time and QP effort for autologous products could be establishing centralised QP hubs where batch and testing data would be compiled and processed automatically, and computer programs would be employed to flag any quality issues i.e. determine the acceptability of testing results in an automated fashion. To get closer to such a vision, automated manufacturing (rather than semi-automated) equipment and real-time monitoring would be required. Furthermore, such vision would still need some level of QP oversight and QP final signature but would significantly ease the product release process (Bicudo et al. 2021).

2.2.4 Modular versus Integrated manufacture

There have been significant technological advances in the field of cell therapy manufacture over the last 5 years. New technologies were introduced and significant progress has been achieved to close and automate processes.

In the context of autologous therapies closed processing decreases the risk of cross-contamination obviating the need to operate in biosafety cabinets in grade B cleanrooms or isolators in grade C cleanrooms. Closing and automating autologous cell therapies minimises process variability which, in the context of dealing with highly variable starting patient material, is highly desirable. Two main closed-processing approaches emerged: the modular (discrete) approach and the integrated (end-to-end) approach (Morrissey et al. 2017; Ball et al. 2018). The modular approach involves employing equipment systems specific for each processing step forming a processing chain while the integrated approach accommodates the execution of all processing steps within one equipment system. An economic assessment was published comparing the two approaches which predicted a cost of goods advantage of modular (or semi-continuous) over integrated manufacturing based on better resource utilisation with the former approach (Lopes et al. 2020). An assessment of the advantages and disadvantages of modular and integrated approaches is provided in **Table 2.5**.

Table 2.5 Modular versus integrated manufacturing solutions for autologous *ex vivo* gene therapies: advantages and disadvantages.

Approach	Advantages	Disadvantages
Modular (discrete)	• More batches can be manufactured per unit time with one processing chain • More flexible scheduling i.e. higher resource utilisation may be achieved • Potentially lower capital costs if the cost of the processing chain does not exceed that of the integrated system • Batch may be rescued if downstream equipment stops working by employing back-up equipment • Allows gradual translation of the manual unit operation to the automated unit operation • Malleable to implementing allogeneic approaches	• Different equipment systems are associated with different tubing sets and hardware costs and hence consumable cost and capital costs could exceed those achieved with the integrated system • Multiple qualification and validation activities – may need more resources; involves more paperwork • Multiple change-over points from one kit to another which could lead to potentially more opportunities for cross contamination; may require temporal segregation which could hinder lean operations • Training required on multiple systems; systems are developed by different suppliers and have differences in software and manipulations required • Since different systems are involved, data integration with a central system (eBMR, ePQS, MES) may be more challenging to implement. • More challenging to ensure traceability
Integrated (end-to-end)	• Lower risk of cross-contamination • Two major operations only: loading and harvesting • Easier to keep track of batch number and records as each equipment unit is dedicated to one batch (easier traceability) • One qualification and validation activity • Personnel training only one piece of equipment • Potentially easier to integrate with a central system (eBMR, ePQS, MES)	• Cannot stagger batches without additional equipment being brought in i.e. one equipment unit per batch • Higher initial CAPEX and lower flexibility • Heavy reliance on one supplier • If the system breaks, the batch is likely jeopardised • Not compatible with allogeneic approaches

eBMR = electronic batch manufacturing records; ePQS = electronic pharmaceutical quality system, MES = manufacturing execution system.

In terms of the modular approach, multiple systems were developed for cell concentration and buffer exchange steps, activation and selection as well as for the cell culture step. With regards to the cell concentration and buffer exchange steps, technologies based on

centrifugation (e.g. Sefia™, Cytiva), counterflow centrifugation (e.g. Elutra®, Terumo BCT; Rotea ™, Thermo Fisher Scientific; ksep®, Sartorius, Göttingen, Germany), membrane filtration (e.g. Lovo®, Fresenius Kabi, Bad Homburg, Germany) and acoustics (e.g. Ekko™, FloDesign Sonics, Wilbraham, Massachusetts, USA) were developed (Li et al. 2021). Furthermore, selection and activation steps can be performed in a closed fashion and key technology players for these steps are the CliniMACs Plus and Prodigy® systems (Miltenyi) employing magnetic beads (Vormittag et al. 2018). On the other hand, acoustic technology is gaining traction in the field of non-paramagnetic selection with MilliporeSigma developing the Acoustic Affinity Cell Sorter (AACS) (Tostoes et al. 2020). With regards to the cell culture step, static (e.g. G-rex), rocking technologies (e.g. Wave™, Xuri™, Cytiva; Biostat® RM wave-mixed bioreactor, Sartorius) and hollow fibre technologies (e.g. Quantum®, Terumo BCT) were developed (Wu et al. 2018; Baudequin et al. 2021). For non-viral vector processes, closed electroporation devices have been developed such as MaxCyte GTx™ (MaxCyte, Gaithersburg, Maryland, USA) and 4D-Nucleofector™ LV Unit (Lonza, Basel, Switzerland). It is likely that at least some of the approved products to date (e.g. Kymriah, Novartis) are manufactured using a modular approach (Tyagarajan et al. 2020). An account of CAR T-cell therapy modular manufacturing with software integration of closed unit operations is provided by Weist et al. (2020) while Jung et al. (2018) discusses hardware module integration using a plug-and-play approach. In the context of allogeneic approaches, the modular approach, following the individual unit operations framework, would suit best. In such case, the development of large scale stirred-tank bioreactors (STR) is paving the way towards industrialising CAR T-cell therapy manufacture (Costariol et al. 2020; Rotondi et al. 2019).

In terms of the integrated (end-to-end) approach, two key systems have been developed that are suitable for autologous *ex vivo* gene therapy manufacture: the Prodigy® (Mock

et al. 2016) and the Cocoon® (Lonza) (Levinson et al. 2018). These are capable to perform wash, selection, activation, transduction and cell culture steps with one equipment unit only in a fully-closed fashion, and should, at least in theory, make manufacturing within cleanroom obsolete (Moutsatsou et al. 2019). The Prodigy® system has been introduced slightly before the Cocoon® system and has already been assessed in the manufacture of multiple engineering and clinical batches (Mock et al. 2016; Zhu et al. 2018; Zhang et al. 2018; Aleksandrova et al. 2019; Ardeshna et al. 2018; Priesner et al. 2016; Silva et al. 2020; Jackson et al. 2020a; Lock et al. 2017; Stroncek et al. 2016; Adair et al. 2016). The Prodigy® system was approved for the manufacture of the now withdrawn Zalmoxis product, manufactured by MolMed for graft-versus-host disease (Moutsatsou et al. 2019). Whilst there is a smaller number of reports of utilising the Cocoon® system, the collaboration between Lonza and the Israeli Sheba hospital has led to at least one patient receiving CAR T-cell therapy manufacturing using this system as part of a clinical trial (Raper 2020). In terms of similarities, the price of hardware and consumable associated with the two systems are in the same ballpark (~$200,000/system, ~$3,000/consumable set) and the proliferation chambers have similar working volumes (~250 ml). A further similarity is the ability of both systems to perform electroporation for gene transfer. The Prodigy® system is both compatible with an inline electroporation unit and Miltenyi is also working on releasing a new Prodigy system with incorporated electroporation capability (Miltenyi 2021; Alzubi et al. 2021). The Cocoon® system, on the other hand, is compatible to the 4D-Nucleofector™ LV Unit (Lonza) (Neo et al. 2020). In terms of contrasts, there are at least three key differences between the two. Firstly, the engineering principle behind the concentration function of the Prodigy® system is centrifugation (Mock et al. 2016), whereas in the case of the Cocoon®, this relies on settling (Shi et al. 2019). Secondly, the Cocoon® system allows efficient scale-out by enabling the arrangement of multiple systems in tree-like structure of 6/8-10 units

per 1 m^2 floor area (Levinson et al. 2018; Ferreira 2018). Thirdly, the Cocoon® system was reported to be able to allow the culture of both adherent and suspension-adapted cells, whilst the Prodigy® system can be used with suspension cell cultures only (Levinson et al. 2018; Moutsatsou et al. 2019). Other platforms are in the process of being developed such as the Autostem project (Ran et al. 2020; Moutsatsou et al. 2019). **Table 2.6** presents a summary of the key technologies options employed for each unit operation for CAR T-cell therapy manufacture.

Table 2.6 Summary of technologies used in the manufacture of CAR T-cell therapies.

Unit operation	Technologies
Collection	• Leukapheresis (Centrifugation) Haemonetics systems; COBE Spectra MCN, COBE Spectra Optia MNC, Spectra Optia IDL and Cardian Trima Accel (Terumo BCT); Amicus (Fresenius Kabi); Alyx (Fresenius Kabi)
Isolation / Enrichment (wash / concentration)	• Centrifugation-based e.g. Haemonetics Cell Saver5+, Sepax™ and Sefia™ (Cytiva); COBE 2991, CARR Unifuge Pilot (Pneumatic Scale Angelus, Stow, Ohio, USA); CliniMACS Prodigy (Miltenyi Biotec) • Counterflow centrifugation-based e.g. Rotea™ (Thermo Fischer Scientific), Elutra® (Terumo BCT); kSep 400, kSep 6000 (Sartorius) • Membrane filtration-based e.g. Lovo (Fresenius Kabi), XCell ATF (Repligen, Waltham, Massachusetts, USA) • Acoustic-based e.g. Ekko™ (FloDesign Sonics)
T-cell subsets selection / isolation	• Immunophenotype-based techniques using the following equipment o CliniMACS PLUS® (Miltenyi Biotec); CliniMACS Prodigy® (Miltenyi Biotec); CTS Dynamag (Thermo Fisher Scientific) • Buoyancy-based separation (Buoyancy-Activated Cells Separation (BACS, by ThermoGenesis, Rancho Cordova, California, USA)
Activation	• Immunophenotype-based techniques using the following reagents o Magnetic beads e.g. CTS Dynabeads CD3/CD28 (Thermo Fisher Scientific); MACS GMP ExpAct Treg beads (Miltenyi Biotec); EasySep (GE Heathcare, Chicago, Illinois, USA and STEMCELL Technologies, Vancouver, Canada) o Non-magnetic beads e.g. MACS GMP TransAct CD3/CD28 beads (biodegradable nanobeads, Miltenyi); Immunocult T-cell activator (STEMCELL Technologies); Expamers (Juno Therapeutics) • Cell lines e.g. culture with APC or aAPCs (e.g. K562 cell line) • Antibodies e.g. culture with soluble anti-CD3 mAbs and IL-2
Modification	• Viral vectors: Lentiviral vectors; gamma-retroviral vectors. • Non-viral vectors: mRNA electroporation (transient expression); Sleeping Beauty transposone/transposase pDNA electroporation (stable expression); mRNA delivery of gene editing tools • Electroporation devices: MaxCyte® GTx (MaxCyte), 4D-Nucleofector™ LV (Lonza), Miltenyi electroporator
Culture	• Rocking motion bioreactor e.g. Xuri/WAVE bioreactor (Cytiva); SmartRocker (Finesse, Thermo Fisher Scientific); Allegro (Pall Corporation, Port Washington, New York, USA); Biostat RM (Sartorius) with Flexsafe bags (Sartorius) or Cellbags (Cytiva) • Gas-permeable bags: VueLife (Saint Gobain, Courbevoie, France), PermaLife (OriGen Biomedical, Austin, Texas, USA) • Gas permeable vessel: G-rex bioreactor (Wilson Wolf) • Automated systems: CliniMACS Prodigy (Miltenyi Biotec); Cocoon™ (Lonza); Quantum (Terumo BCT)
Formulation	If DMSO is required: • Pneumatic mixing, universal cooling plate: SmartMax (Cytiva)
Storage	• Cryopreservation using controlled rate freezers
Thaw	• For vial thawing: VIA Thaw SC2 (Cytiva); Biocision ThawSTAR (BioLife Solutions, Bothell, Washington, USA) • For bag thawing: VIA Thaw CB1000 (Asymptote, New York, New York, USA); Sahara system (Sarstedt, Newton, North Carolina, USA)

2.3 Vector manufacturing processes

This section will address first the manufacture of two main viral vectors used in gene therapy applications. Secondly, it will discuss the manufacture of non-viral vectors such as the plasmid DNA (pDNA).

2.3.1 Viral vector considerations

The key viral vectors employed in gene therapy applications are the lentiviral vector (LV) and the adeno-associated virus vector (AAV). These have different characteristics and applications. **Table 2.7** provides a summary of the differences between these two vectors. In summary, the LV, a relatively unstable ssRNA-virus, is larger than the AAV, a relatively stable ssDNA-virus, it is enveloped and it is associated with a larger transgene cargo when compared to the AAV particle. Some of these differences will be discussed later on when processing details will be provided.

Table 2.7 Key characteristics of lentiviral and adeno-associated virus vector.

Viral Vector	**LV**	**AAV**
Family	Retroviridae	Parvoviridae
Genus	Lentivirus	Dependoparvovirus
Vector biology	Enveloped	Not enveloped
Size (nm)	80-100	20-26
Genome type	Single-stranded RNA (ssRNA)	Single-stranded DNA (ssDNA)
Transgene size (kb)	8	4.7
Infectivity potential	Both dividing and non-dividing cells	Both dividing and non-dividing cells
Genome integration potential	Yes	Yes
Modality	*ex vivo* and *in vivo*	*in vivo*
Tissues targeted	*ex vivo*: • T-cells (Blaeschke et al. 2018; Rapoport et al. 2015; Porter et al. 2015) • Haematopoietic stem cells (Aiuti et al. 2009b; Booth et al. 2016) *in vivo*: • Eye (Zallocchi et al. 2014) • Brain (Palfi et al. 2018) • Respiratory tissue (Alton et al. 2017; Alton et al. 2020) • Liver (Milani et al. 2019)	• Eye (Kumar et al. 2016) • Brain (Kumar et al. 2016) • Respiratory tissue (Katz et al. 2019) • Liver (Pasi et al. 2020) e.g. AAV8 & 9 • Motor neurons (Stevens et al. 2020) • Skeletal muscle (Bryant et al. 2013) e.g. AAV8 & 9 • Kidney (Takeda et al. 2004)e.g. AAV2

Diseases targeted and dose sizes	*ex vivo*:
	• Blood cancers (10^8 – $2x10^9$ TU (Blaeschke et al. 2018; Rapoport et al. 2015))
	• Genetic diseases (10^9 – $2x10^{11}$ TU)
	  ○ Primary immunodefficiencies (Aiuti et al. 2009a; Aiuti et al. 2013; Mamcarz et al. 2019)
	  ○ Haemoglobin disorders (Ribeil et al. 2017; Cavazzana-Calvo et al. 2010)
	  ○ Inherited neurological disorders (ALD, MLD) (Biffi et al. 2013; Cartier et al. 2009)
	in vivo:
	• Eye disorders ($8x10^5$ – $5x10^6$ TU; Zallocchi et al. 2014, Campochiaro et al. 2017, Kong et al. 2008)
	• Parkinson's disease ($2x10^7$ – 10^8 TU, Palfi et al. 2018))
	• Cystic fibrosis (10^8 to > 10^{11} TU, Alton et al. 2020)
		• Inherited neurological disorders (e.g. AADC, $2x10^{11}$ vg; Kumar et al. 2016)
		• Inherited retinal disease (e.g. Luxturna, Sparks Therapeutics for retinal dystrophy $1.5x10^{11}$ vg/eye; FDA 2017b)
		• Haemophilia (2-6 x 10^{13} vg/kg; Pasi et al. 2020)
		• SMA (e.g. Zolgensma, Novartis Gene Therapies $3x10^{14}$ – $1.5x10^{15}$ vg; Stevens et al. 2020)
		• Lipoprotein lipase deficiency (LPLD) (e.g. Glybera, Uniqure: 10^{12} gc/kg; Bryant et al. 2013)

ALD = Adrenoleukodystrophy; MLD = metachromatic leukodystrophy; AADC = Aromatic l-amino acid decarboxylase deficiency; SMA = Spinal muscular atrophy; gc = genome copies; vg = viral genomes; TU = transducing units.

Lentiviruses, a genus of the Retroviridae family, are able to stably integrate the gene of interest in both dividing and non-dividing cells in contrast to gamma-retroviral vectors (Marquez Loza et al. 2019; Cockrell and Kafri 2007; Quinonez and Sutton 2002; Hematti et al. 2004; Montini et al. 2009; Abina et al. 2015). Lentiviruses are more complex than retroviruses from the genomic organisation point of view (Escors and Breckpot 2010). However, given that the former exhibits similar efficiency of gene transfer, long term and high level of transgene expression as retroviruses (g-RV) and are known to be associated with lower risk of insertional mutagenesis, recombinant lentiviruses are used in numerous clinical trials. LV are known to have a lower insertional mutagenesis induction rate compared to g-RV probably due to the fact that LV preferentially integrates in active transcriptional loci rather than near to the start sites of active genes as g-RV tend to do (Modlich et al. 2009; Cattoglio et al. 2010). Key types of lentiviruses are HIV-1 (Human immunodeficiency virus 1), SIV (Simian immunodeficiency virus), FIV (Feline immunodeficiency virus), EIAV (Equine infectious anaemia virus) and Visna. These are enveloped viruses, spherical, with a diameter of 80-100 nm which are secreted in the culture media (Wagner et al. 2009). The most utilised type of lentiviruses is HIV-1. LV is likely to become unstable in culture. The half-life of the LV particles is of ~3-18 hours (Watson et al. 2002; Croyle et al. 2004) at 37°C and that this increases with storage at 4°C (Higashikawa and Chang 2001a). This was attributed to loss of reverse transcriptase activity at these temperatures (Carmo et al. 2009). Latest generation of LV is known as 'self-inactivating' or SIN vectors which are prevented from generating full-length vector RNA in target cells by deleting a vector sequence i.e. the enhancer promoter sequences of the LTR (long terminal repeats) on the transfer plasmid (Zufferey et al. 1998). Current LV generation includes the woodchuck hepatitis virus posttranscriptional regulatory element (WPRE) on the transfer plasmid which showed enhanced transgene expression (Zufferey et al. 1999).

The adeno-associated virus (AAV), a genus from the Parvoviridae family, is a icosahedral protein capsid DNA single-stranded virus which was discovered as a contaminant of adenovirus preparations in 1965 (Atchison et al. 1965). This can infect both dividing and non-dividing cells and has genome integration potential, but typically resides in an episomal state after transduction, rarely integrating into the genomic DNA (Venditti 2021). Production of recombinant AAV (rAAV) was initiated about 37 years ago (Aponte-Ubillus et al. 2018) There are at least 12 natural serotypes associated to different tissue types (Gao et al. 2004). The serotype also dictates whether the AAV is secreted in the culture media or not during processing. Many serotypes other than AAV2 and AAV5 are known to be secreted in the cultured media to various extent which was found to depend on expression conditions (pH/serum presence) and time post-transfection (Adams et al. 2020). Several modifications were performed to maximise cargo capacity and improve manufacturability (Bulcha et al. 2021) .

In terms of modalities approached with these viral vectors, the AAV is typically used *in vivo* whereas LV is used both *in vivo* and *ex vivo,* however it is used predominantly in *ex vivo* applications (Masri et al. 2019). In terms of *in vivo* applications, the target tissues for gene delivery for both vectors are typically the eye, brain, and respiratory tissue while motor neurons and skeletal muscles tend to be targeted with AAV only. Only AAV was used in *in vivo* products that gained marketing approval so far (i.e. Luxturna® and Zolgensma®). AAV is employed in the treatment of inherited neurological disorders, inherited retinal disease, haemophilia, SMA, lipoprotein lipase deficiency. As *ex vivo* gene therapy vectors, LVs have been employed in the treatment of blood cancers and solid tumours by engineering T-cells to express chimeric antigen receptors (CAR) or enhanced T-cell receptors (TCR) (Allen et al. 2017; Casucci and Bondanza 2011; Fesnak et al. 2016a; Fesnak et al. 2017a; Fesnak et al. 2016b; Garfall et al. 2015; Gill and June 2015; Holzinger et al. 2016; Rapoport et al. 2015), enabling them to target and kill tumour

cells based on recognition of tumour-associated antigens (TAAs) such as CD19 and NY-ESO (Rosenberg 2012b; Fesnak et al. 2016b; Hartmann et al. 2017). In the context of HSC gene therapy, LV is employed to insert either absent or mutated genes into CD34+ cells' genomes in order to tackle rare and monogenic disorders (e.g. ADA-SCID, WAS, MLD, X-ALD, X-SCID) and haemoglobinopathies (Aiuti et al. 2013; Aiuti et al. 2009a; Biffi et al. 2013; Cavazzana et al. 2017; Rai and Malik 2016; Ribeil et al. 2017; Rio et al. 2017; Wang and Riviere 2017; Zonari et al. 2017; Cartier et al. 2009; Mamcarz et al. 2019; Greene et al. 2012; Cavazzana-Calvo et al. 2010). As *in vivo* gene therapy vectors, LVs are being clinically tested as a treatment for cystic fibrosis, macular degeneration and Parkinson's disease. Typical dose sizes for these therapies are shown in **Table 2.7.**

2.3.1.1 Viral vector analytics

A high level description of quality control for *ex vivo* gene therapies is provided in **Section 2.2.3.** This section provides more information about the release testing of viral vectors in terms of process and product-related impurity testing and quantification assays.

Viral vector process-related impurities such as residual endonuclease, pDNA and genomic DNA are quantified using ELISA-based methods for endonuclease and PCR-based methods, respectively for DNA.

In terms of product-related impurities, both AAV and LV preparations can be associated with product-related impurities which can compromise their quality.

This issue is more acute in the case of AAV where the key product-related impurity is represented by empty capsids. While some level of empty capsids is thought to aid in the therapeutic effect of AAV-based gene therapies, residual empty capsids may trigger a capsid specific T-cell response, thus posing a significant risk to patients' safety (Qu et al. 2015). Consequently, process flowsheets which remove these impurities have been established and analytical approaches have been developed to robustly measure the

empty-full ratio, representing a critical release test for AAV. This can be performed using a range of orthogonal methods. These are: analytical ultracentrifugation, analytical anion-exchange chromatography and HPLC-based methods. Transmission electron microscopy, UV absorbance at 260 and 280 nm and mass spectrometry can also help complete the picture (Adams et al. 2020).

In the case of LV, a potentially dangerous product-related impurity is represented by LV particles which have the ability to replicate i.e. replication-competent lentiviruses. The transduction of patients' cells with replication-competent retroviruses had led to catastrophic insertional oncogenesis events causing cancers as documented in Booth et al. 2016. Consequently, RCL testing is a critical test that needs to be performed by all LV manufacturers as part of release testing. This is a laborious and expensive test which can take up to a month to be completed. On the other hand, replication-competent AAV testing is not typically required, although concerns around integration safety of AAV vectors remain (Venditti 2021).

Quantification of viral vectors is done typically using viral genome titration employing PCR-based methods as well as capsid quantification (for AAV) or p24 quantification (LV) employing ELISAs.

In terms of viral genome quantification, droplet digital PCR (ddPCR) has been recently developed. This is superior to the quantitative PCR (qPCR) methods since it is less laborious and it does not require a reference standard (Clarner et al. 2021). This uses microfluidics as well as probe-based qPCR technology and has been used to deliver absolute quantification of nucleic acids for the titration of LV (Transfiguracion et al. 2020) and AAV (Clarner et al. 2021). In the case of LV quantification, p24 ELISA is performed alongside functional assays e.g. transducing a known number of a relevant type of cells and analysing the transgene expression thus determining the number of

transducing units. The quality of the LV preparation can be assessed by comparing the mass of p24 (representing a measure of both functional and non-functional virus) to the number of transducing units (functional virus) (Perry and Rayat 2021).

In the context of LV production, the current analytical techniques are known to be highly variable (Masri et al. 2019), industry quoting at best ±30% variability in titre measurements. Segura et al. (2013) presents an exhaustive list of quality assessment tools for proving CQAs for clinical-grade LV and Mccarron et al. (2016) signals the lack of international standards for LV products. As a result, it is challenging to build a fair comparison between flowsheets and this flags the acute need for standardisation of LV titration methods (Zhao et al. 2017; McCarron et al. 2016; Masri et al. 2019). Aiuti et al. (2013), Biffi 2013 et al. (2013) and Ausubel et al. (2012) present LV batch specifications details.

In the context of AAV production, whilst titre measurements tend to be slightly less variable when compared to LV, challenges still remain. An account for quality control of AAV products is provided in Wright (2021).

2.3.2 Viral vector manufacturing processes

Limited capacity and high costs associated with viral vectors garnered much attention particularly in recent years (Kolata 2017). Some of the contributing reasons are the limited scalability achieved with traditional adherent cell culture technologies, the modest process yields achieved with existing downstream processing (DSP) technologies, the process variability, as well as the limited and costly supply of cGMP-grade plasmid DNA (pDNA) used for transient transfection (Masri et al. 2019; Merten et al. 2016).

The following sections will discuss the cell culture technologies used in viral vector manufacture, the expression systems used i.e. the transient transfection system and the producer cell line systems, and the downstream processing considerations.

2.3.2.1 Cell culture technologies

The traditional cell culture approach of viral vectors is based on the adherent culture of HEK293(T) cell lines in multi-layer vessels such as cell factories (Nunc Cell Factory™, Thermo Fisher Scientific) (Allay et al. 2011; Merten et al. 2016; Merten et al. 2014b; Merten 2016). However, typically less than 100 L is harvested per batch (Miskin 2015) via multiple harvests; this may only yield 10s of LV doses for a CAR T-like therapy or less for higher dose size therapies. Other adherent manufacturing platforms have been used to generate cGMP-grade LV and AAV. Sheu et al. (2015) describe a hollow fibre bioreactor (Quantum™, Terumo BCT), run in perfusion mode which was used to generate LV using a transient transfection system. Also, Valkama et al. (2018) and Leinonen et al. (2019) used a fixed bed bioreactor, namely iCELLis® (Pall Corporation) that can be run in perfusion mode to manufacture LV. Moreover, Legmann et al., (2020) described the manufacture of AAV using the iCELLis bioreactor. Another fixed bed bioreactors was developed recently and was trialled successfully in both viral vectors' manufacture i.e. scale-X™ system (Univercells, Charleroi, Belgium) (Leinonen et al. 2020; Lesch et al. 2021). Yet another fixed bed bioreactor system development was recently announced by Corning (New York, US) i.e. the Ascent platform (Todd Upton 2021). Greene et al. (2012) describe the use of microcarriers (Fibra-Cel® microcarrier disks, Eppendorf, Hamburg, Germany) in a 50 L rocking motion bioreactor (Wave™, Cytiva) run in repeat batch mode for the manufacturing of SIN-LV for a SCID-X1 clinical trial with a stable producer cell line. On the other hand, suspension processes for delivering LV have also been developed. Organisations such as Genethon, Oxford BioMedica, Theravectys, bluebird bio and others announced development of LV manufacturing using serum-free suspension cultures and transient transfection (Marceau and Gasmi 2019; Miskin 2016; Zemmar et al. 2015; bio 2016; Bauler et al. 2020). Manufacturers such as Oxford Biomedica and others have successfully scaled their suspension processes up to 200 L

scale (Miskin 2016). For example, and according to the same source, this process requires about 21 days of upstream processing including inoculum build-up, transient transfection at day 22 and downstream processing for two subsequent days. Bluebird bio, on the other hand, has claimed the development of a stable producer cell line based on the 293F cell line able to produce BB305 LV in suspension, serum free culture (Slauson et al. 2016). Furthermore, AAV manufacture is also known to be done in large scale suspension cultures utilising transient transfection (Chahal et al. 2014; Grieger et al. 2016; Collaud et al. 2019).

As mentioned previously, it is known that LV half-life at 37°C is ~3-18 hours (Watson et al. 2002; Croyle et al. 2004) and that this increases with storage at 4°C (Higashikawa and Chang 2001a). Consequently, this impacts on the manner in which cell culture is carried out as well as the length of DSP. For example, multiple product collections (also known as repeat batch mode), are commonly implemented in LV processing due to the low stability of lentiviruses. This can be implemented relatively straightforwardly when using adherent cell culture systems such as the multilayer flasks or the fixed bed bioreactors.

2.3.2.2 Transient transfection

Large scale transient transfection requires large quantities of costly cGMP-manufactured pDNA and transfection reagents, and poses constraints on production scale, as well as on process optimisation (Merten et al. 2016; McCarron et al. 2016; Ferreira et al. 2020; Chen et al. 2020). Furthermore, it is associated with batch-to-batch variability but a lower risk of recombination potential between plasmid DNA components that could generate replication competent viruses (Ferreira et al. 2020; Merten et al. 2014b). Transient transfection of HEK293 and HEK293T cell lines is commonly employed in the manufacture of viral vectors and is performed using multiple pDNA vectors carrying the gene of interest as well as key structural and functional vector genes (Merten et al. 2014b).

Research and clinical-grade viral vector production relies on the multi-plasmid transient transfection of adherent or suspension cultured human embryonic kidney cells HEK293 or HEK293T (293T) cell line (Cockrell, 2007; Segura, 2013). The 293T cell line is derived from HEK293 which was initially employed in the production of LV because they are of human origin, have a proven safety record for the generation of retroviral vectors and are relatively easy to transfect (Ansorge, 2010; Segura, 2007). Optimised transfection requires selection of the appropriate transfection agent adding the correct ratio between transfection agent and plasmid DNA as well as the correct ratio between plasmids required for triggering vector assembly and release (Merten, 2014; Ansorge, 2010). Transfection reagents that have been used historically are: calcium phosphate ($CaPO_4$), lipid-based approaches, polyethylenimine (PEI) and flow electroporation (Segura et al. 2013). The $CaPO_4$ method requires FBS addition to the media and high plasmid DNA mass, exerting a notable toxicity to the cells and high sensitivity to pH. On the other hand, PEI represents an alternative transfection agent that does not require FBS addition to the media, is associated with lower pH sensitivity and lower cytotoxicity than $CaPO_4$ (Merten et al. 2016).

For LV vectors, 2-4 pDNAs are required consisting of the gene of interest vector and the genes encoding structural-based proteins (e.g. gag-pol), regulator proteins (e.g. rev) and envelope proteins (e.g. VSV-g). This is typical of a 3rd generation SIN LV vector created based on the split genome conditional packaging system so as to so as to reduce the risk of replication-competent lentivirus generation (Dull et al. 1998; Merten et al. 2016). On the other hand, for AAV, a virus-free expression system typically requiring 2-3 plasmids carrying the transgene and the packaging *rep/cap* and helper virus auxiliary genes, is the most commonly used platform (Keeler and Flotte 2019). Such virus-free system and the alteration of homologous sequences present in both vector and helper plasmids constitute a strategy to mitigate against the risk of replication-competent AAV (rc-AAV) generation

(Aponte-Ubillus et al. 2018). Typical total plasmid quantities used in transient transfection range between 1-2.5 µg added per million cells. GMP-manufactured pDNA prices per unit mass can vary immensely based on the plasmid production process performance in terms of titre and process yield. Thus, small scale un-optimised processes could be associated with costs per gram in the order of $100,000's/g, whereas large-scale fairly well performing processes could be associated with costs per gram in the order of $50,000/g or less. Since relatively large pDNA quantities may be required per batch, the pDNA percentage cost contribution to a 2,000L viral vector batch cost is expected to be approximately 30% (**Chapter 5**, Comisel et al**.** (2021)) and this is quantified further in the present work. A further implication of the reliance on pDNA and transfection reagent is the need to maintain a continuous and robust supply of these materials throughout the product lifetime. Transient transfection has also been reported to be problematic to implement at thousand litre scales due to challenges around achieving timely preparation of effective polyplexes (Masri et al. 2019; Ansorge 2010) and event-free addition of large volumes of transfection mixtures to cell culture volumes. Moreover, transient transfection imposes limitations on upstream process conditions which hinder process optimisation (Chen et al. 2020). On the other hand, it is associated with shorter development timelines compared to developing alternative expression systems such as packaging or stable producer cell lines (Bussow 2015).

2.3.2.3 Packaging cell lines

Efforts are undertaken to establish packaging and virus-producing cell lines (PCL and VPCL) in order to decrease the reliability on pDNA, ease the purification process and decrease the risk of recombination between transfected plasmids (Segura et al. 2013).

Packaging cell lines represent cell lines engineered to express some or all viral gene components apart from the gene of interest (Ansorge et al. 2010). Whilst this system requires the transient transfection of a reduced number of plasmids to initiate viral vector

production, it does not obviate the need for cGMP-manufactured pDNA supply. Packaging cell lines comprising helper virus genes (e.g. HEK293) have been successfully implemented for AAV production (Keeler and Flotte 2019), however packaging cell lines for LV production have historically proven to be more challenging to develop (Sanber et al. 2015; Ansorge et al. 2010; Merten et al. 2016).

2.3.2.4 Stable producer cell lines

Stable producer cell lines (SPCLs), as alternative systems to transient transfection for viral vector production, have all viral gene components including the transgene incorporated into their genetic package, hence do not require any pDNA addition. SPCLs represent the most common system for recombinant protein production, and, given the manufacturing similarities between viral vector and recombinant protein production, it is expected that SPCLs will become the future workhouse for viral vector production (Keeler and Flotte 2019; Merten et al. 2016). The advantages of SPCL systems include lower raw material costs due to removal of pDNA, improved process robustness and greater potential for optimisation when compared to transient transfection (McCarron et al. 2016; Sanber et al. 2015; Ferreira et al. 2020; Manceur et al. 2017; Forsberg N. 2018). Yet, SPCLs have been historically associated with lengthy cell line development campaigns as well as risks of transcriptional instability resulting in productivity losses over time (Chen et al. 2020). A further challenge associated with developing SPCL for either LV or AAV is the fact that both viral vectors have components which are cytotoxic.

In the case of the LV vector, cytotoxicity is caused by the pseudotyping envelope, VSV-g, the most widely used envelope due to its broad tropism and improved stability during downstream processing (Gutierrez-Guerrero et al. 2020; Merten et al. 2016). This prompted the development of inducible systems such as Tet-on whereby the LV production is triggered by the addition of doxycycline, and the utilisation of low-toxicity

envelopes and hence the development of constitutive systems which continuously express viral vector components (Merten et al. 2016). Sanber et al. (2015) described the construction of a RDpro envelope stable packaging cell line called WinPac which can constitutively produce LV reaching titres of 10^6 TU/ml. Although promising, no accounts of suspension, serum-free production have been yet made using this cell line. Another stable producer cell line which expresses LV constitutively is RD-MolPack cell line using a RD114-TR envelope (Marin et al. 2016). Humbert et al. (2016) describes the development of a cocal envelope producer cell line, adapted to suspension, serum-free growth, producing LV by induction with Sodium Butyrate which elicited higher transduction efficiency of CD34+ and T-cells than VSV-G enveloped LV. However, further optimisation is required since the titres achieved with the cocal cell line in suspension were 3-5 fold lower than those in adherent culture. Amongst these systems, the inducible Tet-on system appears to be the most advanced with several reports of suspension-adapted high producing SPCL published (Chen et al. 2020; Manceur et al. 2017). A process development account is offered by Manceur et al. (2017) whereby a stable producer cell line adapted to suspension, serum-free culture in perfusion mode achieved a cumulative total yield of 8 to 10 x 10^7 TU/ml with a cell-specific LV productivity of 11.5 TU/cell. LV production is induced with cumate and doxycycline which may burden DSP and perfusion mode achieved using acoustic cell filter technology is initiated after induction. Furthermore, Chen et al. (2020) describes an elegant and rapid methodology of LV SPCL generation which could significantly reduce development timelines.

On the other hand, in the case of the AAV, cytotoxicity is caused by the Rep proteins and helper proteins i.e. E2A and E4orf6 (Keeler and Flotte 2019; Hein et al. 2018). This initially prompted the development of infectious recombinant helper viruses (e.g. replication competent adenovirus, baculovirus and herpes simplex virus) used in

conjunction with a variety of cell line types (e.g. HeLa cells, Sf9, Vero, HEK-293) to trigger AAV production (Keeler and Flotte 2019). This approach is less favourable as it involves the manufacture of yet another recombinant virus and potentially, is associated with risks of rc-AAV generation (Aponte-Ubillus et al. 2018). However, an account of helper virus free producer cell lines for AAV was recently reported, whereby the *rep* and *cap* genes as well as transgene and serotype-specific capsid genes were sequentially stably integrated into the CAP cell line (Hein et al. 2018; Fischer et al. 2012). Similarly to the LV SPCL lead examples, the production of AAV particles in this system is also based on an inducible Tet-on system (Hein et al. 2018). Finally, given the cytotoxicity associated with both LV and AAV expression, the long-term production windows typical of mAb manufacture with SPCL, are not possible here, removing a key advantage of SPCL over the transient transfection system experienced in the mAb industry.

A summary table comparing the transient transfection system and the producer cell line system is provided below (**Table 2.8**).

Table 2.8 Transient transfection versus stable producer cell line expression systems: advantages and disadvantages.

	Transient transfection	**Stable producer cell lines**
Advantages	• Flexible • Fast to develop (time)	• Reduced pDNA contaminants to be removed by DSP (time, no of steps) • Safer and of higher quality • Increased reproducibility (less variability) • Reduced LV manufacturing costs (no pDNA)
Disadvantages	• Batch-to-batch variability due to variability in pDNA uptake and expression efficiency • Costly and technically difficult to scale up • Complex USP due to the complex formation and difficult elimination of pDNA in DSP • Large quantity of transfected pDNA may increase the risk of recombination events leading to formation of RCL	• Time consuming to create (development cost) • Challenging implementation of reliable and robust gene expression system – often leaky gene expression of cytotoxic VV components • Depending on the production system used to generate the cell line, partial gene silencing can occur over time

2.3.2.5 Harvest titres

aIn terms of process performance, LV and AAV are associated with vastly different reported titres and productivities. It is worth noting that LV is typically quantified using functional titration methods measuring the transducing units (TU), whereas AAV is quantified using physical titration methods measuring the viral genomes (vg) or capsids. LV titres range between 10^7 and 10^8 TU/ml, with amongst latest accounts quoting 10^9 TU/ml (Bauler et al. 2020) with a typical productivity of 1-40 TU/cell (Merten et al. 2016; Ansorge 2010), whereas AAV titres range between 10^{10} – 10^{11} vg/ml with typical productivities of 10^4 - 10^5 vg/cell (Aponte-Ubillus et al. 2018, Masri et al. 2019, Zhao et al. 2020). Process yield differences between LV and AAV will be discussed in the next section.

2.3.2.6 Downstream processing flowsheets

With the introduction of suspension cell cultures, the viral vector manufacturing processes look more similar to recombinant protein manufacturing flowsheets. However,

the gene therapy sector remains miles away from the productivity and throughputs achieved by recombinant protein manufacturers, namely due to the limited titres and yields achieved. This is likely caused by the use of purification technologies that had been developed for recombinant proteins, hence are not fully suitable for manufacturing larger and more complex biological entities such as LV and AAV particles. Whilst the large scale production processes of LV and AAV may share suspension-adapted cell culture in single-use stirred tank bioreactors, and some unit operations in downstream processing, there are differences DSP flowsheets and in process performance between the two vectors.

General overview of viral vector processing (post-viral vector expression)

Briefly, once the viral vector particle assemble at adequately high levels, the viral vector particles need to be fully released from HEK293(T) cells into the culture media. This may require cell lysis as in the case of some AAV serotypes (e.g. AAV2), but typically occurs naturally by shedding in the case of other AAV serotypes (e.g. AAV9) depending on culture conditions, and in the case of LV particles. The resulting process-related impurities namely the un-ruptured cells and cell debris need to be removed and this is generally achieved using normal flow filtration employing uncharged filtration media to minimise viral vector adsorption to the media. This requires retention ratings within 10 and 0.2 μm (microfiltration range) in a cascading fashion to ensure that the viral vectors flow through into the permeate (Perry and Rayat 2021). Membrane filtration is preferred to depth filtration since a depth filtration step is challenging to fully close. Depth filter media commonly used are cellulose, perlite, diatomaceous earth and resin binders while membrane media is commonly polyethersulfone (PES), nylon, polyvinylidene fluoride (PVDF), and inorganic materials (Raghavan et al. 2019). Reduction in DNA level is typically employed using endonucleases which digest the genomic and unincorporated

pDNA into small fragments, reducing the viscosity of the feed stream and thus, making it easier to process. DNA degradation can be performed either before clarification, in the bioreactor, or after clarification. The subsequent step is the further removal of process-related impurities and product-related impurities typically using chromatography-based separation techniques. Prior to chromatography, it is common to employ a concentration and/or a buffer exchange step using tangential flow filtration techniques known as ultrafiltration/diafiltration (UF/DF) steps typically for two reasons. The first reason to employ a UF/DF step is to concentrate the feed stream, hence reduce the processing times of the subsequent chromatography step in the case of bind-and-elute steps as well as reduce the size of the chromatography column in the case of a flow through step. The second reason to employ a UF/DF step is to change the buffer of the viral particle preparation into a new buffer providing the load conditions required for the subsequent chromatography step. In the case of LV, one to two chromatography steps are employed typically separating out the LV particles based on their surface charge (LV has a negative charge) using anion exchange chromatography media and based on its size using size exclusion chromatography (Merten et al. 2016; McCarron et al. 2016). However, the relatively large viral vector particle sizes (especially the LV) make these unsuitable for the widely used porous bead stationary phases, which means step yields are typically low (Ruscic et al. 2019). In the case of AAV, typically two or more chromatography steps are used due to larger volumes of process-related impurities than in non-lysed processes and the presence of critical product-related impurities. The AAV is associated with specific product-related impurities such as empty AAV capsids which can pose safety concerns in clinic hence need to be removed (Wright 2020). Consequently, AAV processes are associated typically with an initial affinity chromatography step followed by an ion exchange chromatography step, typically an anion exchange step due to AAV's predominantly negative charge (Adams et al. 2020). It is likely that a further UF/DF step

could be employed after the chromatography steps in order so as to formulate the product into the desired formulation recipe. This is then filtered using a 0.22 μm pore size filter and filled and cryopreserved.

A further difference between LV and AAV is linked to the stability profiles of these vectors. LV is unstable at room temperature (Higashikawa and Chang 2001b; Carmo et al. 2008) prompting developers to design processes addressing the short vector half-life through rapid harvest or short processing times at lower temperatures. In contrast, AAV has a good stability profile at room temperature (Gruntman et al. 2015), enabling DSP purification to occur at room temperature and over longer periods of time. The consequence of the stability and size differences between these vectors is that LV processes are commonly associated with a lower overall process yield than the AAV processes i.e. 15-25% vs 25-45% (Masri et al. 2019).

LV processing

In terms of downstream processing of LV, eight clinical-grade LV production flowsheets are shown in **Table 2.9**. Briefly, crude harvest is clarified normally using normal flow filtration of decreasing pore size with uncharged depth filters or membranes. Interestingly, a recent account of lentiviral vector bioprocessing described the successful use of tangential flow depth filtration (TFDF™, Repligen Corporation) to clarify suspension cell cultures achieving recoveries similar or higher than established clarification approaches (Williams et al. 2020). The potential of the adopting TFF-based technology this early in the bioprocess can have multiple advantages. Firstly, it can act as a cell-retention device i.e. the producer cells, which are retained are re-routed back into the bioreactor, whilst LV particles are harvested for purification in a semi-continuous like fashion. Secondly, the implementation of the TFF-based step could mean that a lower number of unit operations may be required which, in turn, may increase the maximum

possible overall process yield. Any excess DNA is degraded using endonucleases such as Benzonase® (Millipore Sigma, Burlington, MA, USA), LV is captured with anion exchange chromatography or concentrated using ultrafiltration or ultracentrifugation. Formulation can be achieved by either size-exclusion chromatography or ultrafiltration/diafiltration (UF/DF) operations. The bulk drug substance is 0.22 μm filtered in most cases, vialled and cryopreserved. Out of eight different published flowsheets (Merten et al. 2011; Aiuti et al. 2013; Miskin 2015; Ausubel et al. 2012; Slepushkin et al. 2003; Greene et al. 2012; De Ravin et al. 2016b; Marceau and Gasmi 2014; Miskin 2016; Kutner et al. 2009a; Burnham M 2017), only one employs purification using ultracentrifugation (UC) (Ausubel et al. 2012). Furthermore, another one uses conventional resin chromatography (Merten et al. 2011; Aiuti et al. 2013) followed by a size exclusion chromatography (SEC) step, which also serves as a formulation step. At least four protocols involve the use of anion exchange (AEX) membrane chromatography followed by UF/DF (Greene et al. 2012; Slepushkin et al. 2003; Kutner et al. 2009a; Wolstein et al. 2014). This reflects the industry's move away from UC and SEC due to their manual and open nature (UC) and limited scalability (SEC) and towards convective chromatographic media and UF/DF for concentration and buffer exchange. The use of AEX monoliths and nanofibers has also been reported with step yields above 80% (Bandeira et al. 2012; Ruscic et al. 2019).

Membrane chromatography is an attractive option because it can be run at higher flowrates than conventional, packed-bed chromatography whilst minimising the shear stress on LV particles which was associated with resin bead chromatography (Rodrigues et al. 2007a; Rodrigues et al. 2007b). But more importantly, keeping processing time short helps preserve LV infectivity (Nilsson 2016). LV harvest can be loaded onto the Mustang Q capsules at 200 ml/min (Slepushkin et al. 2003) compared to 10 ml/min in case of conventional chromatography (Scherr et al. 2002; McCarron et al. 2016). To illustrate

membrane scalability, a 900 ml Mustang Q capsule can process 1,500L of LV harvests per day (Slepushkin et al. 2003) whilst its binding capacity is in the order of 1-10 x 10^{10} TU/ml of membrane according to Kutner et al. (2009b). Bandeira et al. (2012) presents an LV purification process using DEAE CIM monoliths with a step yield of 80% which is about 12% higher than that achieved using conventional chromatographic media (Scherr et al., 2002). In terms of the UF/DF steps, ultrafiltration molecular weight cut-offs for LV processing are between 100 – 500 kDa (Nilsson 2016) and, given that the LV diameter is 100 nm, can go as high as 750 kDa, equivalent of 50 nm (Merten et al. 2014a; Perry and Rayat 2021). Furthermore, ultrafiltration can be run at 17-50 ml/min or more with 90-100% yield (Perry and Rayat 2021; McCarron et al. 2016; Geraerts et al. 2005).

Whilst the LV modality is thought to not impact cGMP DSP flowsheet design, the formulation buffer of choice is likely going to be selected based on whether the product will be used *in vivo* or *ex vivo*. It is typical for *ex vivo* gene therapy products to formulate the LV drug product in the cell culture media which will be used in the cell therapy process. However, in the case of *in vivo* LV products, the buffer of choice will need to be defined hence water for injection is likely to be part of that formulation (Perry and Rayat 2021).

Table 2.9 Lentiviral vector manufacturing flowsheets.

Institution/ Indication	**Genethon /WAS; MolMed/ WAS**	**Oxford BioMedica/ Cancer, PD**	**Beckman Research Institute/HIV**	**Virxsyx/HIV**	**WuXi Hyper-PRO platform/NC**	**St. Jude's Hospital/X-SCID**	**Theravectys/HIV, Cancer; Oxford BioMedica/Cancer,PD; Genethon/NC***	**bluebird bio/BH**
USP Tech., envelope, TT/PCL, FBS/SFM	10-layer trays, VSV-G, TT, FBS				HyperStacks (Corning Cellbind), NC, TT, NC	50-L WAVE reactor (cells immob. onto Fibra-cel disks), PCL (tet-0ff), VSV-G, FBS	STR susp., NC, TT, SFM; STR susp., NC, TT, SFM; STR susp., NC, TT, SFM	NC, VSV-G, TT, NC
TT agent used /no. of plasmids	Calcium-Phosphate /4	NC, sodium butyrate induction/4	Calcium-Phosphate/4	Calcium-Phosphate/2	PEI/4	Not applicable	NC/NC; NC/4; PEI/4	$CaCl_2$/3
Harvest Volume range (L)	24-50	72 per week	Up to 20 per week	36-52	250	~138 (perfusion)	20-1,000; 200; 200	>40
Crude Titre	1-5x10^7 IG/ml	0.2-2x10^6 TU/ml (PD process)	0.5-1x10^6 TU/ml	2.02 x 10^7 TU/ml	1-2 x 10^6 LV particles/mL	0.5-1x10^7 TU/ml	NC; 5 x 10^7 TU/ml; NC	NC
Clarification	1.DepthF (0.8/0.45 um)	1.NFF	1.DepthF (0.45 um)	1.DepthF (DPS, e.g. Sartorius)	1.Filtration	1.DepthF (1.2um/0.45um,, Millipore)	1; 2.DepthF; NC	1
Benzonase	2	2	2	4	3		2; 1	NC
AEC	3 DEAE	3		2. Mustang Q		2.Mustang Q	3; 3	2. Mustang Q
Conc./DF	4	4.UF/DF (HF) and -70degC hold, 6.UF	3.UF/DF 500 kDa 4. Ultracentrifugation (6,000g for 16-20h)	3. UF (HF), 5.DF	2, 4	3. DF	4.UF (TFF); 4.UF/DF and -70degC, 6.UF (OXB)	3.UF/DF
Formulation	5. SEC		5			4. 0.5% HSA		4

Institution/ Indication	**Genethon /WAS; MolMed/ WAS**	**Oxford BioMedica/ Cancer, PD**	**Beckman Research Institute/HIV**	**Virxsyx/HIV**	**WuXi Hyper-PRO platform/NC**	**St. Jude's Hospital/X-SCID**	**Theravectys/HIV, Cancer; Oxford BioMedica/Cancer,PD; Genethon/NC***	**bluebird bio/BH**
Sterile filtration	6	5		6	5	5	5; 5	5
Fill Finish	7	7	6	7	6	6	6.200-5,000 vials; 7	6
Yield	20%	30-40% (PD process)	40%	30%	75%	29-33%	NC	NC (Final titre >10^8 TU/ml)
References	Merten et al. (2011), Aiuti et al. (2013), Biffi et al. (2013), Geraerts et al. (2005), Schweizer and Merten (2010), Stewart et al. (2011)	Miskin (2015), Truran et al. (2009), Schweizer and Merten (2010)	Ausubel et al. (2012)	Slepushkin et al. (2003)	Burnham (2017)	Greene et al. (2012), De Ravin et al. (2016a)	Zemmar et al. (2015), Miskin (2016), Hebben (2015), Marceau and Gasmi (2014)	Kutner et al. (2009a), Negre et al. (2016)

WAS = Wiskott Aldrich Syndrome; PD = Parkinson's disease; NC = not communicated; BH = beta-haemoglobinopathies; NFF = normal flow filtration; SEC = Size Exclusion Chromatography; AEC = anion-exchange chromatography; USP = upstream processing; TT = transient transfection; DPS = decreasing pore size; HF = hollow fiber; DF = diafiltration, DepthF = depth filtration; SFM = serum-free media; FBS = foetal bovine serum; STR = stirred tank bioreactor. * DSP steps information not communicated for Genethon STR process.

AAV processing

In terms of downstream processing of AAV vectors, considerations around the lysis, clarification, DNA degradation, purification steps and concentration steps will be discussed.

An initial trade-off that needs consideration concerns the lysis step. The introduction of a lysis step designed to maximise AAV particle recovery generates a larger volume of process-related impurities which may require additional unit operations to remove which, in turn, decreases the overall process yield (Adams et al. 2020). Lysis reagents compatible with large scale manufacture which are commonly employed are chemical-based such as detergents (e.g. Tween® 20 from Millipore Sigma, Burlington, MA, USA) or high osmolality solutions (acidic buffers such as citrate and low pH) (Kimura et al. 2019; Adams et al. 2020). Triton X-100 represented the gold standard detergent lysis reagent until recently; however this will be banned soon in the European Union due to the environmental impact of its degradation products (Adams et al. 2020). In terms of the clarification step, similarly to the case of LV, depth or membrane filtration is employed. Examples of depth filtration technologies that can be used for viral vector processing are STAX mAx Clarification Platform (Pall Corporation), Millistak+ Pod Depth Filter System (Millipore Sigma, Burlington, MA, USA), or Zeta Plus™ Encapsulated System (3M, Bracknell, United Kingdom) (Adams et al. 2020).

With regards to the DNA degradation step, this can be employed either before or after the clarification step, and, similar to the LV processes, Benzonase® (Millipore Sigma, Burlington, MA, USA), is typically used. However, this endonuclease is sensitive to high salt concentration which is often required to enhance chromatographic purification of AAV. As such, a salt-activated nuclease which is reported to have improved activity at

high salt concentration is under development (i.e. SAN-HQ by ArcticZymes, Tromsø, Norway not yet available in GMP-grade) (Ward 2018).

With regards to AAV purification, chromatography and ultracentrifugation methodologies have been employed to date. Ultracentrifugation is particularly useful for separating empty/full capsids if short development timelines are available. However, this technique is labour intensive, has limited scalability, is challenging to close and is associated with large capital expenditure. In terms of the chromatography flowsheets, at least two chromatography steps are typically employed in AAV purification i.e. a capture step and at least one polishing step. The goal of the capture step is to bind the AAV particles onto the adsorption media whilst impurities follow-through and this is typically achieved using affinity chromatography or hydrophobic interaction chromatography. The current affinity chromatography media usually employ recombinant ligands based on camelid single domain antibody fragments for a range of AAV serotypes (Terova et al. 2018). Examples of commercially available camelid media are AVB Sepharose, Capto™ AVB (Cytiva). Other types of affinity media were developed based on screening of single-domain antibody fragments such as the POROS™ CaptureSelect™ AAVX (Thermo Fisher Scientific) which uses POROS polymer bead matrix and AVIPure® AAV9 (Cytiva) which uses fibro chromatography. Both types of media have the advantage of convective-based mass transfer which accommodates large flowrates (i.e. 150 – 450 cm/h), thus shortening processing times, as well as high binding capacities (Toueille et al. 2018; Adams et al. 2020). An alternative to affinity chromatography as capture step is hydrophobic interaction chromatography using, for example, monolith chromatography i.e. CIMmultus™ OH monoliths (BIA Separations, Ajdovščina, Slovenia), which enables high flowrates to be achieved (Adams et al. 2020). While the capture step using the previously mentioned technologies can deliver decent levels of purity, subsequent chromatography steps are needed to reduce process-related impurities

such as DNA and host cell proteins and product-related impurities such as empty capsids. Polishing chromatography can achieve the removal of most product and process-related impurities. Specifically, anion exchange chromatography is typically used to separate out empty capsids based on the surface net charge difference between the full and empty capsids i.e. empty AAV capsids have a pI of 6.3 while full capsids have pI of 5.9 (Qu et al. 2015). Examples of commercial media used in this step are POROS HQ and Q Sepharose XL, Mustang S ad Mustang Q membranes and CIMmultus^{TM} QA (BIA Separations) (Adams et al. 2020).

In terms of concentration and buffer exchange, similarly to LV, tangential flow filtration is used. PES-based membranes are typically used with molecular weight (MW) cut-offs of 100 kDa or 300 kDa in the case o AAV given AAV's MW of 600 kDa (Qu et al. 2015).

It is worth mentioning that cGMP processes involving helper viruses such as AdV, rHSV or baculovirus typically require a viral clearance step which will not be discussed herein.

In terms of formulation, AAV is formulated using the following excipients: MgCl2 (e.g. 1mM), Tris buffer (e.g. 20mM, pH 8.0), NaCl (e.g. 20 mM) and poloxamer 188 (e.g. 0.005%) as in the case of Zolgensma® (FDA 2019). Luxturna®, however, is formulated using sodium phosphate, with different concentrations of NaCl and poloxamer 188 and without Tris buffer or $MgCl_2$ (FDA 2017a).

2.3.3 Plasmid DNA vector considerations

Plasmid DNA (pDNA) is required for viral vector manufacturing using transient transfection methodology. It is also the delivery system for the transposone/transposase genes via electroporation for stably engineering T-cells (Singh et al. 2015). Besides, the mRNA transcripts of genome editing tools which are delivered into target cells' cytoplasm typically via electroporation, are produced using plasmid DNA and a RNA polymerase such as T7 RNA polymerase (DiGiusto et al. 2016). Moreover, minicircle

(MC) DNA vectors which have emerged as promising gene delivery tools are generated from parental plasmids using site-specific recombination (Sharma et al. 2013; Hudecek et al. 2017; Monjezi et al. 2017; Prommersberger et al. 2021). All these applications flag the relevance of pDNA manufacturing process for the gene therapy sector.

2.3.4 Plasmid DNA vector manufacturing processes

The pDNA is constructed using synthetic biology techniques to encode key elements such as the transfer gene, origin of replication and restriction enzyme sites. Once the plasmid DNA is built, it is transfected into multiple *E. coli* strains. The best producers are selected, tested and a Research Cell Bank (RCB) is derived from which a Master Cell Bank (MCB) is generated (DiGiusto et al. 2016). Clinical grade pDNA is produced using antibiotic-free fed-batch *E. coli* fermentation with reagents from non-animal sources (Rinaldi et al. 2014). Strains commonly used are K12 such as DH5alpha (Schmeer et al. 2017) and BL21 recA endA (Carnes et al. 2011). Plasmid copy number per cell is an important optimisation target as high copy number plasmids can yield up to 1,000 copies per cell thus majorly impacting costs (Rinaldi et al. 2014). According to the same source, lower specific bacterial growth rates are associated with increased plasmid copy number.

Fed-batch mode *E*. coli fermentation leads to higher biomass levels and hence higher plasmid levels than batch mode (Ruiz et al. 2011). Fermentation scales reported for GMP production of plasmid are 50-400 L however much larger scales have been reported for lower quality grades manufacture (Cai et al. 2009). This is typically performed in stainless steel stirred-tank bioreactors and, more recently and to a lower extent and scale, in single-use bioreactors specifically designed for bacterial cultures (Cytovance 2020). Fermentation takes about 2 days and biomass levels tend to range below 100 g dry cell weight/L while pDNA titres can go up to 2.2 g/L (Ongkudon et al. 2011; Xenopoulos and Pattnaik 2014; Williams et al. 2009). The latter can vary quite dramatically depending on

replicon type, plasmid size, sequence or host. For example, Sanofi (France) (formerly known as Centelion) reported pDNA titres in the range of 52.5 ±10 mg/L while VGXI (USA) reported values as high as 1,800 mg/L (Cai et al. 2009; Nelson et al. 2013). **Table 2.10** provides detail on 8 pDNA manufacturing processes including manufacturing scales, process performance and DSP flowsheet designs.

Table 2.10 GMP manufacturing processes for plasmid DNA vectors.

Group / pDNA length	**Beijing University of Technology / 6.2kb***	**VGXI / 3.6kb**	**VGXI, HyperGRO* / 4.22kb, 4.19 kb**	**VGX pharm. and VGXI / 3.8-4.7kb**	**Recipharm/ Cobra / 8.8kb***	**Centre for Genetic Engineering and Biotechnology, Havana, Cuba / 5.5kb***	**Boehringer Ingelheim / NC**	**Centellion, Sanofi / NC**
Fermentation volume/ Fermentation mode	50L/Batch	10L/Batch	320L/batch	400L/Batch	50L/Fed-Batch	5L/Fed-Batch	1-200L/Fed-Batch	400L/Fed-batch
Crude titre (mg/L)	220-233	NC	1,500	Approx. 100	NC	NC	2,400	52.5 +/-10
***in vivo/ex vivo* application**	*in vivo*	*ex vivo*	*in vivo*	*in vivo*	*ex vivo*	*in vivo*	*in vivo*	NC
Centrifugation	1.Cont	1	1	1.Cont	1	2	1	1
Cell lysis	2.AL (cont.), 6.Cold ethanol	2.Airmix Lysis	2.Airmix Lysis	2. AL	2.AL	3.AL	2.AL	2.AL
Solid liquid separation		3.DepthF	3.Filtration	3	3.Centrifugation, 4.DepthF	4.TFF (5x) 100,000 kDa	3	3.DepthF
AEX	5.Source 15Q	4	4. Mustang Q capsule	4.Mustang Q capsule	5	6.Sartobind membrane	5	4
AC	4.PSX				6.PSX			5.TAC
SEC/HIC	3.SEC (Sepharose 6FF)		5.HIC	5.HIC		5.SEC	4.HIC,6.SEC	6.HIC
Concentration	7. Centrifugation	5.TFF	6.UF/DF 50 kDa	6.UF/DF 50 kDa	7.TFF			7.TFF
Formulation	8					7.TFF	7.UF	
Sterile filtration	9	6	7	7	8	8	8	8
Fill Finish	10	7	8	8	9	9	9	9
Yield	58–67 %	NC	30 - 45%	NC	65-76%	50%	NC	average of 60%
References	Hu et al. (2016)	Tiwari et al. (2015)	Nelson et al. (2013)	Cai et al. (2010)	Hitchcock et al. 2010 (2010)	Limonta et al. (2010)	Huber et al. (2008)	Blanche et al. (2005), Cai et al. (2009)

AL = alkaline lysis; HL = heat lysis; PSX = PlasmidSelect Xtra; HIC = hydrophobic interaction chromatography; AEX = anion exchange chromatography; AC = affinity chromatography; SEC = size exclusion chromatography; NFF = normal flow filtration; TAC = thiophilic adsorption chromatography; DepthF = depth filtration.*Protocol has been used in the production of pDNA clinical trial material.

The only form of plasmid DNA that is considered safe and efficacious is the supercoiled configuration (Pillai et al. 2008). It is thought that the larger the plasmid is, the more challenging the purification of the supercoiled form is (Hitchcock et al. 2010; Rinaldi et al. 2014; Xenopoulos and Pattnaik 2014). As a result, each pDNA, especially those destined for viral vector manufacturing, can have a slightly different manufacturing process, characterised by different titres and yields.

In terms of downstream processing, recovery of cell paste is done using centrifugation followed by cell lysis which is normally performed typically using alkaline lysis using NaOH and SDS in order to release the pDNA (**Table 2.10**). Downstream processing of pDNA is more complex than that of LV due to the release of host cell components during the lysis procedure and the need to purify supercoiled isoforms from open circle plasmids and RNA. Typically, DSP consists in a sequence of solid/liquid separation techniques and 2 to 3 chromatography steps with typical process duration of less than two days (Cai et al., (2010), **Table 2.10**). Chemistries used for pDNA purification are anion exchange (AEX), hydrophobic interaction (HIC), mixed-mode chromatography such as thiophilic aromatic adsorption (TAC) and size exclusion chromatographic (SEC) media. These are used in various combinations and sequences (Xenopoulos and Pattnaik 2014). Commonly AEX is used as a capture step and TAC such as PlasmidSelect Xtra (PSX, Cytiva) or HIC are used as polishing or intermediate steps. Concentration and buffer exchange is then carried out using UF/DF (TFF), followed by 0.2 µm filtration and sterile fill (Xenopoulos

and Pattnaik 2014). Depending on scale and alkaline lysis capacity, the DSP takes at least one week. Overall process yields tend to range between 30% and 76% **(Table 2.10**).

Plasmids used in viral vector manufacturing such as plasmids carrying transgenes, are often larger than recombinant proteins of similar molecular weight hence do not adsorb very well onto conventional chromatographic media (Xenopoulos and Pattnaik 2014; Ongkudon et al. 2011). Binding capacities achieved with resins tend to fall below 5 mg/ml of media and are associated with modest flowrates of 150 cm/h (Eon-Duval and Burke 2004). On the other hand, macroporous media such as membranes and monoliths have been employed in purifying plasmids. With membranes, a dynamic binding capacity of 4 mg/ml was achieved with flowrates of 150 ml/min in case of weak AEX Sartobind D membrane (Limonta et al. 2010), whilst up to 10 mg/ml was captured with an AEX DEAE CIM monolith (Bia Separations) run at flowrates as high as 1,000 cm/h (Urthaler et al. 2005).

The grade at which pDNA should be manufactured at depends on its intended use, such that pDNA can be cGMP-manufactured or high quality-grade manufactured (i.e. HQ grade). According to Schmeer et al. (2017), cGMP manufacturing of pDNA is mandatory for *in vivo* applications such as vaccines or pDNA electroporated T-cells expressing CARs or pDNA electroporated haematopoietic stem and progenitor cells (HSCs) (DiGiusto et al. 2016). With regards to the release criteria for pDNA manufactured for the genetic modification of T-cells in clinical trials, an example is provided by Singh et al. (2013). As such, more than 90% of the pDNA in the final product needs to be supercoiled, endotoxin levels must be below 50 EU/mg, HCP levels below 0.3% and RNA below 10%. Schmeer et al. (2017) also provides an account of the quality control testing performed for pDNA.

However, in the case of pDNA destined for viral vector manufacture it is not fully clear whether the pDNA needs to be cGMP-grade and it is somewhat accepted to employ HQ-grade pDNA (Schmeer et al. 2017). The key differences between cGMP-grade and HQ-grade can be related to the manufacturing facility which, in case of cGMP-grade, needs to have an active manufacturing licence, to the documentation level of completeness and traceability and quality of materials. Furthermore, cGMP-grade manufacture requires a cGMP-grade cell bank and QC and QA release of materials (Schmeer et al. 2017; Rinaldi et al. 2014).

With regards to pDNA destined for viral vector manufacture, the quantity of transfer plasmid which carries the therapeutic gene is typically larger than the other plasmids (Geraerts et al. 2005). Merten et al., (2011) provided detail on the amount of pDNA required for a small scale adherent LV manufacturing process using 24 10-layer vessels. **Table 2.11** captures the type of pDNA involved and, its role and the quantities used in the process. Assuming a transfection cell density of 2 x 10^5 cells/cm^2, this translates into a total pDNA requirement of 1.4 μg/10^6 cells. This is similar to AAV reports claiming pDNA requirements in the order of 1.5 μg/10^6 cells (Cameau et al. 2019). Furthermore, reports of 2.5 μg /10^6 cells have been published for both LV and AAV applications (Cesari M. 2017).

Table 2.11 Example of plasmid DNA requirement for LV manufacturing based on Merten et al. (2011).

Type of plasmid	**Plasmid name**	**Encoding for**	**Quantity per CF-10 (μg)**
Transfer plasmid	pRRLW1.6-huWASP-WPREmut6-K	Therapeutic gene	760
Packaging plasmid	pKLgagpol	HIV-1 gag-pol genes	500
Packaging plasmid	pKRev	HIV-1 rev gene	191
Envelope plasmid	pKG	Vesicular stomatitis virus G glycoprotein	270
Total per CF10 (μg)		1,721	
Total per batch (μg)		41,304	

2.4 Conclusion

The gene-modified cell therapy and two vector manufacturing processes i.e. for the LV vector and the pDNA vector, were discussed in terms of classifications, flowsheets and technologies involved. Also, alternative flowsheets whereby reliance on viral vector is removed were discussed, however these still rely on pDNA manufacture. On the other hand, the *in vivo* gene therapies typically require viral vector (LV or AAV) and pDNA processes. Since AAV products are leading the *in vivo* gene therapy clinical investigations, the manufacture of the AAV vector was discussed alongside that of the LV vector. In addition, routes towards eliminating the dependency on pDNA were addressed by discussing the development of stable producer cell lines.

Chapter 3: Materials and methods

3.1 Introduction

Chapter 1 described some of the key questions that gene therapy developers are faced to answer so as to build their way towards achieving commercial viability of their products. Manufacturing strategy and supply chain, process design and viral vector expression system are all key topics which need to be carefully addressed to ensure market success. This chapter describes the decisional tools used to attempt answering some topical questions by capturing the impact of technical and cost assumptions on financial features. These tools were applied to case studies relevant to the industry which are described in **Chapters 4-6**.

Chapter 3 is structured as follows. **Section 3.2** introduces the decisional tools used in this work, describing in detail the advanced gene therapy decisional tool developed as part of this project. **Section 3.3 – 3.7** describe the key components of the novel gene therapy decisional tool developed while **Section 3.8** and **Section 3.9** provide an overview of how data collection was performed and the conclusions section, respectively.

3.2 Decisional tools employed in this project

The work performed during this project employed two key advanced decisional tools. One of the decisional tool employed here was an advanced autologous CAR T-cell therapy decisional tool, previously developed by Pereira Chilima (2019) whilst the other tool was a gene therapy process change evaluation tool which was developed for this project. The gene therapy process change evaluation tool was employed to generate the results presented in **Chapter 5** and **Chapter 6**. On the other hand, the autologous CAR T-cell therapy decisional tool was used for generating the results presented in **Chapter 4** as well as for providing key cell therapy-related inputs for the application of the gene therapy process change evaluation tool in **Chapter 6**. The following paragraph provides

a high level description of the autologous CAR T-cell therapy decisional tool while the remainder of sections will describe the components of the gene therapy process change evaluation tool.

The decisional tool developed by Pereira Chilima (2019) which was employed in this work consisted of two key models specifically designed for autologous CAR T-cell therapy manufacture: a whole bioprocess economics model and a project valuation model. The whole bioprocess economics model included a cost of goods model and a fixed capital investment model, developed to assess the economics competitiveness of a range of technologies and product dose sizes. The project valuation model, built based on risk-adjusted net present value methodology, was developed to assess the profitability differences between centralised and decentralised (multi-site) manufacturing options. **Chapter 1**, **Section 1.4.3**, describes the case studies approached with this tool in another project. **Chapter 4** describes the application of the tool in the case study approached in this project, providing detailed information on new assumptions, key equations and any updates to the equations used in the tool (**Section 4.2**).

3.3 Gene therapy process change evaluation tool architecture

An integrated gene therapy decisional tool (also referred to as the viral vector decisional tool) was developed so as to enable the assessment of the impact of viral vector process changes at various stages in the gene therapy drug development pathway by analysing the costs associated with the entire project lifecycle. The project lifecycle is assumed here to span between the beginning of Phase 1 clinical trial preparation through to the end of the commercial phase.

The tool consists of four components: a whole viral vector bioprocess economics model including a cost of goods (COG) and fixed capital investment (FCI) model (referred to as the COG model), a cost of drug development ($C_{development}$) model, a gene therapy project

valuation model, and a brute force optimisation algorithm for scenario analysis (**Figure 3.1**). These were linked to multiple databases. A detailed list of the inputs to the tool (grouped under clinical trials, process development, manufacturing and cash flow) is shown in **Figure 3.1**. The key tool outputs are the cost of drug development ($C_{development}$) and project lifecycle cost (supported by the sponsor company – sum of $C_{development}$ and cost of commercial phase ($C_{commercial}$)), technology rankings and cost breakdowns (COG per stage and FCI) as well as the profitability ranking (**Figure 3.1**). A brute force optimisation algorithm was developed to rapidly change specific inputs (either one or multiple at a time), run the three models and generate and store the tool outputs. The tool with all its components was built using Microsoft Excel (Microsoft® Corporation, Redmond, WA) coupled with Visual Basic for Applications (VBA, Microsoft® Corporation, Redmond, WA).

The following sections will describe the viral vector bioprocess economics model, the cost of drug development model, the project valuation model and the brute force optimisation approach. To note, only the viral vector bioprocess economics model and the brute force optimisation approach were used in the case study discussed in **Chapter 5** while all components shown in **Figure 3.1**, plus key CAR T-cell therapy decisional tool outputs were used in the case study discussed in **Chapter 6**.

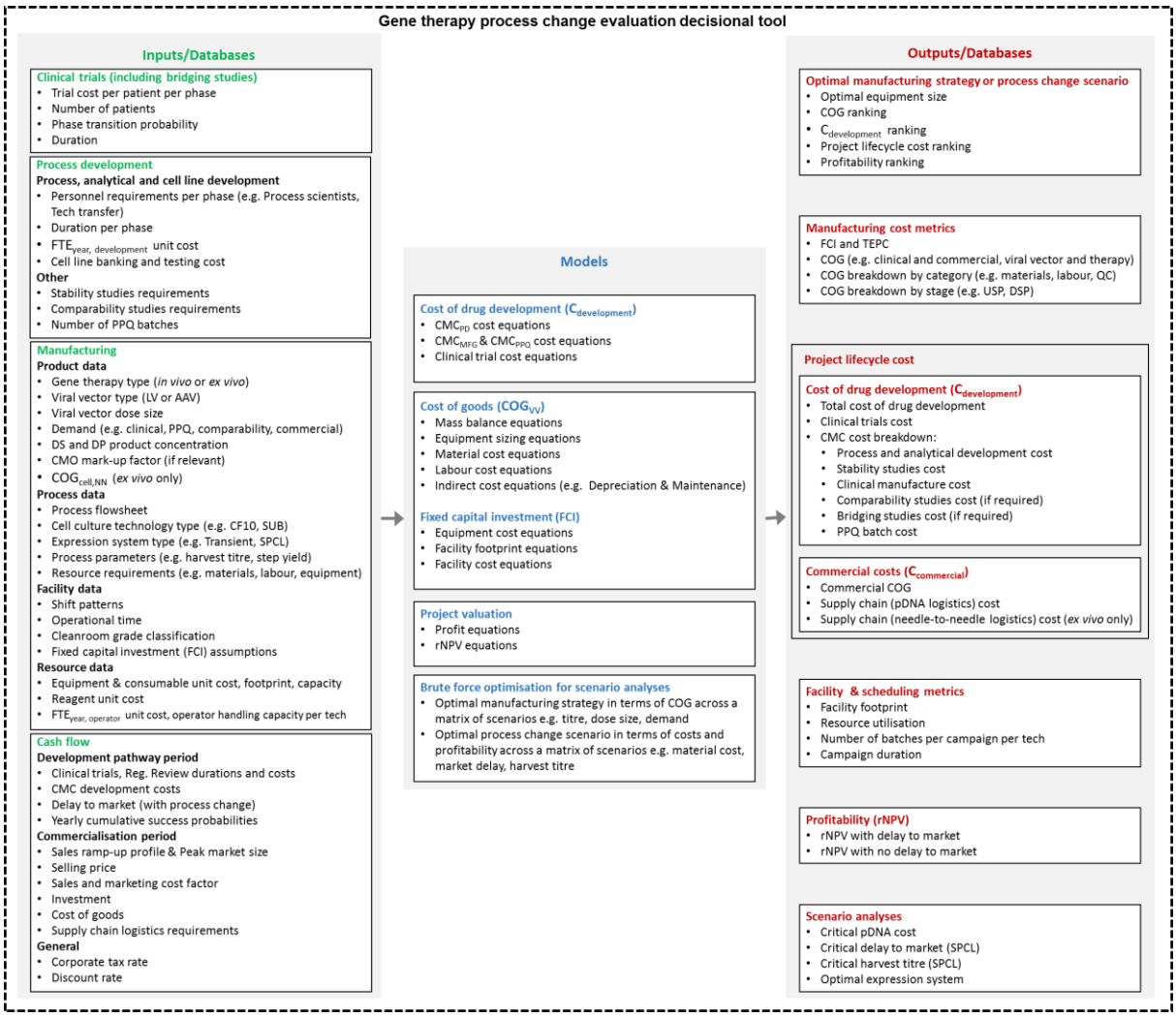

Figure 3.1 Overview of the process change decisional tool. SPCL = stable producer cell line, VV = viral vector, NN = needle-to-needle, FTE = full-time equivalent, Reg. Review = Regulatory Review, TEPC = total equipment purchase cost, PD = process development, PPQ = process performance qualification, MFG = manufacturing, rNPV = risk-adjusted net present value.

3.4 Bioprocess economics model

The viral vector bioprocess economics model consisted of a cost of goods (COG) model and fixed capital investment (FCI) model which were built using Microsoft Excel (Microsoft® Corporation, Redmond, WA) given its transparency and wide usage across the sector. In addition, it included databases containing information about all technologies and flowsheets undergoing evaluation. This model was employed in addressing the challenge of determining the most cost-effective cell culture technology for viral vector manufacture and the optimal configurations across a range of viral vector products and

process performance. The model captures whole bioprocess costs (materials, labour, QC testing, indirect) from cell culture through to downstream processing costs (DSP), and fill finish costs (FF). The process flowsheet and the resource requirements of each unit operation are a function of the viral vector selected to be manufactured. As such, the user can specify product data (e.g. LV or AAV), process data (e.g. cell culture technology, expression system type i.e. transient transfection or SPCL, harvest titre, process yields), facility data (e.g. shift patterns) and resource data (e.g. resource unit costs) (**Figure 3.1**). For each technology, the bioprocess economics model selects the optimal configuration it needs to meet the demand by retrieving technology and configuration-specific information from the database and taking into account a series of constraints (e.g. minimum working volume and maximum number of units per batch). Simultaneously, the FCI and COG are determined for each flowsheet under evaluation and the ranking of cell cultures technologies as well as other non-cost related outputs are provided (e.g. facility footprint, utilisation, manufacturing duration and resource requirements). In addition, for the gene-modified cell therapies, the user specifies the cell therapy-related needle-to-needle costs, namely the cell therapy manufacturing costs, which in this case could be retrieved from the autologous CAR T-cell therapy decisional tool, as well as apheresis and transportation costs.

The bioprocess economics model was initially built for lentiviral vectors and was later adapted for adeno-associated viral vector manufacture evaluations.

The foundations of the bioprocess economics model are represented by mass balance and equipment sizing equations which will be discussed in **Section 3.4.1**. These respond to the inputs provided by the user by calculating resource and facility size requirements which then become inputs into the cost equations designed to output the cost of goods. The cost equations will be described in **Section 3.4.2**.

3.4.1 Mass balance and equipment sizing

This section will describe the key mass balance and equipment sizing equations used in the bioprocess economics model. The key units which this model uses are number of cells, number of viral vector product units (either transducing units, TU, for LV or viral genomes, vg, for AAV) as well as product volume. The number of cells represents the unit used in the seed train and upstream processing parts of the model, while the product units and product volume represent the units used in downstream processing and fill finish parts of the model. As such, the key law used here is that the output units exiting one step represent the input units into the next processing step (unit operation). Since there are losses experienced in most downstream processing unit operations, the product units (PU) exiting a unit operation *n* are determined as follows:

$$N_{PU_{out}} = N_{PU_{in}} \times Y_n \quad \textbf{(3.1)}$$

Where $N_{PU_{out}}$ = number of product units exiting the unit operation *n*

$N_{PU_{in}}$ = number of product units entering the unit operation *n*

Y_n = step yield of unit operation *n*

The process yields values are inputs that are dictated by the users and examples of such values are shown in **Chapter 5** and **Chapter 6**. Since there were some differences in the flowsheets associated with LV and AAV, as described in **Chapter 2** and **Chapter 6**, the model used slightly different sets of equations if the user selected a LV product or an AAV product.

Furthermore, the model was designed to operate in rate mode or in design mode. In rate mode, the key inputs are product characteristics such as viral vector type, dose size, demand, technology and configuration characteristics. The facility utilisation is calculated based on demand input and the type of technology and configuration selected

for manufacture. As such, one of the rate mode outputs is the number of batches required to meet a certain demand. The indirect costs such as labour, maintenance and depreciation are calculated based on facility utilisation and the best performing technology is identified by determining the COG/dose in the case of each candidate and selecting the one with the lowest COG/dose. This approach is compatible with modelling a CMO-type operation and was used for generating the results in **Chapter 5** and **Chapter 6**.

On the other hand, whilst the same inputs are required, the design mode uses an additional input which is the number of batches that need to be manufactured per year so as to maximise facility utilisation. Here, the candidate technology and configuration solutions are screened first to ensure that minimum bioreactor utilisation levels are met before ranking them from a COG perspective. This approach is more suitable to be used when modelling in house manufacture. Since this was not the approach used in generating the results discussed in **Chapter 5** and **Chapter 6,** the design mode will not be extensively discussed.

Rate mode equations

For any given product characteristics in terms of vector type and dose size, the model calculates the number of doses that could be produced per batch using each of the candidate cell culture technologies for all configurations (sizes) available for every technology. Based on this calculation and the input demand (number of doses), the model calculates the number of batches required to satisfy the demand. The equation below shows how the number of doses per batch can be determined using technology and configuration *n* for a LV product **(3.2)** and for an AAV product **(3.3)**.

$$N_{dose,batch,n} \quad \textbf{(3.2)}$$

$$= RoundDown\left(\frac{(V_{h,n} \times T_h \times Y_{DSP} - V_{QC,DS} \times c_{DS}) \times Y_{ff} - V_{QC,DP} \times c_{DP}}{m_{dose} \times (1+F)}\right)$$

Where $V_{h,n}$ = harvest volume produced by technology and configuration *n* per batch (ml)

T_h = harvest titre (TU/ml)

Y_{DSP} = overall DSP yield

$V_{QC,DS}$ = drug substance volume retained for release testing (ml)

$V_{QC,DP}$ = drug product volume retained for release testing (ml)

c_{DS} = drug substance concentration (TU/ml)

Y_{ff} = fill finish yield

c_{DP} = drug product concentration (TU/ml)

m_{dose} = LV product dose size (TU)

F = overage (% surplus of doses acting as back-up)

$$N_{dose,batch,n} = RoundDown\left(\frac{(V_{h,n} \times T_h \times Y_{DSP} \times Y_{ff}) - V_{QC,DP} \times c_{DP}}{m_{dose} \times (1+F)}\right) \quad \textbf{(3.3)}$$

Where $V_{h,n}$ = harvest volume produced by technology and configuration *n* per batch (ml)

T_h = harvest titre (vg/ml)

m_{dose} = AAV product dose size (vg)

$V_{QC,DP}$ = drug product volume retained for release testing (ml)

c_{DP} = drug product concentration (vg/ml)

Y_{ff} = fill finish yield

Y_{DSP} = overall DSP yield

F = overage (% surplus of doses acting as back-up)

To determine the number of batches required to meet demand using technology and configuration *n*, regardless of whether a LV or an AAV product is selected, the following equation was used:

$$N_{batch,n} = MAX\left(\frac{N_{dose,annual}}{N_{dose,batch,n}}\right) \quad \textbf{(3.4)}$$

Where $N_{dose,annual}$ = annual demand (number of doses)

$N_{dose,batch,n}$ = number of doses that can be generated per batch using technology and configuration *n*

Design mode equations

To calculate the harvest volume required per batch, assuming the number of batches per year is given as input, the following equation is used for LV:

$$V_{h,batch} = \frac{\left(\frac{\frac{N_{dose,annual}}{N_{batch,annual}} \times m_{dose} \times (1+F) + V_{QC,DP} \times c_{DP}}{Y_{ff}} + V_{QC,DS} \times c_{DS}\right)}{Y_{DSP} \times T_h} \quad \textbf{(3.5)}$$

Where $N_{dose,annual}$ = annual demand (number of doses)

$N_{batch,annual}$ = number of batches to be produced per year

m_{dose} = LV product dose size (TU)

$V_{QC,DS}$ = drug substance volume retained for release testing (ml)

c_{DS} = drug substance concentration (TU/ml)

$V_{QC,DP}$ = drug product volume retained for release testing (ml)

c_{DP} = drug product concentration (TU/ml)

Y_{ff} = fill finish yield

Y_{DSP} = overall DSP yield

T_h = harvest titre (TU/ml)

F = overage (% surplus of doses acting as back-up)

The equation used for AAV processes varied slightly as the flowsheet looked slightly different to that of the LV processes i.e. no cryopreservation hold step and no concentration step were required, as discussed in **Chapter 6**:

$$V_{h,batch} = \frac{\left(\frac{N_{dose,annual}}{N_{batch,annual}} \times m_{dose} \times (1+F) \ + V_{QC,DP} \times c_{DP}\right)}{Y_{overall} \times T_h} \quad \textbf{(3.6)}$$

Where $N_{dose,annual}$ = annual demand (number of doses)

$N_{batch,anual}$ = number of batches to be produced per year

m_{dose} = AAV product dose size (vg)

$V_{QC,DP}$ = drug product volume retained for release testing (ml)

c_{DP} = drug product concentration (vg/ml)

$Y_{overall}$ = overall yield (DSP and fill finish)

T_h = harvest titre (vg/ml)

F = overage (% surplus of doses acting as back-up)

To check whether the minimum working volume constraint is met, the working volume (V_w) was calculated using the following equation, regardless of product type:

$$V_W = V_{h,batch} / N_h \quad \textbf{(3.7)}$$

Where $V_{h,batch}$ = harvest volume per batch (L)

N_h = number of equal volume harvests performed per batch

Regardless of mode, if the annual demand exceeds the maximum number of batches that can be generated per year in that facility and no larger configuration is available to further scale-up the process, additional manufacturing trains are added. To calculate the number of manufacturing trains (N_{train}) required, the following equation is employed:

$$N_{train} = MAX\left(\frac{N_{batch}}{N_{batch,max}}\right) \quad \textbf{(3.8)}$$

Where N_{batch} = number of batches required to satisfy demand

$N_{batch,max}$ = maximum number of batches that can be manufactured in one train per year

The following paragraphs will describe how the seed train, upstream processing (USP), downstream processing (DSP) and fill finish process areas were scaled in terms of raw materials, equipment and labour requirements. Regardless of process area type, the model identified the most appropriate resource unit size (or type) from the resource database based on the calculated resource requirements. For example, the product volume bag size and cost was determined based on the calculated product volume by checking the resource database for a bag that would have a working volume just slightly larger than the

calculated product volume. If the product volume exceeded the largest available bag size in the resource database, multiple bags of the largest size were selected by the model.

3.4.1.1 Seed train

Since each technology and configuration may be associated with slightly different working volumes, when keeping a constant seeding cell density, this translates into different cell number requirements to be seeded for each scenario. As such, the seed trains associated with each technology and configuration may differ in terms of number of passages (expansion stages), duration and resource requirements. An example of seed train flowsheet for adherent and suspension cell culture is provided below (**Table 3.1).**

Table 3.1 Seed train flowsheets for adherent and suspension technologies.

Seed stage	Adherent	Suspension
1	T175 (175 cm^2 flas)	125 ml (flask)
2	T500 (500 cm^2 flask)	250 ml (flask)
3	L2 (1,272 cm^2 vessel)	3L (flasks)
4	CF10 (6,360 cm^2 vessel)	3L (flasks)
5	CF10 (6,360 cm^2 vessel)	RM50 (50L bag)
6	CF10 (6,360 cm^2 vessel)	RM100 (100L bag)
7		SUB200 (200L bag)

RM = rocking motion bioreactor, SUB = single-use stirred tank bioreactor, CF10 = 10-layer vessels.

Seed train raw materials requirements

The key raw materials costs associated with the seed train are the sum of all cell culture consumables costs and the media costs required in each expansion stage. Cell bank costs were assumed to be negligible in the case of the transient transfection route based on the fact that one cell bank can be used to generate multiple different viral vector products.

To determine the number of viable cells at harvest ($N_{cell,h}$), the following equation was used:

$$N_{cell,h} = N_{cell,seed} \times e^{k \times t} \quad \textbf{(3.9)}$$

Where $N_{cell,seed}$ = number of viable cells seeded

k = specific growth rate (day^{-1})

t = time between seed and harvest (day)

The following equation shows how the number of cell culture consumable units of technology *n* ($N_{unit,n,p}$) was calculated for an expansion stage, *p*, based on the number of cell culture consumable units of technology *n+1*, used at the next expansion stage, *p+1*:

$$N_{unit,n,p} = MAX\left(\frac{N_{unit,n+1,p+1} \times c_{seed} \times A_{n+1}}{c_h \times A_n}\right) \quad \textbf{(3.10)}$$

Where $N_{unit,n+1,p+1}$ = number of cell culture units of technology *n+1* required in the next expansion stage, *p+1*

c_{seed} = seeding cell density (cells/cm^2 or cells/ml)

A_{n+1} = surface area (cm^2) or working volume (ml) of the cell culture technology *n+1*

c_h = harvest cell density (cells/cm^2 or cells/ml)

A_n = surface area (cm^2) or working volume (ml) of the cell culture technology *n*

Furthermore, the media volume required for an expansion stage *p* ($V_{media,p}$) was determined using the following equation:

$$V_{media,p} = V_{unit,n,p} \times N_{unit,n,p} \quad \textbf{(3.11)}$$

Where $V_{unit,n,p}$ = working volume of the cell culture technology unit *n* used in passage *p* (L)

$N_{unit,n,p}$ = number of cell culture units of technology *n*, required in the expansion stage *p*

Seed train equipment

The key seed train equipment considered by the model were biosafety cabinets (BSC) and incubators. To calculate the number of BSC required per seed train process area (N_{BSC}), the number of BSC required per passage was determined, and the highest number of BSC was selected. The following equation was used:

$$N_{BSC} = MAX\left(\frac{N_{unit,n,p}}{c_{BSC,n}}\right) \quad \textbf{(3.12)}$$

Where $N_{unit,n,p}$ = number of units of cell culture technology *n* required per passage *p*

$c_{BSC,n}$ = BSC capacity in terms of number of units of cell culture technology *n* that can be handled by one operator per day

To calculate the number of incubators required per seed train process area ($N_{incub.}$), the number of incubators required per passage was determined, and the highest number of incubators was selected. The following equation was used:

$$N_{incub.} = MAX\left(\frac{N_{unit,n,p}}{c_{incub.,n}}\right) \quad \textbf{(3.13)}$$

Where $N_{unit,n,p}$ = number of units of cell culture technology *n* required per passage *p*

$c_{incub.,n}$ = incubator capacity in terms of number of units of cell culture technology *n* that can fit in the incubator

Seed train labour requirements

To calculate the seed train labour requirement ($N_{op.,seed}$), the following equation was used:

$$N_{op.,seed} = MAX\left(\frac{N_{unit,n,p}}{c_{op.,n}}\right) + 1 \quad \textbf{(3.14)}$$

Where $N_{unit,n,p}$ = number of units of cell culture technology *n* required per passage *p*

$c_{op.,n}$ = operator capacity in terms of number of units of cell culture technology *n* that can be handled per day

1 operator was assumed for media prep

To estimate the seed train duration (t_{seed}), the following equation was used:

$$t_{seed} = \frac{\ln\left(\frac{N_{t,cell}}{N_{0,cell}}\right)}{k} \quad \textbf{(3.15)}$$

Where $N_{t,cell}$ = number of viable cells required to seed the production bioreactor

$N_{0,cell}$ = number of viable cells in the working cell bank vial, after thaw

k = specific growth rate (day^{-1})

3.4.1.2 Upstream processing

Upstream processing raw materials

The key raw materials requirements associated with USP were cell culture bioreactor consumables, media and plasmid DNA. For the rocking motion bioreactor run in microcarrier mode, microcarrier requirement was also accounted for.

In terms of the small scale adherent technologies such as 10-layer flasks (CF10) or the hollow fibre (HF) bioreactor, since up to 36 units were allowed to run in parallel per batch, the following equation was used to determine the number of cell culture consumable units ($N_{unit,n}$) required:

$$N_{unit,n} = MAX\left(\frac{V_{h,batch}}{V_{h,unit,n}}\right) \quad \textbf{(3.16)}$$

Where $V_{h,batch}$ = harvest volume required per batch based on demand (L) (see equation **3.5** and **3.6** above)

$V_{h,unit,n}$ = harvest volume achieved from one cell culture unit of technology *n* (L) (e.g. CF10 or HF)

On the other hand, for all the other cell culture technologies, only one bioreactor was assumed to be used per batch.

In terms of media requirement, this was calculated differently depending on whether the mode of operation associated with the cell culture technology was batch mode (e.g. single-use stirred tank bioreactor), repeat batch mode (e.g. 10-layer vessels or rocking motion bioreactor run with microcarriers) or semi-continuous mode (e.g. hollow fibre bioreactor or fixed bed bioreactor). As such, the media requirement associated with the cell culture technologies run in batch mode equalled the bioreactor working volume. On the other hand, the following equations were used to determine media consumption ($V_{media,n}$) associated with technologies run in repeat batch mode **(3.17)** and semi-continuous mode **(3.18)**:

$$V_{media,n} = V_n \times N_{h,n} \quad \textbf{(3.17)}$$

Where V_n = working volume associated with technology *n* (L)

$N_{h,n}$ = number of harvest performed (including any harvests that go to waste employed in media exchanges steps) associated with technology *n*

$$V_{media,n} = V_n \times (PR_{growth,n} \times t_t + PR_{harvest,n} \times t_h) \quad \textbf{(3.18)}$$

Where V_n = working volume (L) associated with cell culture technology *n*

$PR_{growth,n}$ = perfusion rate associated with the cell growth stage (prior to transient transfection or induction) used when employing cell culture technology *n* (working volumes/day)

t_t = time (day) between inoculation and transient transfection or induction steps

$PR_{harvest,n}$ = perfusion rate associated with the time between transient transfection or induction and harvest used when employing cell culture technology *n* (working volumes/day)

t_h = time (day) between transient transfection or induction and harvest

In terms of plasmid DNA requirement ($m_{pDNA,n}$), this was calculated based on the number of viable cells achieved at the time of transient transfection as well as a factor dictating the mass of plasmid DNA required per million viable cells. The following equation was used:

$$m_{pDNA,n} = \frac{A_n \times c_{transf.}}{10^6} \times R_{pDNA} \quad \textbf{(3.19)}$$

Where A_n = surface area (cm^2) or working volume (ml) of the cell culture technology *n* used in production stage

$c_{transf.}$ = cell density at transient transfection (cells/cm^2 or cells/ml)

R_{pDNA} = plasmid DNA requirement per million viable cells (g)

For rocking motion bioreactor run with microcarriers flowsheet, the following equation was used to determine the microcarrier requirement (m_{mc}) in terms of grams (g):

$$m_{mc} = V_w \times c_{mc} \quad \textbf{(3.20)}$$

Where V_w = bioreactor working volume (ml)

c_{mc} = microcarrier concentration (g/ml)

Upstream processing equipment

The equipment required in USP depended on the type of cell culture technology employed. The multi-layered flask technology (CF10) was associated with BSC and incubator equipment requirements. In this case, the same equations were assumed as shown for the BSC and incubator equipment requirements associated with the seed train. On the other hand, for the rest of the cell culture technologies, one technology-specific control unit was assumed per cell culture unit. For each technology, tube welding equipment was accounted for.

For some technologies, such as those associated with multiple harvests (repeat batch mode or semi-continuous), specific harvest storage equipment was accounted for. This equipment consisted of a harvest bag (consumable), a bag holder, pump, jacket and a heat exchanger.

Upstream processing labour

The labour requirement associated with USP is a function of the number of cell culture units in the case of the non-scalable technologies such as multi-layer flasks or hollow fibre bioreactors or, it is a function of the harvest volume as in the case of the more scalable technologies. The team sizes assumptions are shown in **Chapter 5 (Table 5.2)**.

3.4.1.3 Downstream processing

The equations used for sizing the DSP train in terms of raw materials and consumables will be presented following the same sequence as that shown in the process flowsheets in **Chapter 6**. The strategies for determining DSP equipment and labour requirements are presented also.

Downstream processing raw materials requirements

The raw materials associated with DSP were filters, resins, bags and reagents (endonuclease and buffers). For each unit operation, size appropriate bags for storing product volume and buffers were accounted for.

To calculate the filter area, processing time and volume out associated with the depth filtration step, the following formulae were used:

Depth filter area (A_{DepthF})

$$A_{DepthF} = \frac{V_{in,DepthF}}{c_{DepthF}} \quad \textbf{(3.21)}$$

Where $V_{in,DepthF}$ = harvest volume feeding into the depth filtration step (L)

c_{DepthF} = depth filter capacity (L/m^2)

Depth filtration processing time (t_{DepthF})

$$t_{DepthF} = \frac{V_{in,DepthF}}{A_{DepthF} \times J_{DepthF}} \quad \textbf{(3.22)}$$

Where $V_{in,DepthF}$ = harvest volume feeding into the depth filtration step (L)

A_{DepthF} = depth filter surface area (m^2)

J_{DepthF} = clarification flux ($L/m^2/h$)

Volume out from the clarification step ($V_{out,DepthF}$)

$$V_{out,DepthF} = V_{in,DepthF} + A_{DepthF} \times V_{hold-up} \times (V_{fp\%} + V_{prodFV\%}) \quad \textbf{(3.23)}$$

Where $V_{in,DepthF}$ = harvest volume feeding into the depth filtration step (L)

A_{DepthF} = depth filter surface area (m^2)

$V_{hold-up}$ = hold-up volume (L/m^2)

$V_{fp\%}$ = filter preparation volume (% of hold-up volume e.g. 40%)

$V_{prodFV\%}$ = product recovery flush volume (% of hold-up volume e.g. 60%)

A size-appropriate bag was assumed to be required for the product volume (permeate).

With regards to the endonuclease step, the following equation was used to calculate the amount of endonuclease (in units, $N_{unit,endo}$) required per batch:

$$N_{unit,endo} = V_{out,DepthF} \times R_{endo.} \quad \textbf{(3.24)}$$

Where $V_{out,DF}$ = volume out from the clarification step (ml)

$R_{endo.}$ = endonuclease requirement in terms of concentration (units/ml)

With respects to the chromatography steps (assuming bind-and-elute mode), the following equations were used to determine the volume of chromatographic media required, the column volume and diameter required, the volumetric flux and processing time required per step:

Volume of chromatographic media (V_{resin})

$$V_{resin} = \frac{N_{PU,in}}{DBC} \quad \textbf{(3.25)}$$

Where $N_{PU,in}$ = number of product units (PU i.e. TU or vg) going into the first chromatography step

DBC = dynamic binding capacity in terms of product units (TU or vg) per L of chromatographic media

Column volume (V_{column})

$$V_{column} = V_{resin} \times (1 + R_{overfill}) \quad \textbf{(3.26)}$$

Where V_{resin} = calculated volume of resin required (L)

$R_{overfill}$ = resin overfill (%)

Column diameter (D_{column})

$$D_{column} = \sqrt{\frac{V_{resin} \times 4}{\pi \times H_{bed}}} \quad \textbf{(3.27)}$$

Where V_{resin} = calculated volume of resin required (ml)

H_{bed} = bed height (cm)

Chromatography volumetric flux ($Q_{chrom.}$)

$$Q_{chrom.} = \frac{\left(\frac{D_{column}}{2}\right)^2 \times \pi \times v_{max}}{60\frac{min}{h}} \quad \textbf{(3.28)}$$

Where D_{column} = column diameter (cm)

v_{max} = linear velocity (cm/h)

Chromatography processing time ($t_{chrom.\ op.}$)

$$t_{chrom.\ op.} = \frac{(CV_{eq} + CV_{wash} + CV_{el1} + CV_{el2}) \times H_{bed}}{v_{max}} + \frac{DBC}{N_{PU,in}/V_{in,chrom.}} \times \frac{H_{bed}}{v_{max}} \quad \textbf{(3.29)}$$

Where CV_{eq} = equilibration buffer column volumes

CV_{wash} = wash buffer column volumes

CV_{el1} = elution buffer 1 column volumes

CV_{el2} = elution buffer 2 column volumes

H_{bed} = bed height (cm)

DBC = dynamic binding capacity – product units (TU or vg) per L

$N_{PU,in}$ = number of product units (TU or vg) going into the chromatography step

$V_{in,chrom.}$ = volume going into the chromatography step (L)

v_{max} = linear velocity (cm/h)

Chromatography volume out (the eluate volume containing the product) ($V_{out,chrom.}$)

$$V_{out,chrom.} = V_{column} \times \frac{CV_{el2}}{1 + R_{overfill}} \quad \textbf{(3.30)}$$

Where V_{column} = column volume (L)

CV_{el2} = elution buffer 2 column volumes

$R_{overfill}$ = resin overfill (%)

Chromatographic buffers ($V_{buffer,i}$ where i represents the type of buffer e.g. equilibration, wash etc.)

$$V_{buffer,i} = V_{column} \times CV_{buffer,i} \quad \textbf{(3.31)}$$

Where V_{column} = column volume (L)

$CV_{buffer,i}$ = column volumes of buffer for stage *i* (e.g. equilibration, wash, sanitation)

For the chromatography steps, the model accounted for multiple bags such as bags for equilibration, elution and sanitation buffer as well as the eluate bag.

With regards to the ultrafiltration and diafiltration (UF/DF) step which is employed to concentrate and perform buffer exchange, the following equation was used to determine the membrane area and the diafiltration volume required:

Membrane area (A_{UFDF})

$$A_{UF} = \frac{\frac{(V_{in,UFDF} - V_{out,UF})}{J_{UF}} + \frac{V_{out,UF} \times N_{DV}}{J_{DF}}}{t_{UFDF}} \quad \textbf{(3.32)}$$

Where $V_{in,UFDF}$ = product volume going into the UF/DF step (L)

$V_{out,UF}$ = retentate volume (L)

J_{UF} = membrane flux during the concentration step (L/m^2/h)

J_{DF} = membrane flux during the diafiltration step (L/m^2/h)

t_{UFDF} = time allowed for the UFDF step (h)

N_{DV} = diafiltration volumes

Diafiltration volume ($V_{formulation}$)

$$V_{formulation} = N_{DV} \times V_{out,UF} \quad \textbf{(3.33)}$$

Where N_{DV} = diafiltration volumes

$V_{out,UF}$ = retentate volume (L)

This step was assumed to be associated with the requirement of bag/s for the diafiltration buffer and bag/s for the permeate volume. If either the diafiltration or the permeate volume exceeded the maximum bag volume assumption, the model accounted for additional bags. TAfter the UF/DF step, in the case of the LV product, it was assumed that a fixed drug substance volume was retained for QC testing ($V_{QC,DS}$). Cryobags were assumed to be used for storing drug substance. The following equation was used to determine the number of cryobags ($N_{cryobag}$) required per batch:

$$N_{cryobag} = MAX\left(\frac{V_{out,UFDF} - V_{QC,DS}}{V_{cryobag}}\right) \quad \textbf{(3.34)}$$

Where $V_{out,UFDF}$ = volume resulting from the UF/DF step (ml)

$V_{QC,DS}$ = drug substance volume retained for QC testing (ml)

$V_{cryobag}$ = cryobag working volume (ml)

The diafiltration buffer was assumed to be the formulation buffer which contained cryopreservants such as sucrose. The following equation was used to calculate the cryopreservant requirement (m_{cryo}):

$$m_{cryo.} = N_{cryobag} \times V_{cryobag} \times c_{cryo.} \quad \textbf{(3.35)}$$

Where $N_{cryobag}$ = number of cryobags

$V_{cryobag}$ = cryobag working volume (ml)

$c_{cryo.}$ = cryoprotectant concentration (ml/ml)

Downstream processing equipment requirements

For each unit operation, the following equipment units were assumed to be required. For filtration steps such as depth filtration, these were: filter housing, bag holders, heat exchanger, jacket and sterile tube welding systems. For UF/DF steps, these were: filtration skid (type dependent on membrane area requirements), bag holders and sterile tube welding systems.

For the chromatography step, in the case of the LV product, it was assumed that the column would be packed in-house and it would have a stainless steel casing. The resin was assumed to be renewed once per year, on a per product basis. In the case of the AAV product, on the other hand, it was assumed that the columns were pre-packed, and they were validated to be changed once a year, on a per product basis. Other equipment units assumed for this step were: chromatography skid (type dependent on flow rate requirements), buffer bag holders, as well as jacket and heat exchanger for the LV product only.

For the LV product only, a cryopreservation step was assumed to take place after the UF/DF. The equation used for determining the controlled rate freezer requirements in terms of number of units (N_{CRF}) is shown below:

$$N_{CRF} = MAX\left(\frac{N_{cryobag}}{N_{cryobag,max}}\right) \quad \textbf{(3.36)}$$

Where $N_{cryobag}$ = number of cryobags

$N_{cryobag,max}$ = maximum number of cryobags of drug substance that can be frozen in one day

The number of freezers required for storing the cryopreserved drug substance was calculated using the following formula:

$$N_{freezer} = MAX\left(\frac{N_{cryobag}}{N_{cryobag,max,freezer}}\right) \quad \textbf{(3.37)}$$

Where $N_{cryobag}$ = number of cryobags

$N_{cryobag,max,freezer}$ = maximum number of cryobags of drug substance that can be stored in one freezer

Downstream processing labour

The labour requirement associated with DSP is a function of the harvest volume. The team sizes assumptions are shown in **Chapter 5 (Table 5.4)**.

3.4.1.4 Fill finish

Fill finish raw materials requirements

The raw materials associated with fill finish activities were filters, bags (for product and buffers), tubing sets and cryovials.

As mentioned in the previous section, in the case of LV, it was assumed that the product volume coming out of the UF/DF step would be going into a cryopreservation hold step. The intent of this step is to conserve infectivity whilst performing titre measurement so as to inform the concentration step parameters. On the other hand, in the case of the AAV product, given its superior stability profile, it was assumed that a cryopreservation hold step would not be required, hence a sterile filtration step would occur straight after the UF/DF step. Regardless of viral vector product type, the following equation was used to determine the filter area (A_{SF}) required:

$$A_{SF} = \frac{V_{in,SF}}{c_{sf}} \quad \textbf{(3.38)}$$

Where $V_{in,SF}$ = product volume going into the sterile filtration step (L)

c_{sf} = sterile filter capacity (L/m^2)

Sterile filtration volume out ($V_{out,SF}$)

$$V_{out,SF} = V_{in,SF} + A_{SF} \times V_{prep} \quad \textbf{(3.39)}$$

Where $V_{in,SF}$ = product volume going into the sterile filtration step (L)

A_{SF} = filter area (m^2)

V_{prep} = preparation flush volume (L/m^2)

In the case of LV products, it was assumed that a sterile concentration (UF) step would take place after the sterile filtration step, so as to ensure that the drug product meets the product specifications in terms of drug product concentration. The equation used in order to determine the membrane area required for the ultrafiltration step (A_{UF}) was the following:

$$A_{UF} = V_{in,UF} \times \frac{1 - \left(\frac{V_{in,UF}}{V_{out,UF}}\right)^{-1}}{J_{UF} \times t_{max,UF}} \quad \textbf{(3.40)}$$

Where $V_{in,UF}$ = product volume going into the UF step (L)

$V_{out,UF}$ = volume out of the UF step (L)

J_{UF} = membrane flux (L/m^2/h)

$t_{max,UF}$ =maximum time allowed for the concentration step (h)

In terms of the filling step, the following equation was used to determine the number of cryovials required (N_{vial}) per batch:

$$N_{vial} = MIN\left(\frac{V_{out,fill}}{V_{vial}}\right) \quad \textbf{(3.41)}$$

Where $V_{out,fill}$ = volume exiting the filling step (ml); losses were accounted across this step

V_{vial} = working volume of a cryovial (ml)

The number of cryovials remaining after the vials required for QC testing are retrieved ($N_{vial,released}$) is shown by the following equation:

$$N_{vial,released} = N_{vial} - MAX\left(\frac{V_{QC,DP}}{V_{vial}}\right) \quad \textbf{(3.42)}$$

Where N_{vial} = number of cryovials per batch

$V_{QC,DP}$ = drug product volume to be retained for QC testing (ml)

V_{vial} = working volume of a cryovial (ml)

Tubing set costs were also accounted for by the model in the case of the filling equipment. The number of tubing set required was equal to the number of filling machines times the number of shifts required for performing the filling operations.

Fill finish equipment

While the fill finish filtration steps assumed additional equipment in line with the filtration equipment required in DSP, the filling equipment assumed consisted of an automated filling machine, located within an isolator. The equation used for determining the number of filling machines required ($N_{fill\ eq.}$) is shown below:

$$N_{fill\ eq.} = MAX\left(\frac{N_{vial}}{N_{max,fill\ eq.}}\right) \quad \textbf{(3.43)}$$

Where N_{vial} = number of cryovials per batch

$N_{max,fill\ eq.}$ = maximum number of cryovials that can be filled per operation (up to 3 days of filling were assumed, each day consisting of 3 shifts of 8h)

To determine the filling duration requirement (t_{fill}), the following equation was used:

$$t_{fill} = \frac{N_{vial}}{v_{fill}} \quad \textbf{(3.44)}$$

Where N_{vial} = number of cryovials per batch

v_{fill} = filling rate (no. cryovials/h)

To determine the number of shifts required to perform filling ($N_{shift,fill}$), the following equation was used:

$$N_{shift,fill} = MAX\left(\frac{t_{fill}}{t_{shift}}\right) \quad \textbf{(3.45)}$$

Where t_{fill} = filling duration (h)

t_{shift} = time assumed per shift (h) (e.g. 8h)

To determine the number of controlled rate freezers required ($N_{CRF,ff}$), the following equation was used:

$$N_{CRF,ff} = MAX\left(\frac{N_{vial}}{N_{CRF\ cycle,shift} \times N_{vial\ CRF}}\right) \quad \textbf{(3.46)}$$

Where N_{vial} = number of cryovials per batch

$N_{CRF\ cycle,shif}$ = number of freezing cycles per shift

$N_{vial\ CRF}$ = number of cryovials that can be frozen per cycle

To determine the number of freezers required, equation **3.37** used in the DSP section was employed here as well.

Fill finish labour

To determine the labour requirements associated with fill finish ($N_{ff\ op.}$), the following equation was used if the number of shifts required fell below 3:

$$N_{ff\ op.} = N_{shift} \times 2 \times N_{fill\ eq.} \quad \textbf{(3.47)}$$

Where N_{shift} = number of shifts (e.g. 8h per shift)

$N_{fill\ eq.}$ = number of filling equipment units

If more than 3 shifts were deemed to be required, the following equation was used to determine the number of fill finish operators:

$$N_{ff\ op.} = 3 \times 2 \times N_{fill\ eq.} \quad \textbf{(3.48)}$$

Where $N_{fill\ eq.}$ = number of filling equipment units

3.4.2 Cost of goods

The COG was calculated based on direct and indirect costs. The key direct costs considered here were raw material costs consisting of reagents (e.g. media, plasmid DNA costs (including PEI cost), endonuclease) and consumables (e.g. single-use cell culture units, membranes, filters, resins, cryovials) and QC costs. The indirect costs accounted for were labour, depreciation and maintenance (including monitoring and energy costs). The assumptions on raw materials costs, equipment costs and calculation of FCI are shown in **Chapter 5**, **Chapter 6** and the **Appendix**.

3.4.2.1 Direct costs

The equations used for determining the direct costs such as raw materials (reagents and consumables) costs and QC costs will be described in this section.

Reagents costs

To calculate the cost associated with reagents per batch ($C_{reagent,batch}$), the following equation was used:

$$C_{reagent,batch} = C_{reagent,unit} \times MAX(m_{reagent,batch}/m_{reagent,unit}) \quad \textbf{(3.49)}$$

Where $C_{reagent,unit}$ = cost of reagent per unit

$m_{reagent,batch}$ = quantity of reagent required per batch

$m_{reagent,unit}$ = quantity of reagent required per unit

Consumable costs

To calculate the cost associated with a consumable per batch ($C_{cons.,batch}$), the following equation was used:

$$C_{cons.,batch} = C_{cons.,unit} \times MAX(N_{cons.,batch}/N_{cons.,unit}) \quad \textbf{(3.50)}$$

Where $C_{cons.,unit}$ = cost of consumable per unit (case)

$N_{cons.,batch}$ = number of consumable units required per batch

$N_{cons.,unit}$ = number of consumables per unit (case)

Quality control costs

The annual QC costs ($C_{QC,annual}$) were calculated using the following formula:

$$C_{QC,annual} = C_{QC,batch} \times N_{batch,annual} \quad \textbf{(3.51)}$$

Where $C_{QC,batch}$ = QC cost per batch

$N_{batch,annual}$ = number of batches required per year

The key raw materials costs per unit and the QC costs per batch assumed in this work are presented in **Chapter 5** in the Case study set-up section.

The equation used to compute all direct costs per manufacturing run ($C_{\text{Direct cost, mfg run}}$) where *i* represents each process area type (i.e. seed, USP, DSP and fill finish) is shown below:

$$C_{Direct\ costs,mfg\ run} = N_{batch,annual} \times \left(\sum_{i}^{i=S,U,D,F} (C_{reagent,batch,i} + C_{cons.\ batch,i}) + C_{QC,batch} \right) \quad \textbf{(3.52)}$$

Where $N_{batch,annual}$ = number of batches required per year

i = process area type i.e. seed (S), USP (U), DSP (D), fill finish (F)

$C_{reagent,batch,i}$ = reagents cost per batch associated with process area type *i*

$C_{cons.,batch,i}$ = consumable cost per batch associated with process area type *i*

$C_{QC,batch}$ = QC cost per batch

3.4.2.2 Indirect costs

The indirect cost categories were labour, maintenance and depreciation. While labour requirements were determined based on cell culture technology and number cell culture units (USP) as well as the manufacturing volumes (DSP) handled, maintenance and depreciation costs were calculated based on the calculated fixed capital investment. A detailed factorial methodology for estimating FCI model developed specifically for ATMP products at UCL in collaboration with industry partners was linked to the COG model so as to generate the maintenance and depreciation costs, based on the calculation of FCI (Chilima et al. 2020). The framework calculates the facility size based on information on each flowsheet and subsequently calculates the FCI costs.

Labour costs

To calculate labour costs associated with seed train and USP activities involving multi-layer flasks or hollow fibre bioreactors ($C_{labour,annual,USP}$), the following equation was used:

$$C_{labour,annual,USP} = M \times MAX\left(\frac{N_{unit,n}}{N_{unit,op.,n}}\right) \times Sal_{op.} + C_{gowning,annual} \quad \textbf{(3.53)}$$

Where M = labour multiplier to account for costs related to management and supervisors labour (e.g. 2.2)

$N_{unit,n}$ = number of cell culture units of technology type *n* to be handled

$N_{unit,op.,n}$ = number of cell culture units of technology type *n* that can be handled by one operator

$Sal_{op.}$ = operator annual salary

$C_{gowning,annual}$ = annual gowning costs

On the other hand, the labour costs ($C_{labour,annual}$) associated with the more scalable technologies were estimated based on the working volumes and harvest volumes (configuration) to be handled using the equation below:

$$C_{labour,annual} = M \times L_n \times Sal_{op.} + C_{gowning,annual} \quad \textbf{(3.54)}$$

Where M = labour multiplier to account for costs related to management and supervisors labour (e.g. 2.2)

L_n = labour requirement for technology and configuration *n* (labour requirement of each process area type is described in Se**ction 3.4.1**)

$Sal_{op.}$ = operator annual salary

$C_{gowning,annual}$ = annual gowning costs

The gowning costs were determined based on the following equation:

$$C_{gowning,annual} = \sum_{i}^{i=S,U,D,F} N_{op.,i} \times t_{f,active} \times C_{gown,gr.} \times N_{gown,day} \quad \textbf{(3.55)}$$

Where i = process area type

n = process areas type (i.e. seed (S), USP (U), DSP (D), fill finish (F))

$N_{op.,i}$ = number of operators required per process area type

$t_{f,active}$ = time during which the facility is operational (day) e.g. 330 days per year

$C_{gown,gr.}$ = cost of a gown, depending on cleanroom grade

$N_{gown,day}$ = number of gowns to be used per day by one operator

The USP, DSP and fill finish labour assumptions used in this work are presented in **Chapter 5,** Case study set-up section.

The total labour cost per year was determined using the following equation ($C_{labour,annual}$):

$$C_{labour,annual} = N_{train} \times (C_{labour,seed} + C_{labour,USP} + C_{laboour,DSP} + C_{labour,ff}) \quad \textbf{(3.56)}$$

Where N_{train} = number of manufacturing trains

$C_{labour,seed}$ = seed train annual labour cost

$C_{labour,USP}$ = USP annual labour cost

$C_{labour,DSP}$ = DSP annual labour cost

$C_{labour,ff}$ = fill finish annual labour cost

Fixed capital investment

The maintenance and the depreciations costs categories were calculated as a function of fixed capital investment (FCI). To calculate FCI, the following formula was used:

$$FCI = C_{equipment} + C_{p,support} + C_{logisics\ eq.} + C_{QC,eq} + C_{EMS} + C_{shell} + C_{fitout} + C_{land,yard} + C_{cf} + C_{eng,mng,cf} + C_{con} \quad \textbf{(3.57)}$$

Where $C_{equipment}$ = total equipment cost

$C_{p,support}$ = process support equipment cost

$C_{logisics\ eq.}$ = logistics equipment cost

$C_{QC,eq}$ = QC equipment cost

C_{EMS} = environmental monitoring systems cost

C_{shell} = shell building cost

C_{fitout} = fit-out costs

C_{cf} = contractor's fee

$C_{land,yard}$ = land and yard improvement costs

$C_{eng,mng,cf}$ =project design, engineering, management and consultant's fee costs

C_{con} = contingency costs

To calculate the equipment costs ($C_{equipment}$), the following equation was used:

$$C_{equipment} = N_{train} \times \sum_{j}^{n} C_{equipment,j} \times MAX\left(\frac{N_{unit,j}}{c_{equipment,j}}\right) \quad \textbf{(3.58)}$$

Where N_{train} = number of manufacturing trains

n = all equipment type required e.g. biosafety cabinet, incubator etc.

$C_{equipment,j}$ = equipment j unit cost

$N_{unit,j}$ = number of consumable units required per equipment j

$c_{equipment,j}$ = maximum number of consumable units that can be accommodated by one unit of equipment j

The equipment requirements for each process area type are discussed in **Section 3.4.1** in this chapter.

To calculate the process support equipment cost ($C_{p,support}$), the following equation was used:

$$C_{p,support} = A_{cleanroom,f} \times C_{pe,sqm} \quad \textbf{(3.59)}$$

Where $A_{cleanroom,f}$ = total cleanroom footprint (m^2)

$C_{pe,sqm}$ = process support equipment cost per m^2 of cleanroom

To calculate the logistics equipment cost ($C_{logistics\ eq.}$), the following equation was used:

$$C_{logisics\ eq.} = A_{cleanroom,f} \times C_{logistics\ eq.,sqm} \quad \textbf{(3.60)}$$

Where $A_{cleanroom,f}$ = total cleanroom footprint (m^2)

$C_{logistics\ eq.,sqm}$ = logistics equipment cost per m^2 of cleanroom

To calculate the cleanroom area required per facility ($A_{cleanroom,f}$), the following equation was used:

$$A_{cleanroom,f} = N_{train} \times \frac{(A_{eq.,seed} + A_{eq.,USP} + A_{eq.,hs} + A_{eq.,DSP} + A_{eq.,ff})}{r_{eq.,cr.}} \quad \textbf{(3.61)}$$

Where N_{train} = number of manufacturing trains required per facility

$A_{eq.,seed}$ = total seed equipment footprint (m^2)

$A_{eq.,USP}$ = total USP equipment footprint (m^2)

$A_{eq.,hs}$ = total harvest storage equipment footprint (m^2)

$A_{eq.,DSP}$ = total DSP equipment footprint (m^2)

$A_{eq.,ff}$ = total fill finish equipment footprint (m^2)

$r_{eq.,cr.}$ = ratio of equipment footprint to cleanroom area

In general, to calculate the total equipment footprint per any process area type (e.g. seed, USP, DSP or fill finish) ($A_{eq.,area}$), the following equation was used:

$$A_{eq.,area} = \sum_{i}^{n} A_{eq.,i} \times N_{eq.,i} \quad \textbf{(3.62)}$$

Where $A_{eq.,i}$ = footprint of equipment type *i* (m^2)

$N_{eq.,i}$ = number of equipment type *i*

n = number of different types of equipment

To calculate the QC labs cost ($C_{QC,eq.}$), the following equation was used:

$$C_{QC,eq.} = N_{QC\ lab} \times C_{QC\ eq.,lab} \quad \textbf{(3.63)}$$

Where $N_{QC\ lab}$ = number of QC labs

$C_{QC\ eq.,lab}$ = QC equipment cost per lab

To calculate the environmental monitoring system cost (C_{EMS}), the following equation was used:

$$C_{EMS} = C_{CU} + (N_r \times 3 \times 3) + \left(\sqrt[2]{A_{cleanroom,f} + \left((A_{PAL} + A_{PAL}) \times N_r\right)}\right) \quad \textbf{(3.64)}$$

Where C_{CU} = central environmental monitoring system unit cost

N_r = number of processing rooms

$A_{cleanroom,f}$ = total cleanroom footprint (m^2)

A_{PAL} = personnel airlock footprint (m^2)

A_{MAL} = material airlock footprint (m^2)

To calculate the cost associated with the shell, the following equation was used:

$$C_{shell} = A_f \times C_{shell,sqm} \quad \textbf{(3.65)}$$

Where A_f = total facility footprint (m^2)

$C_{shell,sqm}$ = building shell cost per m^2

To determine the total facility footprint (A_f), the following equation was employed:

$$A_f = A_{clean\ change} + A_{grD} + A_{CNC} + A_{un.} \quad \textbf{(3.66)}$$

Where $A_{clean\ change}$ = total clean change area (m^2)

A_{grD} = grade D area (m^2)

A_{CNC} = controlled not classified area (m^2)

$A_{un.}$ = unclassified area (m^2)

The equation for the total clean change footprint ($A_{clean\ change}$) used is show below:

$$A_{clean\ change} = A_{cleanroom,f} \times \left[N_r \times (r_{cc1} + r_{cc2}) + r_{cco} + r_{cj}\right] \quad \textbf{(3.67)}$$

Where $A_{cleanroom,f}$ = total cleanroom footprint (m^2)

N_r = number of processing rooms

r_{cc1} = ratio of clean change 1 to cleanroom footprint

r_{cc2} = ratio of clean change 2 to cleanroom footprint

r_{cco} = ratio of clean corridor to cleanroom footprint

r_{cj} = ratio of clean janitor to cleanroom footprint

To determine the grade D footprint requirement (A_{grD}), the following equation was used:

$$A_{grD} = N_{QC\ lab} \times A_{cleanroom,f} \times (r_{QC\ lab} + r_{micro} + r_{lab\ c.} + r_{PCR} + r_j) \quad \textbf{(3.68)}$$

Where $N_{QC\ lab}$ = number of QC labs

$A_{cleanroom,f}$ = total cleanroom footprint (m^2)

$r_{QC\ lab}$ = ratio of QC lab to cleanroom footprint

r_{micro} = ratio of microbiology lab to cleanroom footprint

$r_{lab\ c.}$ = ratio of lab corridor to cleanroom footprint

r_{PCR} = ratio of PCR room to cleanroom footprint

r_j = ratio of janitor room to cleanroom footprint

To determine the controlled non-classified footprint (A_{CNC}), the following equation was used:

$$A_{CNC} = A_{cleanroom,f} \times r_{plant} \quad \textbf{(3.69)}$$

Where $A_{cleanroom,f}$ = total cleanroom footprint (m^2)

r_{plant} = ratio of plant level footprint to cleanroom footprint

To determine the unclassified footprint ($A_{un.}$), the following equation was used:

$$A_{un.} = A_{cleanroom,f} \times \sum_{i}^{n} r_i \quad \textbf{(3.70)}$$

Where $A_{cleanroom,f}$ = total cleanroom footprint (m^2)

r_i = ratio of unclassified area to cleanroom footprint

n = total number of different unclassified areas (e.g. waste corridor, change and treatment, logistics, offices, meeting rooms, reception, lorry loading docks, WC etc.)

To calculate the facility fit-out cost (C_{fitout}), the following equation was used:

$$C_{fitout} = A_{gr.B} \times C_{gr.B,sqm} + A_{gr.C} \times C_{gr.C,sqm} + A_{gr.D} \times C_{gr.D,sqm} + A_{CNC} \times C_{CNC,sqm} + A_{un.} \times C_{un.,sqm} + A_{hs} \times C_{coldr,sqm} \quad \textbf{(3.71)}$$

Where $A_{gr.B}$ = grade B cleanroom footprint (including clean change area) in m^2

$C_{gr.B,sqm}$ = grade B cleanroom cost per m^2

$A_{gr.C}$ = grade C cleanroom footprint (including clean change area) in m^2

$C_{gr.C,sqm}$ = grade C cleanroom cost per m^2

$C_{gr.D,sqm}$ = grade D cleanroom cost per m^2

$C_{CNC,sqm}$ = CNC area cost per m^2

$C_{un.,sqm}$ = unclassified area cost per m^2

$C_{coldr,sqm}$ = cold room area cost per m^2 assumed to be required only in the case of multi-layered cell culture technology

A_{HS} = harvest storage area in m^2

To determine the contractors' fees (C_{cf}), the following equation was used;

$$C_{cf} = C_{fitout} \times r_{cf} \quad \textbf{(3.72)}$$

Where C_{fitout} = facility fit-out cost

r_{cf} = ratio of contractors' fees from total facility fit-out costs

To determine the land and yard improvement cost ($C_{land,yard}$), the following equation was used:

$$C_{land,yard} = C_{shell} \times (r_l + r_{yard}) \quad \textbf{(3.73)}$$

Where C_{shell} = shell cost

r_l = ratio of land costs to shell costs

r_{yard} = ratio of yard improvement costs to shell costs

To determine the project design, engineering, management and consultant's fee cost ($C_{eng,mng,cf}$), the following equation was used:

$$C_{eng,mng,cf} = \left(C_{equipment} + C_{p,support} + C_{logisics,eq} + C_{EMS} + C_{p.eq.i.} + C_{QC\ lab} + C_{shell} + C_{fitout} + C_{land,yi}\right) \times r_{eng} \quad \textbf{(3.74)}$$

Where $C_{equipment}$ = total equipment purchase cost

$C_{p,support}$ = process support equipment cost

$C_{logisics,eq}$ = logistics equipment cost

C_{EMS} = environmental monitoring system cost

$C_{p.eq.i.}$ = process equipment installation cost

r_{eng} =engineering, management and consultants fees percentage

Contingency was determined using the following equation:

$$C_{con} = \left(C_{equipment} + C_{p,support} + C_{logisics,eq} + C_{EMS} + C_{p.eq.i.} + C_{QC\ lab} + C_{shell} + C_{fitout} + C_{land,yard}\right) \times \left(1 + r_{eng}\right) \times r_{con} \quad \textbf{(3.75)}$$

Where $C_{equipment}$ = total equipment cost

$C_{p,support}$ = process support equipment cost

$C_{logisics,eq}$ = logistics equipment cost

C_{EMS} = environmental monitoring system cost

$C_{p.eq.i.}$ = process equipment installation cost

$C_{QC\ lab}$ = QC labs cost

C_{shell} = shell building cost

C_{fitout} = fit-out cost

$C_{land,yard}$ = land and yard improvement cost

r_{eng} = engineering, management and consultants fee percentage

r_{con} = contingency percentage relative to project direct costs and fees

Maintenance and depreciation costs

The annual maintenance cost ($C_{maint.,annual}$) was calculated using the following equation:

$$C_{maint.,annual} = FCI \times P_{annual} + C_{monit.,annual} + C_{energy,annual} \quad \textbf{(3.76)}$$

Where FCI = fixed capital investment

P_{annual} = annual percentage (e.g. 10%)

$C_{monit.,annual}$ = annual facility monitoring cost

$C_{energy,annual}$ = annual facility energy cost

To calculate the annual cleanroom monitoring cost ($C_{monit.,annual}$), the following equation was used:

$$C_{monit.,annual} = \sum_{i,j}^{n,m} A_i \times C_{j,sqm} \quad \textbf{(3.77)}$$

Where *i* = process area type (e.g. seed, USP, DSP, fill finish)

n = total number of process areas types

j = cleanroom grade area type (e.g. B, C)

m = total number of cleanroom grade types

$C_{j,sqm}$ = cleanroom monitoring costs per m^2 for grade j

A_i = process area i footprint (m^2)

To calculate the annual energy cost ($C_{energy,annual}$), the following equation was used:

$$C_{energy,annual} = A_{cleanroom,f} \times C_{energy,sqm} \quad \textbf{(3.78)}$$

Where $A_{cleanroom,f}$ = total cleanroom footprint (m^2)

$C_{energy,sqm}$ = energy costs per m^2

The equation used to determine the annual depreciation cost ($C_{depr.,annual}$) is shown below:

$$C_{depr.,annual} = \frac{FCI}{F_{lifetime}} \quad \textbf{(3.79)}$$

Where FCI = fixed capital investment

$F_{lifetime}$ = facility lifetime (years)

As discussed in **Section 3.4.1,** the bioprocess economics model was run in rate mode in order to generate the results described in **Chapter 5** and **Chapter 6**. As such, the indirect costs per manufacturing run were calculated as a percentage of the annual indirect costs, dictated by the facility utilisation level. The following equations were used so as to determine facility utilisation ($F_{utilisation}$) **(3.80)** and manufacturing time ($t_{manufacture}$) **(3.81)**:

$$F_{utilisation} = \frac{t_{manufacture}}{t_{f,active}} \quad \textbf{(3.80)}$$

Where $t_{manufactur}$ = manufacturing time required to deliver for a certain demand (day)

$t_{f,active}$ = time during which the facility is operational (day) per year e.g. 330 days

A campaign-system was used whereby a campaign represented a group of batches sharing one seed train. Two campaign sizes were assumed so as to minimise overproduction scenarios. The manufacturing time required to deliver for a certain demand ($t_{manufacture}$) was calculated using the following formula:

$$t_{manufacture} = N_{campaign_{s1}} \times \left[t_{seed1} + N_{batch_{s1}} \times (t_{USP} + t_{DSP} + t_{FF} + t_{turnaround})\right] + N_{campaign_{s2}} \times \left[t_{seed2} + N_{batch_{s2}} \times (t_{USP} + t_{DSP} + t_{FF} + t_{turnaround})\right] \quad \textbf{(3.81)}$$

Where $N_{campaign_{s1}}$ = number of campaigns of size 1

t_{seed1} = time required to seed batch 1 of campaign size 1

$N_{batch_{s1}}$ = number of batcher per campaign size 1

t_{USP} = upstream processing time

t_{DSP} = downstream processing time

t_{FF} = fill finish time

$t_{turnaround}$ = turnaround time of the titration assay

t_{hold} = hold time

$N_{campaign_{s2}}$ = number of campaigns of size 2

t_{seed2} = time required to seed batch 1 of campaign size 2

$N_{batch_{s2}}$ = number of batches per campaign size 2

The indirect costs associated with a manufacturing run ($C_{indirect,mfg.\ run}$) are calculated using the following equation:

$$C_{indirect,mfg.run} = (C_{labour,annual} + C_{maint.,annual} + C_{depr.,annual}) \times F_{utilisation} \quad \textbf{(3.82)}$$

Where $C_{labour,annual}$ = total labour cost per year

$C_{maint.,annual}$ = maintenance cost per year

$C_{depr.,annual}$ = depreciation cost per year

$F_{utilisation}$ = facility utilisation

The equation used to determine the cost of goods per dose ($COG_{VV/dose}$) is given below:

$$COG_{VV}/dose = \frac{C_{Direct\ costs,mfg\ run} + C_{indirect,mfg\ run}}{N_{dose,annual}} \quad \textbf{(3.83)}$$

Where $C_{Direct\ costs,mfg\ run}$ = direct cost (raw materials and QC) associated with the manufacturing run

$C_{indirect,mfg\ run}$ = indirect cost (labour, depreciation and maintenance) associated with the manufacturing run

$N_{dose,annual}$ = annual demand (number of doses)

3.5 Cost of drug development

A methodology for calculating the cost of drug development ($C_{development}$) activities was implemented based on a similar framework described in Hassan et al. (2016). The $C_{development}$ captured Chemistry, Manufacturing and Controls (CMC) activities such as process development (CMC_{PD} i.e. process and analytical development, tech transfer,

stability studies), process performance qualification (PPQ) batches (CMC_{PPQ}), clinical manufacture (CMC_{MFG}) and clinical trials activities (**Table 3.2**). Preclinical and nonclinical studies costs were not included. For the base case process (i.e. using transient transfection), the CMC activities assumed were process and analytical development, stability studies, clinical manufacture, and process performance qualification (PPQ). In addition to these costs, for a process change scenario such as to a stable producer cell line (SPCL) system, cell line development, cell banking and testing were accounted for, as well as comparability studies and bridging studies costs if the change to SPCL occurred later in development.

The CMC_{PD} costs for the key process development activities were determined using a full-time equivalent (FTE) basis (personnel costs in terms of roles, number of FTEs and duration), apart from comparability studies. The development assumptions input category in **Figure 3.1** is defining the development efforts in terms of personnel costs required in preparation for each critical stage of the project (i.e. clinical trial phases, regulatory review or post-approval process change), associated with the particular product and process data inputs. The manufacturing costs for comparability studies and bridging studies, CMC_{PPQ} and CMC_{MFG} were determined using the bioprocess economics model described in **Section 3.4**, above. Clinical trials costs for each phase and for bridging studies were calculated based on estimated clinical trial cost per patient and the number of patients in each phase. These costs were assumed to include costs for patient enrolment, medical procedures, toxicology and pharmacokinetic laboratory work, hospital staff and clinical infrastructure, data management and clinical supply (McGuire 2013). The product and process data in **Figure 3.1** provides information on the product and process type which may influence development durations (i.e. transient transfection versus SPCL processes) and the clinical trials sizes in terms of number of patients per trial (indication type).

Table 3.2 Assumptions in the process change evaluation framework related to the drug development activities and their cost basis.

Abbreviation	Activity	Details of activity	When they occur	Cost basis
CMC_{PD}	**Cell line, Process & Analytical development**	Cell line development, testing and banking; Process and analytical development, scale-up and optimisation; Tech transfer; Regulatory support; Process characterisation; Process and analytical qualification and validation	Cell line development required only in the SPCL scenarios; Prior to Phase 1, Phase 3 and Regulatory Review; Post-approval: if process change takes place post-approval	$\sum_{k=1}^{N_{activity}} C_{FTE,annual} \times N_{FTE,k} \times t_{,k}$ **(3.84)**
	Comparability studies	Manufacture of batches using both transient transfection and SPCL process; If *ex vivo* gene therapy, additional donor material cell batches need to be generated and transduced with viral vector from comparability batches; Extensive material characterisation of each batch	If there is a process change occurring post Phase 1 clinical trial	$3 \times (COG_{VV,batch,TT} + C_{charact.}) + 3 \times (COG_{VV,batch,SPCL} + C_{charact.}) + 6 \times COG_{cell}$ **(3.85)**
	Stability studies	Create a stability study plan; Carry out analytical tests at various time points in different conditions	Early and late phase clinical trials; At BLA/ MAA filling using PPQ material; These are repeated in case there is a post-approval process change	$\sum_{k=1}^{N_{study}} N_{sample,k} \times C_{test,k}$ **(3.86)**
CMC_{PPQ}	**Process performance qualification**	Run three PPQ batches as part of process validation	Post Phase 3 clinical trial, in preparation for market authorisation application; These are repeated in case there is a post-approval process change	$3 \times COG_{batch,\,Ph3}$ **(3.87)**
CMC_{MFG}	**Clinical manufacture**	Engineering runs; Clinical material generation;	For each clinical trial phase and for potential bridging studies	$\sum_{k=1}^{N_{trial}} N_{batch,k} \times COG_{batch,k}$

Abbreviation	Activity	Details of activity	When they occur	Cost basis
		Includes a phase-appropriate overproduction level for the generation of stability studies material		**(3.88)**
Clinical	**Clinical trials**	Patient information and recruitment; Clinical study management; Data management	For each clinical trial phase and for potential bridging studies	$\sum_{k=1}^{N_{trial}} N_{patient,k} \times C_{patient,k} + C_{overhead,k}$ **(3.89)**

COG = cost of goods, PPQ = process performance qualification, FTE = full-time equivalent, N = number, C= cost, VV = viral vector, TT = transient transfection, SPCL = stable producer cell line, charact. = extensive material characterisation package, t = time, COG_{cell} = cost of manufacturing *ex vivo* cell therapy product using donor leukapheresis, BLA = biologics license application, MAA = marketing authorisation application, y = year, Ph3 = phase 3 clinical trial, $C_{test,k}$ = cost per test used in study k per sample. Nonclinical studies costs were not included.

3.6 Project valuation model

Here, a risk-adjusted net present value (rNPV) project valuation methodology is used to assess the profitability of a gene therapy project as described in Bogdan and Villiger (2010). A positive rNPV indicates an attractive project and the higher the rNPV, the higher the profit promised by a project. To capture the impact of the R&D risks associated with a project's progression through to commercial phase, phase transition probabilities determined for cell therapy projects in Hassan et al. (2016) were adopted here and used to determine the yearly cumulative success probabilities ($P_{CF,t}$) to adjust each cash flow (CF_t) by. The resulting risk-adjusted cash flows were then discounted using the discount factor ($(1+r)^{-t}$) accounting for the time value of money and summed to determine the rNPV:

$$rNPV = \sum_{t=1}^{t=Time} (1+r)^{-t} \times P_{CF,t} \times CF_t \quad \textbf{(3.90)}$$

Where r = discount rate

$P_{CF,t}$ = yearly cumulative success probabilities

CF_t = cash flow at year t

t = year

Time = project lifetime (years)

In terms of the cash flow assumptions (**Figure 3.1**), the user can define the project lifecycle duration in terms of clinical trials, regulatory review, any delay to reaching market (i.e. due to bridging studies or SPCL development duration) and commercial phase durations. Furthermore, the user can input proposed selling price, market uptake rates (building up the revenue stream), discount rates and corporate tax rates. On the other

hand, the bioprocess economics and the cost of drug development models' outputs generated at each time point of the cash flow represent the outgoings, together with additional costs such as those associated with other manufacturing processes and supply chain costs. Product data assumptions impact the cash flow such that, if an *ex vivo* gene therapy is selected, the cash flow will include outgoings related to the cell process manufacture. Supply chain costs are also accounted for since effective supply chain management is required for ensuring supply continuity of key starting materials, raw materials and consumables as well as needle-to-needle logistics if the product is autologous.

3.7 Brute force optimisation

Brute force (BF) optimisation is a method whereby all possible solutions to a problem are produced and then tested to check whether they meet the problem statement. Written in Visual Basic for Applications (VBA, Microsoft® Corporation, Redmond, WA), BF algorithms were employed extensively in this work as means of automating routinely used tasks as well as automating solution search runs. For example, a BF algorithm was built so as to rapidly test the impact of changes in a variety of input values on the tool outputs such as profitability ranking of scenarios of processes utilising different expression systems and identify the optimal solution. Other VBA programs were implemented as part of the tool architecture so as to facilitate the rapid update of tool outputs when changing development or cost of goods assumptions. When searching for the most optimal viral vector cell culture technology, a BF optimization algorithm was used to rapidly evaluate a plurality of demands and batch sizes (number of doses per batch) scenarios using the bioprocess economics model and store outputs such as the optimal sizes amongst all technologies, the ranking of technologies, COG_{VV}/dose, FCI and COG breakdown for each scenario.

3.8 Data collection

The gene therapy process change tool described in this chapter was built using fixed equations and parameters as well as parameter selected by the user. With regards to the fixed equations and parameters, the data used to build this tool were mainly based on the work published by the UCL Decisional Tools Research Group, thorough literature research and extensive discussions with industry and academic experts. Furthermore, with regards to the parameters selected by the user, described in the Case study set-up sections of the **Chapter 4-6,** these were also based on thorough literature research, discussions with experts as well as engaging with cell and gene therapy technology vendors. With regards to **Chapter 4**, since the tool used to generate this work had been already developed, the data collection methods had already been reviewed (Pereira Chilima 2019). However, amendments were performed to the assumptions used by this tool so as to ensure it uses more realistic inputs and hence generates more realistic outputs. The data used to update this tool was obtained from discussions with cell and gene therapy experts such as Bo Kara (Evox Therapeutics, Oxford, United Kingdom), and Fritz Fiesser, Nathalie Moens and Sandro Gomez (GSK Brentford, United Kingdom). The data collected for gene therapy-specific bioprocess economics tool described in this chapter originated from discussions with Bo Kara, Fritz Fiesser, Tarik Senussi (Gyroscope Therapeutics, London, United Kingdom), Paul Carter (Quell Therapeutics, London, United Kingdom), Sean Baker (GSK, Brentford, United Kingdom), James Miskin (Oxford Biomedica, Oxford, United Kingdom), Tania Pereira Chilima (Univercells, Gosselies, Belgium), Sven Ansorge (ExCellThera, Quebec, Canada), Aziza Manceur (National Research Council Canada, Ontario, Canada), Shane Knowles (Pall Corporation, NY, USA), Clive Glover (Pall Corporation, NY, USA), Layka Abbasi (Terumo BCT, Clorado, USA), Hanna Lesch (Kuopio Center, Kuopio, Finland), Michael Greene (iVexSol, MA, USA), Rachel Legmann (Repligen, MA, USA).

3.9 Conclusions

This chapter has described an advanced decisional tool specifically designed to address key questions that developers need to find answers for on their journey to commercialise gene therapy products. To address questions surrounding process design and process performance for viral vector manufacture, the bioprocess economics model, containing a COG and a FCI model, was developed and run in conjunction with brute force optimisation algorithms to generate the results described in **Chapter 5**. On the other hand, to address questions surrounding gene therapy portfolio, impact of process change, manufacturing strategy or raw materials cost variation on financial metrics such as cost of drug development, project lifecycle cost or profitability, additional tool components were built and run to generate the results described in **Chapter 6**. These were the cost of drug development model and the project valuation model using risk-adjusted net present value methodology. The decisional tool was built with modularity and flexibility in mind. For example, at the process level the input dashboards enable different technologies with their own mass balance and resource requirements to be selected for each stage of the process. Whilst at the enterprise level, it is possible to explore scenarios with different attrition rates, costs and durations for each phase of development.

Chapter 4: CAR T therapy supply chain economics and decision-making at the enterprise level

4.1 Introduction

The supply chain of autologous cell and gene therapies was introduced in **Chapter 1** with the alternative enterprise models ranging from single-site centralised manufacture through to the vision for bedside manufacture in the context of CAR T-cell therapy products. The key challenges associated with CAR T-cell therapy manufacture were discussed providing a particular focus on the logistical hurdles and risks of transportation of starting materials and high value products associated with the centralised manufacture paradigm (Papathanasiou et al. 2020). Furthermore the decentralised manufacturing models that have been explored in literature were outlined (Lam et al. 2021; Harrison et al. 2016; Harrison et al. 2017; Lopes et al. 2020; Ran et al. 2020). Moreover, progress achieved so far in process automation that would enable the wider adoption of hospital-based manufacturing models was reviewed (Zhu et al. 2018; Lock et al. 2017; Mukherjee et al. 2021; Jackson et al. 2020b; Marín Morales et al. 2019; Moutsatsou et al. 2019).

This chapter addresses the following CAR T-cell manufacture questions: what are the most optimal enterprise models for decentralised manufacture from profitability and shop-floor logistics perspectives. Furthermore, in the context of addressing the challenges associated with the "GMP-in-a-box" model, what is the impact of different financial agreements between the hospital and the sponsor company on the attractiveness of the "GMP-in-a-box" model. And lastly, what is the impact of QC equipment automation on financial metrics. These questions were addressed using a decisional tool previously described in Pereira Chilima (2019) which was updated with the most recent industry data. Mentioned in **Chapter 3**, this tool consists of an autologous CAR T-cell therapy whole bioprocess economics model which calculates COG and includes a detailed

factorial FCI calculation methodology, as well as a risk-adjusted commercial stage cash-flow model. **Section 4.2** provides new assumptions and information on key equations and any updates to the equations. Thus, the impact of adopting alternative enterprise models to the centralised model was analysed by accounting for cash flows associated with the time point of establishing the manufacturing site/s and entering the market, all the way to the end of the product lifecycle. This chapter builds on the previous work described in Pereira Chilima (2019) by exploring the impact of constraints on facility size on the enterprise models' financial performance and by providing insights into the financial implications of adopting "GMP-in-a-box"-like models and QC automation.

This chapter is organised as follows. **Section 4.2** provides an overview of the case study, the key assumptions surrounding the CAR T-cell product and manufacturing process as well as the enterprise models' characteristics and any other key assumptions. **Section 4.3.1** discusses the profitability and operational feasibility screening performed on the enterprise models while **Section 4.3.2** addresses the ranking of enterprise models across demands and selling prices. **Section 4.3.3** brings the focus onto the "GMP-in-a-box" models by providing a picture of the hospital profits estimated for these models in **Section 4.3.3.1**, assessing their associated maximum values for revenue share and mark-up, respectively, in **Section 4.3.3.2**. Finally, **Section 4.3.3.3** provides an analysis of the impact of automation on COG and profitability and **Section 4.4** provides the conclusion of this chapter.

4.2 Case study set-up

4.2.1 Case study overview

The CAR T-cell therapy decisional tool introduced in **Chapter 3** was employed to explore alternative enterprise models to the centralised paradigm for the autologous gene-modified cell therapy manufacture from profitability and shop-floor logistics perspectives.

In terms of the focus adopted in this chapter on the ATMP supply chain, **Chapter 4** takes a helicopter view and addresses the overall gene-modified autologous supply chain circuit shown in **Figure 4.1**. In the context of the centralised and decentralised manufacturing models, the key activities that were accounted for were leukapheresis collection, transportation (frozen-in, frozen-out), CAR T-cell core manufacture, and CAR T-cell product transportation to the administration site (**Figure 4.1a**). On the other hand, in the case of the hospital-based manufacturing models, the key activities accounted for were leukapheresis and CAR T-cell core manufacture as the leukapheresis collection and the product administration sites were assumed to be located within the same hospital site (**Figure 4.1b**).

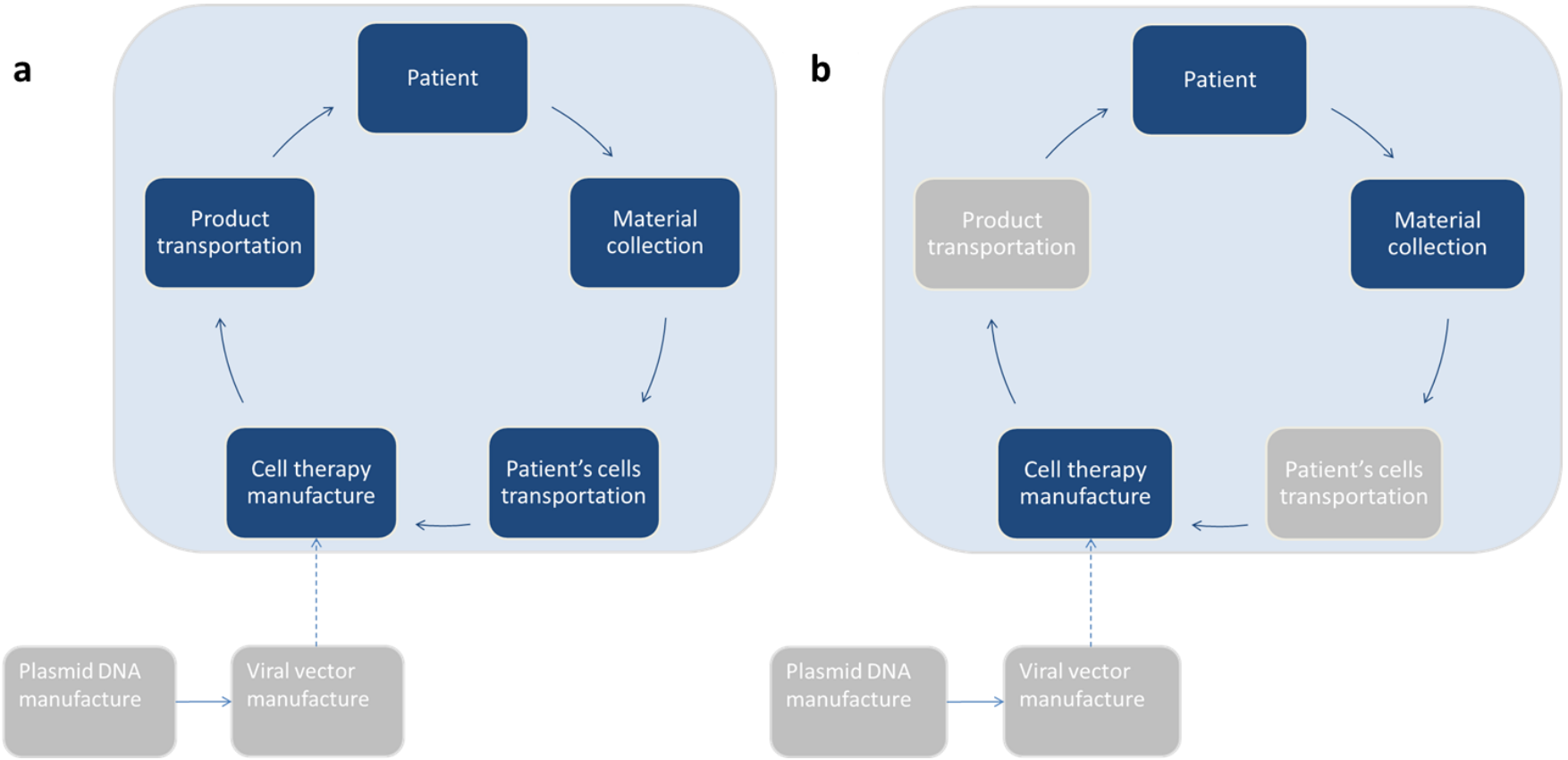

Figure 4.1 Gene therapy supply chain diagram presenting the autologous gene-modified cell therapy focus adopted in **Chapter 4** where the key areas accounted for in the analyses are shown in blue for **a)** the centralised and the regional models and for **b)** the hospital-based manufacturing models. The areas not included were greyed out. The patients' cells (leukapheresates) as well as the final product were assumed to be transported frozen in the case of the centralised and regional models.

Whilst the centralised (single-site) model is associated with advantages to the sponsor company of full control over the manufacturing site and being the sole recipient of the reimbursement, it is perceived to be associated with high capital investment and risks related to logistics and potentially slow response to market fluctuations (Medcalf 2016; Trainor et al. 2014). On the other hand, decentralised manufacturing models benefit from less complex or no transportation needs and potentially lower capital investment based on the possibility of leveraging existing facilities. However, multiple manufacturing sites require multiple manufacturing licences, oversight and, potentially reimbursement share schemes between sponsor company and manufacturing partners (Harrison et al. 2017; Harrison et al. 2016). These trade-offs will be analysed in this chapter. The first objective was to determine the number of sites limits for each decentralised model based on a range of demands from profitability and operational feasibility perspectives and analyse the profitability and investment ranking of the models. The second objective was to explore the feasibility of the bedside manufacturing models in terms of the hospital financial metrics across a range of selling prices, and the impact of future improvements in QC equipment automation on costs and profitability.

This work encompassed the analysis of four enterprise models associated with different capital investment, running costs and responsibility distribution assumptions in the context of autologous CAR T-cell therapy manufacture across a range of demands and selling prices. Apart from the centralised model, three decentralised enterprise models are presented: the regional model and two hospital-based models: the rented hospital and "GMP-in-a-box" (GMPiB) bedside manufacturing models. The GMPiB bedside manufacturing models consisted of a model where reimbursement is shared between the sponsor company and the hospital model and another model where the hospital operates in a CMO-like fashion. The next sections detail the key assumptions related to the CAR

T product, the associated manufacturing process, QC and the enterprise models' characteristics.

4.2.2 Key CAR T-cell therapy product assumptions

The case study describes the commercialisation options for an autologous CAR T-cell therapy product with a dose size of 250 million CAR T-cells, a demand ranging between 1,000 and 10,000 doses/year and a selling price ranging between $160,000 and $400,000/dose based on existing products information on the market (FDA 2018a; Jørgensen et al. 2020; Munshi et al. 2021). The genetic modification of the patients' T-cells was assumed to be achieved using a lentiviral vector.

The costs associated with establishing leukapheresis collection and final product administration centres have not been accounted for given the lack of visibility over the financial data of such partnerships. Furthermore, in this analysis, supply chain management costs associated with needle-to-needle logistics and sourcing of starting materials such as viral vectors were not captured, as the data was not available when the work was performed. Moreover, the cost of drug development is not included in this analysis. However, the supply chain related costs as well as the cost of drug development for a range of cell and gene therapy products were captured in the case studies described in **Chapter 6**.

4.2.3 Key CAR T-cell therapy manufacturing process assumptions

4.2.3.1 Process flowsheet

The 10-day long core manufacturing process of the specific CAR T-cell therapy described here was assumed to be performed using an integrated USP/DSP platform (INT) such as the CliniMACS Prodigy® (Milteny Biotec, Bergisch Gladbach, Germany) device system. All core manufacturing steps post-thaw of the leukapheresate, other than the initial cell separation step (elutriation) and the cryopreservation step at the end of the process were

assumed to take place on the INT system. The flowsheet assumed is shown in **Figure 4.2**. The elutriation step was assumed to take place on an elutriation system such as the Elutra® while cryopreservation step was assumed to be performed using a controlled-rate freezer.

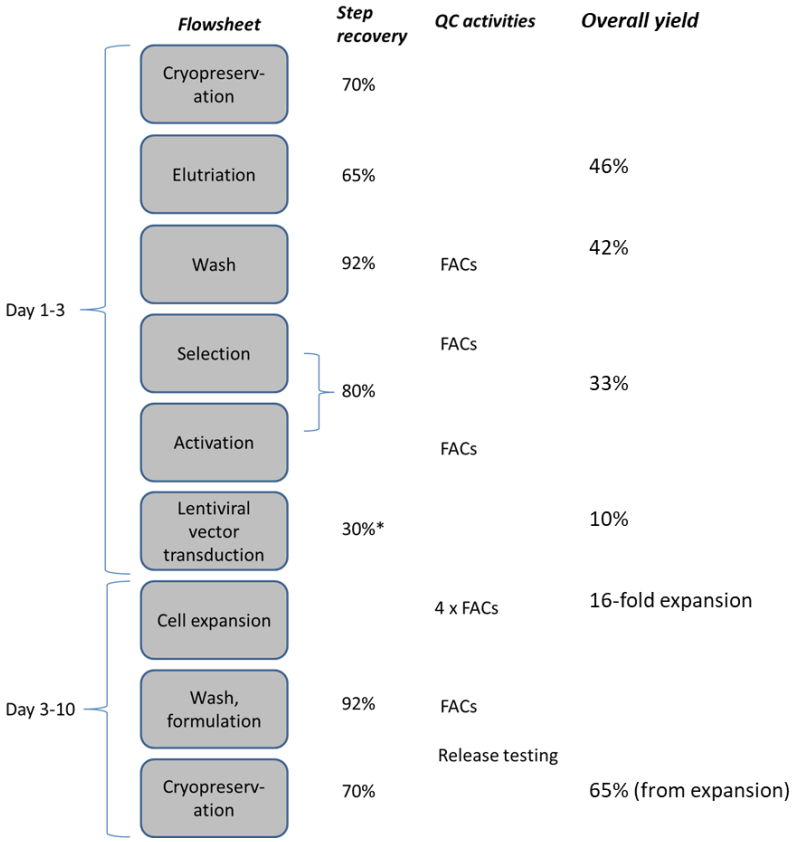

Figure 4.2 CAR T-cell process flowsheet assumed. FACs – Fluorescence-activated cell sorting. * 30% represents the transduction efficiency assumed.

Thus, the first steps assumed in the core manufacturing process of the CAR T product were cell separation, a washing step followed by the selection of the T-cells since the leukapheresate consists of lymphocytes, monocytes and in a small proportion, red blood cells, granulocytes, platelets and tumour cells (Fesnak and O'Doherty 2017). The cell separation was assumed to be achieved using elutriation while the T-cell selection was assumed to be achieved using CD3 and CD28 antibody-conjugated magnetic beads (e.g. CliniMACS CD4 Reagent and CliniMACS CD8 Reagent by Miltenyi Biotec). The next step was the activation of T-cells which was assumed to be performed within the cell

culture chamber using CD3/CD28 nanomatrix (e.g. TransAct, Miltenyi Biotec) (Lock et al. 2017). This was followed by the gene modification step using a lentiviral vector carrying the CAR transgene at a multiplicity of infection (MOI) of 5 transducing units (TU) per cell. The cells were then assumed to enter the expansion step where they were regularly fed in order to proliferate. Sampling for in process control was assumed to take place at multiple points in the process in order to count the number of viable and transduced T-cells and hence assess the quality and progress of the process. Here, it was assumed that the cells reached the required numbers by day 10, and were then washed, formulated, harvested, filled and cryopreserved.

4.2.3.2 Step recoveries and starting T-cell numbers

In terms of process recovery, the percent recovery of T-cells is shown in **Figure 4.2.** The overall process recovery across the steps before transduction (i.e. thaw, elutriation, wash, selection and activation) was assumed to be 33%. The transduction efficiency was assumed to be 30%, meaning that only 30% of T-cells were assumed to be successfully transduced and hence express CARs on their surface as per values routinely obtained in industry (Blaeschke et al. 2018). Moreover, the DSP yield post-expansion, for the wash, formulation, harvest and final cryopreservation steps was 65%. In addition, QC losses were accounted for with 10 million cells required for release testing, reference and retain samples.

In terms of the T-cell expansion step, it was assumed that the T-cells would reach a doubling time of 2 days after the activation step. Consequently, it was assumed that the cells would increase in numbers by ~16-fold from the end of the viral transduction step to the end of the expansion step. Thus, the equation used in order to determine the number of T-cells to be collected from the leukapheresate to start the process with so as to achieve a dose size of 250M CAR T-cells/dose is shown below:

$$N_{leuk.} = \frac{\left(\frac{m_{dose}}{Y_{cryo_2}} + m_{QC}\right)}{Y_{cryo_1} Y_{elutr}\, Y_{wash_1} Y_{act} Y_{trans} Y_{wash_2} e^{kt_{growth}}} \quad \textbf{(4.1)}$$

where:

$N_{leuk..}$ = minimum number of T-cells to be collected in leukapheresis

m_{dose}= CAR T-cell dose size

m_{QC} = number of cells retained for QC

k = specific growth rate (day^{-1}) (assumes constant growth rate as simplification)

t_{growth} = cell growth duration between activation and end of expansion (day)

Y_{cryo_2} = DP cryopreservation step yield

Y_{cryo_1}= cryopreservation step yield (leukapheresate)

Y_{wash_1} and Y_{wash_2} = wash step yield

Y_{elutr} = elutriation step yield

Y_{act}= activation and selection step yield

Y_{trans} = transduction efficiency

Thus, it was assumed that about 190 million T-cells are required to start the process with in order to achieve the dose size assumed in this case study. This was cross-checked against the likely ranges of number of T-cells present in leukapheresis per patient (Allen et al. 2017) as well as the range of number of T-cells that CAR T processes employing the CliniMACS Prodigy system start with based on discussions with industry experts.

Given the high variability in the quality of patients' starting material driven by different profiles of disease and history of medication regimes, it was assumed that 5% of the batches would fail per year.

4.2.3.3 Quality control: in process control and release testing

It was assumed that eight T-cell counts would be performed as part of the IPC schedule. These were assumed to be required to analyse the number of T-cells (% CD3+ T-cells) pre and post-selection, the number of transduced cells (% CD3+ T-cells, % CAR T-cells) as well as to monitor the general progress of the cell culture.

In terms of release testing, it was assumed that flow cytometry would be employed for measuring viability, identity (CAR and CD3+ expression) and stability (Roddie et al. 2019). With regards to measuring safety, sterility and endotoxin testing was assumed alongside PCR-based methodology for assessing vector copy numbers, presence of replication competent lentivirus (RCL), and mycoplasma (Wang and Rivière 2016).

The assumptions surrounding analytical equipment requirements and capacity for the flow cytometer and PCR instruments are shown in **Table 4.1**.

Table 4.1 Analytical equipment requirements.

Parameter	Flow cytometry instrument	PCR instrument
Sample prep requires BSC	yes	yes
No. samples that can be analysed at the same time	4	4
Duration of running test (including preparation and read-out time), hours	6	6
Number of samples that can be run per day	8	8

PCR = polymerase chain reaction.

The equation used for calculating the FACS machine or PCR equipment numbers requirement is shown below:

$$N_{anaytical,equip} = MAX\left(\frac{N_{process,parallel}}{N_{max,test,shift}}\right) \textbf{(4.2)}$$

Where

$N_{process,parallel}$ = number of batches run in parallel

$N_{max,test,shift}$ = maximum number of tests that can be analysed with one analytical equipment unit per shift

To determine the maximum number of tests that can be analysed with one analytical equipment unit per shift, the following equation was used:

$$N_{max,test,shift} = N_{sample,unit} \times \frac{t_{shift}}{t_{analysis}} \textbf{ (4.3)}$$

Where

$N_{sample,unit}$ = number of samples that can be analysed at the same time using one analytical equipment unit

t_{shift} = shift duration (h)

$t_{analysis}$ = analytical equipment operation time (h)

4.2.3.4 QC automation assumptions

To increase the attractiveness of the hospital-based manufacturing models (analysis shown in **Section 4.3.3.3**), analytical equipment automation implementation was evaluated. The scenario in which equipment such as the flow cytometry and the PCR instruments would become automated such that no manual aseptic sample preparation or read-out time would be required was explored in this chapter. The table associated with **Figure 4.10 (Section 4.3.3.3)** shows the assumptions in terms of analytical equipment cost increases and reduction in three labour categories requirements (i.e. production, QC and QP) associated with three levels of automation (i.e. low, medium and high). Furthermore, costs for adopting automation-supporting software platforms were also accounted for based on the assumption that full fruition of automation adoption would be

possible only if the appropriate infrastructure would be in place. As such, one-off costs of either 1M or 5M USD were assumed to account for the implementation of electronic pharmaceutical quality system (ePQS), manufacture execution system (MES) and electronic batch records system (eBMR).

The key assumption here was that different analytical automation degrees (low, medium and high) were associated with subsequent increases in analytical equipment cost and the associated consumable cost. The benefit of automation was translated into decreases in the requirement of different labour categories.

Whilst the basis for decreasing QC labour requirement with increase in analytical automation is somewhat self-explanatory, the basis for reduction in the production personnel and QP time requirements will be discussed further. The basis for reduction in production labour requirement with increase in analytical equipment automation was the assumption that the production team is also responsible for performing IPC activities such as cell counts using the flow cytometry instrument. As such, if such equipment became automated, it was assumed that a team of production operators would be able to handle more INT units in parallel than at base case (3 INT units/team). Furthermore, the basis for decreasing QP release time with increase in analytical automation was the assumption that the novel analytical equipment would have data storage and data trending capabilities called out by software packages such as the ePQS, MES and eBMR. This was assumed to allow the creation of robust data bases increasing process and product understanding which would then help QPs speed up the release process.

4.2.3.5 Production scheduling

The manufacturing capacity requirement in terms of the number of processes (batches) that need to be run in parallel was calculated based on the annual demand and the process

duration using the following two equations. This was determined by first identifying the number of manufacturing slots per year:

$$N_{batch,parallel} = \frac{D_{annual}}{N_{mfg\ slot}} \textbf{ (4.4)}$$

$$N_{mfg\ slot} = \frac{t_{active}}{t_{process}} \textbf{ (4.5)}$$

Where

D_{annual} = annual demand

$N_{mfg\ slot}$ = number of manufacturing slots

t_{active} = time (day) in which the manufacturing facility is active and operating

$t_{process}$ = production duration (day)

4.2.4 Key costs assumptions

The key cost categories assumed in this work were the cost of goods, the fixed capital investment, the facility preparation costs and other costs. As part of the other costs, sales and marketing as well as corporate taxes were assumed. Depending on the enterprise model, transportation costs were also included.

An important assumption applied in this work was that the manufacturing facility where Phase 3 clinical trial (or equivalent) would be performed was already in place and different from the facility used at market launch. Thus, this work captured the costs associated with building and/or preparing (depending on enterprise model) the commercial manufacturing facility for market launch and did not include costs associated with clinical trials or the CMC costs associated with these.

4.2.4.1 Cost of goods

The cost of goods was assumed to consist of direct costs such as leukapheresis, raw materials (reagents and consumables) and QC materials as well as indirect costs such as labour and facility-related costs and were computed using the COG model previously described in Pereira Chilima (2019). Each of these categories will be described in the sections below. Another angle of assessing COG was assumed to be given by the sum of the core manufacturing costs (within the manufacturing facility), plus the supply chain costs associated with leukapheresis and transportation.

Direct costs assumptions

The direct costs represent a function of material utilisation per manufacturing one batch and are shown in **Table 4.2**.

Table 4.2 Direct costs breakdown per CAR T-cell batch.

Direct costs breakdown	**Type**	**Value**
Leukapheresis (materials and labour)*		\$10,000
Raw materials	Consumables	\$4,995
	Viral Vector	\$8,129
	Reagents	\$1,205
QC materials		\$15,000
Total direct costs/batch		\$39,330

Consumables include tubing set costs; *based on Meehan et al. (2000).

As per **Table 4.2,** other than leukapheresis costs, which sits outside of the core manufacturing costs, an important manufacturing-related direct cost was identified as the viral vector cost. This was assumed to be ~\$8,000/dose and was calculated using the following formula:

$$LV_{cost/batch} = N_{cell,transd.} \times MOI \times \frac{LV_{cost}}{10^6} \textbf{ (4.6)}$$

Where

$N_{cell,transd.}$= number of T-cells just before the transduction step

MOI = multiplicity of infection (TU/cell)

LV_{cost} = LV cost per million of transducing units (TU)

The LV dose size of $4x10^8$ TU was calculated by the CAR T model's mass balance and the LV cost was assumed to be $20 per million of TU. The ballpark LV cost was obtained from LV process economics evaluations performed for the gold-standard adherent 10-layer vessel process.

The methodology employed for calculating the LV cost assumed no "at point-of-use" losses. This meant that, since no variations in T-cell numbers between batches were assumed, the LV product vials' content was assumed to be used entirely in the transduction step (without any LV waste). However, it is worth noting that this methodology is likely underestimating the real cost of LV associated with the CAR T manufacture for the following reasons. Firstly, it is likely that additional LV quantities are assumed per CAR T batch as part of a wider contingency strategy i.e. for a second batch in the case of batch failure. Furthermore, given the typically high LV titre variability, it is likely that there will be notable differences in the output of different LV batches in terms of number of doses/batch. Consequently, to guard against the negative impact of such variability, LV manufacturers would likely overestimate the LV volumes sold such that, should they experience a lower titre, they can ensure enough LV is provided to the CAR T manufacturers. These considerations are addressed in the next chapters of this thesis by assuming larger LV dose sizes for this type of therapies.

Indirect costs assumptions

The indirect costs were assumed to consist of labour and facility-related costs. Four key labour categories were assumed: production labour, QC and QA labour, QP labour and supervisors. On the other hand, the facility-related costs were assumed to include facility maintenance costs, energy costs, monitoring costs and depreciation. **Table 4.3** shows the

key costs assumptions related to the indirect costs category. These were calculated on a per year basis. The equations used for determining the indirect costs are shown in **Chapter 3**.

Table 4.3 Indirect costs assumptions associated with CAR T-cell therapy manufacture.

Assumptions	Parameter	Value	Unit
Facility running costs	No. of active days	330	Days/year
	Process length	10	Days
	Depreciation period	10	Years
Labour requirements	No. batches per QC operator	2	-
	No. cleanrooms per $QC_{monitoring}$ scientist	1	
	No. QA scientist: QC scientist	0.5	-
	No. batches per QP	2	-
	No. supervisors & managers: no. of process operators	0.7	-
	Max no. batches per QC lab	10	-
	No. INT units per team of 2 production operators	3	-
Costs	Annual salary	120,000	$/operator
	Facility energy costs	637	$/m^2 /year

4.2.4.2 Fixed capital investment

The fixed capital investment was determined using a detailed factorial methodology for estimating FCI and footprint as described in Chilima et al. (2020), described in **Chapter 3**. The key equipment costs are shown in **Table 4.4**.

Table 4.4 Key equipment costs associated with CAR T-cell therapy manufacture.

Equipment	Cost
Integrated USP/DSP system (INT)	$235,000
Controlled rate freezer	$30,000
Flow cytometry instrument	$100,000
PCR instrument	$50,000

4.2.4.3 Facility preparation costs

The facility preparation costs were assumed to include the costs associated with obtaining the manufacturing licence, engineering and process performance qualification batches as well as the tech transfer and comparability studies (**Table 4.5**). In addition, facility insurance was assumed to be required only in the case of the centralised and the regional models at a cost of 1% of FCI.

Table 4.5 Key facility preparation costs associated with CAR T-cell therapy manufacture.

Facility preparation costs	**Million USD**
Manufacturing licence	3
Tech transfer and comparability studies	1.85
3 PPQ batches and 5 engineering batches	0.41
Total facility preparation costs	5.26

4.2.4.4 Profitability assessment and cash flow assumptions

The methodology used here to assess the profitability of the enterprise models was the risk-adjusted net present value methodology described in **Chapter 3**. The particular risk-adjusted net present value model employed in this work was previously developed by Pereira Chilma (2019). In terms of the cash flow assumptions, **Table 4.6** shows the assumptions surrounding patient demand ramp-up, corporate tax, sales and marketing (S&M) costs as well as the probability of the product to reach market. A 5% batch failure rate was assumed for each of the enterprise models.

Table 4.6 Key cash flow assumptions used to compute the risk-adjusted net present value for different enterprise models employed in CAR T-cell therapy manufacture.

Parameter	**Value**
Patient demand ramp-up	40% at year 1, 2 70% at year 3, 4, 5 100% at year 6, 7, 8, 9, 10
Corporate tax	21%
S&M	5%
Discount factor	11%
Cumulative success probabilities	For Ph1 to Ph2: 87% For Ph2 to Ph3: 56% For Ph3 to Reg. Review: 40% For Reg. Review to market: 36%

S&M = sales and marketing; Ph = clinical trial phase; Reg. = regulatory.

4.2.5 Description of the enterprise models analysed

The enterprise models analysed in this work will be discussed next. **Section 1.3.2** provides a discussion of the key supply chain models for autologous gene-modified cell therapies. Apart from the gold-standard, centralised manufacturing model, four distributed (decentralised) manufacturing models were defined i.e. the regional model and three hospital-based manufacturing models. The hospital-based manufacturing models assumed in this work were the rented hospital model and two "GMP-in-a-box" models. The centralised model was assumed to represent the scenario in which the sponsor company would use a single manufacturing facility to supply a large territory e.g. a site in California, USA, supplying the American continent or both the US and European markets. For the regional model, however, it was assumed that the sponsor company would use multiple sites to supply either a large market or multiple markets e.g. multiple sites in the US and/or multiple sites in Europe. On the other hand, the hospital-based models assumed a partnership between the sponsor company and hospitals. As such, for the rented hospital model, it was assumed that manufacturing, led by the sponsor company's staff, would occur in the cleanrooms of hospital centres, for which the sponsor company would pay rent. For the "GMP-in-a-box" models, however, it was assumed that manufacturing, led by the hospital's staff, would occur in the hospital's controlled non-classified (CNC) areas. This was assumed to be possible in the near future based on the closed nature of the INT system assumed herein and the assumption that control over manufacture and product quality could be ensured. In return, the sponsor company would either share a percentage of revenue with the hospital sites (the GMPiB_A model) or they would be charged a mark-up on top of the expenses of the hospitals (the GMPiB_B model). **Table 4.7** provides a summary description of each model in terms of capital investment requirements, facility preparation cost, running costs, charges and transportation costs and indicates also the stakeholders responsible for each key activity.

Table 4.7 Description of the enterprise models analysed in the CAR T-cell therapy manufacture case study.

		Centralised	Decentralised*			
			Regional **	Hospital-based		
				Rented Hospital (HSP)	"GMP-in-a-box" (GMPiB_A) ***	"GMP-in-a-box" (GMPiB_B) ***
Description		Single manufacturing site	Multiple manufacturing sites	Cleanroom in hospital sites (hotel model)	Reimbursement shared b/w sponsor and hospital model	Semi-CMO model
Capital investment		Equipment + Facility	Equipment + Facility	Equipment (includ. QC equip.)	Equipment (includ. QC equip.)	Equipment (includ. QC equip.)
Commercial facility prep costs	Facility insurance	S	S	N/A	N/A	N/A
	Tech transfer	S	S	S	S	S
	Comparability studies	S	S	S	S	S
	Site license	S	S	S	S	S
	Engineering runs	S	S	S	S	S
	PPQ batches	S	S	S	S	S
Running costs	Materials	S	S	S	S	S
	Production Labour	S	S	S	H	H
	QC, QA Labour	S	S	S	H	H
	QP Labour	S	S	S	S	S
	Equipment overheads	S	S	S	S	S
	Facility overheads****	S	S	H	H	H
Charges to the sponsor definitions	Facility charge	N/A	N/A	1.2 x (facility depreciation + cleanroom monitoring + facility maintenance) **(4.7)**	1.2 x (QC facility depreciation + QC maintenance + QC,QA labour) **(4.8)**	1.6 x (QC facility depreciation + QC maintenance + Production labour + QC,QA labour) **(4.9)**
	Hospital charge	N/A	N/A	N/A	5% of sales to cover production nurses and hospital profit	N/A
Transportation costs		$3,000/dose	$1,500/dose	N/A	N/A	N/A

*It was assumed that the demand would be equally distributed across the decentralised sites; ** It was assumed that the number of sites chosen to satisfy certain demand did not affect transportation costs; *** refers to bedside / point of care; **** facility overheads = facility overheads – equipment overheads; S = sponsor company, H = hospital site, FCI = fixed capital investment, b/w = between, N/A = not applicable, QA = quality assurance, QC = quality control, QP = qualified person, PPQ = process performance qualification.

With regards to the centralised and the regional models, these were assumed to be associated with the largest capital investment. Either one (centralised model) or multiple (regional model) commercial manufacturing facilities were assumed to be built, fitted-out and prepared for manufacture. In the case of the centralised model, it was assumed that the facility would be built, equipped and prepared for peak demand manufacture within 3 years. On the other hand, in the case of the regional model (as well as for the rest of the decentralised models), it was assumed that the sites would come online at the rate of the predicted increase in market demand. Consequently, it was assumed that the sponsor company would be in full charge of running the site/s and hence were assumed to receive full reimbursement. In terms of transportation costs, it was assumed that $3,000 and $1,500 per dose were the total transportation costs associated with the centralised model, and the regional model, respectively.

On the other hand, the hospital-based manufacturing models were assumed to be associated with lower capital investment levels; only equipment procurement was assumed to be required for these models as manufacturing was assumed to take place on the hospital sites' premises. In terms of facility preparation costs, these were assumed to be the same as in the case of the regional model apart from the facility insurance costs which was assumed to not be required (**Table 4.7**). However, the facility running costs were assumed to be slightly different depending on the share in responsibilities between the sponsor company and the hospitals. In the case of the rented hospital model, manufacturing was assumed to be performed in cleanrooms, hence it was assumed that the hospital sites would need to have cleanroom facilities in place. Also, these were

operated in a hotel-like mode meaning that the sponsor company was assumed to bring in their own production, QC and QA teams to operate the hospital's cleanrooms. This arrangement was assumed to incur an annual rent or facility charge payable by the sponsor company to the hospital sites. This was calculated based on the estimated maintenance, depreciation and monitoring costs associated with the hospital's cleanrooms as well as a mark-up of 20% (**Table 4.7**). In the case of the GMPiB models, cleanrooms would not be required as manufacturing was assumed to be possible within CNC environment given the closed nature of the INT system. In this case, it was assumed that the hospital staff rather than sponsor company staff performed manufacturing and QC and QA activities. Furthermore, it was assumed that each hospital site would have invested in QC laboratory facilities in order to facilitate the adoption of autologous products' manufacture on their premises. Consequently, the sponsor company was assumed to pay for the services provided by the hospital sites. The first GMPiB model, GMPiB_A, assumed that the payment for the hospital's services would be done via an annual revenue share of 5%, referred to as "hospital charge" in **Table 4.7.** In addition, it was assumed that the hospital sites would contract out their QC testing services to the sponsor company for a facility charge. This was calculated based on the QC and QA labour costs, as well as the QC laboratory facilities' depreciation and maintenance costs and a mark-up of 20% (**Table 4.7**). On the other hand, in the case of the second GMPiB model, the GMPiB_B, rather than agreeing on a revenue share scheme, it was assumed that the hospital sites would contract out their manufacturing and QC services to the sponsor company at a higher, yet fixed, mark-up. The facility charge in this case was calculated based on production, QC and QA labour costs, QC laboratory facilities maintenance and depreciation and a mark-up of 60% (**Table 4.7).** No transportation costs were assumed to be incurred in the case of the hospital-based models as the leukapheresis, product manufacture and product administration were assumed to be co-located at the hospital site.

4.3 Results and discussion

This section addresses critical challenges surrounding manufacturing strategy faced by companies commercialising autologous gene-modified cell therapies such as CAR T-cell therapies. It provides an overview assessment of alternative enterprise models to the centralised manufacture paradigm and an outlook towards enabling the implementation of bedside manufacturing models. Initially, the minimum and maximum number of sites for each regional model were identified from profitability and operational feasibility perspectives for a range of demands. Next, the ranking of enterprise models was assessed from a risk-reward perspective by analysing the profitability and fixed capital investment of each model for a range of demands and selling prices. The bedside manufacturing models were further analysed to provide a picture of the hospital financial metrics with variation in selling prices. Further to this, target key parameters for negotiation between sponsor company and hospitals were identified. In the context of in-process control activities representing a key challenge preventing adoption of bedside manufacturing models, the impact of QC automation on cost of goods and profitability was assessed.

4.3.1 Profitability and operational feasibility screening of enterprise models

To establish a fair comparison between enterprise models, screening of the optimal number of manufacturing sites for the regional models from a profitability and operational feasibility point of view was initially performed. Profitability was assessed using a risk-adjusted net present value (rNPV) methodology. On the other hand, operational feasibility was assessed by determining the number of integrated USP/DSP system (INT) units (e.g. CliniMACs Prodigy, Miltenyi systems) that would need to be manipulated per manufacturing site at any one time.

Figure 4.3 shows the impact on profitability of a range of number of sites for all four regional enterprise models at 3 demands (1,000, 5,000 and 10,000 doses/year) and 2 selling price levels ($400,000/dose (a) and $160,000/dose (b)). It also indicates the

profitability associated with the centralised model (1 site) as a straight red dotted line. The point where the decentralised rNPV graphs (regional, hospital, GMPiB_A or GMPiB_B) crosses the centralised rNPV graph reveals the number of sites which would lead to a similar rNPV value between the centralised and that decentralised models. This was deemed to be the maximum number of sites of each regional model as any site number above it would lead to lower profitability than the centralised model.

4.3.1.1 Profitability screening

Market demand affects the number of sites which is profitable to establish. At a demand of 1,000 doses/year, the highest number of sites that can be established whilst ensuring a similar or higher profitability level between the decentralised models and the centralised model ranged between 4-6. However, this increased to 10-20 at 5,000 doses/year and 20-40 at 10,000 doses/year across decentralised models. This is driven by the ratio of the costs associated with establishing and running one regional site to the costs associated with one centralised site. The lower this ratio, the more sites could be established using the decentralised models. When the site number increases beyond the thresholds shown in **Figure 4.3** (maximum number of sites), the decentralised models become less profitable than the centralised model because the costs to establish and run the additional sites become larger than the costs associated with the centralised model.

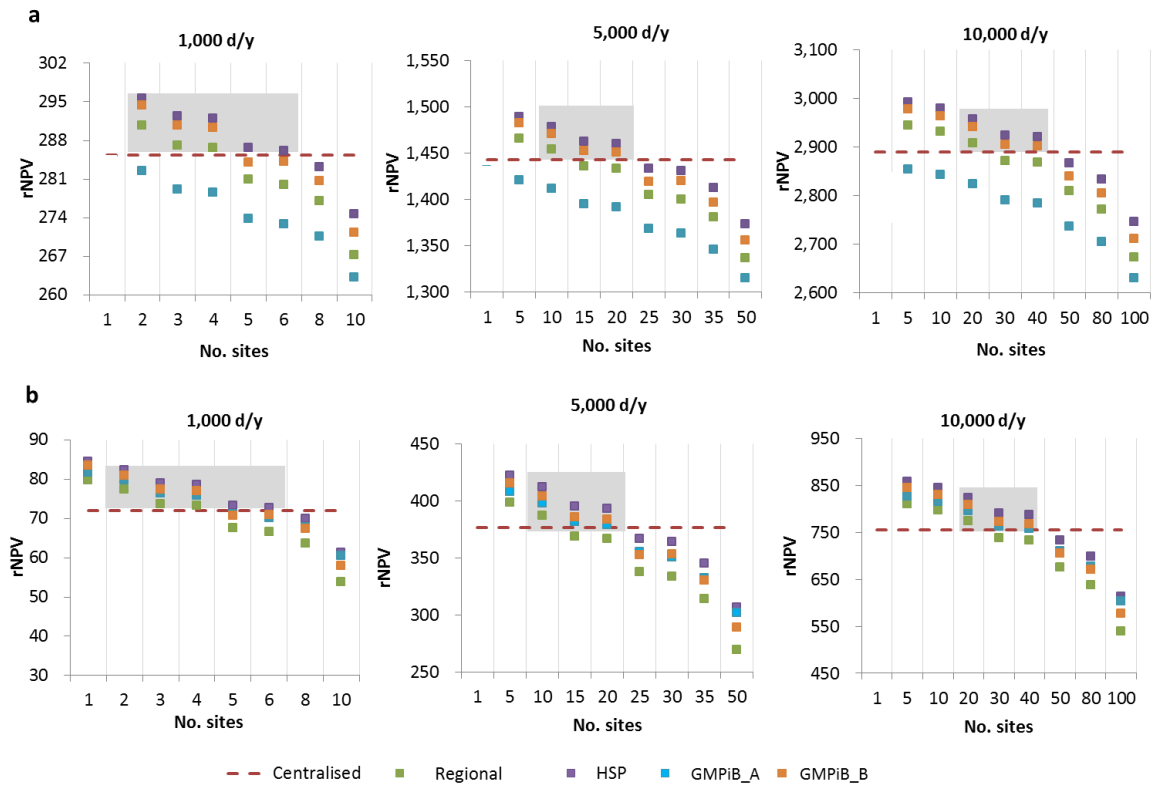

Figure 4.3 Impact of number of sites on the profitability (in million USD) of decentralised models relative to the centralised model profitability at a selling price of **a)** 400,000/dose and **b)** $160,000/dose for three market demands of 1,000, 5,000 and 10,000 doses/year. The centralised model is assumed to be associated with one manufacturing facility hence its profitability is shown as a constant for each demand (red dotted line). The grey area indicates the corresponding number of sites that are feasible to be established from both profitability and operational feasibility perspectives in the case of the hospital-based models. rNPV = risk-adjusted net present value, d/y = doses/year, HSP = Rented hospital model, GMPiB_A = bedside manufacture (reimbursement shared between sponsor and hospital), GMPiB_B = bedside manufacture (semi-CMO model), SP = selling price.

The rented hospital model (HSP) was associated with the highest profitability while the regional model was associated with the lowest profitability across regional models regardless of selling price. The maximum number of sites associated with the rented hospital model was 6, 20 and 40 sites while the regional model was associated with maximum 4, 10, 20 sites at 1,000, 5,000 and 10,000 doses/year, respectively. With respects to the GMPiB_B model, this ranked in between regional and rented hospital models regardless of selling price (**Figure 4.3**) with maximum 4-5, 20, 40 sites at 1,000, 5,000 and 10,000 doses/year, respectively. On the other hand, the profitability

performance of the GMPiB_A model varied drastically with selling price, being competitive with the GMPiB_B model at a low selling price while scoring much lower than the centralised model at a high selling price across demands. Any number of sites below the thresholds above mentioned would mean a higher rNPV value relative to the centralised model. These rankings and their justification are further discussed in **Section 4.3.2**.

The next section dwells on identifying the minimum number of sites for each model and demand scenario.

4.3.1.2 Operational feasibility screening

Whilst the previous section gave an indication of the maximum number of sites to be established from a profitability perspective, this section focuses on identifying the minimum number of sites that can be established from a shop-floor logistics perspective in the case of the regional models. Furthermore, it explores the operational feasibility of the centralised model across demands (**Figure 4.4)**.

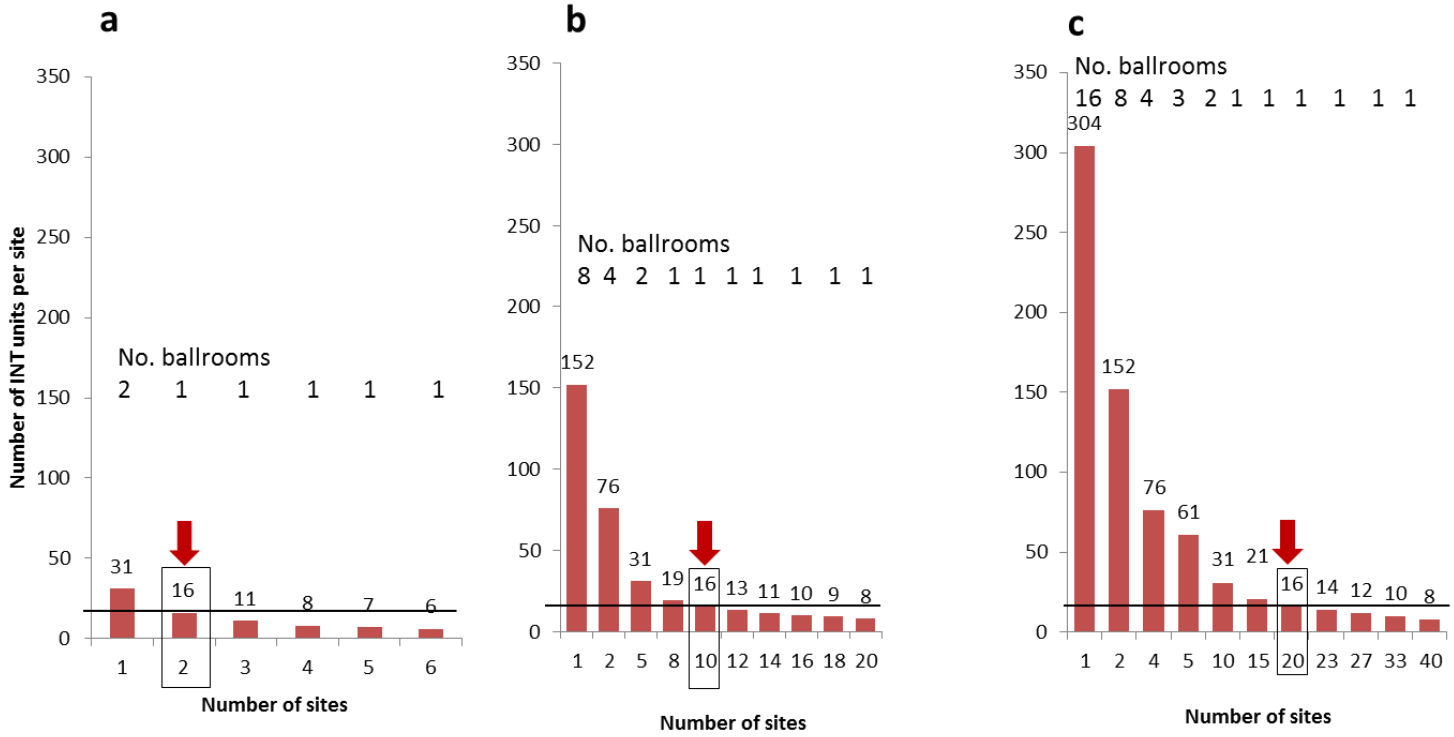

Figure 4.4 Manufacturing capacity requirements per site in terms of number of integrated USP/DSP system (INT) units across a range of number of sites at a) 1,000, b) 5,000 and c) 10,000 doses/year. The red arrow and rectangle indicate the minimum number of sites associated with the hospital-based models. INT = integrated USP/DSP system (e.g. Prodigy, Miltenyi Biotec).

The operational feasibility criterion was considered to be met if the number of integrated USP/DSP system (INT) units run in parallel at any one time per site was below a certain threshold which is dictated by the manufacturing facility size constraints i.e. the shop floor logistics. For the hospital-based models (i.e. rented hospital, GMPiB_A and GMPiB_B), it was assumed that the manufacturing facility size would be smaller than that of the centralised and regional models due to the complex functionality of hospitals. As such, it was assumed that no more than 16 INT units could be manipulated per hospital site, regardless of hospital-based model type, at any one time based on literature accounts (Lopes et al. 2020). On the other hand, in the case of the centralised and regional models, whilst their associated facility sizes do not have constraints dictated by other institutions, the facility size could not exceed a certain threshold either due to operational burdens and risk. Thus, it was assumed that a site could consist of up to 4 ballrooms, hosting 20 INT units each. To perform this operational feasibility screening, the tool was tasked to output the number of INT units required per site for all demands and number of sites scenarios analysed in the previous section (**Figure 4.3).**

To put the results of the profitability screening into perspective, the analysis revealed that the number of INT units per site associated with the maximum number of sites for the hospital-based models ranged between 6-8 units at 1,000 doses/year and 8 units at the higher demands (**Figure 4.4**). This was deemed to be feasible based on the constraints mentioned above. Furthermore, the analysis revealed that the number of INT units per site associated with the maximum number of sites for the regional model from a profitability perspective was 8 units at 1,000 doses/year and 16 units at the higher demands (**Figure 4.3).**

On the other hand, the 16 INT units per site constraint meant that the minimum number of sites for the hospital-based models from an operational feasibility perspective

corresponded to 2 sites at 1,000 doses/y, 10 and 20 sites at 5,000 and 10,000 doses/year, respectively (**Figure 4.4**). Moreover, the 4 ballrooms per facility constraint dictated that the minimum number of sites for the regional model from an operational feasibility perspective corresponded to 2 sites at 5,000 doses/y and 4 sites at 10,000 doses/year (**Figure 4.4**).

With respect to the operational feasibility of the centralised model across demands, it was found that the centralised facility size needed for outputting 5,000 and 10,000 doses/year required 8 ballrooms at 5,000 doses/year and 16 ballrooms at 10,000 doses/year. Given the operational infeasibility, it was assumed that the centralised model would be replaced by the regional model at 5,000 and 10,000 doses/year.

Therefore, this analysis revealed that the range of feasible number of sites for the hospital-based models associated with competitive profitability levels when compared to the centralised model was 2 - 6, 10 - 20 and 20 - 40 sites at 1,000, 5,000 and 10,000 doses/year, respectively. Moreover, it was found that the centralised model would not be feasible from a shop-floor logistics perspective at large demands, hence 2 and 4 regional facilities were assumed to replace it at 5,000 and 10,000 doses/year.

Based on this screening study, the minimum number of decentralised sites (i.e. 2 at 1,000 doses/year, 10 at 5,000 doses/year and 20 at 10,000 doses/year) was selected for further analysis of the enterprise models.

4.3.2 Reward versus Investment analysis of the enterprise models

Whilst the previous section identified the feasible ranges of number of sites for all the enterprise models from profitability and the operational feasibility perspectives, this section focuses on analysing the profitability and investment ranking across models.

Figure 4.5 shows the reward (profitability) and investment (fixed capital investment – FCI) levels for the enterprise models when associated with minimum number of decentralised sites at 1,000, 5,000 and 10,000 doses/year respectively, at two selling price levels ($400,000 and $160,000/dose). Thus 2, 10 and 20 sites are plotted for the decentralised models at the low, medium and high demand, respectively. The regional model is shown additionally as associated with 2 and 4 sites at 5,000 and 10,000 doses/year, respectively (**Figure 4.5ii,iii**). This is shown as a viable alternative to the centralised model given the prohibitively high number of integrated USP/DSP system (INT) units that would be associated with one site at these large demands (**Figure 4.4**). The most attractive enterprise models are located in the lower right-hand-side quadrant relative to the centralised model based on higher profitability and lower FCI levels when compared to the centralised model.

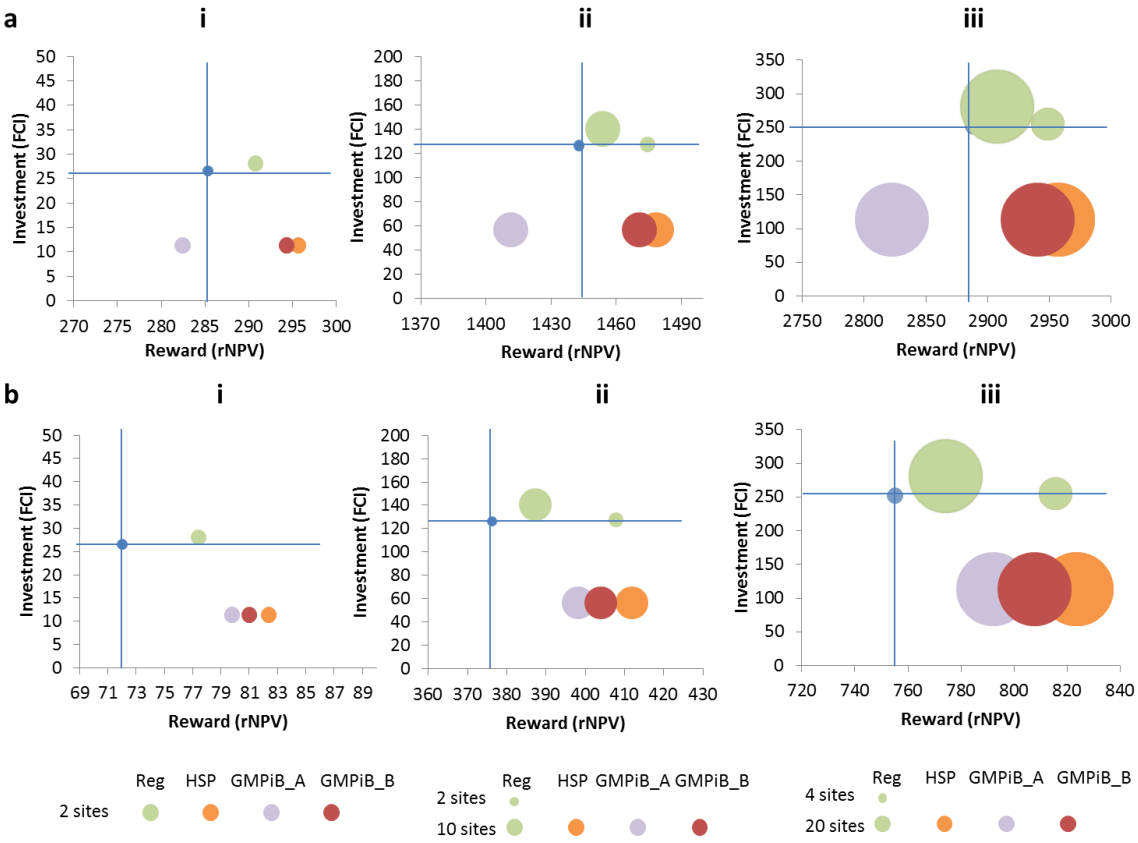

Figure 4.5 Assessment of reward (rNPV in million USD) and investment (FCI in million USD) for all enterprise models when the selling price is **a)** $400,000/dose and **b)** $160,000/dose at **i)** 1,000, **ii)** 5,000 and **iii)** 10,000 doses/year. The minimum number of sites identified in the previous section were plotted for each regional model against the centralised model (blue circle). The size of the bubble represents the number of sites. The blue lines indicate the position of the centralised model, feasible only at the 1,000 d/y demand. Where rNPV = risk-adjusted net present value, FCI = fixed capital investment, Reg = regional model, HSP = rented hospital model, GMPiB_A = bedside manufacture (reimbursement shared between the sponsor and the hospital), GMPiB_B = Bedside manufacture (semi-CMO).

From both profitability and investment perspectives, the rented hospital model was found to be the most attractive, followed by the GMPiB_B across selling prices. This can be attributed to the fact that the rented hospital and GMPiB_B models are associated with much lower investment levels than the centralised and regional models (**Figure 4.5)**, as these two models leverage on existing hospital facilities. Moreover, the two hospital-based models are associated with no transportation costs as leukapheresis collection, manufacture and administration are assumed to occur at the same hospital centre (in the regional model, these activities occur at different locations). The rented hospital site

scores better than the GMPiB_B because of differences in labour assumptions between the two models. In the case of the rented hospital model, it was assumed that the labour (production, QC and QA) would be hired and paid by the sponsor company and the hospital unit would operate in a hotel mode. On the other hand, in the case of the GMPiB_B, it was assumed that the labour would be hired and paid by the hospital and that the hospital unit would operate in a semi-CMO-like mode, hence a mark-up was applied on top of those costs (**Table 4.7)**. Consequently, the labour costs charged by the hospital to the sponsor company in the GMPiB_B scenario were higher than those associated with the rented hospital model (shown in the facility charge column in **Figure 4.6** and **Figure 4.7**).

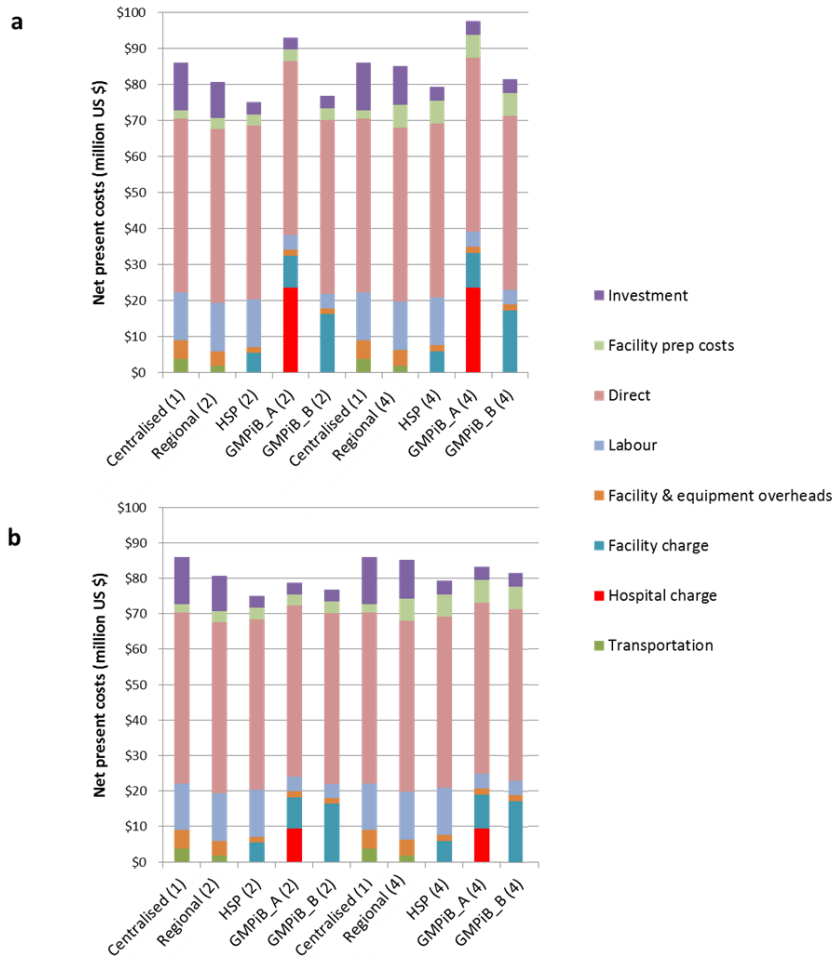

Figure 4.6 Net present cost breakdown for enterprise models employed in CAR T product manufacture for a demand of 1,000 doses/year at a selling price of **a)** $400,000/dose and

b) $160,000/dose. The number in brackets shows the number of manufacturing sites assumed for each model. Where HSP = rented hospital model, GMPiB_A = bedside manufacture - reimbursement shared between the sponsor and the hospital model, GMPiB_B = Bedside manufacture - semi-CMO model.

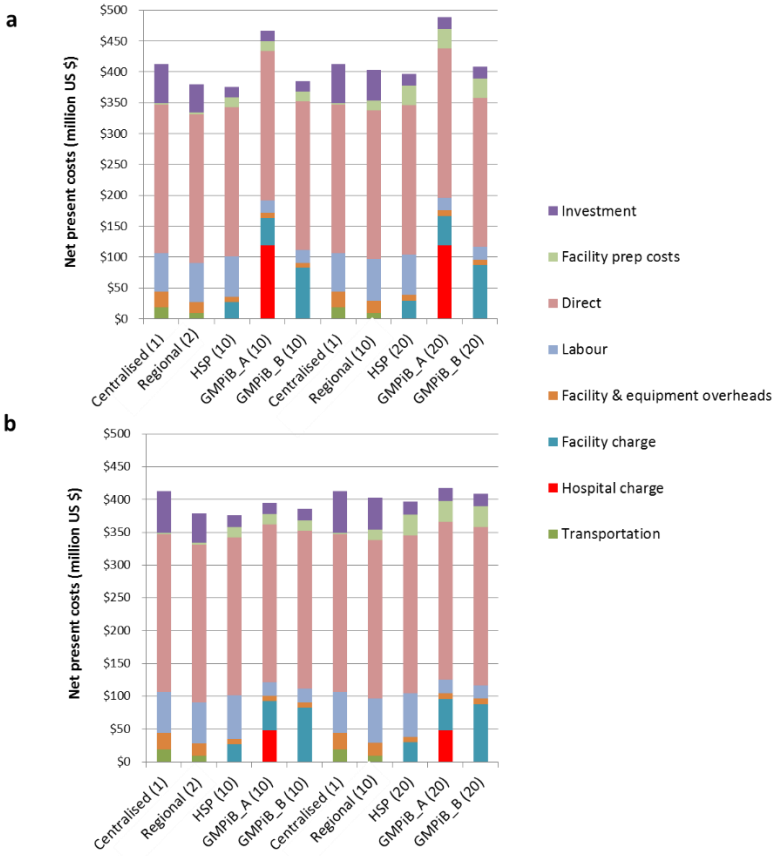

Figure 4.7 Net present cost breakdown for enterprise models employed in CAR T product manufacture for a demand of 5,000 doses/year at a selling price of **a)** $400,000/dose and **b)** $160,000/dose. The number in brackets shows the number of manufacturing sites assumed for each model. HSP = rented hospital model, GMPiB_A = bedside manufacture - reimbursement shared between the sponsor and the hospital model, GMPiB_B = Bedside manufacture - semi-CMO model.

Whilst the GMPiB_A and GMPiB_B are associated with the same FCI, the GMPiB_A model was shown to be competitive with the GMPiB_B model at a low selling price and was found to be the least competitive model from profitability perspective at a large selling price (**Figure 4.5).** The key difference between the two GMPiB models is that the GMPiB_A model relies on revenue share between the sponsor and the hospital (referred to as hospital charge) whereas the GMPiB_B relies on full reimbursement to the sponsor (**Table 4.7**). In addition, the GMPiB_A model states that the hospital charges the sponsor

for QC services whereas the GMPiB_B model states that the hospital charges the sponsor for both manufacture and QC services (both referred to as facility charges, **Table 4.7**). As a result, at a low selling price, GMPiB_A scored only slightly lower than its counterpart from a profitability perspective because the hospital charge plus the facility charge for QC services slightly exceeded the facility charge incurred in the case of the GMPiB_B model (**Figure 4.6b, Figure 4.7b**). However, at a high selling price, GMPiB_A scored the worst from a profitability perspective because the hospital charge (which increases proportionally with the selling price) led to the largest NPC across enterprise models (**Figure 4.6a, Figure 4.7a**).

Furthermore, the centralised model was found to be associated with the lowest profitability at a selling price of $160,000/dose and the second-lowest at $400,000/dose across demands. Since the infeasibility of the centralised model was demonstrated at the large demands of 5,000 and 10,000 doses/year, the 1,000 doses/year ranking will be discussed (**Figure 4.5).** The centralised model scored worse than the regional model because of its higher investment net present costs (NPC, **Figure 4.6**, **Figure 4.7**). This is because the decentralised sites were assumed to be built in stages, ahead of the predicted ramp-up of the patient demand, while the centralised site was assumed to be built and equipped for the peak demand from the market entry time-point. Furthermore, the transportation costs associated with the regional model were assumed to be half of those associated with the centralised model (**Table 4.7**).

Despite high investment and charging of transportation costs, the regional model employed to replace the centralised model at 5,000 and 10,000 doses/year was found to be the second most profitable across selling prices, after the rented hospital model (**Figure 4.5ii,iii**). That is because of lower overall facility preparation costs when compared to the

rented hospital and the GMPiB models, no facility or hospital charges and similar labour costs (**Figure 4.7**, **Table 4.7).**

Although the rented hospital model appears to be the most attractive across the models analysed here, it is also the least flexible and scalable since not many hospital centres exist which have cleanroom facilities. The second most attractive scenario was the regional model. However, this remains associated with some level of risk due to the transportation of the leukapheresate to the manufacturing site and of the product back to the patient for administration. Therefore, the GMPiB models are further explored to identify the conditions in which they would be the most attractive enterprise models.

4.3.3 GMPinaBox models: high level feasibility assessment

The second part of this chapter discusses the impact of the agreement type between the sponsor company and the hospitals and the impact of variation in selling price on hospital profits in the case of the GMPiB models. Moreover, it discusses the parameters which would make such models at least as attractive as the gold standard i.e. the centralised model at low demands and the regional model at the higher demands. The final section of this chapter discusses the challenges associated with the implementation of the GMPiB models and introduces automation as mitigation strategy, providing an assessment of its impact on COG/dose.

4.3.3.1 View on hospital profits for the GMPiB models

Since the GMPiB models assume that the hospital staff would be in charge of manufacturing and QC, the hospital's estimated outgoings (expenses to the hospital) and revenue were plotted in **Figure 4.8** for a range of selling prices at 1,000 doses/year. The key assumption used here was that the hospital staff would have the same salaries as operators employed in cleanrooms.

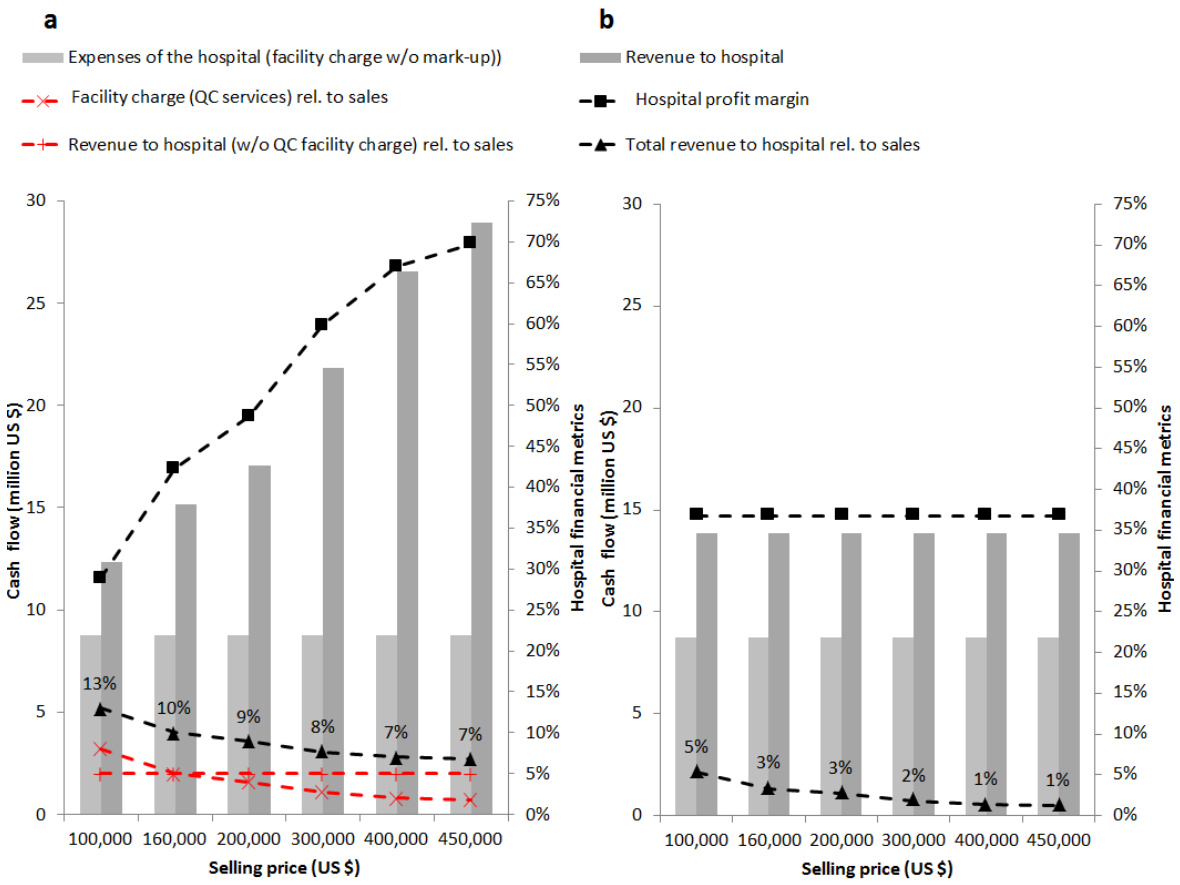

Figure 4.8 Hospital expenses and revenue for **a)** GMPiB_A and **b)** GMPiB_B model at 1,000 doses/year and 4 sites for a range of selling prices. The hospital staff salary was assumed to be the same as the salary of the operators working in the cleanroom. Where hospital profit margin = (revenue to hospital – expenses of the hospital)/revenue to hospital, QC = quality control, HSP = hospital, rel. = relative, w/o = without.

In the case of the GMPiB_A model, as the revenue to hospital stream increased with selling price (dark grey columns, **Figure 4.8a**), the profit to the hospital also increased as the expenses of the hospital (light grey columns, **Figure 4.8**) remained the same. Thus, while the hospital profit margin (revenue to hospital – expenses to the hospital relative divided by the revenue to hospital) was 42% at a low selling price of $160,000/dose, this increased to 67% at a selling price of $400,000/dose (black squares, **Figure 4.8**). On the other hand, in the case of the GMPiB_B model, since no revenue share was assumed between hospital and sponsor and a fixed charge was applied instead, the hospital profit margin was constant and equal to 37% (black squares, **Figure 4.8b**). Therefore, the ratio

of total revenue to hospital to product sales (black triangles, **Figure 4.8)** was larger for the GMPiB_A model than for the GMPiB_B model and decreased with increasing selling price. This ranged between 13% and 7% in the case of the GMPiB_A model and between 5% to 1% in the case of the GMPiB_B model. The reason why this ratio decreased with selling price is because both models employ a facility charge which is independent of selling price. For the GMPiB_A model, apart from the revenue share (red pluses, **Figure 4.8a**), a facility charge for the QC services provided by the hospital (red crosses, **Figure 4.8a**), calculated based on the estimated QC and QA labour costs and overheads and a mark-up of 20% was applied (**Table 4.7).** On the other hand, the facility charge in the case of the GMPiB_B model was calculated based on the production staff cost, QC services cost and a mark-up of 60%. These results show that even at a lower selling price of $160,000/dose, the sponsor's outgoings (i.e. revenue to hospital, dark grey column) and hence the hospital profit margin were higher for the GMPiB_A model than for its counterpart **(Figure 4.8a,b**). Consequently, this explains why the GMPiB_A model was inferior to GMPiB_B model from a profitability perspective at a selling price of $160,000/dose in **Figure 4.5b.** The hospital profit margins linked to autologous CAR T-cell manufacturing reported in this work are well above the average US total median hospital profit margins which is estimated at ~4% (Singh and Wheeler 2012). However, the hospital profit margins did not account for product administration costs or hospitalisation charges for any specialised medical care.

These results illustrate the impact of negotiations between stakeholders and the financial consequences of agreeing to a too high revenue share between the sponsor and the hospital partners. As such, comprehensive assessments should be performed to determine the most favourable partnership schemes across a range of commercialisation scenarios.

4.3.3.2 Key parameters' maximum values for the GMPiB models

To mitigate against profit losses when choosing a GMPiB-like model, this section discusses the maximum revenue share and mark-up values a sponsor company should be negotiating against across a range of selling prices, demands and number of sites (**Figure 4.9**). The tool was tasked to find the maximum revenue share for the GMPiB_A model and the maximum mark-up for the GMPiB_B model which would lead to the same profitability as the centralised model at 1,000 doses/year or the regioanl model at 5,000 doses/year (**Figure 4.9**). The tool calculated the maximum revenue share or mark-up based on the difference between the GMPiB models (when assuming no revenue share or mark-up) and the centralised or regional models. Furthermore, the analysis was performed for the minimum and maximum number of sites identified in the screening study provided at the beginning of this chapter. Thus, any values lower than those shown in the matrix of **Figure 4.9** would lead to a higher profitability for the GMPiB model/s when compared to the centralised/regional models. **Figure 4.9** also shows the hospital profit margins associated with the identified maximum revenue share and mark-up values.

	Demand		1,000 d/y		5,000 d/y	
	Relative to		Centralised (1 site)		Regional (2 sites)	
	No. sites		2 sites	4 sites	10 sites	20 sites
GMPiB_A maximum revenue share	Selling price/dose	$160,000	9.9%	7.3%	3.5%	0.8%
		$200,000	8.0%	5.9%	2.8%	0.7%
		$250,000	6.4%	4.7%	2.2%	0.5%
		$300,000	5.3%	3.9%	1.8%	0.4%
		$350,000	4.5%	3.3%	1.6%	0.4%
		$400,000	4.0%	2.9%	1.4%	0.3%
GMPiB_B maximum mark-up			168%	115%	49%	3%

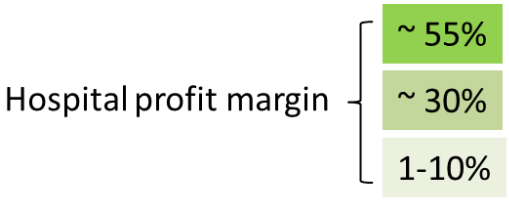

Figure 4.9 Maximum revenue share for the GMPiB_A model across a range of selling prices and mark-up for the GMPiB_B model determined for a demand of 1,000 and 5,000 doses/year. These represented the values which led to the GMPiB model's profitability to match either that of the centralised model at 1,000 doses/year or that of the regional model with 2 sites, at 5,000 doses/year. Also, these were determined for the case of two number of sites scenarios i.e. 2 and 4 sites at the lower demand and 10 and 20 sites at the higher demand. The hospital profit margin is equal to hospital revenue minus the expenses of the hospital and divided by hospital revenue. GMPiB_A = bedside manufacture - reimbursement shared between the sponsor and the hospital model, GMPiB_B = Bedside manufacture - semi-CMO model; d/y = doses/year.

Generally, the maximum revenue share and mark-up decreased with increases in demand and number of sites. In addition, the maximum revenue share decreased with increase in selling price (i.e. highest in top left corner and lowest in bottom right corner, (**Figure 4.9**). These values were found to be above the base case of 5% market share and 60% mark-up, respectively, at a demand of 1,000 doses/year, depending on selling price in the case of the GMPiB_A model, and below the base case values at a demand of 5,000 doses/year. Specifically, the maximum revenue share ranged between ~6% (at 4 sites) and ~10% (at 2 sites) at 1,000 doses/year and low selling prices and between 0.3% and 3.5% at 5,000 doses/year. On the other hand, the maximum mark-up ranged between 168% at 2 sites

and 115% at 4 sites for the 1,000 doses/year scenario and dropped to 49% at 10 sites and 3% at 20 sites for the 5,000 doses/year scenario. This was driven by the ranking of the GMPiB models relative to either the centralised model at 1,000 doses/year or the regional model with 2 sites, at 5,000 doses/year. At 1,000 doses/year, the GMPiB models were more profitable than the centralised model depending on selling price, while at 5,000 doses/year, the GMPiB models were less profitable than the regional model (**Figure 4.5).**

In terms of the hospital profit margins incurred by the maximum revenue share and mark-up values, it was found that margins of ~55% could be achieved at 1,000 doses/year, ~30% for the 2 sites scenario and a modest 1-10% for the 4 sites scenario at 5,000 doses/year. This suggests that the GMPiB models could be most attractive for smaller demands and number of sites. On the other hand, the GMPiB models implemented at higher demands and number of sites could potentially be viable if working with public-funded healthcare systems where hospital profits are not targeted.

4.3.3.3 Impact of automation on COG and profitability

GMPiB models are currently considered challenging to implement. One of the challenges is that they require manufacturing licence which, amongst others, requires proof of control over the GMP activities in the facility via the implementation of a pharmaceutical quality system (PQS). Since the hospital partner has their own quality processes which are non-GMP, defining who is responsible for what and building a functional and efficient PQS system is likely to be a significant challenge. A further area of concern when it comes to CAR T manufacture represents the labour-consuming in process control (IPC). It is hypothesised that automation of quality control (QC) could be the stepping stone to enabling routine bedside CAR T manufacture. This section is addressing the impact of employing automated, more expensive QC equipment systems, associated with more costly tubing sets, on cost of goods and profitability if labour requirements decreased by

a range of levels. Since flow cytometry and PCR are the most employed technologies for IPC of CAR T products' manufacture, it was assumed that these technologies would be upgraded to achieve a range of automation levels. Thus three different levels of automation were considered i.e. low, medium and high. It was assumed that a low level of QC equipment automation was associated with automated data analysis and storage in a cloud-like system, available for data trending activities and others. This was assumed to lead to a minimum 23% labour reduction. In addition to the low automation characteristics, the medium automation was assumed to be associated with automated sample preparation while the high automation was assumed to be associated, additionally, with a higher throughput. These levels were assumed to lead to a minimum 45% and 63% labour reduction, respectively. Furthermore, all levels of QC equipment automation were assumed to require the acquisition of a suite of software systems to enable maximising labour savings. These were electronic PQS (ePQS), batch manufacturing records (eBMR) and manufacturing execution systems (MES) and were assumed to incur an upfront cost of either 1M US $ (**Figure 4.10i**) or 5M US $ (**Figure 4.10ii**). The legend in **Figure 4.10** details on the assumptions used for each level of automation in terms of impact on costs and labour requirements.

a

i $1M US software cost

Labour reduction level	QC equipment cost increase: Low	Medium	High
Low	1%	6%	11%
Medium	-3%	1%	7%
High	-6%	-2%	3%

ii $5M US software cost

Labour reduction level	QC equipment cost increase: Low	Medium	High
Low	6%	10%	16%
Medium	2%	6%	11%
High	-2%	3%	8%

b

i $1M US software cost

Labour reduction level	QC equipment cost increase: Low	Medium	High
Low	0%	-3%	-8%
Medium	4%	1%	-3%
High	7%	4%	0%

ii $5M US software cost

Labour reduction level	QC equipment cost increase: Low	Medium	High
Low	-4%	-7%	-11%
Medium	0%	-3%	-7%
High	3%	0%	-4%

Legend

QC equipment cost increase	Base case	Low	Medium	High
QC equipment cost fold increase	1	1.5	2	2.5
QC consumable cost fold increase	1	1.15	1.3	1.5
Labour reduction level	**Base case**	**Low**	**Medium**	**High**
No. batches per production operator team	3	4	6	8
No. batches per QC op.	2	3	5	7
Release time per QP (hours)	20	18	15	9
Average labour saving	0%	23%	45%	63%

Figure 4.10 Impact of QC automation levels captured as **a)** change in COG/dose from base case and **b)** change in rNPV from the base case for the GMPiB_B model at a demand of 1,000 doses/year and a selling price of $160,000/dose when an upfront software cost was assumed to be **i)** 1M US $ and **ii)** 5M US $. Where QC = quality control, QP = qualified person. The base case QC consumable cost was approximated to $15,000/batch.

In terms of the impact on COG/dose, if the QC equipment cost increase level matched the expected level of automation achieved i.e. labour reduction level, the COG/dose was found to be insignificantly changed (<5%) at a low software cost level (**Figure 4.10a,i**). However, if the QC equipment cost increase level did not match the expected level of automation achieved or if the software costs level were higher, the COG/dose was found to be impacted (**Figure 4.10**). If a high level QC equipment cost increase led to a low or

medium labour reduction level (23% and 45%), the COG/dose increased between 11-16% and 7-11%, respectively, depending on software costs. On the other hand, if a low level of QC equipment cost increase over-achieved and led to a high labour reduction level (63%), the COG/dose decreased by 6% and 2%, depending on software costs.

In terms of the impact on profitability, it was found that the QC automation levels analysed here did not have an impact at a selling price of $400,000/dose (data not shown) but did exert an impact at a selling price of $160,000/dose (**Figure 4.10b**). At a selling price of $160,000/dose, if the QC equipment cost increase level matched the expected level of automation achieved i.e. labour reduction level, the GMPiB_B model's profitability was found to be insignificantly changed (within +/-5%) **(Figure 4.10b**). However, if the QC equipment cost increase level did not match the expected level of automation achieved, profitability was found to be impacted (**Figure 4.10**). If a high level QC equipment cost increase led to a low or medium labour reduction level (23% and 45%), profitability decreased between 8-11% and 3-7%, respectively, depending on software costs. On the other hand, if a low level of QC equipment cost increase over-achieved and led to a high labour reduction level (63%), profitability increased by 7% and 3%, depending on software costs. The reason why the profitability of the GMPiB_B model was not affected at a higher selling price was because the higher revenue level achieved absorbed the impact of fluctuations in the outgoings.

These results indicate that the QC equipment cost increase level had a higher impact than the labour reduction level on COG/dose and profitability. A potential reason for that was that, apart from the QC fixed cost, the QC equipment cost includes tubing set cost, which was assumed to be a direct cost thus affecting the COG/dose at a higher extent, while the labour costs were assumed to be indirect costs.

The question remains whether any of the combinations of achieved automation level and software costs would be considered sufficient to de-risk the implementation of hospital-based manufacturing and enable the GMPiBs model to be adopted by sponsor companies.

4.4 Conclusions

This chapter assessed a range of enterprise models for CAR T-cell therapy manufacture from profitability and operational feasibility perspectives, and identified the impact of automation on key financial metrics for bedside manufacturing models. This analysis is relevant since the centralised model may not be the most optimal solution for the supply of large demands of autologous gene-modified cell therapies given the limit in the number of processes that can be run robustly in parallel and the risks associated with transportation.

The profitability and operational feasibility screening results revealed the minimum and maximum number of sites for each decentralised model for a range of demands as well as the maximum demand that could be met by the centralised model (1 site). It was found that 2-4, 10-20 and 20-40 manufacturing sites were feasible for the decentralised models at 1,000, 5,000 and 10,000 doses/year, respectively. Furthermore, it was found that the centralised model (1 site) would unlikely be feasible from a shop-floor logistics perspective at a demand of 5,000 doses/year using the integrated processing approach.

The ranking of the enterprise models from a profitability and investment point of view at various demands and selling prices was further explored. It was found that the rented hospital model was the most attractive following by the bedside manufacture CMO-like model (GMPib_B) and the regional model at low demands and changed to the rented hospital and the regional model at higher demands. The profitability of the bedside manufacturing model where revenue was assumed to be shared between the sponsor

company and the hospital partners (GMPiB_A) was found to be highly impacted by selling price.

Analysis of the impact of selling price on key financial metrics of the hospital partners and a high level financial feasibility assessment for the bedside manufacturing models was provided. It was found that the hospital profit margins ranged between 40% and 67% between selling prices of $160,000 and $400,000/dose when 5% of reimbursement was assumed to be shared with the hospital partners (GMPiB_A model). On the other hand, when a CMO-like model was assumed (GMPiB_B), the hospital profit margins were found to be around 37% when assuming a 60% mark-up on the hospital partners' expenses. Furthermore, the maximum revenue share and mark-up values leading to the bedside manufacturing models to be as profitable as the centralised and regional models were identified across a range of selling prices, demands and number of sites.

Since a key challenge preventing the adoption of the bedside manufacturing models is considered to be the labour-consuming in-process control, the impact of QC automation on cost of goods and profitability was assessed. This analysis shows that large increases in QC equipment costs (up to 250%), matched or not by achieving the expected labour reduction level (i.e. up to 63%), as well as upfront software costs do not exert a large impact on COG/dose (i.e. -7% and 12% change). Further to this, it did not impact profitability at a high selling price of $400,000/dose. However, at a lower selling price of $160,000/dose, if a high or medium cost for QC automation would only a yield a low level of labour reduction, the profitability of the GMPiB_B model would be lower than at base case. This analysis could be extended to quantify the impact of achieving higher batch success rates as a result of QC automation adoption on financial metrics.

Beyond the specific set of case studies presented here it is worth noting the broader applicability of the decisional tool. The tool has been used in further optimisation

exercises where different avenues to achieving COG reductions were explored i.e. by limiting the process expansion duration, decreasing T-cell doubling time, decreasing viral vector requirement and increasing transduction efficiency (Pereira Chilima, 2019). It can be used to model allogeneic CAR T processes and such a case study is presented in Pereira Chilima (2019). Other allogeneic approaches e.g. utilising iPSC technology could also be modelled using this tool. However, the tool is not readily amenable to modelling *in vivo* CAR T manufacturing approaches i.e. mRNA/lipid nano-particle-mediated approaches. On the other hand, the viral vector decisional tool described in **Chapter 3** could be amenable to model mRNA manufacturing processes.

Chapter 5: Lentiviral vector process economics: an upstream processing appraisal

5.1 Introduction

Chapter 4 described an analysis of the impact of decentralisation extent of automated autologous CAR T-cell therapy manufacture on profitability and operational feasibility and provided a high level analysis of the implementation of "GMP-in-a-box"-like manufacturing model. The focus of **Chapter 5** shifts away from the helicopter-view adopted in **Chapter 4**. Instead, **Chapter 5** zooms into a key dependency of many *ex vivo* gene therapies, a critical component of their supply chain, the lentiviral vector component (**Figure 5.1)**. As such, viral vector-specific models were developed and added to the cell and gene therapy decisional toolkit, alongside the tool used in **Chapter 4**. The viral vector decisional tool was described in **Chapter 3**.

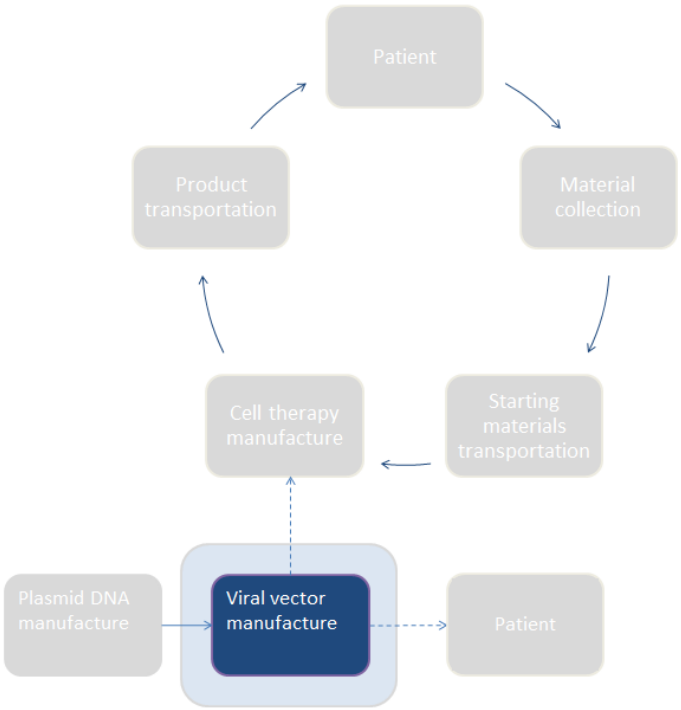

Figure 5.1 Gene therapy supply chain diagram presenting the focus adopted in **Chapter 5** where the area accounted for in the analyses, the lentiviral vector manufacture, is shown in blue. The areas not included were greyed out.

Chapter 1 provided an overview of the lentiviral vector products used in marketed products or in clinical trials while **Chapter 2** discussed the manufacturing processes including the cell culture technologies and expression systems typically employed, as well as downstream and analytics considerations. Viral vector costs are perceived to represent a major component of the material manufacturing costs for CAR T-cell therapies (Forsberg 2018; Technology 2019; Challener 2019) and this can be even more pronounced in the haematopoietic stem cell (HSC) gene therapy context (DiGiusto et al. 2013; Abou-El-Enein et al. 2013). Hence, there is a strong drive towards decreasing LV manufacturing costs to maximise the commercial feasibility of cell and gene therapy products.

This chapter presents the application of the decisional tool to investigate cost rankings of the currently available cGMP-grade LV manufacturing cell culture technologies across a wide range of LV products, clinical and commercial demand and harvest titre. Furthermore, the target process performance required to lower LV-associated costs down to critical threshold levels is explored. Briefly, the decisional tool components employed in this study consisted in a viral vector whole bioprocess economics model, which included a cost of goods model and fixed capital investment model coupled to a brute force search algorithm.

This chapter is organised as follows. **Section 5.2** presents the overview of the case study, describes the technologies chosen for investigation, the process assumptions as well as scheduling and facility assumptions. Five different cell culture technologies (10-layer vessels, hollow fibre bioreactors, fixed bed bioreactors, rocking motion bioreactors run with microcarriers and single-use stirred tank bioreactor run in suspension-mode) using a fixed DSP and fill finish flowsheets are assessed from a COG perspective (**Section 5.3.1** and **Section 5.3.4**). The analysis provides the COG breakdown for each of these

technologies and the key cost drivers (**Section 5.3.2** and **Section 5.3.3**). Moreover, it presents the harvest titre targets to achieve specific COG savings (**Section 5.3.5**) as well as the impact of changing specific productivity assumptions and switching from transient transfection to stable producer cell line on technology ranking (**Section 5.3.6**).

5.2 Case study setup

5.2.1 Case study overview

The decisional tool described in **Chapter 3** was used to explore the rankings of commercially available cell culture technologies utilised in cGMP compliant LV manufacturing from a COG perspective. This analysis was carried out across a range of annual demands and LV dose sizes representative to a variety of LV products employed in CAR T/TCR, HSC gene therapies and in *in vivo* applications for indications shown in **Table 1.1**, **Chapter 1**. Importantly, at the core of the present analysis is the assumption that the LV products manufactured using the selected candidate cell culture technologies can be proven as comparable to the standard technology, i.e. 10-layer vessels.

In terms of dose size, **Table 5.1** provides key assumptions as well as the equation used in determining the LV dose size for a hypothetical CAR T/TCR product. The LV dose size of 2 x 10^9 TU/dose was chosen to be the base case scenario for a hypothetical CAR T/TCR product, and a potential lower dose of 2 x 10^8 TU/dose was also explored in the sensitivity scenarios (Blaeschke et al. 2018). Based on the reported dose ranges (**Table 2.7**), representative HSC gene therapy dose sizes of 2 x 10^{10} and 2 x 10^{11} TU/dose were selected for analysis. It is assumed that only one dose is required per patient and that the dose size does not change as a result of different patients' weight. It was assumed that the CQA requirements for the *in vivo* LV would not be dissimilar from those of an *ex vivo* product, namely in terms of safety. The same manufacturing process could be used therefore for both types of products.

Table 5.1 LV dose size considerations for CAR T/TCR products.

Parameter	Assumption	References
No. CD3+ T cells in leukapheresate (N_{Cstart})	0.6 x 10^9 – 2 x 10^9 Base case: 1.2 x 10^9	Allen et al. (2017)
Process yield up to transduction step (%) (Y_{pT})	33%	Cryopreservation/thaw (70%): Ostrowska et al. (2009) Elutriation (65%): TERUMO BCT protocol Cell wash (92%): Kabi (2019) Selection/activation (80%): Willasch et al. (2010)
Multiplicity of infection (MOI as TU/cell); No. transduction hits (N_{TH})	0.2-8; 1 Base case: 5; 1	Milone et al. (2009); Rapoport et al. (2015)
Equation to determine CAR T/TCR LV dose size (TU/dose)	$LV_{dose} = N_{Cstart} \times Y_{pT} \times MOI \times N_{TH}$ Base case LV dose size = 1.2 x10^9 x 33% x 5 x 1 ≃ **2 x 10^9 TU/dose**	

Although CAR T and TCR products are inherently different, it was decided to refer to them as a class of products due to similarities at the manufacturing level. TU = transducing units.

Five different single-use cell culture technologies were identified to have demonstrated cGMP compliant manufacturing of LV vectors based on literature review (Aiuti et al. 2013; Sheu et al. 2015; Valkama et al. 2018; Greene et al. 2012; Miskin 2015; Miskin 2016). Aside from the standard 10-layered vessels (e.g. Cell Factory™) hereby referred to as "CF10", hollow fibre - "HF" (e.g. Quantum™), fixed bed - "FB" (e.g. iCELLis™), rocking motion - "RMmc" (e.g. Wave™) and single-use stirred tank bioreactors - "SUB" (e.g. Mobius, Merck, Massachusetts, USA) were chosen as candidate technologies in the analysis. To note, RMmc bioreactors were assumed to be run using microcarriers such as Fibra-Cel® microcarrier disks. The most prominent difference between these technologies was that cell cultures in CF10, HF, FB and RMmc were run in adherent-mode whereas the SUB cell culture was run in suspension-mode. Key process and cost parameters of candidate cell culture technologies are presented in **Table 5.2, Table 5.3**, and **Table 5.4.**

Table 5.2 Key process and cost parameters associated with candidate cell culture technologies.

Parameters	**CF10**	**HF**	**FB**	**RMmc**	**SUB - suspension**
Surface area (cm^2)/unit	6,360	21,000	$66x10^6 – 3.33x10^6$	$2.4x10^5 – 6.00x10^6$	NA
Working volume (WV, L)/unit [1]	1	0.18	70	5, 10, 25, 100, 250	50, 100, 200, 500,1000,2000
No. perfusion days prior to harvest initiation (T_{ph})	NA	2.5	2.25	NA	NA
No. of batch harvests (NH)	2	NA	NA	2	1
No. perfusion days for harvest (T_h)	NA	2	2	NA	NA
Max. no. of units/batch [2]	36	36	1	1	1
Perfusion rate (PR, WV/day)	NA	PR_{ph}: 13.7 PR_h:14.8	PR_{ph}: 0.18 (FB66); 0.35 (FB133); 0.9 (FB333) PR_h: 0.7 (FB66); 1.4 (FB133); 3.6 (FB333)	NA	NA
Total media consumption per run (L)	WV x NH	WV x (PR_{ph} x T_{ph} + PR_h x T_h)	WV x (PR_{ph} x T_{ph} + PR_h x T_h)	WV x NH	WV x NH
Total harvest volume per unit (L)	WV x NH	T_h x WV x PR_h	T_h x WV x PR_h	WV x NH	WV x NH
Plasmid requirement (µg/million cells)	2.5	2.5	2.5	2.5	2.5
Media consumption (ml) per million cells per day of harvest [4]	0.786	0.640	0.375	0.208	0.786

Parameters	CF10	HF	FB	RMmc	SUB - suspension
Productivity (TU/cell/day) to achieve the same harvest titre of 10^7 TU/ml [5]	7.86	6.35	3.75	2.08	7.86
Pure TU/batch [6]	2.37 x 10^{10}	2.33 x 10^{11}	7.26x10^{10} – 7.7x10^{11}	7.26x10^{10} – 7.7x10^{11}	7.26x10^{10} – 3.39x10^{12}
USP labour requirements (no. operators per batch)	>5 units: 0.25 <5 units: 2	>5 units: 0.2 <5 units: 2 [3]	4 (FB66), 5 (FB133, FB333) [3]	4 (RMmc6, RMmc120), 5 (RMmc240, RMmc600) [3]	3 (SUB50, SUB100), 4 (SUB200, SUB500, SUB1000, SUB2000)
Consumable costs (USD/unit)	500	12,000	19,000 – 29,400	420 – 1,400	6,300 – 18,800
Associated equipment cost (USD/unit)	20,000; 20,000 (BSC & incubator costs)	150,000	325,000	80,000 – 325,000	250,000 – 437,500

[1] Minimum WV = 10% vessel volume;
[2] Per cleanroom suite;
[3] Additional labour for the night shift included due to continuous harvesting (20% of day time capacity);
[4] Media consumption per million cells per day refers to harvest volume/(total number of cells in bioreactor at transfection/10^6)/number of harvest days;
[5] Specific productivity (TU/cell/day) = Harvest titre (TU/ml) x Harvest volume (ml)/(transient transfection cell density (cells/cm^2) x SA (cm^2) x no. of harvest days) for adherent processes or Productivity (TU/cell/day) = Harvest titre (TU/ml) x Harvest volume(ml)/(transient transfection cell density (cell/ml) x working volume (ml)) for the suspension (SUB) process;
[6] Accounts for retained material, material needed for QC and overall yield.
ph = prior harvest, h = harvest, TU = transducing units; WV = working volume; NH = number of batch harvests; NA = not applicable.

Table 5.3 Key mass balance, DSP and fill finish process parameters assumptions.

Culture mode	**Technology**	**Harvest Volume (L/unit)**	**Cell density (seeding; transfection)**
Adherent	Technology (surface area in m^2): CF10(0.6) HF(2) FB(66); FB(133); FB(333) RMmc60(60); RMmc120(120); RMmc240(240) RMmc600(600) [1]	2 5.33 100; 200; 500 50; 100; 200; 500	$5x10^4$ cells/cm^2; $2x10^5$ cells/cm^2
Suspension	Technology (working volume in L): SUB(50); SUB(100); SUB(200); SUB(500); SUB(1000); SUB(2000)	50; 100; 200; 500; 1,000; 2,000	3.18×10^5 cells/ml [2]; 1.27×10^6 cells/ml [2]
Downstream steps	**Process parameter**	**Value**	
DSP			
Clarification	Step yield	80%	
	Filter capacity (adherent/suspension) (L/m^2)	60 / 20	
	Flux (LMH)	40	
DNA degradation	Endonuclease requirement (U/ml of feed)	25	
AEX	Step yield	40%	
	DBC (TU/ml)	$5x10^8$	
	Column bed height (cm)	20	
	Max. linear velocity (cm/h)	100	
UF/DF	Step yield	80%	
	Target DS concentration (TU/ml) [3]	$10^8 – 10^9$	
	Flux (LMH)	55	
	Max. concentration time (h)	2	
	Max. diafiltration time (h)	2	
	Retained DS volume for QC and other purposes (ml)	100	
Fill Finish			
Thaw and 0.2 µm filtration	Step yield	75%	
	Filter capacity (L/m^2)	250	
	Flux (LMH)	100	
UF	Step yield	96%	
	Max. concentration time (h)	2	
	Flux (LMH)	55	
	Target DP concentration (TU/ml) [3]	$10^9 – 10^{10}$	
Fill	Step yield	95%	
	Cryovial total volume (ml), space efficiency (%)	1-100, 75%	
	Thaw yield	100%	
	Retained DP volume for QC and other purposes (ml)	100	
Overall			
DSP	**Overall DSP yield**	**26%**	
Fill Finish	**Overall Fill Finish yield**	**68%**	
DSP & Fill Finish	**Overall DSP & Fill Finish yield**	**17%**	

DSP = downstream processing, LMH= litre per m^2 per hour, TU = transducing units, U = units, AEX = anion exchange chromatography, DBC = dynamic binding capacity, UF/DF = ultrafiltration/diafiltration.
[1] Fibra-cell disks concentration = 0.02 g/ml of working volume;
[2] The suspension process cell density was calculated using: CF10 surface area x CF10 cell density/CF10 working volume;
[3] Final concentrations are functions of LV dose size;
DSP and fill finish unit operations were assumed to be single-use, with the exception of AEX column (self-packed) which could be reused as many times as needed on a per year basis.

Table 5.4 Key lentiviral vector process costs assumptions.

Category	Cost parameter	Value
Materials	Fibra-cel disks (USD/g)	7
	Plasmid DNA cost (include. PEI, USD)/g	74,000
	Depth filter (USD/m^2)	613
	Endonuclease (USD/5M U)	12,000
	AEX resin (USD/L)	300
	UF membrane (USD/ m^2)	613
	CellGro formulation buffer (USD/ 500 mL)	207
	Filter (USD/0.6 m^2)	260
Labour	Operator salary (USD)	120,000
	Labour multiplier (to account for supervisors and management)	2.2
	Seed labour	f(no. units/seed train) + 1 for media prep.
	USP labour	f(technology), see **Table 5.2**
	DSP labour [1] (no. operators in DSP/batch), HV stands for harvest volume/batch	2 (HV≤ 50 L); 3(HV≤ 100 L, 4 (HV≤ 500 L), 5(HV≤ 1,000 L), 8 (HV≤ 2,000 L)
	Fill finish labour	2/filling machine
	Seed no. shifts/day	1
	USP no. shifts/day	2 apart from CF10 and SUB which require one shift only; night shift requires 20% of day shift labour
	DSP no. shifts/day	2; night shift requires 50% of day shift labour
	FF no. shifts/day	3
Indirect	Depreciation period (years)	7
	Maintenance (%FCI)/year	10%
	Class B monitoring costs ($/$m^2$)/year	7,232
	Class C monitoring costs ($/$m^2$)/year	1,012
	Energy ($/$m^2$)/year	637
QC	QC (USD/batch)[2]	40,000
Other	Overage (%)	10%

USP = upstream processing, DSP = downstream processing, UF = ultrafiltration, HV = harvest volume/batch, FCI = fixed capital investment, FF = fill finish, QC = quality control.
[1] USP and DSP labour can work on either of the process areas. Includes buffer prep and equipment prep labour;
[2] QC costs contains both labour and material costs. No QP costs accounted for.

5.2.2 Lentiviral vector process overview

All of the above-stated technologies were assumed to be employed in a transient transfection LV manufacturing process using a 4-plasmid system mediated by polyethylenimine (PEI) using a HEK293T cell line and serum-free media. Whilst the pDNA requirement typically ranges between 1-5 µg per one million cells at transfection step (Inc. 2018; Merten et al. 2016), the base case pDNA mass was selected to be 2.5 µg/10^6 cells **(Table 5.2**). This is associated with the same DSP and fill finish flowsheet operated in batch mode, and duration so as to mitigate biases (**Table 5.3**). **Table 5.5** summarises the schedule associated with each cell culture technology from seeding the production bioreactors to fill finish. Irrespective of technology, the seed train duration was variable as it was assumed to be a function of manufacturing scale and it was associated with different costs depending on culture mode (**Table 3.1, Chapter 3)**. In this chapter, differences in license costs for GMP cell lines were assumed to be negligible for the cost of goods calculations.

The HF and FB bioreactors are intrinsically perfusion systems, whereas the rest operated in batch (SUB) or repeat batch-mode (CF10 and RMmc). In the case of CF10 and RMmc, LV containing media was collected, chilled and replaced with fresh media on Day 3. On Day 4 the final collection took place and the two product volumes were pooled prior to DSP. In the case of the RMmc technology, intermittent product collections were assumed to be carried out between Day 3 and Day 4. Product collection on HF and FB was assumed to be continuous across ~2 days and all collections were pooled prior to DSP (**Table 5.5**). The perfusion rate parameters and total media consumption were based on literature (Valkama et al. 2018; Sheu et al. 2015) but were adjusted to the assumed schedule as the best approximation of possible commercial production scenarios (**Table 5.2, Table 5.3, Table 5.5)**. The SUB bioreactor was assumed to be harvested only once as is typical with

suspension culture so as to avoid the logistical hurdles associated with executing a "media exchange" step on a stirred tank bioreactor at scale.

Table 5.5 Schedule of production activities for candidate technologies.

Tech	Day 0	Day 2	Day 3	Day 4	Day 9
CF10	Seed	Transfect	Harvest & chill; Replenish media	Harvest; Pool; DSP; Cryo-freeze	Thaw FF Cryo-freeze
HF	Seed; Start perfusion (via EC loop)	Stop perfusion and transfect (via IC loop); Re-start perfusion (via EC loop) Start perfusion and harvest (via IC loop, ~12h post-transfection) & chill	Harvest & chill	Stop perfusion/ harvest; Pool; DSP; Cryo-freeze	Thaw FF Freeze Cryo-freeze
FB	Seed; Start perfusion	Stop perfusion and transfect; Re-start perfusion (6 hours post-transfection); Start harvest (12h post-transfection) & chill	Harvest & chill	Stop perfusion/ harvest; Pool; DSP; Cryo-freeze	Thaw FF Cryo-freeze
RMmc	Seed	Transfect	Harvest & chill Replenish media	Harvest; Pool; DSP; Cryo-freeze	Thaw FF Cryo-freeze
SUB (STR)	Seed	Transfect		Harvest; DSP; Cryo-freeze	Thaw FF Cryo-freeze

ff = fill finish, EC = extracapillary loop, IC = intracapillary loop.

In terms of estimating the infectious harvest titre, it was assumed that all cell culture technologies achieve the same infectious titre in the total collected harvest volume of 10^7 TU/ml as measured using RT-qPCR methodology and that the LV preparations have the same quality (Barczak et al. 2015). The authors are aware that the quality of the LV preparation, which is impacted by vector biology and other factors, has a significant impact on MOI and hence on final number of LV doses that can be generated from one

batch. It is thus assumed that the LV generated using all cell culture technologies would be characterised by the same ratio of physical to infectious particles falling between 100 and 250 (Marceau and Gasmi 2014). “Infectious harvest titre” and “harvest titre” are used interchangeably in this work. The consequence of assuming a constant harvest titre and cell density across technologies, whilst assuming other different process parameters, was that the specific productivity, defined as the total number of collected TU divided by the total number of cells at transfection and divided by the number of harvest days, was different between technologies. It was the lowest for RMmc and FB (**Table 5.2**) due to the high surface area per working volume and the double harvest per batch assumed in these systems. In practice, concerns have been raised around carrying out transient transfection in these technologies as it could result in low specific productivities due to either limited contact area between adherent cells on the Fibra-Cel disks and the liquid phase containing the PEI: plasmid DNA complexes in the case of RMmc or due to heterogeneous cell distributions discovered across the height of the bed in the case of FB (Valkama et al. 2018; Lesch et al. 2015).

An overall process yield of 17% was calculated from the assumed step yields (**Table 5.3**). DSP was assumed to be carried out at 2-6°C using jacketed product holding and buffer bags so as to preserve infectivity. Given that variations in harvest titre are commonplace in viral vector processes (Geraerts et al. 2006; Merten et al. 2014b; Masri 2019), it was assumed that filling consistent LV dose size per cryovial could be achieved by implementing a freezing step of the drug substance during which infectious titre measurement would be performed.

5.2.3 Key lentiviral vector manufacturing assumptions

When it comes to the number of bioreactors used per batch, it was assumed that only one FB, RMmc or SUB bioreactor could be run per batch. If the demand input led to more

batches per year than the number of batches that could be manufactured using one bioreactor, the model scaled out the process to allow multiple bioreactors to be selected per cleanroom (up to six). Each train comprised a bioreactor with its own seed, DSP and fill finish equipment. On the other hand, up to 36 units per batch were assumed in the case of the CF10 and HF. Moreover, HF, FB and RMmc bioreactors come in fixed bed formats implying that they often produce excess material as all harvest volume per unit would be further processed. In line with that, it was assumed that also the SUB bioreactors would operate at maximum working volume and all harvest volume would be further processed. In terms of cleanroom classification, it was assumed that seeding and fill finish activities took place in a Grade B cleanroom whereas USP and DSP took place in a Grade C cleanroom irrespective of cell culture technology. The only exception to this rule was that the USP area of the CF10 process was designated as Grade B due its semi-closed nature.

Also, it was assumed that the facility was operated with shift patterns as dictated by the cell culture technology choices and process stage (**Table 5.4**) for up to 330 days per year allowing for two annual shutdowns. The maximum number of batches/year was 30 and was split in campaigns of up to 5 batches depending on demand. Each campaign was assumed to share the same seed train. Furthermore, the case study was set up based on the assumption that the manufacturer sought to generate all demanded LV material as quickly as possible; hence the model was set to minimise the number of batches manufactured per demand while maximising batch size. Also, it was assumed that the facility would be utilised for manufacturing other viral vector products after generating the demanded LV volume. Consequently, labour, maintenance and depreciation costs associated with each technology were calculated as a function of the annual facility utilisation.

5.3 Results and discussion

5.3.1 Deterministic COG analysis of processes utilising different cell culture technologies for LV manufacturing

A deterministic COG analysis of processes utilising five different cell culture technologies was run for a hypothetical base case CAR T/TCR LV product with a dose size of 2 x 10^9 TU across a range of demands. The range of demands was representative of early and late phase clinical trials (10 - 300 doses/trial) and different commercial manufacturing scenarios (500 – 10,000 doses/y) (**Figure 5.2a,b**). **Figure 5.2a** shows the COG_{LV}/dose for each technology across demands whereas **Figure 5.2b** shows the total COG associated with the number of batches required to satisfy each demand for each technology. The number of batches and manufacturing trains (if different from 1) required to meet those demands with each configuration plotted, are shown in **Figure 5.2c**. It was assumed that all candidate technologies achieved an infectious harvest titre of 10^7 TU/ml. Additionally, it was assumed that the CF10 and HF batches were run with the maximum

number of 36 units/batch while the FB, RMmc and SUB with one unit per batch.

c

	Clinical trials demand (no. doses/trial)				Commercial demand (no. doses/y)			
	10	100	200	300	500	1,000	5,000	10,000
Technology	No. batches/trial (1 train)				No. batches/year, No. trains (if no. trains>1)			
CF10	1	10	20	30	50, 2	100, 4	500, 17	1000,34
HF	1	1	2	3	5	10	48,2	95, 4
FB66/RMmc120/SUB100	1	4	7					
FB133/RMmc240/SUB200	1	1	2	3	5	9	45,2	90,3
FB333/RMmc600/SUB500				1	2	3	15	29
SUB2000				1	1	1	4	7

Figure 5.2 Candidate technologies ranking at a dose size of 2 x 10^9 TU/dose and harvest titre of 10^7 TU/ml based on **a)** COG_{LV}/dose, **b)** Overall COG_{LV}/demand and **c)** The number of batches across a range of demands representative of both clinical trials and commercial manufacturing for a large indication. Grey cells show that a particular configuration is not a candidate for a particular demand. Multiple manufacturing trains were allowed per facility to satisfy demands. Light blue cells show the configurations which require more than one manufacturing train. The maximum number of units per batch in the case of CF10 and HF is 36 whereas for FB, RMmc and SUB is 1. CF10 = 10-layer vessels, HF = hollow fibre bioreactor, FB = fixed bed bioreactor, RMmc = rocking motion bioreactor run with microcarriers, SUB = single-use stirred-tank bioreactor, TU = transducing units.

The analysis identified the optimal configuration of each candidate technology across each of the demand scenarios (**Figure 5.2**). The most cost-effective FB, RMmc and SUB configurations for early phase clinical trials with 10 patients were found to be FB66, RMmc120 and SUB100, respectively. On the other hand, for Phase 3 clinical trials and commercial manufacturing, the most cost-effective FB and RMmc configurations were found to be FB333 and RMmc600. In terms of SUB and large-scale manufacturing, three different SUB configurations were investigated (SUB200, SUB500 and SUB2000). The SUB200 represents the largest scale to which transient transfection has been scaled successfully to date, in suspension cell culture, and the larger scales (SUB500 and SUB2000) represent possible scales if the feasibility of transient transfection is demonstrated in the future above the 200 L scale. The optimal SUB scales for late phase clinical trials and commercial manufacture were identified as SUB500 at 300, 500 and 1,000 doses/y, and SUB2000 at 5,000 and 10,000 doses/y.

The tool explored the rankings of the different candidate technologies and the impact of demand on COG. Irrespective of demand, the tool predicted that SUB was the most cost-effective technology, assuming successfully scaled-up transient transfection at scales above 200 L. SUB was the most cost-effective technology in clinical trials despite the fact that SUB100 produced two-fold more material than the demand of 10 doses/trial. SUB50 was not an optimal configuration as it was found to be unable to deliver any doses per batch post-purification due to the low overall process yield as well as the drug substance and drug product volumes needed for QC and retains. The cost benefit of SUBs relative to CF10 increased with demand from being 8% cheaper at early phase trials to 90% at late phase clinical trials to being over 95% cheaper for large commercial demands. This translated into SUB COG_{LV}/dose values of $84,400 USD to $4,300 USD to $1,200 USD.

The SUB offered also cost savings relative to the more scalable adherent options of FB and RMmc of 14% and 19%, respectively, for early phase clinical trials and 17% and 32%, respectively, for late phase clinical trials and commercial demands. If there is a preference to use adherent technologies, then switching to FB and RMmc could lead still to significant COG_{LV}/dose savings relative to CF10 of 94% and 92%, respectively, at late phase clinical trials and commercial scales.

In terms of the CF10 and HF technologies, these incur the highest COG_{LV}/dose across demands in excess of $38,000 USD/dose in the case of CF10 and $9,300 USD/dose in the case of HF at large scale. This is mainly due to their constrained scalability dictated by “scaling out” rather than “scaling up” i.e. increasing the facility footprint to fit the required number manufacturing trains to host manufacturing of a small-scale and expensive process in the case of HF or labour-intensive process in the case of CF10. Sustaining manufacturing using the CF10 technology throughout the project lifetime requires building multiple facilities as the maximum demand that this technology can deliver, with one manufacturing train of 36 CF10 units and 30 batches/y, is only 330 doses/y at the base case dose size of 2×10^9 TU (**Figure 5.3**).

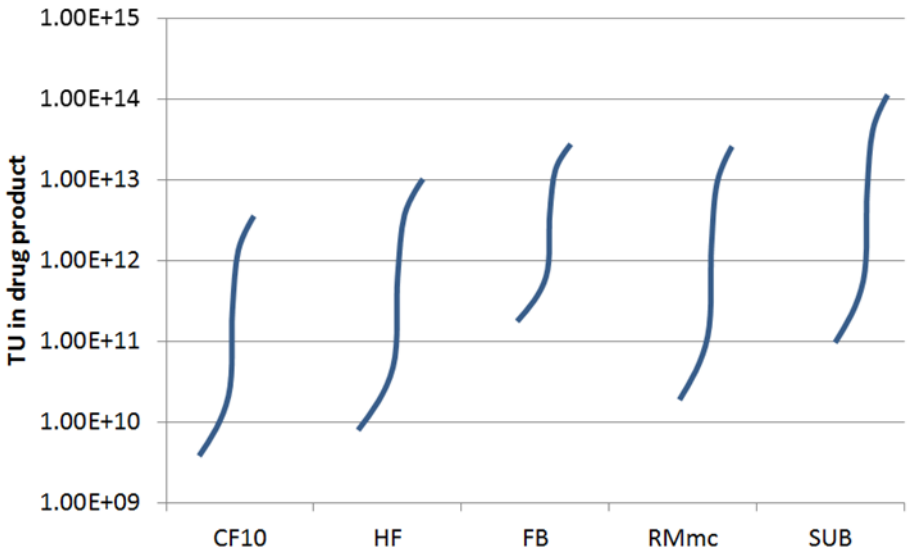

	CF10	HF	FB333	RMmc600	SUB2000
No. CAR T LV doses/y (2×10^9 TU/dose)/train	330	3,480	11,550	11,550	50,760

Figure 5.3 Conceptual representation of a technology S-curve illustrating the evolution of cell culture technologies used in lentiviral vector manufacturing obtained at base case assumptions. The lower limit of each S-curve are the number TUs in drug product achieved per year (30 batches/y) when the minimum number of units is used in case of CF10 and HF whereas in case of FB, RMmc and SUB when the smallest configurations are used at maximum capacity. Conversely, the upper limit of each S-curve is represented by the number of TUs in drug product per tear (30 batches/y) achieved when the maximum number of CF10 and HF units are used per batch whereas in case of FB, RMmc and SUB when the largest configurations are used at maximum capacity. The number of CAR T doses accounts for the base case process yields (**Table 5.3**) and 10% overage per batch. The plotted TU numbers per technology do not take into account losses due to testing/retains (i.e. 100 ml drug substance and 100 ml drug product).

The steeper decrease in COG_{LV}/dose with increase in scale that the tool captured for the SUB technology when compared to the other technologies can be explained by the fact that the SUB benefits from a broader scalability compared to all other candidate technologies i.e. the largest SUB configuration, SUB2000, was assumed to deliver 2,000 L harvest per batch whereas FB333 and RMmc600 configurations (the largest ones) were assumed to deliver maximum ~500 L harvest per batch. As a result, while at low demand (300 doses/y) the number of batches required to meet demand is the same amongst these

three technologies and equal to 1, the number of SUB2000 batches at 10,000 doses/y is ~4-fold lower compared to the number of FB333, RMmc600 or SUB500 batches (7xSUB2000 batches versus 29xFB333/RMmc600/SUB500 batches, **Figure 5.2c**). Consequently, SUB2000 benefits from lower indirect and labour costs when compared to the FB333 and RMmc600 technologies as it was assumed that the facility can be utilised for manufacturing other similar products after the LV order has been delivered. The authors have checked that the COG/dose values generated by this tool fall in the right ballpark by engaging in discussions with industry experts throughout the execution of the project and during the preparation of the manuscript.

In terms of the total COG_{LV} associated with manufacturing of all LV doses required per demand (**Figure 5.2b**), COG_{LV}/demand ranges from one million US dollars at early stage clinical trials to ten million US dollars at late stage clinical trials and ten million US dollars to above one hundred million US dollars at 10,000 doses/y.

In terms of the LV cost contribution to CAR T drug substance COG_{DS}/dose, for a case where LV cost contribution to the CAR T COG_{DS}/dose represents between 15-20% when manufactured using CF10, switching to SUB500 would reduce that cost contribution to ~1%. In terms of the LV cost contribution to the total raw material costs, this would mean a decrease from 24-33% in the case of the CF10 process down to 2% in the case of the SUB500 process (data not shown). Despite the superiority of the SUB technology over the FB and RMmc technologies from a COG_{LV}/dose perspective across scale, the percentage cost reductions these technologies achieved relative to CF10 COG_{LV}/dose were not dissimilar (**Figure 5.2a**) suggesting that these technologies could also provide cost-effective solutions for cell and gene therapy manufacturers.

5.3.2 COG_{LV}/dose breakdown at base case scenario

The tool was then used to generate COG_{LV}/dose breakdowns so as to identify the key cost drivers contributing to the technology ranking presented in the previous section. **Figure 5.4** shows the COG_{LV}/dose breakdown for all technologies on the basis of different cost categories such as raw materials (reagents and consumables), labour, QC and indirect costs (**Figure 5.4a**) and of different process stage costs such as seed train (inoculum generation), USP, harvest storage, DSP and fill finish costs (**Figure 5.4c**, **Figure 5.5**). This data is representative for a LV product with a dose size of 2 x 10^9 TU across multiple demands. The cost reductions achieved by switching away from CF10 on each cost category are shown in **Figure 5.4b** at 100 and 1,000 doses/y. The raw material cost breakdown is also shown at a demand of 1,000 doses/y in **Figure 5.6.**

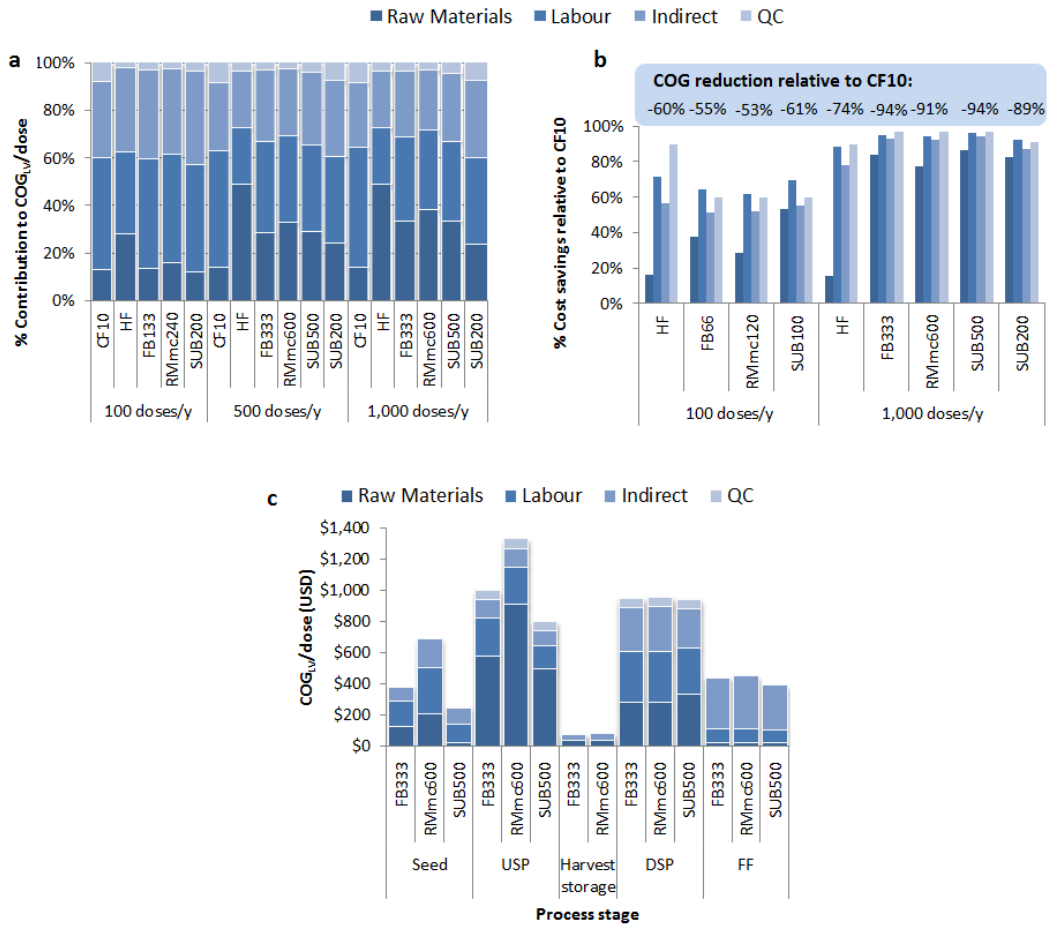

Figure 5.4 Lentiviral vector cost of goods breakdown at a dose size of 2x10^9 TU on the basis of **a)** Cost category at 100, 500 and 1,000 doses/y, **b)** Reduction in category costs achieved when switching away from CF10 at 100 and 1,000 doses/y; **c)** Process stage cost

category at 1,000 doses/y in the case of FB333, RMmc600 and SUB500, Harvest storage costs include indirect and raw material costs only and apply only for adherent technologies where multiple harvests are carried out. QC costs are equally distributed between USP and DSP in figure **c**. For details about what each cost category includes, see **Section 5.2**.

From a cost category perspective, the tool showed that, in general, labour and indirect costs dominated COG_{LV}/dose at the lower demands in the order of 100 doses/y while raw materials dominated at the higher demands above 500 doses/y for the more scalable technologies (FB, RMmc, SUB). For CF10, the demand did not have an effect on the cost breakdown (**Figure 5.4a**) given the scale-out approach. In general, at 100 doses/y, labour and indirect costs each accounted, on average, for ~35% and 40% of the total COG_{LV}/dose, followed by raw material costs and QC. At 1,000 doses/y, on the other hand, raw material costs contributed to ~40% of COG_{LV}/dose in the case of FB333, RMmc600 and SUB500 and ~50% in the case of HF. Raw material costs dominated COG_{LV}/dose at the commercial demands since facility overheads were spread over more doses while raw material costs per dose remained the same. In the case of the SUB200 and the higher commercial demands, the raw material cost contributions were lower (26%) due to the higher number of batches required to meet demand when compared to SUB500 (5xSUB200 vs 2xSUB500 batches, **Figure 5.2c**), driving indirect and labour costs up. In terms of QC costs, its contribution was the lowest (2-10% depending on technology) and it did not change with increase in demand as the volume of drug substance (DS) and drug product (DP) required for QC and retains was fixed per batch. QC costs were consistently highest for CF10 technology due to the highest number of batches required per demand (**Figure 5.2c**).

The cost reductions in COG_{LV}/dose that can be achieved when moving away from CF10 and towards the more scalable technologies are highlighted in **Figure 5.4b**. At low demands (100 doses/y), more significant cost savings of 60-70% are observed for QC and

labour costs while the raw material and indirect costs are reduced by 30-50%. On the other hand, at higher demands (1,000 doses/y), the savings associated with the switch increased to ~80-90% across all cost categories driven by the differences in scalability.

In terms of process stage costs, the tool predicted that USP and DSP stages were the most expensive stages, followed by fill finish and seed, irrespective of demand or technology (**Figure 5.5**). USP costs dominated the COG_{LV}/dose for CF10 and HF due to large raw material and labour costs associated with running multiple cell culture units in parallel per batch. The USP cost contribution in the case of HF was higher than for CF10 due to the large hollow fibre consumable unit cost. HF's DSP and fill finish costs were lower when compared to CF10's because of the lower number of batches needed (1 x HF vs 10 x CF10). For the more scalable technologies (FB, RMmc, SUB), the USP, DSP and fill finish costs had the highest contributions, with the first two process stages being slightly more expensive than the fill finish stage (~30%, ~30%, ~18% respectively). In terms of process stage cost differences amongst cell culture technologies, **Figure 5.5** and **Figure 5.4c** show that, irrespective of manufacturing scale, seed and USP costs associated with the SUB technology were lower than those associated with FB and RMmc of similar size.

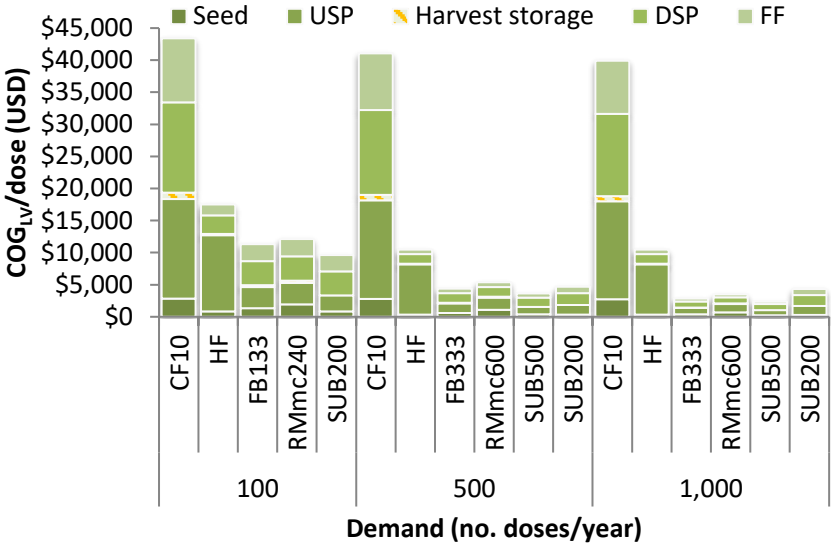

Figure 5.5 COG_{LV}/dose breakdown in terms of process stage costs at 100, 500 and 1,000 doses/year. Dose size = 2 x 10^9 TU, base case assumptions.

To analyse the root cause of this observation and, ultimately, to understand the COG_{LV}/dose differences amongst the scalable cell culture technologies, the tool was tasked to generate the process stage cost category breakdown at a demand of 1,000 doses/y (**Figure 5.4c**). It was found that raw material and labour costs associated with seed and USP stages were significantly lower in the case of SUB when compared to FB and RMmc. In the seed stage, the SUB cost savings in terms of raw material costs (80% relative to either FB or RMmc) and labour costs (30% relative to FB and 60% relative to RMmc), were due to assuming different seed train cell culture technologies (**Table 3.1**, **Chapter 3**). Specifically, the n-1 stage in the case of FB333 and RMmc600 relied on utilising multiple CF10 units as opposed to a single 100 L rocking motion bioreactor in the case of SUB500. As a result, 60 and 100x10-layer units were needed in the case of FB333 and RMmc600, respectively, which in turn, drove up the number of biosafety cabinets, and incubators, as well as the number of operators, when compared to the SUB500 candidate. In the USP stage, the SUB cost savings in terms of raw material costs (15% relative to FB and 46% relative to RMmc) were attributed to additional media

consumption during cell growth stage (**Table 5.2**) and larger pDNA costs due to higher cell numbers present at transfection. In terms of the labour costs savings predicted when choosing SUB (37% relative to either FB or RMmc), these were attributed to multiple harvest days associated with the adherent technologies.

When it comes to the raw material cost breakdown (**Figure 5.6**), USP single-use components costs dominated in the case of CF10 and HF (34% in the case of CF10 and 82% in the case of HF) whilst pDNA had the highest cost contribution in the case of the scalable technologies (41%, 46% and 36% in the case of FB333, RMmc600 and SUB500, respectively). While at 1,000 doses/y, pDNA costs had a contribution to the overall COG_{LV}/dose of 13-19% in the case of the scalable technologies, this contribution increased to 15-28% at 10,000 doses/y. This represents a solid basis to drive efforts towards eliminating these costs by switching to a stable producer cell line system which removes any plasmid requirements. The second largest driver in the case of FB333 and RMmc600 technologies was the single-use USP components amounting to 22% for each and media (13% for FB333 and 11% for RMmc600).

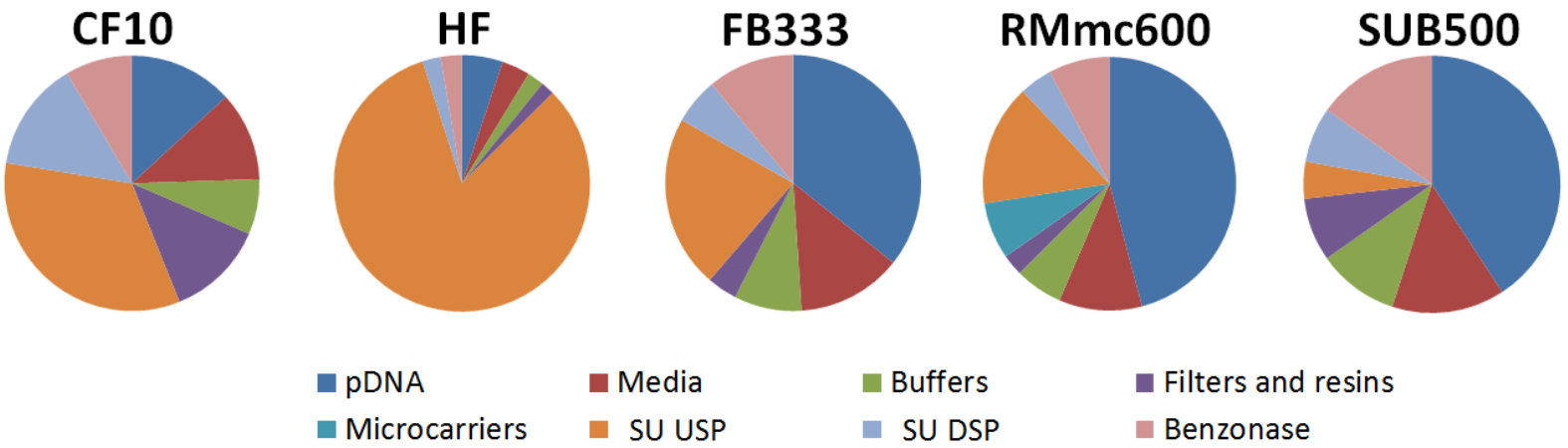

Figure 5.6 Lentiviral vector raw material cost breakdown at a dose size of $2x10^9$ TU at 1,000 doses/y for all candidate technologies. pDNA costs refer to plasmid DNA costs plus transfection reagent costs. SU = single-use components costs, TU = transducing units. SU USP costs contain both seed and USP consumables such as cell culture units used in inoculum growth, production cell culture units and harvest bags. Media cost includes the growth media and production media costs as well as contributing working cell bank costs used in inoculum growth per batch. SU DSP costs refer to bags, bottles and vials costs incurred in both DSP and fill finish activities. Buffers costs contain all chromatography buffer costs as well as the formulation buffer cost and DMSO. Filters and resins contain all filters/membranes and resin costs.

5.3.3 Sensitivity analysis

A sensitivity analysis was run in the context of all cell culture technologies in a scenario where the dose size was 2 x 10^9 TU and the demand was fixed at 1,000 doses/y. Tornado plots for CF10 and SUB200 are shown as these are arguably the most utilised cell culture technologies in the industry at the moment (**Figure 5.7**). Six process parameters and four key raw material cost drivers were included in this analysis. Each of these was varied one at a time, by a fixed percentage (±10% in the case of process parameters and ±30% in the case of the raw material costs) and the impact was captured as the percentage change in COG_{LV}/dose relative to the base case value. Resizing was allowed upon variations in process parameters.

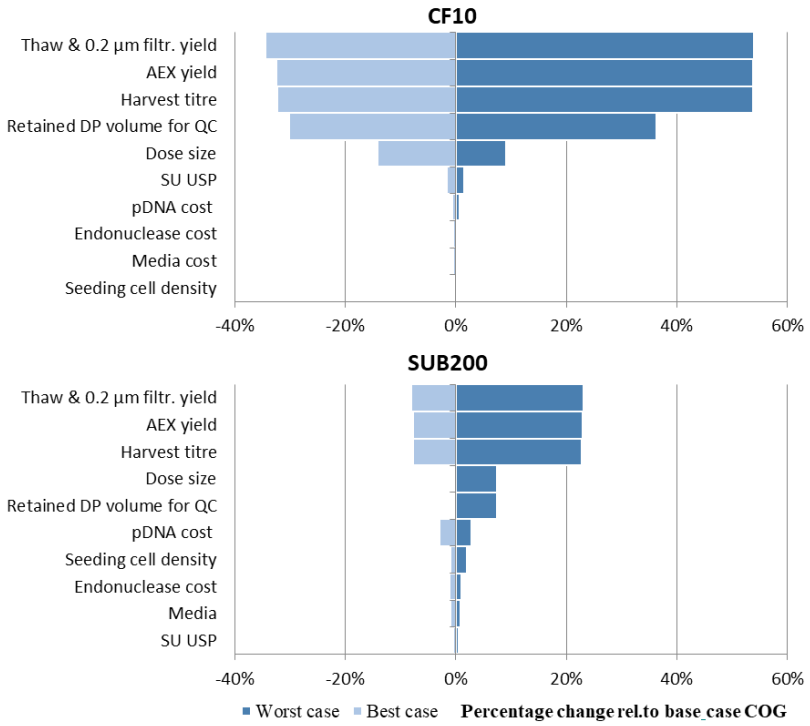

Figure 5.7 Tornado diagrams for CF10 and SUB200 technologies obtained at 1,000 doses/y and dose size of 2 x 10^9 TU showing the impact on COG_{LV}/dose when key process and costs parameters were varied one at a time by a fixed percentage from base case values. Thaw & 0.2 µm filtration yield, AEX yield, harvest titre, dose size and retained drug product (DP) volume for QC and seeding cell density were varied by ± 10% while pDNA, endonuclease, media and SU USP (single-use USP components) costs were varied by ±-30%. It was assumed that the values of these parameters were known of prior to facility and process sizing i.e. resizing was permitted. pDNA cost comprised

transfection reagents costs. AEX stands for anion exchange chromatography. Base case values for each parameter are in **Table 5.2**, **Table 5.2**, **Table 5.3** and **Table 5.4**.

The tool predicted that thaw & 0.2 μm filtration yield, AEX yield and harvest titre had a similar impact on COG_{LV}/dose and the largest impact of all parameters across technologies. Furthermore, it showed that variation in these process parameters (e.g. a 10% decrease in thaw & 0.2 μm filtration yield) had a much higher impact on COG_{LV}/dose in the case of CF10 (54% increase) compared to the other more scalable technologies such as SUB200 (23% increase, **Figure 5.7**) due to the reduced batch size of the CF10 (11 doses/batch under base case assumptions). The analysis also revealed that a 10% decrease in the base case values of the most impactful process parameters had a greater impact on COG_{LV}/dose than a 10% increase; this can be attributed to the additional number of batches required when the yields decrease by 10%.

In terms of a 10% increase in either the retained drug product (DP) volume for QC, or the dose size, these had a significant impact on COG_{LV}/dose in the case of CF10 (36%) and a lower impact on the scalable technologies (~8%). On the other hand, the impact of a 10% decrease in either of these parameters on the COG_{LV}/dose of the scalable technologies was zero because it did not add a sufficiently high number of doses in order to lead to a reduction in the number of batches required to meet demand (**Figure 5.7**). Amongst all the process parameters looked at, seeding cell density variation had the lowest impact on COG_{LV}/dose across technologies with the exception of FB133 and RMmc240 where up to 9% and 6% COG_{LV}/dose reductions could be achieved if seeding cell density decreased by 10% (data not shown).

In terms of the key raw material cost drivers, the impact of their variation on COG_{LV}/dose was significantly lower than that of the process parameters (<±5%) for all technologies. Plasmid DNA cost increase by 30% led to an insignificant change (1-4%); in the case of

all technologies at 1,000 doses per year and did not significantly change at higher manufacturing scales.

As authors are aware that a ±10% variation in infectious titre may not be reliably captured with currently available viral vector analytics, the impact of spontaneous variation of ±30% in harvest titre (no resizing allowed) was also assessed. If harvest titre dropped by 30%, no single dose consisting of $2x10^9$ TU could be achieved with the CF10 process while a 56% increase in COG_{LV}/dose was predicted in the case of the SUB200 (data not shown). In contrast, if titre increased by 30%, COG_{LV}/dose savings of 66% and 42% were predicted by the model for CF10 and SUB200, respectively.

5.3.4 Impact of different LV product characteristics on the ranking of cell culture technologies used in LV manufacturing

The LV process economics tool was employed to assess the ranking of the cell culture technologies used in LV manufacturing, the manufacturing feasibility and the COG_{LV}/dose for a variety of LV products associated with different dose sizes, demands and harvest titres that can be achieved (**Figure 5.8**). Doses representative of CAR T LV, TCR LV and *in vivo* LV products (2×10^8 TU and 2×10^9 TU) and of HSC gene therapy (HSC GT) LV products (2×10^{10} TU and 2×10^{11} TU) were explored (shown as column headers in **Figure 5.8**). Demand was varied between 100 and 10,000 doses/y to reflect potential sale volumes for CAR T and TCR LV products (e.g. acute lymphoblastic leukaemia (ALL), diffuse large cell B-cell lymphoma (DLBCL)), *in vivo* LV products (e.g. Parkinson's disease), and HSC GT LV products (e.g. beta-thalassemia (B-thal), sickle cell disease (SCD)). Harvest titre was varied between low titre of 5×10^6 TU/ml, medium titre of 10^7 TU/ml and high titre of 10^8 TU/ml (shown as row headers in **Figure 5.8**) so as to represent routinely achieved titres in typical CF10 processes as well as future targets which could be achieved with process optimisation and vector engineering. The

analysis was run for 2 different scenarios. **Figure 5.8a** is representative of a scenario in which a company demonstrated adaptation of an adherent cell line such as HEK293T to suspension culture. **Figure 5.8b**, on the other hand, illustrates a scenario in which it was decided to move forward with an existing adherent cell line, hence SUB was dismissed from the analysis.

a

		CAR T/TCR or *in vivo* LV products		HSC GT LV products	
		Dose size (TU/dose)			
	Harvest titre	2×10^8	2×10^9	2×10^{10}	2×10^{11}
100 doses/year	Low	SUB200 (1)	SUB500 (1)	SUB2000 (4)	SUB2000 (37,2,1)
	Medium	SUB100 (1)	SUB200 (1)	SUB2000 (1)	SUB2000 (10)
	High	CF10 (1:4)	CF10 (1:10)	SUB200 (1)	SUB500 (3)
1,000 doses/year	Low	SUB500 (1)	SUB1000 (3)	SUB2000 (31,2,1)	SUB2000 (367,13, 3)
	Medium	SUB200 (1)	SUB500 (3)	SUB2000 (9)	SUB2000 (92,4,1)
	High	CF10 (1:10)	SUB200 (1)	SUB500 (3)	SUB2000 (7)
5,000 doses/year	Low	SUB2000 (1)	SUB2000 (7)	SUB2000 (153,6,1)	SUB2000 (1834, 61, 11)
	Medium	SUB1000 (1)	SUB2000 (4)	SUB2000 (45,2,1)	SUB2000 (459, 16, 3)
	High	SUB100 (1), CF10 (1:35)	SUB200 (4)	SUB2000 (4)	SUB2000 (33,2,1)
10,000 doses/year	Low	SUB1000 (3)	SUB2000 (14)	SUB2000 (306,11,2)	SUB2000 (3667, 123, 21)
	Medium	SUB500 (3)	SUB2000 (7)	SUB2000 (90,3,1)	SUB2000 (917, 31, 6)
	High	SUB200 (1)	SUB500 (3)	SUB2000 (7)	SUB2000 (66,3,1)

b

		CAR T/TCR or *in vivo* LV products		HSC GT LV products	
		Dose size (TU/dose)			
	Harvest titre	2×10^8	2×10^9	2×10^{10}	2×10^{11}
100 doses/year	Low	FB133 (1)	FB333 (1)		
	Medium	CF10 (1:36), FB66 (1)	FB133 (1)		
	High	CF10 (1:4)	CF10 (1:10)	FB133 (1)	FB333 (3)
1,000 doses/year	Low	FB333 (1)	FB333 (7)		
	Medium	FB133 (1)	FB333 (3)		
	High	CF10 (1:10)	CF10 (2:36), FB133 (1)	FB333 (3)	FB333 (29)
5,000 doses/year	Low	FB333 (4)	FB333 (33)		
	Medium	FB333 (2)	FB333 (15)		
	High	CF10 (1:35)	FB133 (4)	FB333 (15)	FB333 (145,5,1)
10,000 doses/year	Low	FB333 (7)	FB333 (66)		
	Medium	FB333 (3)	FB333 (29)		
	High	FB133 (1), CF10 (2:36)	FB333 (3)	FB333 (29)	FB333 (290,10,2)

COG_{LV}/dose (USD)
> $500,000
$100,000 – $500,000
$50,000 – $100,000
$10,000 – $50,000
$1,000 - $10,000
< $1,000

Figure 5.8 Optimal cell culture technologies for LV manufacturing across a range of dose sizes and harvest titres for demands of 100, 1,000, 5,000 and 10,000 doses/y when **a)** SUB was a candidate technology and **b)** SUB was not a candidate technology. Low, medium and high harvest titres values in the row headers are: $5x10^6$, 10^7 and 10^8 TU/ml. Each cell contains the most cost-effective cell culture technology and configuration, the number of batches per year required (in brackets) followed by the number of units/batch required in the case of CF10. If more than one manufacturing train was required (up to 30 batches/year/ manufacturing train), then the second number in the brackets represents

the number of manufacturing trains (up to 6 trains per facility), followed by the number of manufacturing facilities. Multiple technologies are stated in each box if the second ranked technology percentage COG_{LV}/dose difference relative to the most optimal technology was below 5%. The legend on the right-hand side shows the colour code for COG_{LV}/dose ranges to indicate the COG_{LV}/dose of the most optimal technology for each scenario. Infeasible scenarios are shown in grey cells. Dark grey cells illustrate scenarios in which one batch cannot generate enough material for a dose while light grey cells illustrate scenarios in which more than 6 manufacturing trains are required per facility in order to generate the demanded number of doses. Maximum number of CF10 and HF units per batch = 36 and maximum number of FB, RMmc and SUB units per batch = 1. The processes are resized for each combination of dose size, harvest titre and demand. HSC GT= haematopoietic stem cell gene therapy, TU= transducing units.

The tool was used to identify the most cost-effective technology across a matrix of dose, demand and harvest titre combinations. For a scenario in which SUB was a feasible option, the tool predicted that SUB was predominantly the most optimal technology across the matrix (**Figure 5.8a**). On the other hand, in the case when SUB was not an option, FB was found to be predominantly the most optimal technology across the matrix (**Figure 5.8b**). In both cases exceptions existed where CF10 competed with SUB (**Figure 5.8a**) or FB (**Figure 5.8b**). These occurred where the more scalable technologies were oversized compared to CF10; this can be seen for combinations of low dose sizes representative of CAR T, TCR and *in vivo* LV products, high harvest titre and demand below and equal to 5,000 doses/y in the case where SUB was a feasible option (**Figure 5.8a**) and 10,000 doses/y where SUB was not an option (**Figure 5.8b**). The CF10 cost optimality assumes that cGMP-compliant small scale downstream equipment is available on the market to process the low volumes of material.

The matrices also highlight where even current scales of SUB or FB would not be feasible to meet demand which are indicated by grey cells (**Figure 5.8**). When SUB is an option (**Figure 5.8a**), this tends to be seen in cases for the highest dose (2×10^{11} TU) representative of HSC GT LV products combined with lower harvest titres. When SUB is not an option (**Figure 5.8b**), this region increases in size to cover doses equal and above to 2×10^{10} TU combined with lower harvest titres, as well as high demands even at higher

harvest titres. For these regions, the capacity of the existing technologies means that multiple trains (> 6) and multiple facilities would be required to meet demand. In certain cases (dark grey cells, **Figure 5.8b**), one batch would not generate enough material for a dose given the yields and volumes required for QC and retains. In these cases, efforts to reduce dose size, increase harvest titre and/or increase process recovery are critical to enable feasible processes. Such options could include decreasing LV dose size by optimising the CD34+ manufacturing process (MacArthur et al. 2019; Tang et al. 2019; Zonari et al. 2017) or utilisation of new pseudotyping strategies (Boudeffa et al. 2019), or increasing LV infectious harvest titre by optimising transfection efficiency via optimised vector engineering (Uchida et al. 2019)**.**

Figure 5.8 highlights also COG_{LV}/dose benchmarks across different dose size, demand and harvest titre combinations. For scenarios representative of CAR T/TCR and *in vivo* LV products, COG_{LV}/dose values range from <$1,000 USD at low dose size ($2x10^8$ TU/dose), high demand (e.g. DLBCL) and high harvest titre to $10,000-$50,000 USD at high dose size ($2x10^9$ TU/dose), low demand (e.g. ALL) at low harvest titre. In contrast, for higher LV dose sizes associated with HSC GT therapies, COG_{LV}/dose ranges from $1,000 – $10,000 USD at low dose size ($2x10^{10}$ TU/dose), high demand (e.g. sickle cell disease) and high harvest titre to in excess of $500,000 USD at high dose size ($2x10^{11}$ TU/dose), low demand (e.g. beta-thalassemia) and low harvest titre. Hence LV costs for HSC GT therapies can be ~2-20-fold or ~4-200-fold higher at the low and high doses, respectively relative to CAR T/TCR LV costs at $2x10^9$ TU/dose (**Figure 5.8a**). The LV cost contribution to the cost of the final *ex vivo* gene therapy was discussed earlier for CAR T/TCR products (**Section 5.3.1**). In comparison, for a case where LV cost contribution to a larger LV dose HSC GT product COG_{DS}/dose was 90%, as obtained using the CF10 process, switching to SUB2000 is predicted to drop that LV cost

contribution down to 21% (assuming a COG_{DS}/dose of ~$50,000 USD, excluding apheresis costs and viral vector costs).

5.3.5 Harvest titre performance targets

Given that harvest titre was shown to have a large impact on COG_{LV}/dose (**Figure 5.7**), the tool was then used to determine the target harvest titre and specific productivity that each of the cell culture technologies should achieve in order to drive the COG_{LV}/dose down to a specific target cost value (**Figure 5.9**). It was assumed that the harvest titre increases would be achieved through increases in specific productivity. These may be achieved by optimisation of media composition or the transfection process and vector engineering without causing significant changes to cell numbers at seeding or transfection, harvest volumes, labour requirement or schedules. The analysis was carried out for two hypothetical scenarios: for a CAR T LV product and for 2 HSC GT LV products. The CAR T LV product was representative of a diffuse large B-cell lymphoma (DLBCL) LV product with a dose size of 2×10^9 TU and a peak demand of 5,000 doses/y. In this case, the target COG_{LV}/dose chosen was $1,000 USD/dose (**Figure 5.9**), as this value would ensure that for a case where the LV cost contribution relative to the CAR T COG_{DS}/dose ranged between 15-20%, as experienced with the traditional CF10 process, the LV cost contribution would drop to ~1%. In the second scenario, the two LV products were representative of sickle cell disease (SCD) LV products with dose sizes of 2×10^{10} TU (HSC GT medium dose size LV product) and 2×10^{11} TU (HSC GT high dose size LV product) with a peak demand of 1,000 doses/y. The target COG_{LV}/dose chosen here was based on achieving a similar fold decrease in COG_{LV}/dose relative to the CF10 process as that achieved in the DLBCL CAR T LV product example. Coupled with published cell and gene therapy product costs and in house assumptions, the target COG_{LV}/dose for the SCD LV product was rounded-up to $10,000 USD/dose for both

SCD LV products which represents a LV cost contribution to the gene-modified cell therapy COG_{DS}/dose below 20% (**Figure 5.9**).

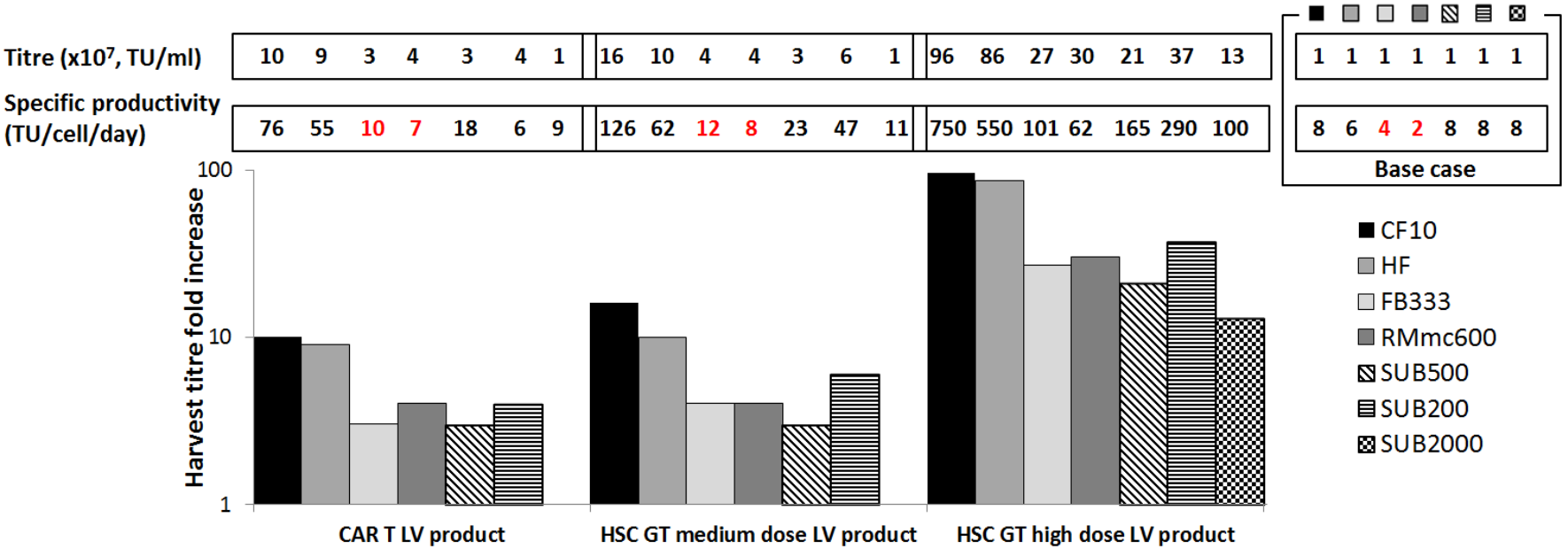

Figure 5.9 Target process performance in terms of target harvest titre fold increase determined for candidate technologies for a CAR T LV product ($2x10^9$ TU/dose) at 5,000 doses/y leading to a target COG_{LV}/dose of $1,000 USD/dose; two different HSC GT LV products ($2x10^{10}$ TU and $2x10^{11}$ TU/dose) at 1,000 doses/y leading to a target COG_{LV}/dose of $10,000 USD/dose. Base case harvest titre and specific productivity values for all technologies are shown in the legend above on the right-hand side. Specific productivity equations can be found in the footnotes of **Table 5.2**. TU = transducing units.

The tool predicted the fold increases in target harvest titre and specific productivities across doses and technology relative to the base case value of 1 x 10^7 TU/ml (**Figure 5.9**). These spanned from ~1 to 10-fold in the context of the CAR T LV product, ~1 to ~20-fold and ~10 to ~100-fold in the context of the HSC GT medium dose size and the high dose size LV products, respectively, depending on technology (**Figure 5.9**). In terms of the non-scalable technologies' target performance, to reach the target cost contributions to the gene-modified cell therapy COG, harvest titres and specific productivities need to reach a 10-fold increase in the context of the CAR T LV product and that of the HSC GT medium dose size LV product. On the other hand, up to 100-fold harvest titre and specific productivity increase would be required in order to reach target cost contribution in the case of the HSC GT high dose size LV product. In contrast, in terms of the adherent scalable and suspension SUB500 technologies' target performance, harvest titres and specific productivities need only to double or triple in the context of the CAR T LV product and that of the HSC GT medium dose size LV product and increase 20-30 fold for the HSC GT high dose size LV product. If operation in SUB2000 proves feasible, then hardly any increase would be required in the context of the CAR T LV product and the HSC GT medium dose size LV product, while a 13-fold increase would be needed for the HSC GT high dose size LV product.

With regards to analysing the specific productivity gains required for the CAR T LV product and the HSC medium dose size LV product examples, the tool predicted that the FB and RMmc need to reach similar specific productivities to the CF10 or the SUB base case values (~8 TU/cell/day) (**Figure 5.9**). This translates to a 3-4 fold increase in specific productivity from the base case values for FB and RMmc. In other words, should a process development team target, and achieve, equivalent specific productivity levels between the FB or RMmc and the CF10, the target LV cost contributions to the CAR T LV and to the HSC GT medium dose size product would be reached with these scalable

adherent options; this is on the basis of the herein assumed base case cell densities, harvest volumes and yields.

5.3.6 Impact of FB process optimisation in a transient transfection versus a stable producer cell line scenario on technology COG ranking

This work has focused so far on COG_{LV}/dose analysis in a transient transfection scenario, where a lower specific productivity was assumed to be achievable with the FB technology compared to the CF10 or SUB. This section analyses how the ranking of FB versus SUB processes changes if the specific productivity of FB was as high as that of the SUB (increase from ~4 to ~8 TU/cell/day). In addition, the impact of expression system scenarios on the COG_{LV}/dose was explored, namely transient transfection versus an inducible stable producer cell line (SPCL). It was assumed that the SPCL does not need any transfection step, and hence no pDNA.

It was assumed that the same harvest titre would be achieved by all technologies, while the same theoretical specific productivity would be achieved with the FB by increasing media consumption and hence the perfusion rate. This was implemented by assuming that the FB333 harvest volume per bioreactor can be increased from 500 L to ~1,000 L while assuming that the schedule, harvest titre and transfection cell density remained the same as the base case scenario (**Figure 5.10b**). It is hypothesised that the higher specific productivities in FB for the transient transfection scenario would require transfection process optimisation in addition to higher perfusion rates, whereas only the latter would be needed for the SPCL scenario.

a

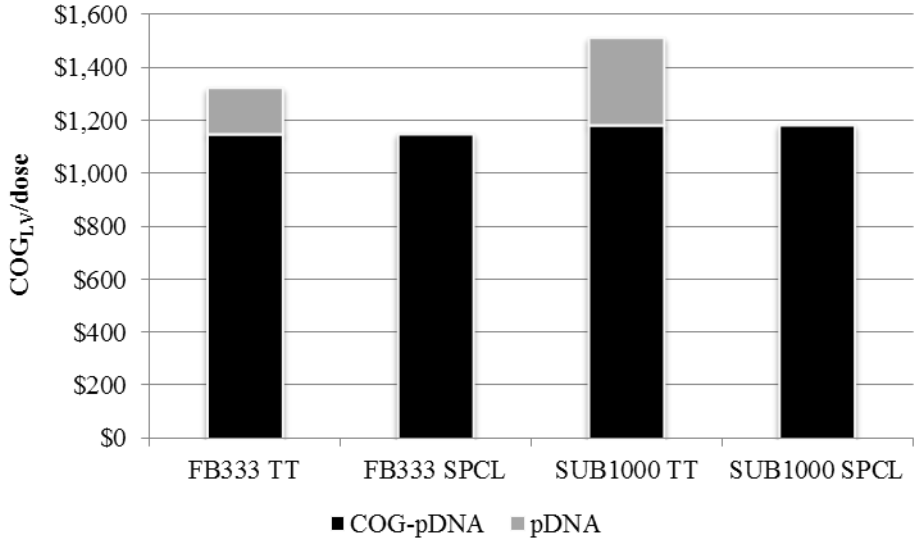

b

Parameter	FB333 base case	FB333 optimised	SUB1000
Total cells in bioreactor at transfection	$2 \times 10^5 \times 333 \times 10^4 = 6.66 \times 10^{11}$	$2 \times 10^5 \times 333 \times 10^4 = 6.66 \times 10^{11}$	$1{,}000 \times 10^3 \times 1.27 \times 10^6 = 1.27 \times 10^{12}$
No. harvest days	2	2	1
Harvest volume/unit (ml)	500×10^3	$1{,}047 \times 10^3$	$1{,}000 \times 10^3$
Perfusion rate (wvd)	500/70/2= 3.57	1,047/70/2= 7.48	NA
Harvest titre (TU/ml)	10^7	10^7	10^7
Total TU in harvest/ batch (TU)	$500 \times 10^3 \times 10^7 = 5 \times 10^{12}$	$1.047 \times 10^3 \times 10^7 = 1.047 \times 10^{13}$	$1{,}000 \times 10^3 \times 10^7 = 10^{13}$
Specific productivity (TU/cell/harvest day)	$5 \times 10^{12}/(6.66 \times 10^{11})/2 =$ 3.75	$1.05 \times 10^{13}/(6.66 \times 10^{11})/2 =$ 7.86	$10^{13}/(1.27 \times 10^{12})/1 =$ 7.86

Figure 5.10 Impact of optimising FB333 process and of switching from a transient transfection system to a stable producer cell line system (SPCL) on technology ranking at 5,000 doses/y and a dose size of $2x10^9$ TU showing **a)** COG_{LV}/dose breakdown for the optimised FB333 transient transfection process (FB333 TT) and for the SUB1000 transient transfection process (SUB1000 TT) and the COG_{LV}/dose for the FB333 run using a SPCL (FB333 SPCL) and for the SUB1000 run using a SPCL (SUB1000 SPCL) and **b)** Key parameters that should be altered to achieve an optimised FB333 process whereby the specific productivity is conserved between FB333 and SUB1000 alongside the base case parameters. It was assumed that the only difference between the SPCL process and the TT process is the lack of the pDNA cost. Both technologies require 7 batches in order to satisfy the 5,000 doses/y demand. Costs regarding the one-off stable producer cell line development, testing and release, as well as the supply chain costs associated with the consistent plasmid supply in the transient transfection scenario were not accounted for in this analysis. TU = transducing units, wvd = working volumes per day.

Figure 5.10a shows the COG_{LV}/dose breakdown at 5,000 doses/y for a 2 x 10^9 TU/dose for the optimised transfection FB333 process and the SUB1000 configuration for both the transient transfection and SPCL scenarios. FB333 was evaluated against the SUB1000 to achieve a similar number of doses per batch. In a transient transfection scenario, the tool predicted that the optimised FB333 was more cost-effective than the SUB1000 achieving cost savings of 13%. In such a scenario, the technology ranking across different LV products (**Figure 5.8a**) would differ from that obtained at base case specific productivity assumptions as FB would replace SUB as the optimal technology for demands that translate to harvest volumes between 200 L and 1,000 L/batch. On the other hand, in an SPCL scenario, the FB333 and SUB1000 COG_{LV}/dose values were very similar, with only a 3% difference. The reason why FB did not maintain its cost-effectiveness over SUB in an SPCL scenario is the fact that the FB333 plasmid cost was significantly lower in the optimised transient transfection scenario due to the lower number of cells at transfection in the FB333 compared to the SUB1000 (**Figure 5.10a**). In such a scenario, the technology ranking across indications (**Figure 5.8a**) would change such that FB and SUB would be shown as the optimal technologies for demands that translate to harvest volumes between 200 L and 1,000 L/batch.

Figure 5.10a highlights also the impact of removing the pDNA costs when switching from transient transfection to SPCL. This can result in overall COG savings of 15% to 30% at these larger scales of FB333 and SUB1000.

5.4 Conclusions

This work describes an integrated decisional tool consisting of a bioprocess economics model and an optimisation algorithm that can be used to assess the economic competitiveness of a range of cell culture technologies used in viral vector manufacturing. Applied to an industrially relevant case study on lentiviral vector manufacture, the tool highlighted the cost-effectiveness of five available technologies, key cost drivers, scalability limitations and process development targets to lower costs for a range of products. At base case assumptions, the results showed that the suspension stirred-tank bioreactor was the most optimal technology across demands, followed by the fixed bed bioreactor, achieving cost savings between 94-97% when compared to the traditional 10-layer process at large demands. These results are aligned with industry-led publications, for example Cameau et al. (2019), who found that fixed bed bioreactor technology and suspension technology were superior to planar technology, in the context of AAV manufacture. A detailed COG_{LV}/dose breakdown analysis was provided so as to trace back the key base case assumptions impacting the ranking. The tool generated technology rankings for a range of LV products across a matrix of different dose, demand and harvest titre scenarios. The SUB was predominantly the most optimal technology if suspension mode culture was available while FB was the most optimal if adherent mode was preferred instead in terms of COG_{LV}/dose values. The tool highlighted the scalability limitations of technologies and COG_{LV}/dose orders of magnitude. Ultimately, commercial demand should drive the decision to either stick to adherent or move to suspension cell culture whereby the latter option should be chosen for large indications as it is associated with the highest scalability potential. It is common that the criticality of switching to a GMP cell line in a timely fashion is overlooked, especially in academic settings. The development or licensing of a suitable GMP cell line should be done early, as early as in nonclinical stage so as to ensure that the data achieved in nonclinical studies

can be relied on to establish a regulatory-satisfactory clinical development program, and to avoid the requirement of comparability studies. Consequently, manufacturers should assess early on what type of cell culture technology they will need in commercial manufacture (demand-driven decision) as this will influence what type of cell line (adherent or suspension-adapted) they should invest in. Harvest titre targets were identified for each technology so as to minimise the LV cost contribution to gene-modified cell therapy costs for a range of products. Furthermore, this study showed that if the FB achieved the same specific productivity as the SUB, the FB became more cost-effective than the SUB in a transient transfection scenario and as cost-effective as the SUB in a stable producer cell line scenario for harvest volumes up to 1000 L.

Overall, this tool can be employed to generate a comprehensive picture of the current limitations and characteristics of different technologies for LV manufacture and can be extended to explore other vector products such as AAV. As demonstrated in this chapter, the decisional tool can help viral vector manufacturers predict clinical and commercial manufacturing budgets required, assess the economic competitiveness of different technologies for commercial scale prior to establishing the "locked-in" process design and determine process improvement targets required to justify switching to a new technology. Hence, such analyses help inform R&D decisions so as to deliver cost-effective commercial processes and, ultimately, more widely accessible advanced therapeutic medicinal products (ATMPs).

This chapter focused on the cost of goods consequences of different cell culture technologies and expression systems. The next chapter extends this to consider the drug development costs that would be associated with a process change from a transient to a stable expression system, such as the extra cell line development costs to develop a stable producer cell line.

Chapter 6: Gene therapy process change evaluation framework: transient transfection and stable producer cell line comparison

6.1 Introduction

The previous chapter presented an analysis of multiple cell culture technologies used in the manufacture of lentiviral vectors from a cost of goods perspective, identified the cost drivers, manufacturing scale limitations and characterised the impact of plasmid DNA (pDNA) cost on COG_{LV}/dose. However, **Chapter 5** only touched on the impact of switching from a transient transfection system to a stable producer cell line (SPCL) system by capturing the impact of the pDNA cost removal, without capturing the implications of performing such a process change on cost of drug development or profitability. **Chapter 6** addresses the impact of moving away from transient transfection, towards a SPCL system at different stages in the drug development pathway from cost of goods, cost of drug development, overall project lifecycle cost and profitability perspectives. This work goes beyond analysing just the lentiviral vector-based products, by including an analysis of the adeno-associated virus (AAV) vector products as well. The decisional tool used to generate the results presented in **Chapter 4** and **Chapter 5**, was extended to incorporate a cost of drug development model as well as a project valuation model, specifically translating the impact of the process change activities costs and timings on profitability. Furthermore, the viral vector bioprocess economics model was expanded to include data related to AAV processes such as titre, step yields, dynamic binding capacity, chromatographic media costs, as well as an additional chromatography step. This extension of the decisional tool is described in **Chapter 3**.

Chapter 2 discussed the advantages and disadvantages of transient transfection and SPCL systems, addressing differences in drug development duration (process and cell line-related), running costs and process robustness (**Section 2.3**). In terms of transient

transfection, it captured plasmid DNA requirements and, later on informed on reported pDNA cGMP-grade costs. In terms of SPCL, it described the published accounts of SPCL systems for both LV and AAV as well as the challenges towards developing such cell lines.

The questions addressed in this chapter are directed towards understanding the financial incentives towards switching to SPCL at four different points in the drug development pathway, in the case of four gene therapy products. These were an autologous CAR T-cell product LV product and a HSC LV product, an *in vivo* LV product and an AAV product. Specifically, the decisional tool was tasked to output the pDNA cost contribution in the case of each of these products' $COG_{overall}$/dose. Furthermore, the impact of switching SPCL at different time points was quantified from a cost of drug development, an overall project lifecycle cost and a profitability perspective. The impact of a range of pDNA cost values, SPCL harvest titres and development duration on the ranking between the two expression systems was described from cost of goods, cost of drug development and profitability perspectives.

In terms of the supply chain angle that this chapter adopts, this is a holistic view, similar to that presented in **Chapter 4**, by measuring the impact of process change on key financial metrics associated with the supply chain of gene therapy products. **Figure 6.1** shows the view adopted in this chapter for autologous *ex vivo* gene therapies (a) and *in vivo* gene therapies (b). As such, in the case of the autologous *ex vivo* gene therapies, the costs associated with both the cell processing component and the viral vector component throughout the drug development pathway and product lifecycle were accounted for. On the other hand, for the *in vivo* gene therapies, given their off-the-shelf nature, only the costs associated with the viral vector component throughout the drug development pathway and product lifecycle were accounted for.

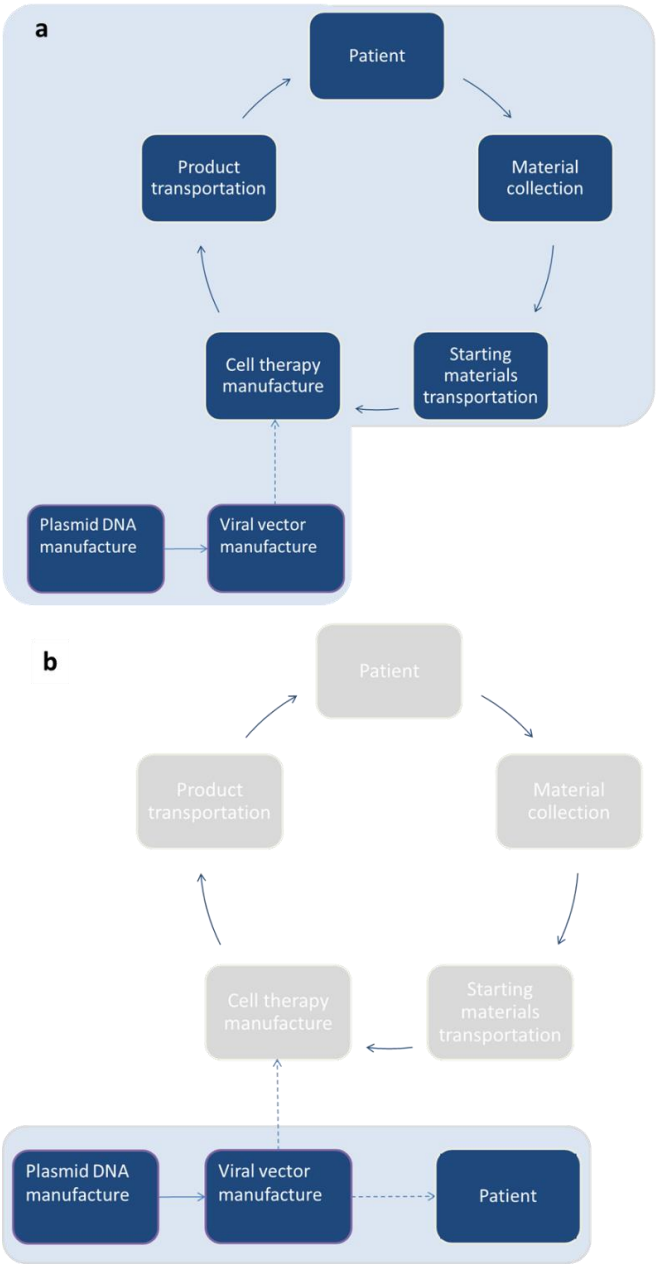

Figure 6.1 Gene therapy supply chain diagram showing the focus adopted in **Chapter 6** where the key areas accounted for in the analyses are shown for **a)** the autologous *ex vivo* gene therapies and for **b)** off-the-shelf *in vivo* gene therapies. The areas not included were greyed out.

The remainder of this chapter is organised as follows. **Section 6.2** provides an overview of the case study, introducing the assumptions surrounding the products and process change scenarios to be analysed, as well as the key process assumptions related to the AAV product. Furthermore, it describes the assumptions adopted with regards to the impact of implementing a process change at different stages in the drug development pathway on costs and timelines. Lastly, it discusses the manufacturing strategy, supply

chain and cash flow assumptions. **Section 6.3.1** discusses the pDNA cost contribution on $COG_{overall}$/dose for each product type. **Section 6.3.2** and **Section 6.3.3** describe the cost of drug development and project lifecycle cost and their breakdowns for each product type and process change scenario analysed. Furthermore, **Section 6.3.4** captures the profitability associated with each product and process change scenario as well as summarises the findings achieved thus far. Also, **Section 6.3.5** presents a series of scenario analyses quantifying the impact of pDNA, SPCL harvest titre and development durations on profitability ranking, as well as cost of goods and cost of drug development savings.

6.2 Case study set-up

6.2.1 Case study overview

The decisional tool was used to explore the performance of the SPCL system against the transient transfection system used in cGMP viral vector manufacture in terms of cost of drug development ($C_{development}$), project lifecycle cost and profitability. Whilst the switch to SPCL is reported to lead to higher process robustness, potentially higher productivity and a reduction in running costs due to the elimination of the pDNA costs, the development of an SPCL takes longer than the development of a transient transfection process (McCarron et al. 2016; Sanber et al. 2015; Ferreira et al. 2020; Manceur et al. 2017). Consequently, there may be a risk of delaying the market entry of the product, assuming all the assumptions are the same as for a transient transfection route. The first objective of the analysis was to examine these trade-offs and learn whether the COG savings achieved when switching to SPCL would outweigh the $C_{development}$ and the impact on profitability of potential delays to market associated with the SPCL route. The second objective was to identify the conditions necessary for the SPCL to be more attractive than transient transfection from cost of drug development and profitability perspectives.

These analyses were carried out for four hypothetical gene therapy product types associated with different pDNA cost contributions to the overall cost of goods per dose ($COG_{overall}$/dose), hence different degrees of COG savings achieved when switching to SPCL system. Moreover, for each product type, the transient transfection scenario was compared against three different scenarios in which SPCL was introduced at various time points in the drug development pathway. These scenarios were the switch to SPCL for material supply for Phase 1 clinical trials (SPCL-Ph1), the switch to SPCL for Phase 3 clinical trials (SPCL-Ph3), and the switch to SPCL post-approval (SPCL-PA) (**Table 6.1**). The next subsections describe the key assumptions related to the product-specific characteristics, drug development lifecycle, viral vector processes, impact of expression system of choice on costs and timelines and cash flow assumptions.

Table 6.1 Process change scenarios indicating when the switch in expression system occurs.

Scenario	Phase 1	Phase 2	Phase 3	Regulatory Review	Post-approval
Transient transfection	Transient transfection	Transient transfection	Transient transfection	Transient transfection	Transient transfection
SPCL-PA	Transient transfection	Transient transfection	Transient transfection	Transient transfection	SPCL
SPCL-Ph3	Transient transfection	Transient transfection	SPCL	SPCL	SPCL
SPCL-Ph1	SPCL	SPCL	SPCL	SPCL	SPCL

SPCL = stable producer cell line, Ph = clinical trial phase

6.2.2 Product-specific characteristics

To increase the relevance of this analysis, the trade-offs associated with both expression systems and the impact of process change at various time points were analysed in the context of products with similar characteristics to currently commercialised ATMPs. Amongst the four gene therapy product types analysed here, two were assumed to be autologous gene-modified cell therapies using lentiviral vectors (LVs) whereas the other two were assumed to be off-the-shelf *in vivo* gene therapies based on the lentiviral vector

(LV) and on the adeno-associated virus vector (AAV). **Table 6.2** presents key characteristics associated with each product type in terms of therapeutic indications, dose sizes, predicted selling prices and peak annual demands. Regardless of product type, it was assumed that the therapy would consist of the administration of one single dose of gene therapy.

Table 6.2 Key assumptions for the characteristics of each product type modelled in the case study.

Product type characteristics	**Gene-modified cell therapies**		***in vivo* gene therapies**	
	CAR T_{LV}	**HSC_{LV}**	**LV**	**AAV**
Indication	Blood cancer	Sickle cell disease	Cystic fibrosis	Spinal muscular atrophy
Therapy type	Autologous	Autologous	Off-the-shelf	Off-the-shelf
Clinical demands (patients/trial)	20, 40, 100	5, 15, 50	5, 15, 50	5, 15, 50
Peak demand (patients/year)	2,250	500	500	500
VV dose size (TU or vg/dose)	$2x10^9$	$2x10^{10}$	$2x10^{11}$	$7x10^{14}$
VV drug product concentration (TU or vg/dose)/ml	10^9	10^{10}	10^{10}	$2x10^{13}$
Cell process dose size	250M	150M	-	-
VV scale - in early clinical	SUB100	SUB1000	SUB2000	SUB200
VV scale - in late clinical & commercial	SUB500	SUB2000	SUB2000	SUB2000
No. of batches/trial	2, 3, 3	2, 2, 2	3, 4, 7	2, 2, 2
No. of batches/peak demand	7	5	46	6
Costs captured	Cell processing + LV	Cell processing + LV	LV	AAV
S&M % of sales	5%	5%	5%	5%
Selling price (x 1,000 US $)	400	1,800	1,800	1,800

Key references on dose sizes: Hartmann et al. (2017), Harrison (2019), FDA (2018b), FDA (2019) and on demands: Pagliarulo (2019), Orphanet (2020). CAR T = chimeric antigen receptor T-cell, HSC = haematopoietic stem cell gene therapy, S&M = sales and marketing, VV = viral vector, TU =

transducing units, vg = viral genomes, LV = lentiviral vector, AAV = adeno-associated virus vector, SUB = stirred tank single-use bioreactor, M = million. SUB100 indicates a 100L bioreactor (working volume. The most cost-effective VV manufacturing scales were determined using the COG model.

6.2.3 Development and impact on timelines

In terms of the drug development lifecycle assumptions, each product type analysed here was assumed to undergo three clinical trial phases so as to prove safety and efficacy based on the traditional biopharmaceutical journey. In terms of the CMC development activities, it was assumed that process and analytical development would occur prior to Phase 1, prior to Phase 3 clinical trials and prior to regulatory review (Farid et al. 2020). The numbers of patients per trial as well as the clinical trial costs assumed per patient are shown in **Table 6.2** and **Table 6.3**.

Table 6.3 Key assumptions for the cost of drug development model.

Key assumptions for the cost of drug development ($C_{development}$) model	**Value**
CAR T cell process clinical cost/patient (without C_{VV})[a]	$75,000
HSC cell process clinical cost/patient (without C_{VV})[b]	$50,000
$FTE_{development}$ year cost[b]	$150,000
SPCL banking costs (includes testing)[b]	$600,000/product
Viral vector clinical manufacture overproduction[c]	Ph1: 250%, Ph2: 250%, Ph3: 125%
Extensive characterisation package cost (in addition to base case QC costs) [b]	$100,000/batch
Stability studies cost (early and late stage clinical trials)[b]	$500,000 at Ph1 and Ph3 $1,000,000 using PPQ material Additional $1,000,000 if process change post-approval
Clinical trial cost/patient at Ph1, Ph2 and Ph3; in bridging study [d]	Ph1: $45,200/patient + $100,000 (overhead)
	Ph2: $69,700/patient + $206,500 (overhead)
	Ph3 or BS: $74,800/patient + $277,000 (overhead)
Bridging study size and duration [b]	10 patients, 1 year

C_{VV} = viral vector cost/dose (determined using the COG model and applied a mark-up), FTE = full-time equivalent, CAR T = chimeric antigen receptor T-cell therapy, HSC = haematopoietic stem cell gene therapy, Ph = clinical trial phase, QC = quality control, BS = bridging study.
[a] Generated using an internal CAR T whole bioprocess model.

[b] Based on discussions with industry experts.
[c] Based on overproduction values in Farid et al. (2020).
[d] Based on values for MSC products Hassan et al. (2016), given the lack of any other more recent data.

The later the switch to SPCL takes place in the drug development pathway, the more extensive the process development (PD) efforts were. **Table 6.4** shows the key roles, number of FTEs, durations and costs per clinical trial phase preparation for transient transfection and each process change scenario. The development of an SPCL was assumed to require 4 cell line scientists and a project manager on top of the personnel requirements for a transient transfection process. Generally, additional process development time was assumed to be required for the SPCL route of approximately one year on top of the transient transfection route to accommodate any process optimisation and early product comparability requirements. The personnel numbers and the process development assumptions were based on discussions with industry experts. In the case of switching to SPCL for Phase 3 or post-approval, additional CMC activities were assumed to be required such as extensive comparability studies, potential clinical bridging studies (e.g. to address limitations of the comparability studies and/or regulatory requirements) and repetition of stability studies and PPQ batches (for the switch to SPCL post-approval only). As a result, in the case of the switch to SPCL post-approval, 2 years were assumed to be needed to perform the switch.

Table 6.4 Key assumptions for viral vector process development in preparation for clinical trial phases.

Stages	**Phase I**		**Phase III**		**Reg. Review (PD)**		**Post-approval**
Scenario	**Transient, SPCL-Ph3, SPCL-PA**	**SPCL-Ph1**	**Transient, SPCL-Ph1, SPCL-PA**	**SPCL-Ph3**	**Transient**	**SPCL-Ph1, SPCL-Ph3, SPCL-PA**	**SPCL-PA**
# Project manager	1	2	2	2	2	2	2
# Process scientists	6	6	6	6	12*	11*	12*
# Analytical development	2	2	4	4			
# Cell line scientists	0	4	0	4	0	1	4
# Tech-transfer	2	2	4	4	0	0	4
# Regulatory support	2	2	2	2	5	5	5
# QC/QA	2	2	2	2	4	4	4
Total # personnel	15	20	20	24	23	23	31
Duration (year)	0.5	1.3	1	2	1.5	1.5	2
Total FTE year	7.5	26.7	20	44	34.5	34.5	56.8
Cost (million US $)	1.13	3.8	3.0	7.2	5.18	5.18	9.3

SPCL = stable producer cell line, SPCL-Ph1/SPCL-Ph3 = switch to SPCL for Phase 1/3 clinical trial, SPCL-PA = post-approval switch to SPCL; FTE = full-time equivalent. If values were the same between scenarios, these were grouped under the same column heading. For gene-modified cell therapy products, additional personnel for process development of the cell therapy component were accounted for, assuming similar effort to those associated with the viral vector component (transient transfection route). *For the Reg. Review and Post-approval stages, the personnel under process scientists and analytical development were grouped in the 'Process scientists' row.

In terms of the risks of delays to market, it was assumed that only the switch for Phase 1 and the switch for Phase 3 scenarios would have the potential to incur delays to market. In the scenario of switching to SPCL for Phase 1, since additional development activities are required such as cell line development prior to process development, it was assumed that the duration of these additional activities would lead to an equal delay to market, relative to the transient transfection route. The 10-month estimate duration for stable producer cell line development was based on discussions with industry and comprised activities such as cloning, screening and selection iterations, evaluation of selected clones in a platform suspension process, confirmation of downstream processing (including product quality) well as qualification and characterisation of the cell line. However, for the other two process change scenarios, no delay in hitting the market was assumed provided that comparability studies were successful based on the assumption of starting Phase 1 at the same time as the transient transfection option and planning ahead the process change efforts. For the switch to SPCL post-approval, it was assumed that product launch would occur at the same time as with the transient transfection process. However, the SPCL process would come online one year later hence the commercial costs reductions due to the switch to SPCL would be felt only one year after entering the market. Nonetheless, if there were limitations of the comparability studies and/or regulatory feedback driving the need for a bridging study, it was assumed that this would cause a one year delay to market in the case of the switch to SPCL for Phase 3 scenario. On the other hand, no delay was assumed in the case of the switch to SPCL post-approval. Instead, it was assumed that the product launch would still occur on time with the transient transfection process but the SPCL process would come online two years later.

There were two key differences assumed in the development costs amongst product types. The first was related to the manufacturing costs for clinical supply and PPQ batches given the differences in product COG/dose as a result of the viral vector type, product modality,

dose size and clinical demands (**Table 6.2**). The second key difference was product modality (i.e. *ex vivo* or gene-modified cell therapy or *in vivo* gene therapy application) that affected the overall development costs. For the gene-modified cell therapy products, the costs associated with cell therapy development were accounted for alongside the costs associated with the development of the LV process. In terms of cell therapy process and analytical development and stability studies costs, these costs were assumed to be the same as those for the LV component and the transient transfection route, given the lack of visibility over such costs. It was assumed that comparability studies would be carried out also at the cell therapy level (**Chapter 3, Table 3.2**, equation **3.85**). Furthermore, if comparability was not proved, cell therapy clinical manufacture for bridging studies was assumed. For the switch to SPCL post-approval scenario, the cell therapy stability studies and PPQ batches were assumed to be repeated using lentiviral vector generated with the SPCL process **Table 6.5**.

Table 6.5 Process change-driven drug development activities assumed in each SPCL scenario.

Activities	**SPCL-Ph1**	**SPCL-Ph3**	**SPCL-PA**
Cell line development and cell banking	✓	✓	✓
Comparability studies		✓	✓
Repeat stability studies			✓
Repeat PPQ			✓
Bridging studies		(✓)	(✓)

SPCL-Ph1 = switch to SPCL for Phase 1 clinical trial, SPCL-Ph3 = switch to SPCL for Phase 3 clinical trial, SPCL-PA = switch to SPCL post-approval, PPQ = process performance qualification. In terms of additional activities associated with the cell therapy component triggered by the switch to SPCL, it was assumed that comparability studies would be carried out also at the cell therapy level. Thus, six manufacturing batches using donor cells were assumed to be required. Furthermore, if comparability was not proved, cell therapy clinical manufacture for bridging studies was assumed. For the switch to SPCL post-approval scenario, the cell therapy stability studies and PPQ batches were assumed to be repeated as well using lentiviral vector generated with the SPCL process.

In terms of the cell therapy clinical manufacture costs and PPQ costs, the clinical costs per patient were calculated based on in house assumptions and are shown in **Table 6.3.**

Furthermore, the appropriate orchestration of development activities in the context of autologous gene-modified cell therapy products was assumed (**Figure 6.2**).

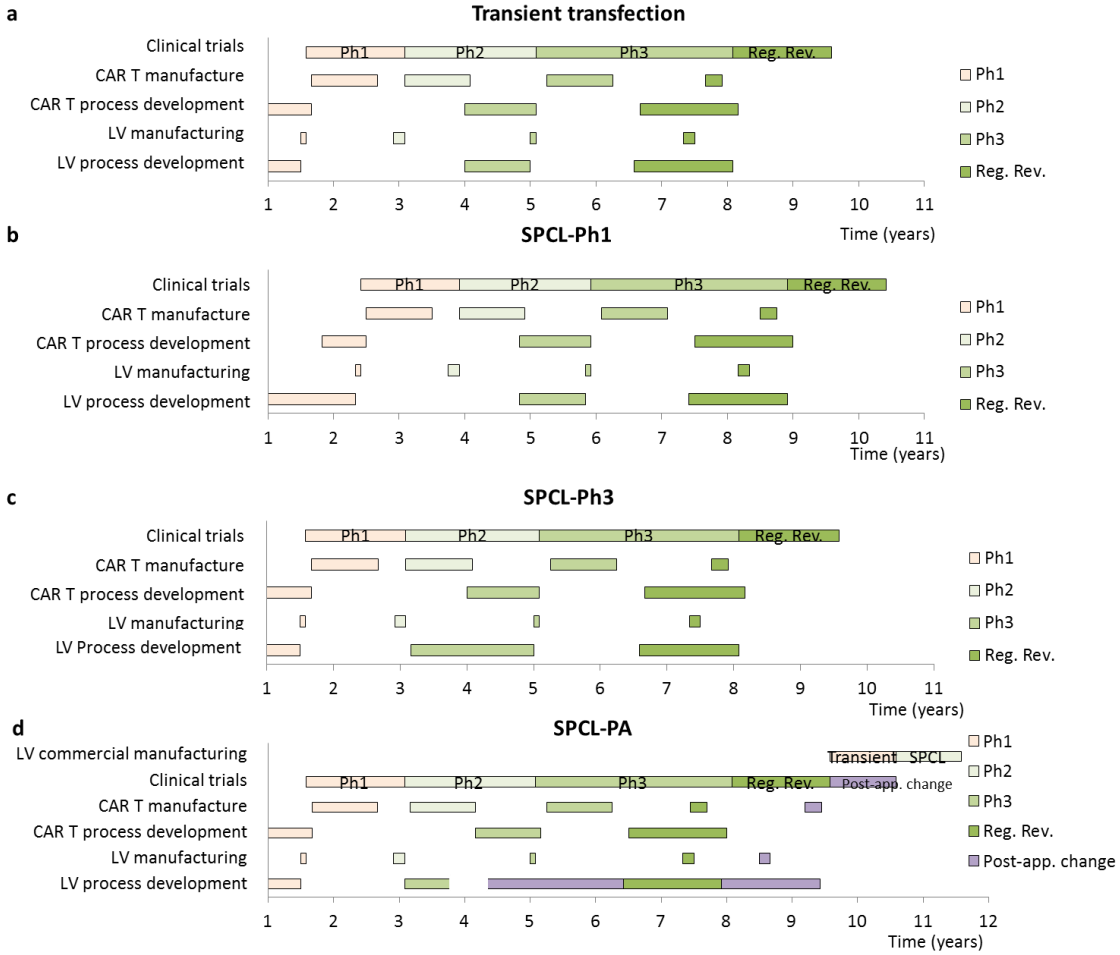

Figure 6.2 Development activities timelines for the CAR T product example for **a)** transient transfection and for each process change scenario i.e. **b)** switch to SPCL for Phase 1 Clinical trial (SPCL-Ph1), **c)** switch to SPCL for Phase 3 Clinical trial (SPCL-Ph3), **d)** switch to SPCL post-approval (SPCL-PA). SPCL= stable producer cell line, Ph = clinical trial phase, Reg. Rev. = regulatory review, Transient = transient transfection, Post-app. = post-approval.

6.2.4 Viral vector processes

Regardless of viral vector type (i.e. LV or AAV), it was assumed that the choice of expression system (i.e. transient transfection or SPCL) would not result in changes in process schedules, DSP flowsheet or process performance at base case scenario.

The LV and AAV vector manufacturing processes assumed here were not dissimilar from an upstream processing (USP) perspective. However, the downstream processing (DSP)

strategies employed for purifying these viral vectors were different due to the differences in physical and biochemical proprieties among LV and AAV particles (**Figure 6.3, Table 6.6**). In terms of the production strategy adopted for the three LV products (i.e. CAR T_{LV}, HSC_{LV} and $LV_{in\ vivo}$), it was assumed that these would share the same process flowsheet and schedule and would be associated with the same process performance (i.e. harvest titre and process yields) (**Table 6.6**).

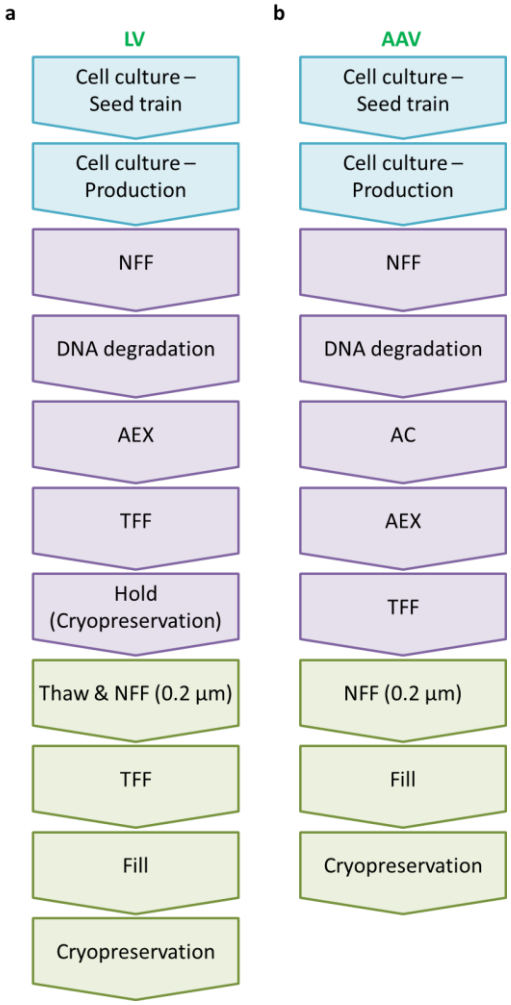

Figure 6.3 Viral vector flowsheets assumed for **a)** the lentiviral vector (LV)-based products and **b)** the adeno-associated virus (AAV) vector product. In the case of the AAV flowsheet, the AAV was assumed to be expressed extracellularly. AEX = anion exchange chromatography, NFF = normal flow filtration, TFF = tangential flow filtration.

Table 6.6 Process parameters and performance assumptions for lentiviral vector (LV) and adeno-associated virus vector (AAV).

Process area	Process parameter	LV	AAV
USP			
	Seeding cell density (cells/ml)	$3.2x10^5$	$3.2x10^5$
	Transfection cell density (cells/ml)	$1.3x10^6$	$1.3x10^6$
	Harvest titre (TU/ml for LV and vg/ml for AAV)	10^7	10^{11}
DSP			
Clarification	Step yield	80%	95%
	Filter capacity (L/m^2)	20	20
	Flux (LMH)	40	40
DNA degradation	Endonuclease requirement (U/ml of feed)	25	25
Chromatography	Number of chromatography step	1	2
	Separation media type	AEX	Affinity, AEX
	Step yield	40%	70%; 70%
	DBC (TU/ml or vg/ml)	$5x10^8$	$3x10^{12}$; $1x10^{13}$
	Column bed height (cm)	20	20; 20
	Max. linear velocity (cm/h)	100	100; 20
UF/DF	Step yield	80%	95%
	Target DS concentration (TU/ml or vg/ml) *	$10^8 – 10^9$	$2x10^{13}$ **
	Flux (LMH)	55	55
	Max. concentration time (h)	2	2
	Max. diafiltration time (h)	2	2
	Retained DS volume for QC and other purposes (ml)	100	0
Fill Finish			
0.2 µm filtration	Step yield (incl. thaw step)	75%	86% (no thaw)
	Filter capacity (L/m^2)	250	250
	Flux (LMH)	100	100
UF	Step yield	96%	-
	Max. concentration time (h)	2	-
	Flux (LMH)	55	-
	Target DP concentration (TU/ml or vg/ml) *	$10^9 – 10^{10}$	-
Fill	Step yield	95%	95%
	Cryovial total volume (ml), space efficiency (%)	1-100, 75%	50, 75%
	Thaw yield	100%	100%
	Retained DP volume for QC and other purposes (ml)	100	100
Overall			
DSP	**Overall DSP yield**	**26%**	**44%**
Fill Finish	**Overall Fill Finish yield**	**68%**	**82%**
DSP & Fill Finish	**Overall DSP & Fill Finish yield**	**17%**	**36%**

TU = transducing units, vg = viral genomes, LMH = $L/m^2/h$, DBC = dynamic binding capacity, DS= drug substance, DP = drug product, QC = quality control. USP = upstream processing, DSP = downstream processing, AEX = anion exchange chromatography. * Final concentrations are functions of LV dose size. In the case of the AAV product, it was assumed there would not be a freeze (cryopreservation) hold step prior to fill-finish, hence there was no thaw step involved. Furthermore, no drug substance ultrafiltration step was deemed to be required. These assumptions were based on literature as well as validation from industry experts. ** represents drug product in the case of AAV.

From a USP perspective and regardless of expression system of choice, both LV and AAV were assumed to be produced in suspension serum-free cell culture in single-use stirred-tank bioreactors run in batch mode, following the same seed train flowsheet and USP schedule **(Chapter 5)**. Additionally, no lysis step was assumed for the AAV process since the AAV product was assumed to belong to an AAV serotype which would be released into the media to a satisfactory extent (e.g. AAV9) (Adams et al. 2020). In terms of the transient transfection expression system, it was assumed that the cell lines used for manufacture of either viral vector type (LV or AAV) would be an existing GMP HEK293-based cell line and the transfection reagent utilised would be Polyethylenimine (PEI). A total pDNA requirement of 2.5 micrograms per million cells at transfection step was assumed for either viral vector type based on literature ranges (Merten et al. 2014b; Merten et al. 2016; Marceau and Gasmi 2014; Ansorge et al. 2010; Masri et al. 2019). A two-plasmid system consisting of a helper pDNA containing the Rep-Cap and adenoviral helper sequence and a pDNA containing the gene of interest was assumed for AAV (Grimm et al. 1998; Penaud-Budloo et al. 2018). On the other hand, a four-plasmid system consisting of one gene of interest pDNA and 3 helper pDNAs was assumed for LV. The base case total plasmid cost per gram was assumed to be $60,000 which represents the lower end of the cGMP-manufactured pDNA costs range reported in industry (Cesari M. 2017). A discussion surrounding plasmid DNA cost variation is presented in **Chapter 1, Section 1.2.2**. In terms of the stable producer cell line expression system, a pDNA-free and helper virus-free Tet-on inducible system was assumed for both LV (Chen et al. 2020; Manceur et al. 2017) and AAV (Hein et al. 2020). Production was assumed to require 293T-based cell lines in the case of LV (Chen et al. 2020; Manceur et al. 2017) or a similar system to CEVEC's Amniocyte Production (CAP) cell line, in the case of AAV (Zeh et al. 2019; Fischer et al. 2012).

From a DSP perspective, the DSP flowsheet, step yields and duration were slightly different amongst viral vector types. Furthermore, the expression system of choice was assumed to not have an impact on DSP. As an overview, for the DSP flowsheets for both vector types, it was assumed that the harvested cell culture would be clarified using normal flow filtration, then undergo a DNA degradation step, be purified using chromatography and finally be concentrated and diafiltered. **Table 6.6** shows the assumed DSP and fill finish flowsheets and step yields for both LV and AAV. Given the differences in DSP flowsheets between the two vectors described in **Chapter 2, Section 2.3** (Merten et al. 2016; Li et al.; Adams et al. 2020; Masri et al. 2019; Forsberg 2018), it was assumed that two chromatography steps would be employed for AAV i.e. an affinity step using the AAVX resin (POROS™ CaptureSelect™, Thermo Fisher Scientific, Waltham, Massachusetts, US) and a anion-exchange (AEX) step run in bind-and-elute mode. The key reagent costs, production labour and QC assumptions can be found in **Chapter 5, Section 5.2**.

6.2.5 Manufacturing strategy, supply chain and cash flow assumptions

With respects to the development and manufacturing strategy, it was assumed that all development and manufacturing activities for viral vectors would be outsourced to a CDMO, while those for the cell therapy component would occur in-house. This represents a commonly adopted approach in the cell and gene therapy industry. To implement that, the viral vector COG and $C_{development}$ models were configured to operate under CDMO assumptions and a mark-up of 40% was applied on all costs. Consequently, the COG model assumed that labour and cleanroom costs would be charged based on facility utilisation. On the other hand, with respects to the development and manufacturing strategy assumed for the cell therapy component in the case of the gene-modified cell therapy products, it was assumed that in-house development, clinical and commercial manufacture facilities would already be in place. Moreover, the needle-to-needle costs

assumed here for the cell therapy component included apheresis, core manufacturing (raw materials, labour, QC and facility-related costs) and transportation costs. **Table 6.3** shows the clinical needle-to-needle costs (clinical COG_{cell}) per patient while **Table 6.7** shows the commercial needle-to-needle costs (commercial COG_{cell}) per patient associated with the CAR T and HSC cell therapy.

Table 6.7 Key assumptions for the cost of goods model.

Key assumptions for the cost of goods (COG) model	**Value**
CAR T cell process commercial cost/patient (without C_{VV})	$47,000
HSC cell process commercial cost/patient (without C_{VV})	$30,000
$FTE_{operator}$ year cost	$120,000
pDNA cost/g (GMP-manufactured price/g)*	$60,000
% CMO_{VV} mark-up	40%

C_{VV} = viral vector cost/dose (determined using the COG model and applied a mark-up), FTE = full-time equivalent, CAR T = chimeric antigen receptor T-cell therapy, HSC = haematopoietic stem cell gene therapy, CMO_{VV} = contract manufacturing organisation delivering viral vector manufacture services, pDNA = plasmid DNA.*The transfection reagent cost was also accounted for and was calculated as 20% of the pDNA cost/g.

Table 6.8 provides key information on supply chain, commercialisation, and cash flow assumptions used in this work. In terms of supply chain management considerations, it was assumed that supply chain specialists would be required to support the viral vector processes, specifically the transient transfection option, for all product types and the cell therapy processes in the case of the CAR T and HSC products. With respects to the supply chain support to the viral vector (VV) processes, 3 FTEs were accounted for per year in the commercial stage to ensure consistent supply of cGMP-manufactured pDNA and PEI required for transient transfection. On the other hand, to support the needle-to-needle logistics for the gene-modified cell therapy products 3 FTEs per clinical trial and 10 FTEs per year were accounted for in the development and commercial stages, respectively.

Table 6.8 Key assumptions for the gene therapy project valuation model.

Key assumptions for the Gene therapy project valuation model	**Value**
Duration of Ph 1 Clinical Trial	1.5 years
Duration of Ph 2 Clinical Trial	2 years
Duration of Ph 3 Clinical Trial	3 years
Duration of Regulatory Review	1.5 years
Duration of Commercial phase	10 years
ex vivo cell gene therapy supply chain FTEs/year in clinical; commercial	3;10
pDNA supply chain FTEs/year (commercial-only)	3
Corporate tax	21%
Discount rate	10%
Sales and marketing (% Sales)	5%
Sales ramp-up profile	25% (Y1), 50% (Y2), 100% (Y3-10)
Transition probability - Ph 1 to 2	87%
Transition probability - Ph 2 to 3	64%
Transition probability - Ph 3 to Reg. Review	71%
Transition probability - Reg. Review to market	91%
Overall Phase I to market clinical success rate	36%

Y = year, Reg. Review =regulatory review, Ph = clinical trial phase, pDNA = plasmid DNA.

6.3 Results and discussions

The integrated framework was used to analyse the impact of switching from transient transfection to SPCL at different stages in the gene therapy product development (i.e. for Phase 1, Phase 3 and post-approval) on economic indicators in the case of four different gene therapy product types.

The base case differences between transient transfection and SPCL expression systems were multiple, affecting all models of the integrated framework. For transient transfection, cGMP-manufactured pDNA and supply chain management costs were assumed. On the other hand, for SPCL, higher cell line, process & analytical development costs, potentially higher harvest titres as well as delays to market were accounted for. Initially, the cost of goods (COG) model was run so as to determine the $COG_{overall}$/dose for each product type and the key cost structure differences between product types assuming the same titre being achieved by the two expression systems. Next, the rankings of cost of drug development ($C_{development}$) and the project lifecycle cost to the sponsor company were determined for each process change scenario and product type.

Furthermore, profitability measured using the net present value (rNPV) methodology was assessed and profitability rankings were generated for each process change scenario and product type. Finally, scenario analyses exploring the impact of pDNA cost, delay to market when choosing to switch to SPCL for Phase 1, and SPCL harvest titre on profitability ranking, $C_{development}$ and COG were carried out.

6.3.1 Cost of goods analysis for expression systems used in viral vector manufacturing

As an initial step in the process change analysis, the COG model was used to generate the overall cost of goods per dose ($COG_{overall}$/dose) and the cost savings achieved when removing the pDNA cost in the case of the SPCL system. The COG model was employed to determine the viral vector cost per dose excluding the pDNA cost (C_{VV}/dose) and the pDNA cost per dose (C_{pDNA}/dose) for each product type. In the case of the *in vivo* viral vector products, the viral vector cost plus the pDNA cost per dose represented the overall cost of goods per dose ($COG_{overall}$/dose). On the other hand, in the case of the gene-modified cell therapies, cell therapy cost of goods (COG_{cell}/dose, including apheresis and transportation but excluding viral vector costs) values obtained with the CAR T decisional tool used in **Chapter 4,** plus the C_{VV}/dose and C_{pDNA}/dose represented the $COG_{overall}$/dose. Prior to introducing the $COG_{overall}$/dose and breakdowns trends (**Figure 6.4c**), given that the selected products belonged to different product families (**Table 6.2**), the viral vector manufacturing capacity requirements are described for each product type (**Figure 6.4a,b**).

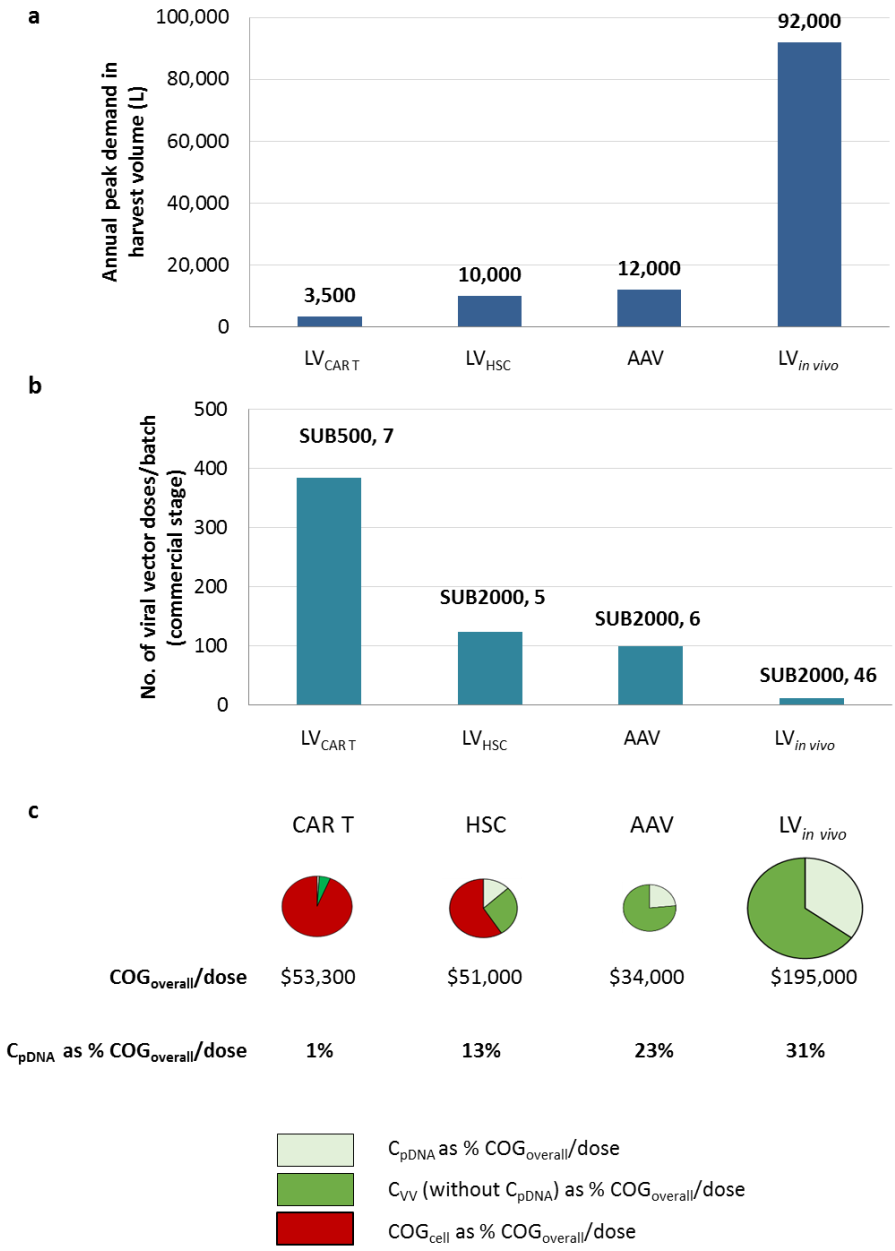

Figure 6.4 Comparisons between product types in commercial stage in terms of **a)** Annual peak demand in viral vector harvest volume, **b)** Number of viral vector doses that can be manufactured per batch using the commercial manufacturing scale bioreactor and **c)** Cost of goods evaluation for the transient transfection expression systems across product types showing overall cost of goods per dose ($COG_{overall}$/dose) as bubble size, $COG_{overall}$/dose breakdown in terms of cell therapy cost of goods (COG_{cell} /dose) shown in red, viral vector cost without the plasmid DNA cost (C_{VV}/dose) shown in green and pDNA cost (C_{pDNA}/dose) shown in light green. The C_{VV}/dose and C_{pDNA}/dose were obtained by applying a 40% mark-up to the COG_{VV}/dose and C_{pDNA}/dose generated using the viral vector bioprocess economics model described in **Chapter 3**. COG_{cell}/dose refers to the cost of goods associated with the cell therapy component and it included apheresis and transportation costs. The annual viral vector harvest volume accounted for the QC and retains volumes required per batch. The equations used for determining the annual harvest volume for LV ($V_{h,annual,LV}$) and AAV ($V_{h,annual,AAV}$) are given in the **Appendix**.

The COG model was employed to identify the most cost-effective SUB configuration (bioreactor size, number of batches required and facility utilisation) for each product type based on the inputs shown in **Table 6.2** i.e. dose size, peak annual demand and viral vector-specific input assumptions. This was found to be the 2,000L working volume bioreactor (SUB2000) for all product types, however, since only two batches using SUB2000 were determined for the $LV_{CAR\ T}$ product (data not shown), it was decided to select the 500L working volume bioreactor (SUB500) for the $LV_{CAR\ T}$ product. The reason why manufacturing of the $LV_{CAR\ T}$ product using two SUB2000 batches annually was considered unfavourable was that a minimum of three batches per run were assumed to be required for validation purposes. As such, 7 batches using a SUB500 bioreactor were required for the $LV_{CAR\ T}$ product, 5 and 6 batches using SUB2000 for the LV_{HSC} and AAV products, respectively, and 46 batches using the SUB2000 for the $LV_{in\ vivo}$ product (**Figure 6.4b)** per year in commercial phase, at peak demand.

Given the differences in values and units for dose and titre across the product types, these were translated into the manufacturing capacity requirement in terms of the annual viral vector harvest volume requirement and scale of production to facilitate comparison (**Figure 6.4a**). The viral vector annual harvest volume required was lowest for the $LV_{CAR\ T}$ product (3,500L), followed by LV_{HSC} and AAV (10,000L and 12,000L), and was largest for the $LV_{in\ vivo}$ product (92,000L). The annual harvest volume for the $LV_{CAR\ T}$ product was lowest despite being associated with a 4.5-fold larger annual demand than the other LV products. This can be explained by its 10- to 100-fold lower dose size compared to LV_{HSC} and $LV_{in\ vivo}$ products, respectively. On the other hand, the annual harvest volume for the AAV product was found to be similar to that of the LV_{HSC} product once the differences in harvest titre, dose size, process flowsheets and process yields assumed between these two products were accounted for (**Table 6.2, Table 6.6).** Furthermore, **Figure 6.4b** shows the number of doses that can be generated per batch for each product

type. The number of doses per batch was highest for the $LV_{CAR\ T}$ product (385), followed by LV_{HSC} (123) and AAV (100) and was smallest for the $LV_{in\ vivo}$ product (12).

Figure 6.4c shows the overall cost of goods per dose ($COG_{overall}$/dose, shown as bubble size) assuming a transient transfection expression system as well as the breakdown in terms of the cell therapy cost of goods (COG_{cell}/dose, shown in red for the gene-modified cell therapy products only), viral vector cost (C_{VV}/dose, shown in dark green) and pDNA cost (C_{pDNA}/dose, shown in light green) percentage contributions. The $COG_{overall}$/dose was the lowest for the AAV product ($34,000/dose), followed by the gene-modified cell therapy products (~$50,000/dose) and finally by the $LV_{in\ vivo}$ product ($195,000/dose) (**Figure 6.4c).** Despite the larger number of viral vector doses per batch produced for the gene-modified cell therapy products (**Figure 6.4b)** resulting in a lower C_{VV}/dose, when accounting for the COG_{cell}/dose, the $COG_{overall}$/dose values were higher than that of the AAV product (**Figure 6.4c).** The $LV_{in\ vivo}$ $COG_{overall}$/dose magnitude was a reflection of the very small number of doses (12) that can be generated from a SUB2000 batch due to the very large dose size (2×10^{11} TU/dose) (**Figure 6.4b).** In terms of the pDNA cost contribution to the $COG_{overall}$/dose for each of product type and hence the percentage $COG_{overall}$/dose savings achieved when switching to SPCL, the highest savings were found for the $LV_{in\ vivo}$ (31%) and AAV (23%) products (**Figure 6.4c).** On the other hand, the gene-modified cell therapy products were associated with savings in the order of 13% in the case of the HSC product and 1% in the case of the CAR T product (**Figure 6.4c).** This ranking was driven by the viral vector process type (whether AAV or LV) as well as the viral vector percentage cost contribution to the $COG_{overall}$/dose for each product in the case of the gene-modified cell therapy products. In terms of viral vector process type, the cost savings achieved when switching to SPCL were higher for the $LV_{in\ vivo}$ product (31%) than for the AAV product (23%) despite assuming SUB2000 as the commercial production scale for both products (**Figure 6.4b,c).** This was because other material costs

in the AAV process bear a heavier weight than the equivalent materials costs in the LV processes (e.g. affinity chromatography resin for AAV versus conventional AEX chromatography resin for LV). On the other hand, the cost savings achieved when switching to SPCL for the gene-modified cell therapy products were lower than for the *in vivo* products due to the diminished viral vector percentage cost contribution to the $COG_{overall}$/dose. The C_{VV}/dose percentage contribution plus the C_{pDNA} percentage contribution to $COG_{overall}$/dose ranged between 41% ($21,000 US/dose) and 6% ($3,300 US/dose) for the HSC and CAR T products, respectively, with the SUB processes in a transient transfection scenario.

6.3.2 Cost of drug development analysis for expression systems used in viral vector manufacturing

The impact of switching to SPCL at different time points on cost of drug development ($C_{development}$) was analysed against the scenario of sticking with transient transfection, for each product type. The time points of switching to SPCL considered were: for Phase 1 (SPCL-Ph1), for Phase 3 (SPCL-Ph3) and post-approval (SPCL-PA). The focus here was to assess the trade-off between the increase in development costs and the reduction in clinical manufacture and PPQ costs associated with the SPCL scenarios and how this changed from one product type to another. The key cost categories building up the cost of drug development ($C_{development}$) were process development (CMC_{PD}), clinical manufacture (CMC_{MFG}), clinical trials, and PPQ (CMC_{PPQ}). The CMC_{PD} costs consisted of process and analytical development costs, tech transfer, stability studies costs (for all scenarios), cell line development costs and cell banking costs (for the SPCL scenarios only) and comparability and bridging studies costs (for SPCL-Ph3 and SPCL-PA scenarios only). A comprehensive list of the activities performed within each category is provided in **Table 3.2**, **Chapter 3** whilst differences in clinical demand across products can be found in **Table 6.2**. In the case of gene-modified cell therapy products, the

development, clinical manufacture and PPQ cost categories are shown for both the lentiviral vector and the cell therapy so as to indicate their separate contributions to the final cost of drug development.

The tool predicted that the stage at which the SPCL switch was implemented had a significant impact on the cost of drug development ($C_{development}$) ranking across process scenarios (**Figure 6.5).** The post-approval and late phase process change scenarios (SPCL-PA and SPCL-Ph3) were associated with the highest $C_{development}$ whereas the change to SPCL for Phase 1 (SPCL-Ph1) or the no change scenario (i.e. transient transfection) led to significantly lower $C_{development}$, regardless of product type.

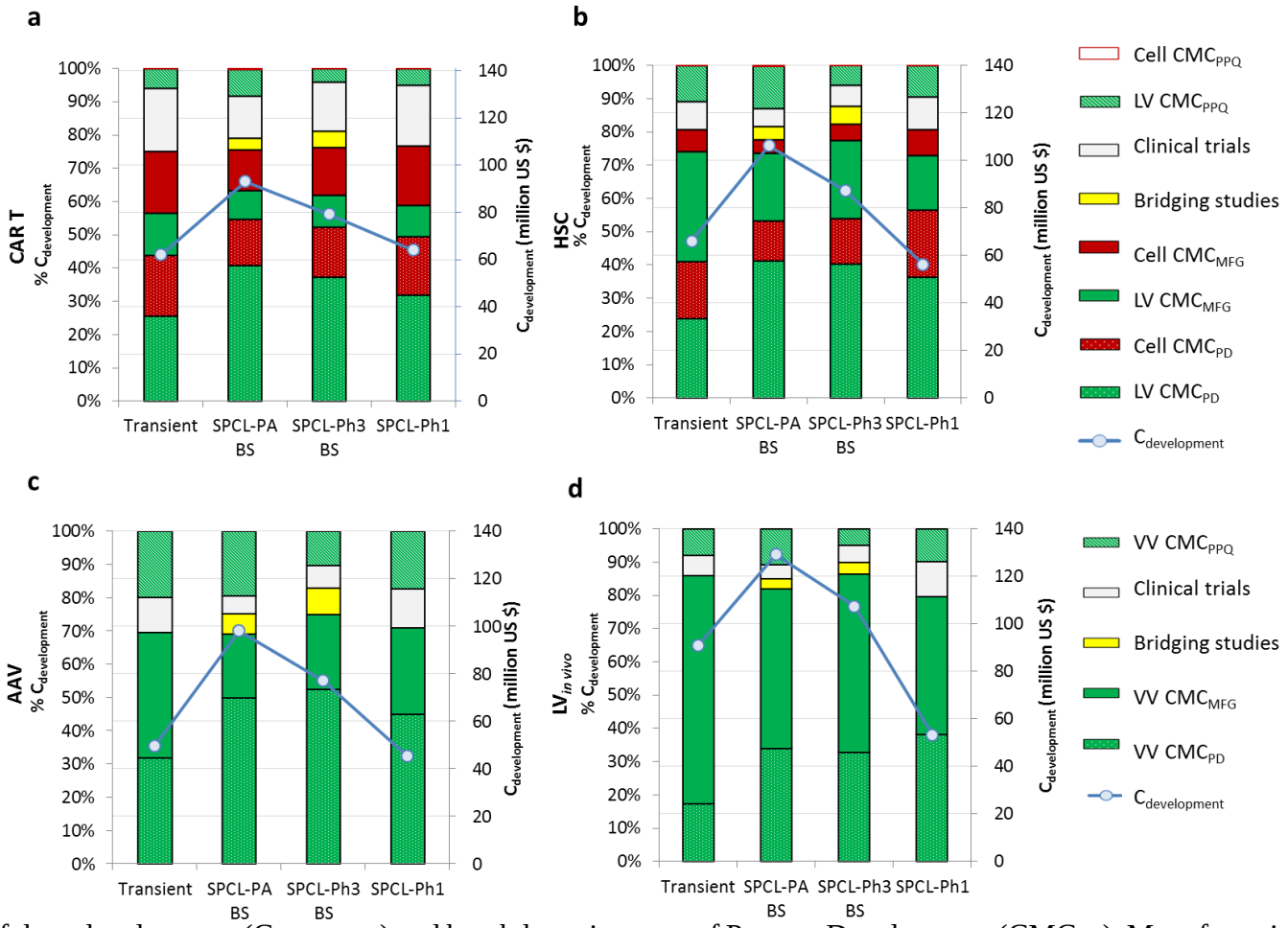

Figure 6.5 Cost of drug development ($C_{development}$) and breakdown in terms of Process Development (CMC_{PD}), Manufacturing (CMC_{MFG}), clinical trials and PPQ (CMC_{PPQ}) for each product type: a) CAR T, b) HSC, c) AAV and d) $LV_{in\ vivo}$ and expression system scenario i.e. transient transfection and switch to Stable producer cell line (SPCL) system for Phase 1 (SPCL-Ph1), for Phase 3 (SPCL-Ph3) and post-approval (SPCL-PA). For the gene-modified cell therapy products, cell therapy development costs are also shown (i.e. Cell CMC_{PD}, Cell CMC_{MFG}, Cell CMC_{PPQ}). Bridging studies were assumed to be required in the case of SPCL-Ph3 and SPCL-PA and were assumed to include 10 participants. Definitions of the drug development activities shown herein are provided in **Table 3.2**. CMC = chemistry manufacture and control, PD = process development, MFG = manufacture, PPQ = process performance qualification, PD = process development, cell= cell therapy, VV = viral vector, BS = bridging studies, Transient = transient transfection.

The $C_{development}$ was largest for the post-approval (SPCL-PA) and late phase (SPCL-Ph3) process change scenarios due to the addition of comparability studies and bridging studies costs, plus additional stability studies and PPQ batch costs in the case of SPCL-PA scenario only. Furthermore, there were two $C_{development}$ ranking trends amongst process scenarios across product types. For the CAR T product (**Figure 6.5a**), the change to SPCL for phase 1 was associated with similar $C_{development}$ to the transient transfection scenario because the higher process development costs (LV CMC_{PD}) costs due to SPCL development were offset by the savings in clinical manufacture (CMC_{MFG}) and PPQ batch (CMC_{PPQ}) costs. On the other hand, for the HSC, AAV and $LV_{in\ vivo}$, the change to SPCL for phase 1 was associated with a lower $C_{development}$ than the transient transfection scenario due to larger savings in clinical manufacture (CMC_{MFG}) and PPQ batch (CMC_{PPQ}) costs resulting from the larger pDNA percentage cost contributions to $COG_{overall}$ (**Figure 6.5b-d**). In terms of assessing the impact of the bridging studies assumed to be required in the case of the SPCL-Ph3 and SPCL-PA scenarios, the contributions to cost of drug development $C_{development}$ was found to be low, ranging between 2% and 9% across product types and process change scenarios (**Figure 6.5).** Therefore, the tool predicted that should bridging studies not be required, the $C_{development}$ ranking would not change.

In terms of the $C_{development}$ ranking across product types, the lowest cost was associated with the AAV, followed by the CAR T and HSC products, followed by the $LV_{in\ vivo}$ product (**Figure 6.5).** This ranking was driven by the clinical manufacture (CMC_{MFG}) cost ranking in line with the $COG_{overall}$/dose ranking shown in **Figure 6.4c** as well as the differences in development costs amongst product types. **Figure 6.5** shows that clinical manufacture costs (VV CMC_{MFG}) dominated in the case of $LV_{in\ vivo}$ product (40-60%) whereas process development costs (CMC_{PD}) dominated in the case of CAR T, HSC and AAV (38%-55%). The reason why CMC_{PD} costs dominated in the case of the gene-modified cell therapies was the fact that the cell therapy development costs were also

accounted for. For the transient transfection scenario, despite assuming equivalent effort, the development costs were slightly higher for the LV than for the cell therapy component because the LV activities were outsourced. For the process changes scenarios, the LV process development costs (LV CMC_{PD}) were significantly higher than those for the cell therapy component (Cell CMC_{PD}). This was due to SPCL development, banking and testing costs, additional process development efforts and, for the SPCL-Ph3 and SPCL-PA scenarios, comparability studies requirements. The CMC_{PD} cost breakdown for the CAR T product is shown in **Figure 6.6.**

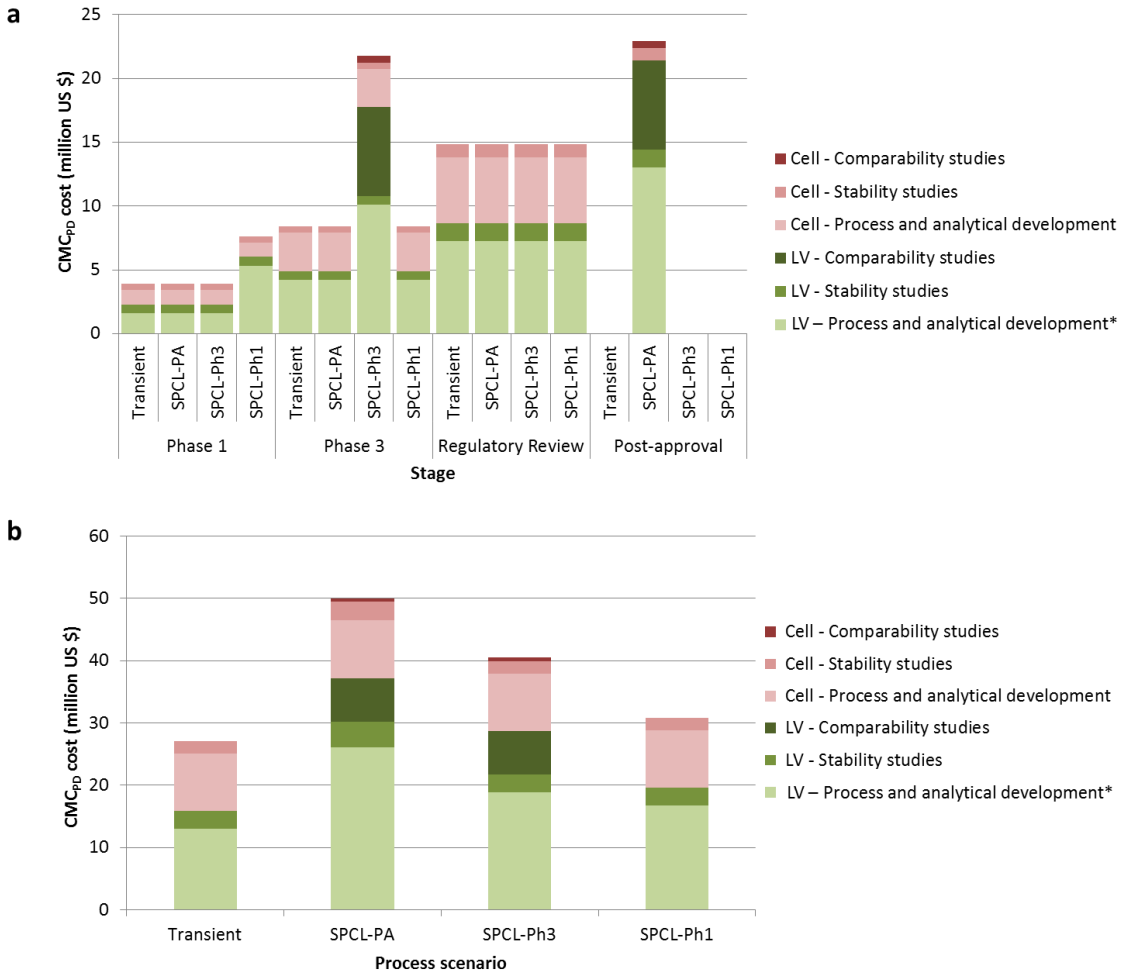

Figure 6.6 CMC_{PD} activities costs breakdown for each process scenario for the CAR T product, showing **a)** breakdown per phase and **b)** overall breakdown in terms of process and analytical development, stability studies and comparability studies for both LV and the cell process components. The LV – Process and Analytical development costs* associated with the SPCL scenarios contain the SPCL development cost, SPCL banking and testing costs as well as additional process and analytical development costs. CMC = chemistry, manufacturing and controls, PD = process development, SPCL = stable

producer cell line, Transient = transient transfection, SPCL-PA = switch to SPCL post-approval, SPCL-Ph3 = switch to SPCL for Phase 3 clinical trial, SPCL-Ph1 = switch to SPCL for Phase 1 clinical trial.

6.3.3 Project lifecycle cost analysis for expression systems used in viral vector manufacturing

The effect of switching to SPCL at different time points on project lifecycle cost was assessed against the transient transfection scenario for each product type (**Figure 6.7**). The trade-off analysed here consisted of higher development costs but lower clinical and commercial manufacturing costs associated with the SPCL scenarios. The project lifecycle cost was defined to comprise the cost of drug development ($C_{development}$) and the commercial cost of goods and supply chain costs ($C_{commercial}$) (**Figure 6.7**). For the gene-modified cell therapies, the $C_{development}$ and $C_{commercial}$ were split between the viral vector component ($C_{development\text{-}LV}$ and $C_{commercial\text{-}LV}$) and the cell therapy component ($C_{development\text{-}cell}$ and $C_{commercial\text{-}cell}$). Additionally, a further scenario was assessed, a post-approval switch scenario in which the bridging study using SPCL viral vector material was assumed to fail, hence transient transfection was assumed to be used throughout commercial phase (SPCL-PA-FC). No delays to market or bridging studies requirements were assumed to be associated with the SPCL scenarios apart from in the case of the SPCL-PA-FC scenario.

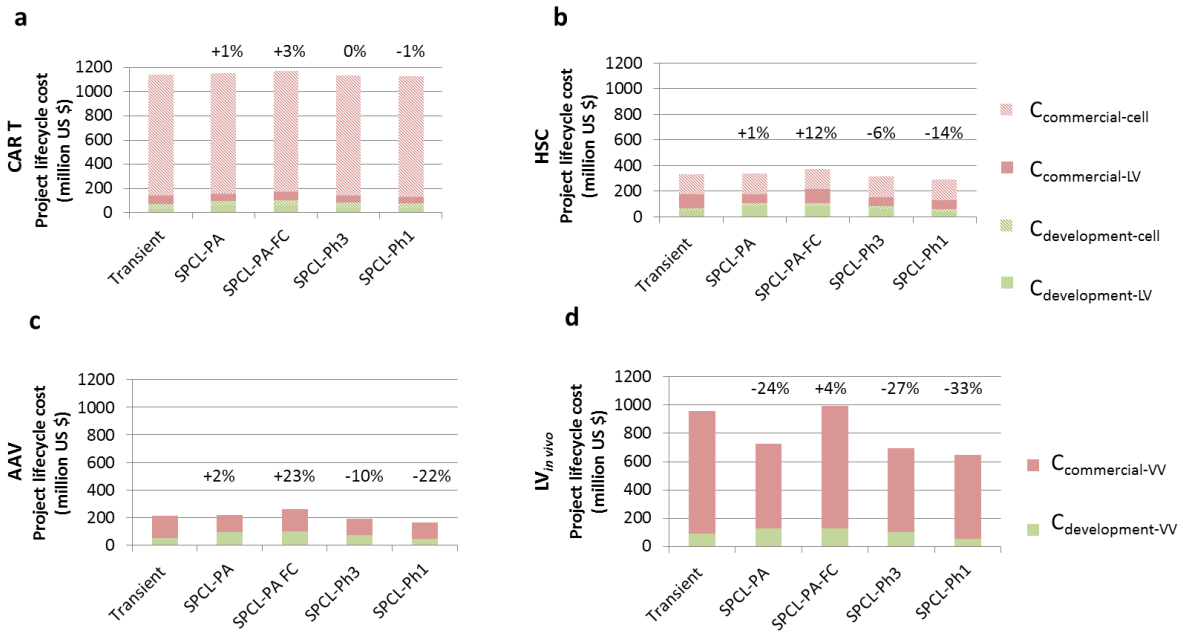

Figure 6.7 Project lifecycle cost in terms of cost of drug development ($C_{development}$) and cost of commercial stage ($C_{commercial}$) supported by the sponsor company for each product type: **a)** CAR T, **b)** HSC, **c)** AAV and **d)** $LV_{in\ vivo}$ and expression system scenario i.e. transient transfection (Transient) and switch to Stable producer cell line (SPCL) system for Phase 1 (SPCL-Ph1), for Phase 3 (SPCL-Ph3) and post-approval (SPCL-PA). The Project lifecycle cost is the sum of cost of drug development ($C_{development}$) and cost of commercial stage ($C_{commercial}$). The $C_{commercial}$ includes commercial cost of goods and pDNA supply chain costs, and for the gene-modified cell therapy products only, it also contains needle-to-needle logistics, apheresis, manufacture and transportation costs. No delays to market and no bridging studies were assumed for the SPCL-Ph1, SPCL-Ph3 and SPCL-PA scenarios. An additional process scenario is shown, a SPCL-PA-like scenario where the bridging study failed, hence transient transfection was used throughout commercial (SPCL-PA-FC). In the case of the gene-modified cell therapies only, the project lifecycle breakdown shown presents both viral vector and cell therapy cost components. The values shown above data points in represent the percentage project lifecycle cost difference between each scenario and the transient transfection scenario relative to transient transfection. VV = viral vector, Transient = transient transfection.

The previous section showed that switching to SPCL post-approval (SPCL-PA) was associated with the largest $C_{development}$ while switching to SPCL for Phase 1 (SPCL-Ph1) or sticking with transient transfection were the most attractive scenarios from a $C_{development}$ perspective, depending on product type. However, when analysing the project lifecycle cost (PLC) ranking, the switch to SPCL-PA scenario was predicted to be as attractive as transient transfection in the case of CAR T, HSC and AAV products (i.e. 1 to 2%) or significantly more attractive than transient transfection (i.e. -24%) for the $LV_{in\ vivo}$ product

(**Figure 6.7)**. For the CAR T product, this was the case due to the very low ratio of $C_{development}$ to PLC (i.e. 5-8%) since a larger demand was assumed for this product (2,250 doses/year) and the modest drop in $C_{commercial}$ when eliminating pDNA costs given the low pDNA cost contribution to $COG_{overall}$/dose. For the HSC and AAV products, as these were associated with a lower demand (500 doses/year) and a slightly lower $COG_{overall}$/dose than the CAR T product, the ratio of $C_{development}$ to PLC was higher (i.e. 20-31% and 24-43%, respectively). Coupled with a larger contribution of pDNA costs to the $COG_{overall}$/dose, the SPCL-PA scenario's PLC were similar to those of the transient transfection scenario because the cost savings achieved in $C_{commercial}$ were similar to the additional development costs associated with the SPCL-PA scenario.-While the $LV_{in\ vivo}$ product was associated with the same demand as the HSC and AAV products, the $LV_{in\ vivo}$ product was also associated with a low ratio of $C_{development}$ to PLC, similar to the CAR T product, because of the high $COG_{overall}$/dose associated with this product and hence a high $C_{commercial}$. Here, the significantly lower PLC of the SPCL-PA scenario relative to transient transfection could be justified by the large cost savings achieved in $C_{commercial}$ due to the significant pDNA cost contribution to the $COG_{overall}$/dose. These cost savings in commercial stage were higher than the additional development costs associated with the SPCL-PA scenario.

Furthermore, in most cases, ranking based on PLC showed that switching to SPCL for Phase 1 or for Phase 3 was significantly better than sticking with transient transfection. Whilst it was expected that the SPCL-Ph1 scenario would be associated with lowest PLC costs due to lower C_{vv}/dose (**Figure 6.4c)** and lowest or similar $C_{development}$ to the transient transfection scenario (**Figure 6.5)** switching to SPCL for Phase 3 scenario was also predicted to be attractive from a PLC perspective (**Figure 6.7**). This can be attributed to the cost savings achieved in commercial stage as a result of lower C_{vv}/dose when compared to the transient transfection scenario, exceeding the SPCL-related development

costs. On the other hand, in the case of the CAR T product, the difference in PLC between the SPCL-Ph1 and SPCL-Ph3 scenarios and the transient transfection scenario was negligible as a result of the very low viral vector cost contribution to the $COG_{overall}$/dose. With respects to the switch to SPCL post-approval scenario in which comparability studies failed (SPCL-PA-FC), it was found that the HSC and AAV products would be associated with significantly higher PLC while the CAR T and $LV_{in\ vivo}$ products would be associated with no significant changes in PLC relative to transient transfection. The PLC were found to be 12% and 23% larger than those in the transient transfection scenario, for the HSC and AAV products, respectively. In this case, the impact of failing comparability studies on PLC was significant given the high ratio of $C_{development}$ to PLC. In contrast, for the CAR T and $LV_{in\ vivo}$ products, the PLC associated with the SPCL-PA-FC scenario was found to be only 3-4% higher than those for the transient transfection scenario due to the very low $C_{development}$ to PLC ratios associated with both product types.

6.3.4 Profitability analysis and ranking summaries of expression systems used in viral vector manufacturing

6.3.4.1 Profitability analysis

While the previous sections analysed the drug development and project lifecycle cost trade-offs when switching to SPCL at various time points against the transient transfection scenario, this section analyses the effects of the switch and of potential delays to market on profitability (**Figure 6.8a-d).** The risk-adjusted net present value (rNPV), the profitability indicator used here, was determined for each product type and process scenario (i.e. transient transfection, switch to SPCL for Phase 1 (SPCL-Ph1), for Phase 3 (SPCL-Ph3) and post-approval (SPCL-PA) (**Figure 6.8**). Delays to market were assumed only for the SPCL-Ph1 and SPCL-Ph3 scenarios. For the SPCL-Ph1 scenario, a 10-month delay to market was assumed based on the 10-month SPCL development duration. On the other hand, for the SPCL-Ph3 scenario, a one year delay to market was assumed due to

the hypothesis that a one-year bridging study would be required. The additional process change scenario described in the previous section i.e. SPCL-PA-FC was included in this analysis.

Although switching to the SPCL system during drug development (SPCL-Ph1 and SPCL-Ph3) offered the lowest project lifecycle cost (PLC) (**Figure 6.7**)**,** if this results in delays to market of 10-12 months, these options become the least favourable from a profitability perspective (**Figure 6.8).**

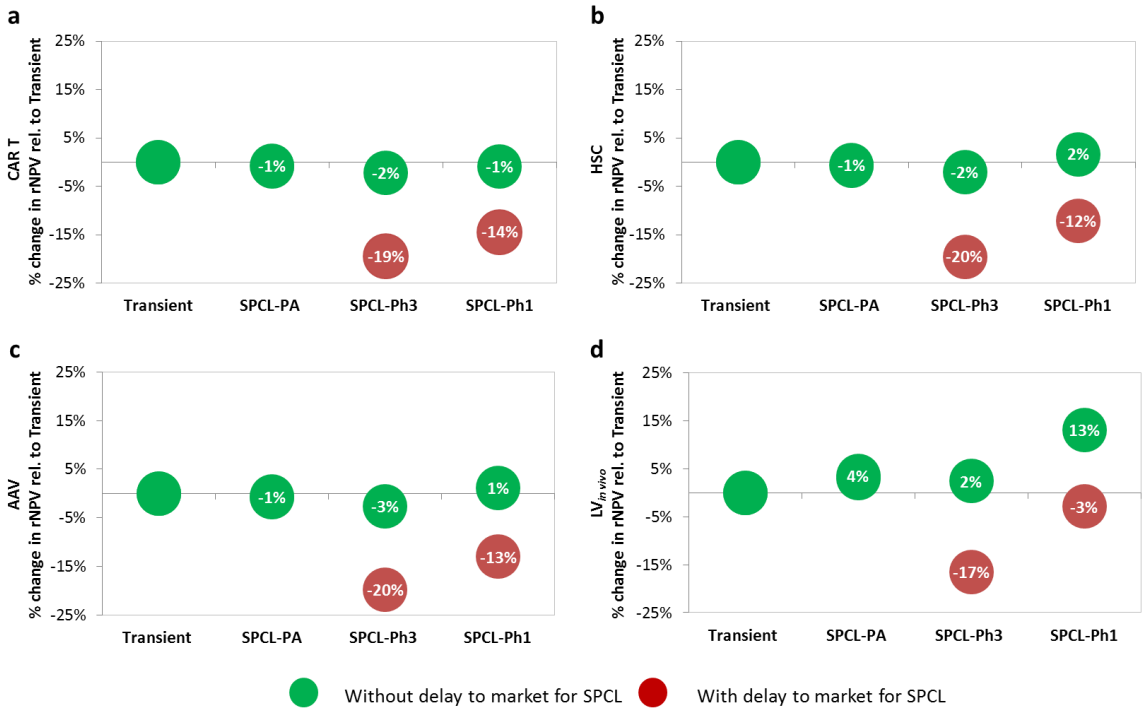

e

Product type	Best strategy according to cost and profitability metrics			
	Cost of development	Project lifecycle cost	Profitability	
			Without delay to market for SPCL	With delay to market for SPCL
CAR T	Transient / SPCL-Ph1	All equivalent	All equivalent	Transient / SPCL-PA
HSC	SPCL-Ph1	SPCL-Ph1	All equivalent	Transient / SPCL-PA
AAV	SPCL-Ph1	SPCL-Ph1	All equivalent	Transient / SPCL-PA
$LV_{in\ vivo}$	SPCL-Ph1	SPCL-Ph1	SPCL-Ph1	Transient / SPCL-PA / SPCL-Ph1

Figure 6.8 Percent change in profitability measured as risk-adjusted net present value (rNPV) relative to transient transfection for each process change scenario for **a)** CAR T,

b) HSC, **c)** AAV and **d)** $LV_{in\ vivo}$ products. e) Best strategy in terms of cost of drug development ($C_{development}$), project lifecycle cost (PLC, $C_{development}$ + $C_{commercial}$) and profitability (rNPV) for all product types (best to the worst order). $C_{commercial}$ = cost of commercial stage, $C_{development}$ = cost of drug development. Process change scenarios: sticking with transient transfection (Transient), switching to stable producer cell line (SPCL) system for Phase 1 (SPCL-Ph1), for Phase 3 (SPCL-Ph3) or post-approval (SPCL-PA) assuming no delay to market (green) and delays to market (red) for the SPCL-Ph3 and SPCL-Ph1 scenarios. For the SPCL-Ph3 scenario, a one year delay to market was assumed if bridging studies were requested by the regulators while for the SPCL-Ph1 scenario, a 10-month delays to market was assumed to occur due to stable producer cell line development duration. While the SPCL-PA scenario includes bridging studies spanning for one year, these activities were assumed not to cause delays to market.

Since there were two ranking trends observed with respect to the SPCL-Ph1 and the transient transfection scenarios in the context of no delay and delay to market, the profitability results for the CAR T, HSC and AAV products are discussed first followed by those for the $LV_{in\ vivo}$ product. Then the profitability of the switch to SPCL post-approval (SPCL-PA & SPCL-PA-FC) scenarios is discussed. In a no delay to market scenario, the tool predicted that all scenarios would score a similar rNPV to the transient transfection scenario (within ± 5%) for the CAR T, HSC and the AAV products (**Figure 6.8a-c).** This was expected because of the small contributions of the viral vector PLC (sum of $C_{development\text{-}VV}$ and $C_{commercial\text{-}VV}$, **Figure 6.7**) to the overall net present cost (NPC) that included the cell therapy PLC (sum of $C_{development\text{-}cell}$ and $C_{commercial\text{-}cell,}$ for the HSC and CAR T products), sales and marketing costs and taxes (**Figure 6.9a**).

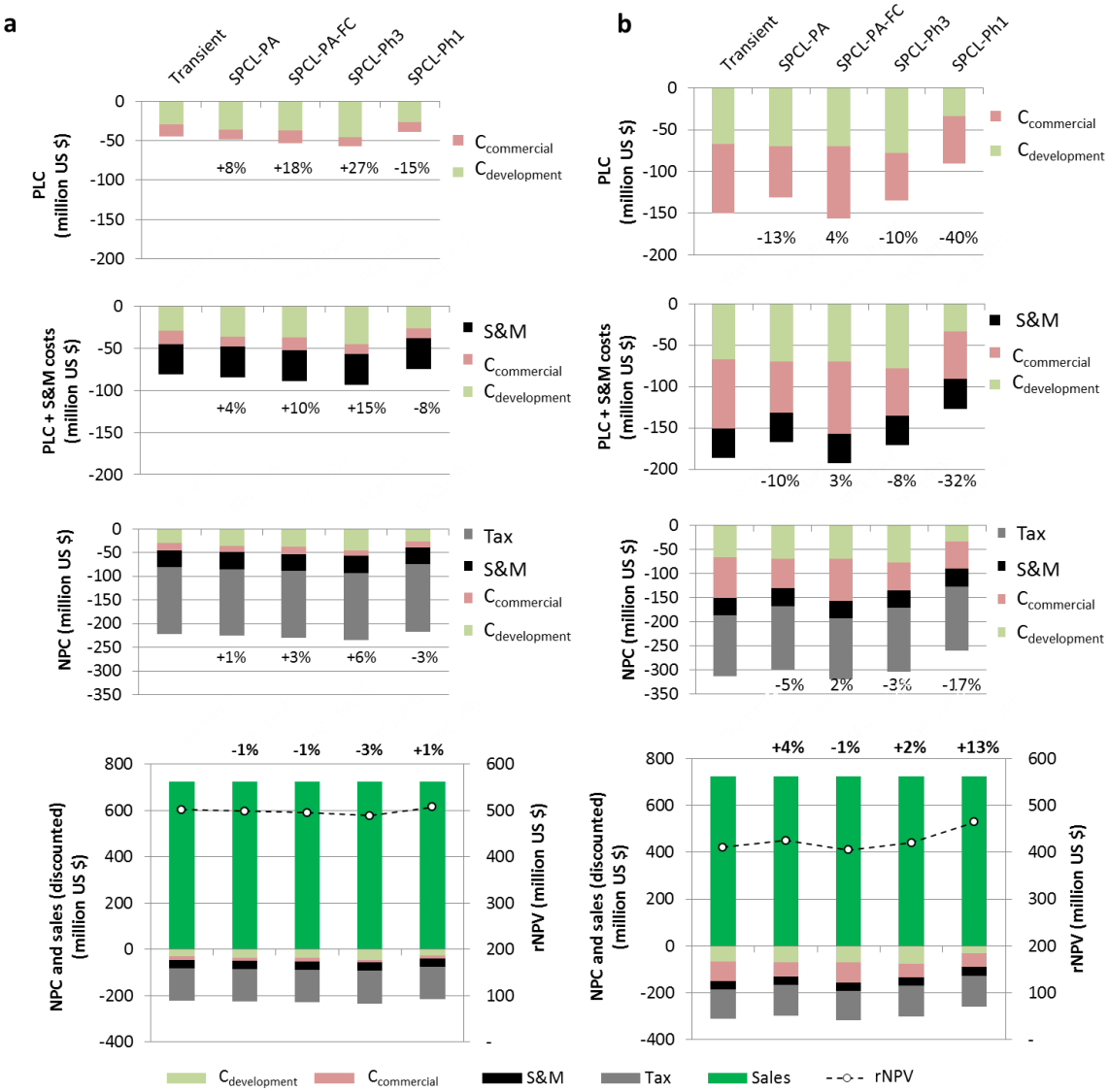

Figure 6.9 Net present cost (NPC) breakdown for transient transfection, switch to SPCL post-approval (SPCL-PA and SPCL-PA-FC), for Phase 3 (SPCL-Ph3) and for Phase 1 (SPCL-Ph1) scenarios for a) the AAV product and b) the $LV_{in\ vivo}$ product. No delays to market were assumed for any of these scenarios. The costs were risk-adjusted based on clinical phase's success rates and were also discounted at a rate of 10% per year. S&M = sales and marketing costs, rNPV = risk-adjusted net present value, $C_{commercial}$ = commercial costs (commercial cost of goods and supply chain costs), $C_{development}$ = cost of drug development; SPCL= stable producer cell line, SPCL-PA-FC = switch to SPCL post-approval and failed comparability studies (bridging studies were assumed in this scenario only).

In contrast, in a delay to market scenario, while the SPCL-Ph3 scenario was associated with the lowest profitability levels for all four product types (16-20% lower), SPCL-Ph1 scenario was associated with low profitability levels for the CAR T, HSC and AAV products (12-14% lower). The lack of revenue associated with 10-12 months delay

decreased significantly the rNPV levels due to the very high selling prices associated with these products (**Figure 6.10a**). The reason for SPCL-Ph3 scenario's lower performance when compared to the SPCL-Ph1 scenario was its higher NPC and 2 month longer delay to market compared to the SPCL-Ph1 scenario (**Figure 6.10a**).

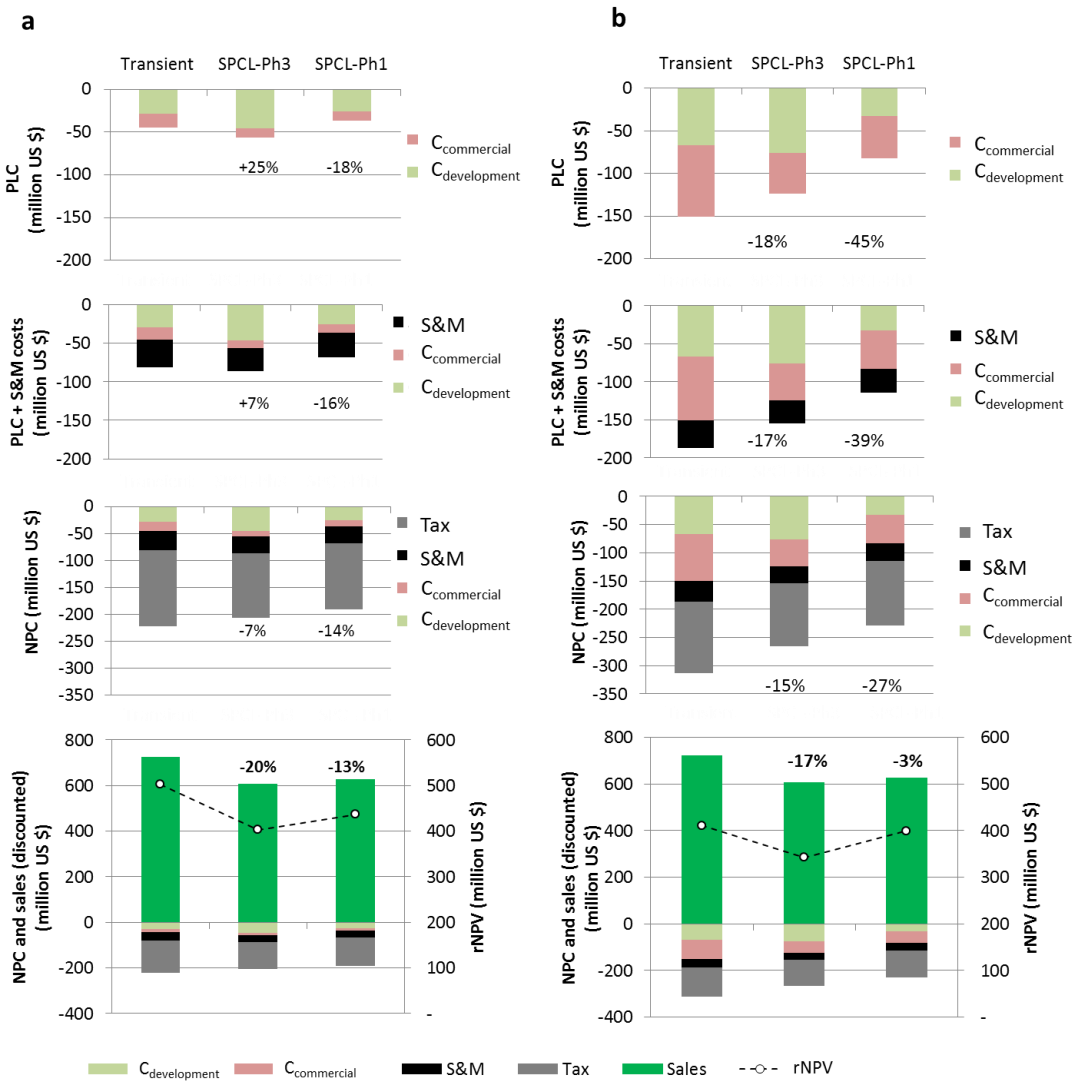

Figure 6.10 Net present costs (NPC) breakdown for transient transfection, switch to SPCL for Phase 3 (SPCL-Ph3) and for Phase 1 (SPCL-Ph1) scenarios for **a)** the AAV product and **b)** the LV*in vivo* product. A 12-month delay to market was assumed for the SPCL-Ph3 scenario and a 10-month delay to market was assumed for the SPCL-Ph1 scenario. Bridging studies were assumed for the SPCL-Ph3 scenario. The costs were risk-adjusted based on clinical phase's success rates and were also discounted at a rate of 10% per year. S&M = sales and marketing costs, rNPV = risk-adjusted net present value, $C_{commercial}$ = commercial costs (commercial cost of goods and supply chain costs), $C_{development}$ = cost of drug development; SPCL= stable producer cell line, SPCL-PA-FC = switch to SPCL post-approval and failed comparability studies (bridging studies were assumed in this scenario only).

On the other hand, for the $LV_{in\ vivo}$ product, the SPCL-Ph1 scenario was associated with superior profitability (+13%) over the transient transfection scenario in a no delay to market scenario and did not lose its competitiveness when a delay to market was assumed. For the no delay to market scenario, this can be attributed to the higher PLC contribution to the overall NPC and NPV (**Figure 6.9b**) given the larger $COG_{overall}$/dose associated with this product as well as the highest pDNA cost contribution (**Figure 6.4c**) when compared to the other products. For the delay to market scenario this can be attributed to the drop in revenue caused by the 10-month delay being counterbalanced by the reduced costs when switching to SPCL (i.e. PLC and hence NPC) (**Figure 6.10b**).

Whilst the SPCL-PA scenario was found to be the least attractive from a cost of drug development perspective, this scenario was equivalent to the transient transfection route across product types from PLC and rNPV perspectives (within ± 5%), even when accounting for the impact of failing comparability studies (SPCL-PA-FC). This was caused by the dominance of the sales contribution to rNPV triggered by the high selling prices and the avoidance of delays to market. Since there are other benefits associated with the SPCL route which were not captured in this analysis (i.e. higher process robustness and quality control profile), these results suggest that switching to SPCL post-approval may represent the least risky strategy from a profitability point of view.

6.3.4.2 Ranking summaries of expression systems and relationship to product type characteristics

Figure 6.8e shows an integrated table of the cost and profitability rankings of the process scenarios analysed so far so as to help visualise the association between transient transfection and SPCL ranking and the pDNA percentage cost contributions to $COG_{overall}$ for each product type.

From a cost of drug development ($C_{development}$) and project lifecycle cost (PLC) ranking perspective, the four product types could be grouped into two categories: the very low versus the medium-high pDNA percentage cost contribution to the $COG_{overall}$/dose i.e. the CAR T versus the HSC, AAV and $LV_{in\ vivo}$ products. Regardless of product type, switching to SPCL early in development was favourable in terms of $C_{development}$ and PLC values; for the CAR T product, this position was tied with sticking with transient transfection (**Figure 6.5, Figure 6.7**).

From a profitability ranking perspective, the four product types could be grouped into two categories: the low-medium versus the high pDNA percentage cost contribution to the $COG_{overall}$/dose i.e. CAR T, HSC and AAV versus the $LV_{in\ vivo}$ product (**Figure 6.8e).** For the first category, if no delay to market was assumed, the expression system did not appear to make a difference on profitability, regardless of the time point of implementing the switch to SPCL. When assuming a delay to market, the transient transfection and the S-PA scenarios (including S-PA-FC) were found to be the most profitable, followed by the S-P1 and the S-P3 scenarios (**Figure 6.8a-c).** For the second category, if no delay to market was assumed, the S-P1 scenario led to significantly higher profitability compared to the transient transfection scenario. In contrast, when delay to market was assumed, the transient transfection, S-P1 and S-PA scenarios (including S-PA-FC) were found to be equally profitable, followed by the S-P3 scenario (**Figure 6d**).

Stable packaging cell lines are an attractive option for viral vector manufacture as they require a fraction of the pDNA costs associated with the transient transfection route. A stable packaging cell line could, at least in theory, be used to manufacture multiple viral vector products by changing the transgene pDNA. If the stable packaging cell line system resulted in a quarter of the pDNA requirement of transient transfection and removed the need for cell line development for each viral vector product, the cost of drug development

would be lower than that of the transient transfection route and slightly lower than that associated with the producer route. With regards to the project lifecycle cost, the packaging route would be associated with slightly higher values than the producer route but much lower than the transient transfection route. In terms of profitability, the packaging route is predicted to perform similarly to the producer route associated with no delay to market, and to perform better than the producer route associated with a similar delay, regardless of product type.

6.3.5 Scenario analyses

This section explores the impact of changing different key costs and process parameters on profitability ranking between transient transfection and the switch to SPCL for Phase 1 (SPCL-Ph1) scenarios. A sensitivity analysis was performed to justify the parameters selected in the scenario analysis (**Figure 6.11**). These were delay to market, harvest titre and pDNA cost. Firstly, pDNA cost impact on profitability is explored so as to identify pDNA cost levels with potential to change the profitability ranking i.e. either favouring SPCL or transient transfection (**Figure 6.12**). Lastly, the cumulative impact of SPCL harvest titre in conjunction with delay to market reductions and pDNA cost on rNPV, $C_{development\text{-}VV}$ and COG levels is discussed (**Figure 6.13**).

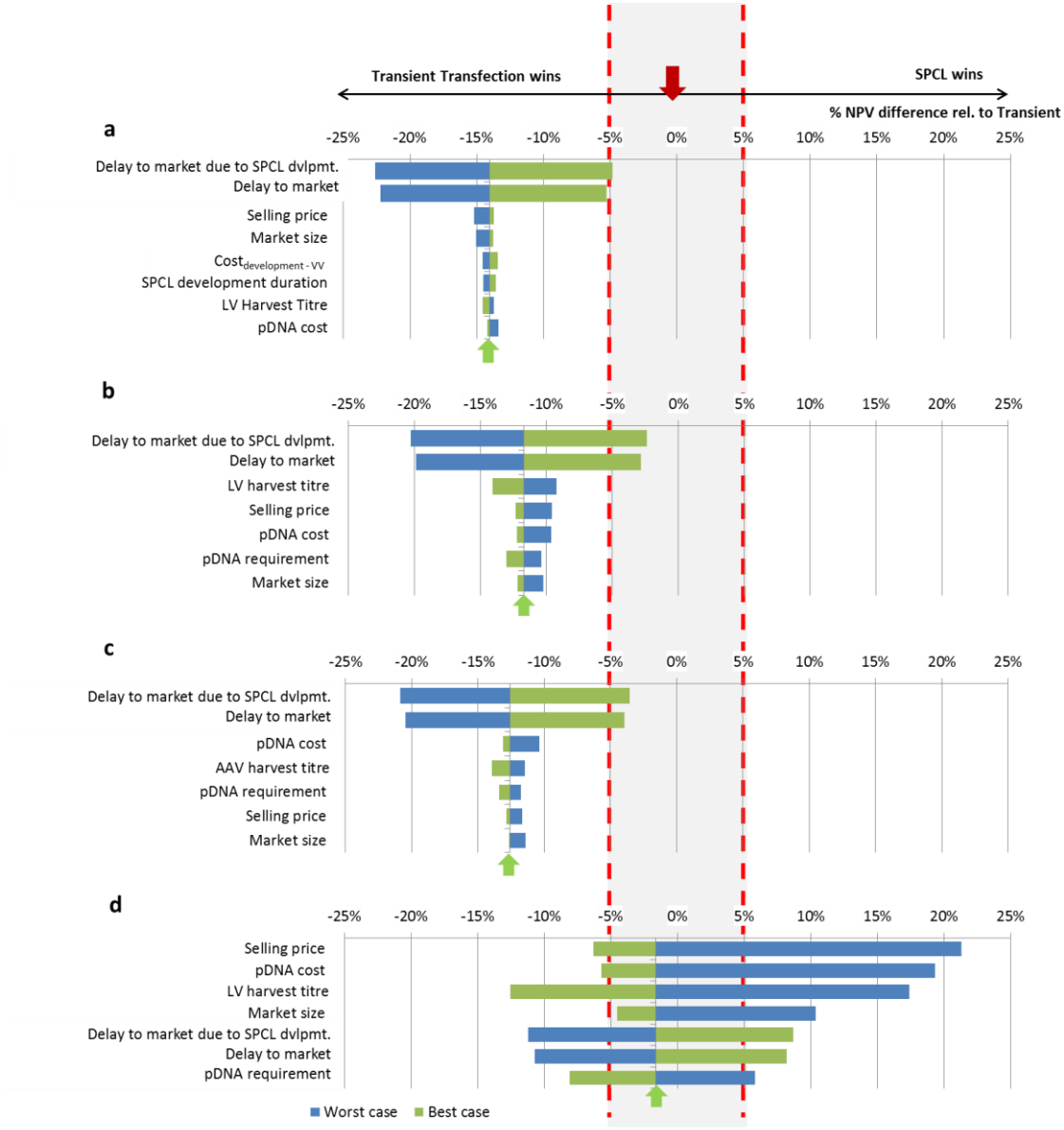

Figure 6.11 Sensitivity analysis showing the impact of varying one parameter at a time on the profitability ranking between transient transfection and the switch to SPCL for Phase 1 (SPCL-Ph1) scenarios for **a)** CAR T, **b)** HSC, **c)** AAV and **d)** LV*in vivo* products. The x-axis shows the percentage profitability difference between these scenarios relative to transient transfection. The arrows above it indicate that SPCL-Ph1 is more profitable if the percentage profitability difference is positive while transient transfection is more profitable if the percentage profitability difference is negative. The green arrows indicate the percentage profitability difference between scenarios at base case. The grey area surrounded by the dashed red lines indicate a profitability difference of ± 5% where the scenarios were considered equally attractive. Each parameter was varied by ±50% with the exception of cGMP-manufactured pDNA price which was varied between $20,000 and $250,000/g. The delay to market due to SPCL development parameter involved varying the delay to market associated with the SPCL-Ph1 scenario as well as the PD effort associated with SPCL development whereas the delay to market parameter involved varying the delay to market only (and keeping the PD effort the same as that at base case scenario).

6.3.5.1 Impact of pDNA cost on profitability ranking of expression systems used in viral vector manufacturing

The cost and profitability rankings generated for the four product types and expression system scenarios were based on a commercial stage pDNA cost of $60,000/g. Since accounts of both high quality and cGMP-manufactured pDNA cost per gram vary significantly, this section explores the critical pDNA cost levels predicted to impact the profitability ranking between transient transfection and the switch to SPCL for Phase 1 (SPCL-Ph1) scenarios (**Figure 6.12a**). Should either or both pDNA cost and pDNA requirement increase per viral vector batch, **Figure 6.12b** explores the impact on the $COG_{overall}$/dose and pDNA cost contributions at the critical pDNA cost for each product type. The analysis was performed for both instances of no delay to market and a 10-month delay to market associated with the SPCL-Ph1 scenario.

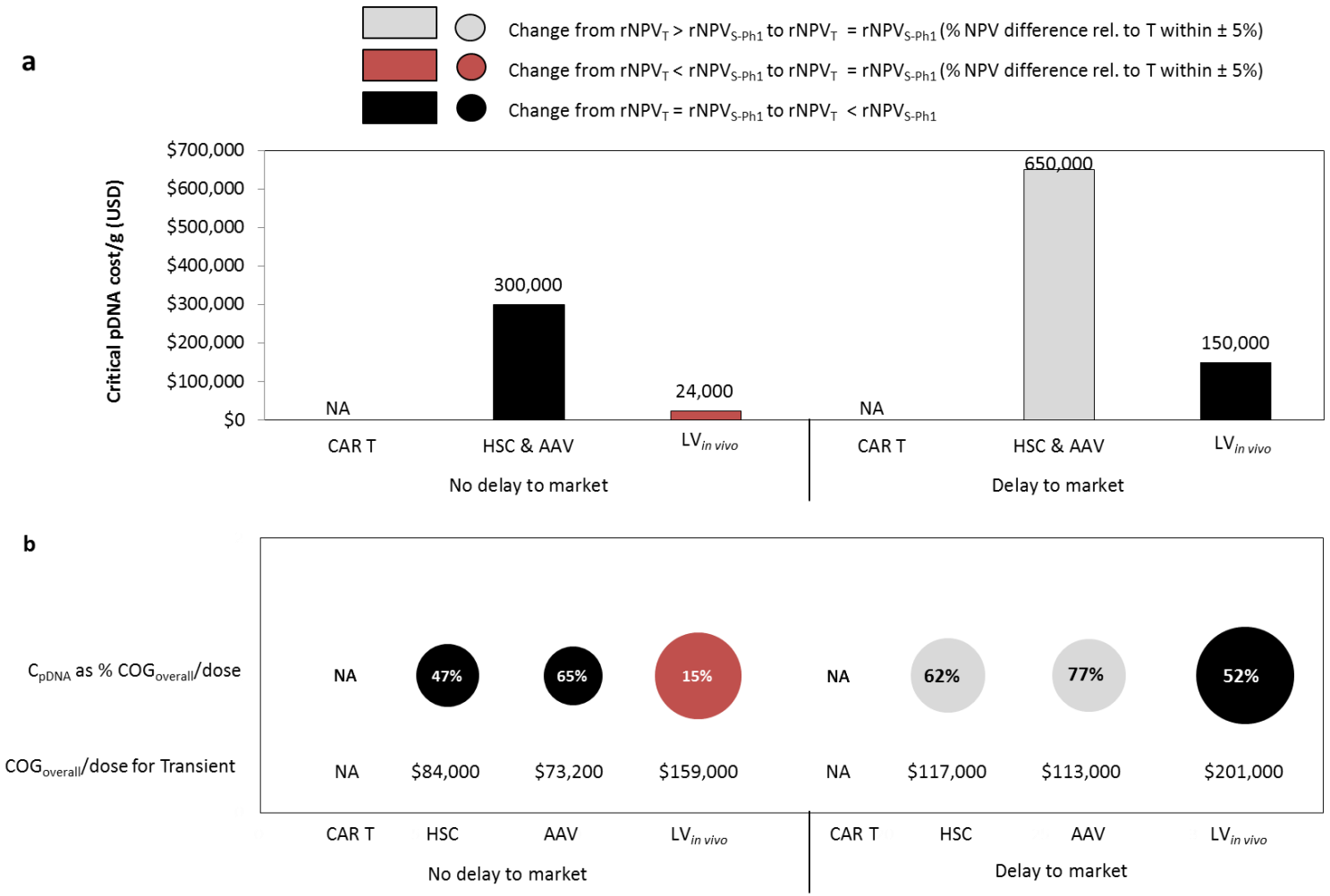

Figure 6.12 Commercial scale pDNA cost impact on profitability ranking showing **a)** critical pDNA cost/g and **b)** the pDNA cost contribution to the $COG_{overall}$/dose generated by the critical pDNA cost/g for each product type in the case of no delay to market and a 10-month delay to market associated with the switch to SPCL for Phase 1 (SPCL-Ph1) scenario. Bubble size represents the $COG_{overall}$/dose in the case of each product type while the percentage value within each circle shows the pDNA cost contribution to the overall cost of goods per dose ($COG_{overall}$/dose). T = transient transfection, S-Ph1 = SPCL switch for Phase 1, NA = not applicable, C_{pDNA} = cGMP-manufactured cost of plasmid DNA.

While the pDNA cost had no impact in the case of the CAR T product due to the negligible pDNA cost contribution to $COG_{overall}$/dose, pDNA cost fluctuations elicited changes in profitability ranking for the other products given the higher pDNA cost contributions to their $COG_{overall}$/dose. In the context of the CAR T product, increasing the pDNA cost even 10-fold had no impact on the ranking in either of the no delay or delay to market instances (**Figure 6.12a**). For HSC and AAV products, the critical pDNA cost that would change the ranking from transient transfection being equal or better than SPCL-Ph1 to SPCL-Ph1 being better or equal to transient transfection was found to be $300,000/g without delays to market and $650,000/g with delays to market. This would correspond to an increase in the pDNA contribution to the COG/dose from 13% and 23% for the HSC and AAV products (**Figure 6.4c**), respectively, to 47% and 65% in a no delay to market scenario and 62% and 77% in a delay to market scenario (**Figure 6.12b**). Since the critical pDNA costs identified for these two products fall within the reported price ranges, this analysis shows that the commercial stage pDNA cost has a large impact on profitability ranking between the transient transfection and SPCL-Ph1 scenarios. For the $LV_{in\ vivo}$ product which required the largest manufacturing capacity, the critical pDNA cost that would change the ranking from SPCL-Ph1 being better or equal to transient transfection to transient transfection being equal or worse to SPCL-Ph1 was found to be $24,000/g without delays to market and $150,000/g with delay to market. This would correspond to a decrease in the pDNA contribution to the COG/dose from 31% (**Figure 6.4c)** to 15% in a no delay to market scenario and an increase to 52% in a delay to market scenario (**Figure 6.12b**). Based on the reported pDNA price ranges, these results suggest that the pDNA process would require further optimisation in order to ensure that transient transfection would be more favourable than the SPCL-Ph1 scenario.

6.3.5.2. Conditions required to justify switching from transient transfection to SPCL in the context of viral vector manufacturing from cost and profitability perspectives

This work has focused so far on one advantage which the SPCL system has over transient transfection, the removal of the pDNA requirement, which has an impact on material costs and supply chain management costs, but other potential benefits include superior harvest titres. The tool was employed to identify the conditions in terms of harvest titre and delay to market associated with the switch to SPCL for Phase 1 (SPCL-Ph1) scenario and the pDNA cost in the transient transfection scenario that would satisfy set criteria for switching to SPCL for each product type. The profitability superiority criteria set entails that the profitability of the SPCL-Ph1 needs to be more than 5% higher than that of transient transfection while the COG_{VV}/dose and $C_{development\text{-}VV}$ should be minimum 60% and 25%, respectively, lower than those of transient transfection. These criteria were chosen based on discussions with industry experts. **Figure 6.13** shows the conditions required to satisfy these criteria in dark green. This figure was assembled based on profitability, COG and $C_{development}$ ranking data (**Figure 6.14, Figure 6.15, Figure 6.16, Figure 6.17).** SPCL harvest titre (shown as row headers, **Figure 6.13**) was varied between 0.5-50-fold from the base case. These values represent both routinely achieved titres with the transient transfection system (low end) as well as potential titre values that SPCL systems could deliver (high end). The commercial-stage pDNA cost was varied from the base case value of $60,000/g (**Figure 6.13i** column), to $250,000/g (**Figure 6.13ii** column) to $600,000/g (**Figure 6.13iii** column) in an attempt to capture the pDNA cost accounts of as many industry players as possible. The different unit pDNA costs could also be interpreted as different starting pDNA levels required per viral vector batch. For example, a requirement of 2.5 $\mu g/10^6$ cells at a pDNA cost of $60,000/g will have the same impact on the COG/batch as 0.6 $\mu g/10^6$ cells at a pDNA cost of $250,000/g.

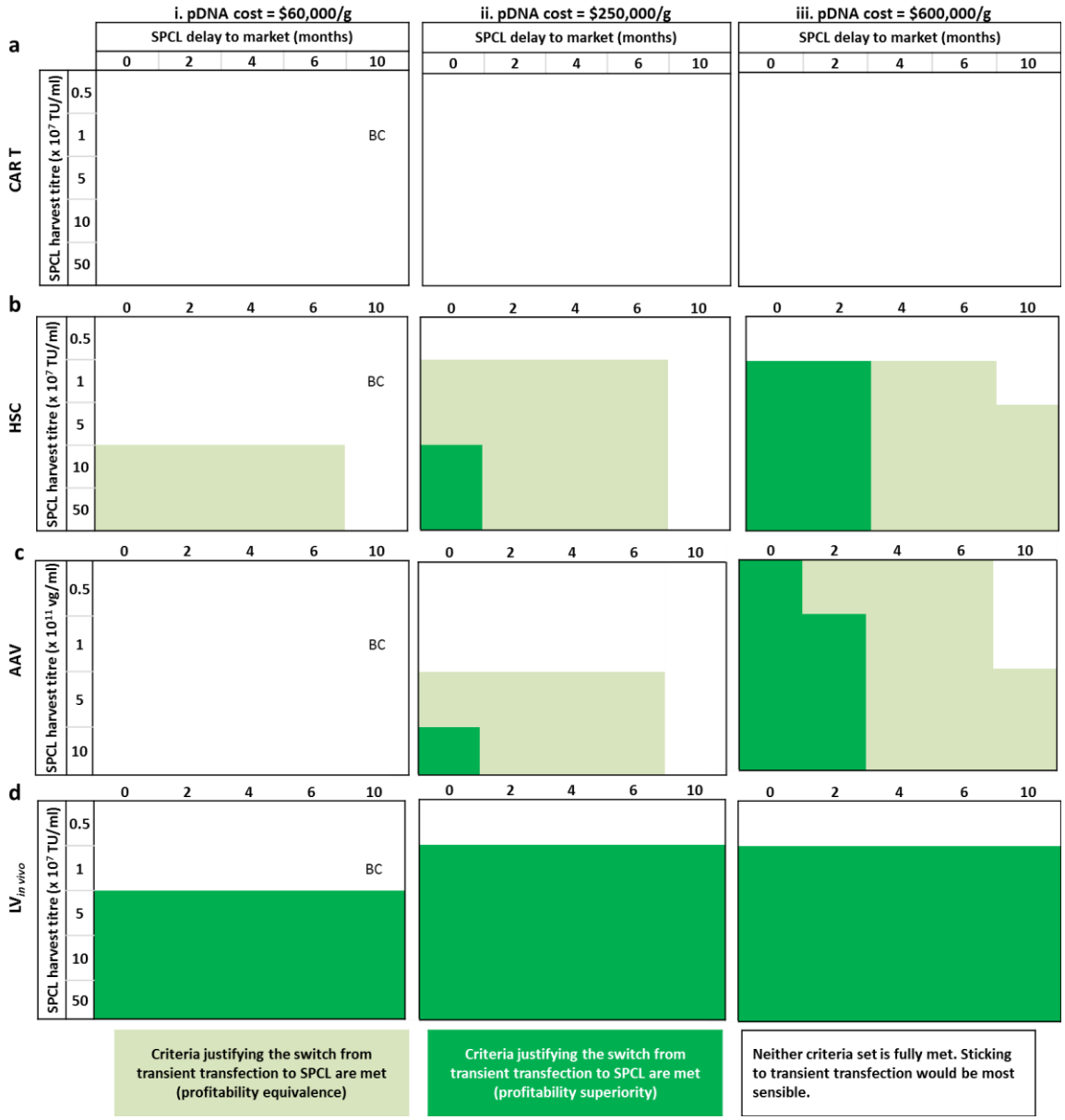

Figure 6.13 Matrix of contour plots showing the sensitivity of the ranking of the switch to SPCL for Phase 1 (SPCL-Ph1) versus transient transfection to delay to market, harvest titre associated with SPCL and pDNA cost conditions for a) CAR T, b) HSC, c) AAV and d) $LV_{in\ vivo}$ products. The values of the pDNA costs explored were i) $60,000/g (base case), ii) $250,000/g and iii) $600,000/g. The shaded regions indicate where the SPCL-Ph1 scenario satisfied the profitability equivalence criteria set (light green) or profitability superiority criteria set (dark green) relative to transient transfection. The profitability equivalence criteria set required that there would be a ±5% difference in profitability between the stable expression system relative to transient transfection. The profitability superiority criteria set required that the profitability of the SPCL-Ph1 be more than 5% higher than that of transient transfection. Both criteria sets required also savings of at least 60% in the cost of viral vector (CVV/dose) and 25% in the cost of drug development for

the viral vector component ($C_{development,VV}$), respectively, for the SPCL-Ph1 scenario relative to transient transfection.

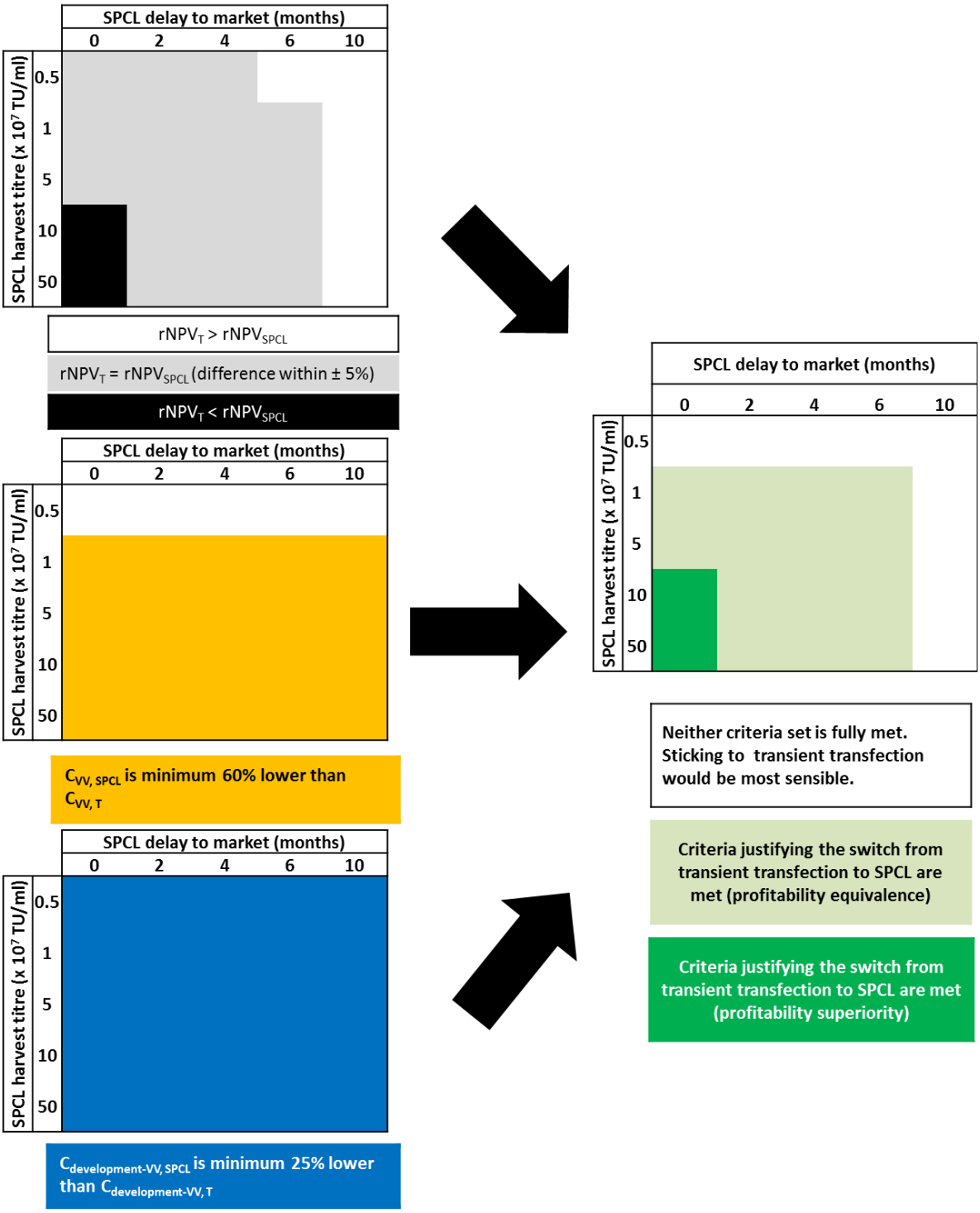

Figure 6.14 Illustration showing how the matrix of contour plots in **Figure 6.13** was created using the data shown in **Figure 6.15**, **Figure 6.16** and **Figure 6.17**. T = transient transfection, SPCL = stable producer cell line, rNPV = risk-adjusted net-present value, C_{VV} = viral vector cost, $C_{development\text{-}VV}$ = cost of drug development associated with the viral vector component.

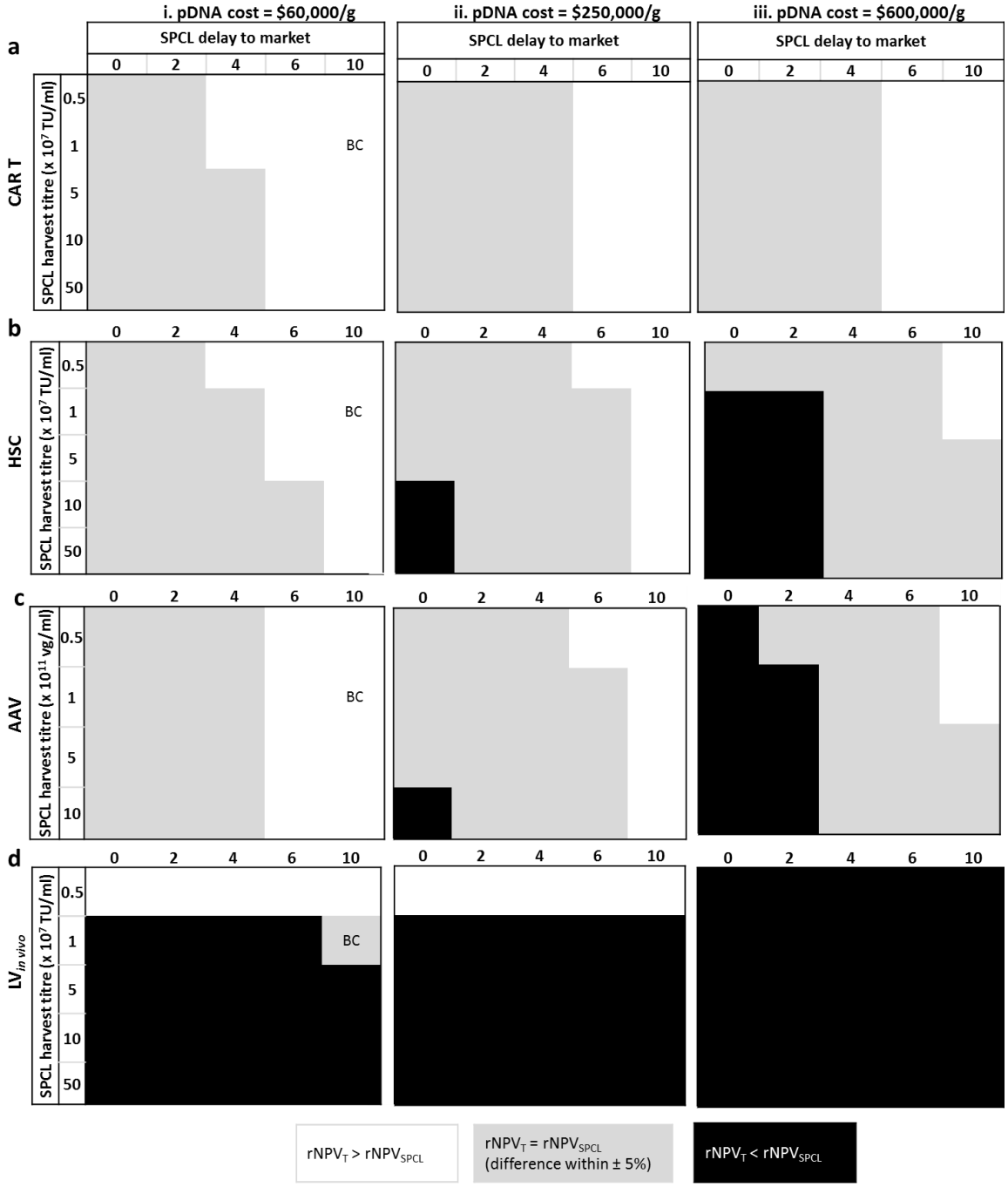

Figure 6.15 Matrix of contour plots showing the sensitivity of the profitability ranking between the switch to SPCL for Phase 1 (SPCL-Ph1) scenario versus transient transfection scenario to delay to market, harvest titre associated with SPCL and pDNA cost conditions for **a)** CAR T, **b)** HSC, **c)** AAV and **d)** $LV_{in\ vivo}$ products at pDNA costs of **i)** $60,000/g (base case), **ii)** $250,000/g and **iii)** $600,000/g. T = transient transfection, SPCL = stable producer cell line, BC = base case scenario, rNPV = risk-adjusted net present value.

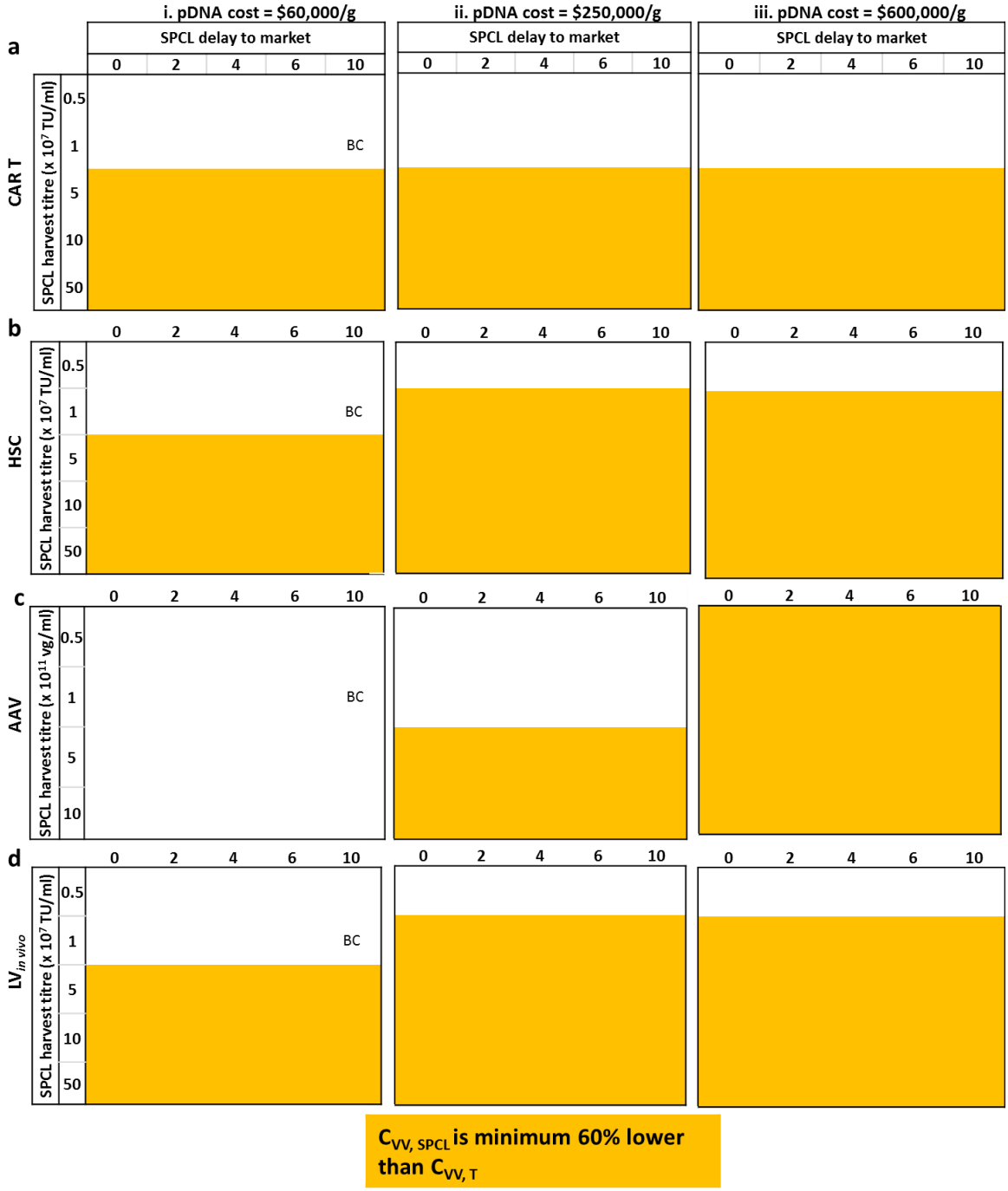

Figure 6.16 Matrix of contour plots showing the delay to market, harvest titre and pDNA cost conditions leading to minimum 60% savings in the cost of viral vector (C_{VV}) achieved with the SPCL system when switching for Phase 1, relative to transient transfection for **a)** CAR T, **b)** HSC, **c)** AAV and **d)** $LV_{in\ vivo}$ products at pDNA costs of **i)** $60,000/g (base case), **ii)** $250,000/g and **iii)** $600,000/g. T = transient transfection, SPCL = stable producer cell line, BC = base case scenario.

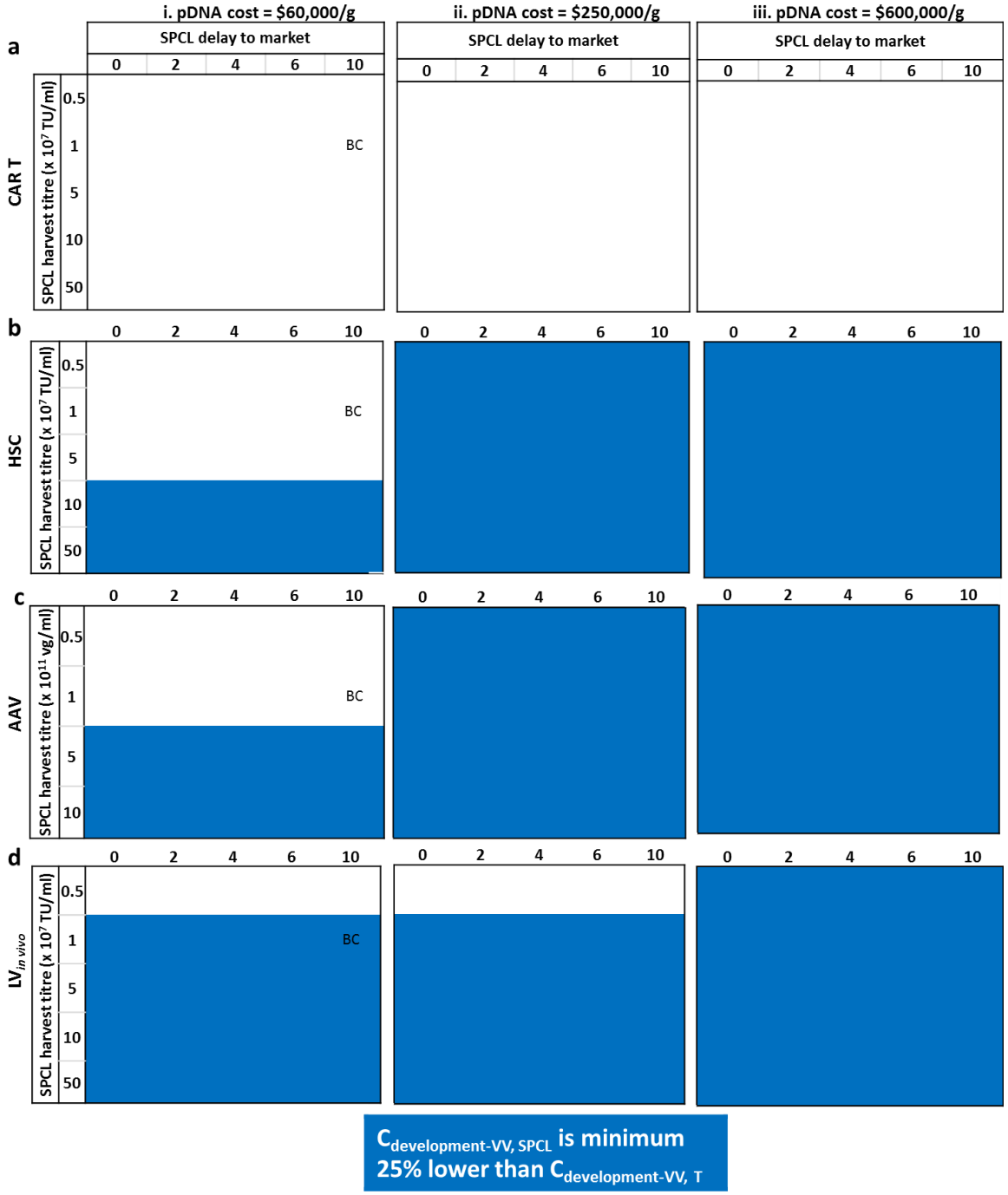

Figure 6.17 Matrix of contour plots showing the delay to market, harvest titre and pDNA cost conditions leading to minimum 25% savings in the cost of drug development associated with the viral vector component ($C_{development\text{-}VV}$) achieved with the SPCL system when switching for Phase 1, relative to transient transfection for **a)** CAR T, **b)** HSC, **c)** AAV and **d)** $LV_{in\ vivo}$ products at pDNA costs of **i)** $60,000/g (base case), **ii)** $250,000/g and **iii)** $600,000/g. T = transient transfection, SPCL = stable producer cell line, BC = base case scenario.

The overarching message here is that with decrease in delay to market and increase in harvest titre associated with the SPCL system as well as pDNA cost increase, the switch to SPCL-Ph1 scenario becomes more favourable than transient transfection from a profitability perspective (**Figure 6.15**). This effect is amplified by the percentage pDNA cost contribution to the $COG_{overall}$/dose associated with each product type; this can be seen with the increasing window size for profitability superiority (dark green shaded areas) moving both downwards with product type and across with pDNA cost. For products associated with a low pDNA cost contribution to the $COG_{overall}$/dose such as the CAR T product, the criteria set could not be met in full i.e. transient transfection was preferable (**Figure 6.13i-iii**, **Figure 6.15**, **Figure 6.16**, **Figure 6.17**). For the product types associated with medium pDNA cost contributions to the $COG_{overall}$/dose (HSC, AAV) the profitability superiority criteria was found to be particularly sensitive to the pDNA cost, the delay to market and the SPCL harvest titre (**Figure 6.13b,c**, **Figure 6.15**, **Figure 6.16**, **Figure 6.17**). For example, in the case of the HSC product, a pDNA cost of $60,000/g was found to favour the transient transfection scenario irrespective of delays to market and titre (**Figure 6.13b,i).** However, at a pDNA cost of $250,000/g, if there was no delay to market and the SPCL harvest titre was 10-fold higher than that achieved with transient transfection (i.e. 10^8 TU/ml), SPCL-Ph1 was found to be the most favourable (**Figure 6.13b,ii**). If the pDNA cost increased further to $600,000/g, the window of operation increased with no SPCL harvest titre increase required and a maximum delay to market of 2 months (**Figure 6.13b,iii).** For products associated with high pDNA cost contributions to $COG_{overall}$/dose such as the $LV_{in\ vivo}$ product, the profitability superiority criteria was met in the majority of conditions analysed (**Figure 6.13d**). Exception to this rule was identified at an SPCL harvest titre of 5×10^6 TU/ml across pDNA costs scenarios and 10^7 TU/ml at the base case pDNA cost (**Figure 6.13d**).

6.4 Conclusion

This work describes a decisional tool consisting of a bioprocess economics model coupled with a cost of drug development model, a project valuation framework and optimisation algorithm built to assess the economic competitiveness of a range of process design and process change scenarios. The tool was applied to an industrially-relevant case study on viral vector manufacture associated with four gene therapy product types: the CAR T, haematopoietic stem cell (HSC) gene therapy, AAV and $LV_{in\ vivo}$ products. The tool highlighted the cost of goods, cost of drug development, project lifecycle cost and profitability associated with sticking with transient transfection or switching to a stable producer cell line (SPCL) system at various time points in the case of each product type. At base case assumptions, the results showed that employing transient transfection in viral vector manufacture exerts a small impact on the overall cost of goods per dose associated with the CAR T product, a higher impact on an HSC and AAV product and the largest impact on an $LV_{in\ vivo}$ product. From a cost of drug development perspective, it revealed similar or lower cost of drug development associated with the SPCL when switching to SPCL for Phase 1 (SPCL-Ph1) compared to the transient transfection scenario across product types. Furthermore, the analysis indicated that switching to SPCL later on in development (for Phase 3 or post-approval) led to the highest cost of drug development due to the addition of comparability studies and also bridging studies costs. The tool was then used to explore the project lifecycle cost across process scenarios and product types to weigh up the cost of goods savings against the higher cost of drug development associated with process changes. This revealed that switching to SPCL post-approval leads to similar or even lower project lifecycle cost compared to the transient transfection scenario. Regarding the profitability ranking across the process change scenarios for each product type, it was found that the SPCL-Ph1 scenario led to similar profitability levels relative to transient transfection scenario for most product types when no delays to market

were assumed. However, when delays to market were assumed, the early switch to SPCL scenarios were associated with significantly lower profitability compared to transient transfection. Exception to this rule was the $LV_{in\ vivo}$ product which was found to be more profitable in a no delay to market instance, and as profitable as transient transfection scenario when delay to market was assumed, attributed to its large pDNA cost contribution to the $COG_{overall}$/dose. Furthermore, this study presented the critical pDNA cost levels which would cause changes in profitability ranking and explored the cumulative impact of decreases in delay to market associated with the SPCL-Ph1 scenario, increases in pDNA cost levels and increases in harvest titres achieved with the SPCL system. Additionally, it highlighted the conditions required in order to meet the industry-vetted criteria for switching from transient transfection to SPCL for Phase 1 from a profitability, cost of viral vector/dose and cost of drug development perspective. This tool can be employed to generate a detailed and comprehensive picture of the trade-offs associated with different process designs and process change scenarios and for a variety of cell and gene therapy product types. Such analyses help inform R&D decisions so as to increase the chances of successful commercialisation journeys for advanced therapeutic medicinal products (ATMPs).

Chapter 7: Process validation in cell and gene therapy

7.1 Introduction

Process validation represents a critical milestone in the commercialisation journey of medicinal products which is performed typically during Phase 3 clinical trials. Cell and gene therapy process validation is not dissimilar to that of biopharma products and it includes thorough assessment of the equipment, facility (cleanrooms), materials and analytical methods to ensure that product quality is safeguarded. However, cell and gene therapies are associated with unique challenges due to their higher complexity than biopharma products as well as their relative infancy when compared to biopharma products. Given gene therapies' recent take-off, the cell and gene therapy sector is still working towards developing suitable manufacturing and analytical technologies able to achieve more productive and robust processes. As such, thorough consideration of raw materials' quality and supply chain, as well as process flowsheet and technologies employed, should be carried out early on in process development. This should be done as part of creating manufacturing strategies which include consideration of the potential product demands, and assessments of the economic feasibility of using the selected technologies for commercial manufacture. Performing such analyses and devising such strategies early on may safeguard against needing to carry out process changes later in the drug development pathway which is expensive and could lead to delays to market. This thesis has addressed the topic of process change at various points in the drug development pathway by describing the application of an in house built decisional tool tasked to evaluate the financial consequences of switching from transient transfection to stable producer cell lines. Furthermore, in the context of process design, this thesis also emphasises the impact of switching to scalable cell culture systems on economic metrics in the context of viral vector manufacture.

Preparation for process validation activities is approached commonly using the Quality by Design (QbD) framework which has at its core the thorough and structured understanding of the product and process (Lipsitz et al. 2016). The first step in this framework is identifying the target product profile which contains information on desired characteristics of the product such as indication, likely patient population and identity. Assuming a process development plan is in place and, hence product and process understanding is generated, the critical quality attributes (CQAs) start to be collated. The CQAs of each product are purity, identity, safety and efficacy and, for each of the CQAs to be demonstrated, qualified and validated analytical methods are required. The quality target product profile includes all the analytical methods to be employed as well as the specification ranges that need to be achieved in order to prove that every product CQA has been met. In the context of viral vector production, purity testing typically entails measuring product and process-related impurities, safety testing is performed using sterility, mycoplasma and endotoxin testing while efficacy testing can be done using cell-based assays.

To ensure that the CQAs are always met, the critical process parameters (CPPs) need to be identified. These are parameters which, upon changes in their values, may cause a change in the product CQAs or, in other words, may lead to analytical test results outside of the specification range. Example of process parameters that could be critical are cell culture temperature, pH, production time frame and agitation rate. Process development is instrumental in generating information on the impact of process parameter fluctuations and the design of experiments (DoE) methodology is typically employed so as to generate design spaces and windows of operation (Campbell et al. 2015). Working within the window of operation means that if the critical process parameters fall within a pre-defined range (minimum and maximum value), the product CQAs will be met. A further step in

the QbD pathway is establishing control strategies to ensure that if the process parameters change, these are brought back within the normal operating range (Lipsitz et al. 2016).

Process validation activities include ensuring that the equipment and analytical methods have been qualified and validated by reviewing user requirement specifications and ensuring that design qualification and installation and operational qualification are in place. Furthermore, the equipment needs to have been serviced within its calibration period. Once the equipment is in good shape, the next activities are production of a variable number of engineering batches and finally, three process performance qualification batches. In process control and release testing needs to be show that all the CQAs have been robustly met.

The remainder of this chapter will address the key validation challenges faced by *ex vivo* and *in vivo* gene therapies.

7.2 Validation challenges in cell and gene therapy

One of the most critical process validation challenges associated with gene therapies is process variability and lack of robust and sensitive enough analytical methods availability. Process variability is of crucial concern since the key reason why process validation activities are integrating part of the commercialisation journey is to prove that one can robustly and reproducibly manufacture a product which meets all CQAs namely safety, efficacy, purity and identity.

Common sources of variability between *in vivo* an *ex vivo* gene therapies are the use of biological materials such as viral vectors, plasmid DNA or serum as well as the often constrained process automation levels. In terms of autologous *ex vivo* gene therapies, additional sources of variability are starting material collection procedure and cell quality (patient-health driven), manual processing, formulation and transportation conditions and product administration. For example, in the case of autologous CAR T products, ensuring

process robustness is very challenging due to the inherent variability of the patient's cells as well as the variability in the lentiviral vector preparation. To tackle the variability brought in by patient materials, allogeneic *ex vivo* gene therapies are being developed. However, they also face challenges related to ensuring that no product would lead to graft-versus-host disease. Furthermore, given that commercial manufacturing of autologous CAR T-cells has followed so far a centralised model, transportation conditions as well as the formulation of choice (fresh versus frozen) and product administration tend to add additional variability to the mix. On the other hand, following a bedside manufacturing model would remove the variability coming from transportation and formulation but would likely introduce new sources of variability, rooted in the limited oversight that the sponsor company can exert over hospitals' activity. A decentralised manufacturing approach is likely to cause process validation hurdles since process validation activities would need to be performed for each manufacturing site and each site would need to prove consistent and robust manufacturing, comparable to that of the other sites. It is envisaged that process validation challenges associated with decentralised manufacture will be resolved once fully automated and integrated manufacturing & QC solutions as well as advanced and validated software and data management systems will become widely available on the market. On a biological level, a further source of variability in the *ex vivo* gene therapy product quality is the random integration of the lentiviral vector into patients' cells. As long as viral vectors such as retroviruses and transposone/transposase plasmid DNA systems are used, there will be a risk of insertional tumourigenicity. To circumvent this issue, gene editing tools such as CRISPR-Cas9 which integrate the therapeutic gene to specific genome loci known to be safe, which do not require viral vector delivery, should be developed.

The main cause for variability in lentiviral vector preparations, as mentioned above, tends to be the employment of transient transfection processes which require plasmid DNA

preparations. The process of preparing the transfection mix (plasmid DNA and transfection reagent) which is added to the viral vector cell culture media has been reported to be rather manual, hence a source for introducing further variability. A solution towards diminishing process variability of viral vectors would be the departure from the transient transfection system by implementing stable producer cell lines for manufacturing viral vectors. In terms of AAV preparations, a key process validation challenge is proving consistent removal of product-related impurities such as the empty capsids.

Given the infancy of the sector, products tend to be developed in academic environments which typically use manual intensive processes and R&D-grade materials. Sometimes, the focus is mainly on transitioning the process from an R&D process to a GMP process, with limited consideration given to the commercialisation outlook of that product, and generating clinical data as fast as possible. The consequences of going down that path tend to be that process changes need to be implemented mid-way through the drug development pathway or even post-approval. If mid-way post-approval, the process validation activities are likely intensified, being accompanied by extensive reviews of comparability and additional stability studies. If post-approval, additional to the comparability and stability studies, process validation needs to be repeated altogether.

However, perhaps one of the most stringent process validation challenges that the sector is facing with regards to viral vector manufacture, is the lack of robust qualitative and quantitative analytical methods. As such, viral vector developers are faced with needing to develop orthogonal methods by employing multiple different analytical tests to try and paint a picture of the viral vector quality and quantity as best as they can.

The case studies described in this thesis have addressed some of the process validation topics mentioned above. The consequences of implementing a process change at various

stages in the commercialisation journey have been assessed for a range of gene therapy product types. In additions, the impact of QC automation was analysed in the context of addressing the process validation challenges associated with bedside manufacturing of autologous CAR T-cell therapy.

Chapter 8: Conclusions and future work

8.1 Introduction

This thesis describes the application of an advanced decisional tool designed to answer key questions that developers are currently seeking answers for on the topics of easing supply chain burdens and ensuring financial viability of cell and gene therapy products. Multiple case studies were built with the focus of exploring manufacturing strategy options which would simplify the supply chain of both autologous and off-the-shelf gene therapies as well as minimise running costs via flowsheet selection and process optimisation. In light of the relative immaturity of the industry, this work captured the impact of adopting alternative supply chain models for autologous CAR T-cell manufacture and alternative flowsheets for lentiviral vector manufacture as well as the impact of viral vector process changes at various development stages on financial metrics. Briefly, the impact of the COVID-19 pandemic on the cell and gene therapy sector especially on supply chains was highlighted. Herein, the key contributions of each chapter are summarised and future work that could bring valuable insights on these topics is proposed.

8.2 Key contributions

8.2.1 Manufacturing processes and technologies

As an initial step of the project described by this thesis, an extensive literature review of the manufacturing processes associated with a wide range of cell and gene therapies was performed. The manufacturing processes of the key components of cell and gene therapy products, namely, the cell therapy, viral vector and plasmid DNA are described. **Chapter 2** provides a classification of *ex vivo* gene therapies based on their cell therapy component manufacturing processes. It discusses representative process flowsheets and key technologies, and it analyses the modular versus integrated manufacturing paradigm.

Furthermore, **Chapter 2** describes the key characteristics and process flowsheets of critical viral vectors such as the lentiviral vector (LV) and the adeno-associated virus vector (AAV) and describes alternatives to the transient transfection expression systems. Lastly, a review of the plasmid DNA manufacturing processes is presented. For each component (e.g. cell therapy, viral vector and plasmid DNA), analytical methods considerations are included. **Chapter 2** offers an exhaustive picture of the means to produce cell and gene therapies such as viral vector and non-viral vector-based autologous and allogeneic *ex vivo* gene therapies and viral vector-based *in vivo* gene therapies. The results of this investigation formed part of the foundations for performing the work discussed in this thesis.

8.2.2 CAR T therapy supply chain economics and decision-making at the enterprise level

Chapter 4 provided an analysis of the feasibility and ranking of a range of decentralised enterprise models relative to the centralised manufacture model for commercial manufacture of autologous CAR T-cell therapies employing an integrated end-to-end manufacturing platform. This work focused further on exploring two key gaps associated with bedside manufacture models adopting "GMP-in-a-box" approaches such as the impact of revenue schemes between the sponsor company and the hospital network and the impact of QC automation. The specific focus on the feasibility of "GMP-in-a-box" manufacturing models from a profitability perspective and the assessment of QC automation options in this context have not been reported so far in literature.

Whilst the impact of the number of manufacturing sites on profitability had been documented already, there is no published account of an assessment of the critical number of sites associated with different types of decentralised models that we are aware of. This work explored the minimum and maximum number of sites for each model type

accounting for constraints related to maximum number of manufacturing platforms that can be run reliably per site and profitability metrics when compared to the centralised model. Based on the assumptions adopted, it was found that 2-4, 10-20 and 20-40 manufacturing sites would meet the set feasibility criteria for the decentralised models at 1,000, 5,000 and 10,000 doses/year, respectively. Furthermore, the tool predicted that one centralised facility generating 5,000 doses/year using an integrated end-to-end manufacturing platform solution would unlikely be feasible from a shop-floor logistics point of view due to the large number of ballrooms associated with it. At 5,000 doses/year and above, it is proposed that at least two facilities should be run so as to decrease risk.

In terms of the ranking of the enterprise models from profitability and investment perspectives, the decisional tool predicted that the bedside manufacturing models would be more attractive than the regional model, which was found slightly more attractive than the centralised model. Amongst the bedside models, the rented hospital model relying on sponsor company's operators to manufacture patients' therapies in the hospital site cleanrooms' was the most attractive model. This was followed by the "GMP-in-a-box" models, in which it was assumed that the hospital staff would perform manufacture and QC activities within the CNC environment of hospital sites. However, it was found that if the revenue share scheme relied on a fixed revenue share percentage, the "GMP-in-a-box" model was only attractive at low selling prices.

The dependency on selling price identified in the case of the "GMP-in-a-box" model was further explored to identify critical fixed revenue share percentage values which would ensure that this model would be associated with a superior profitability level when compared to the centralised/regional model. Furthermore, since one of the key requirements quoted by the industry as being paramount for the adoption of bedside

manufacture models is QC automation, the tool explored the impact of automation of process control activities on COG and profitability.

This study showed that decentralisation of autologous CAR T manufacture may be viable depending on the number of sites established and confirmed that it is the route forwards at very large demands. Furthermore, it explored the bedside manufacture route by analysing the impact of agreements amongst stakeholders as well as the impact of introducing automated, more expensive QC equipment.

The user cases of the CAR T-cell therapy decisional tool are determining the most cost-effective CAR T therapy manufacturing flowsheets and technologies (either for autologous or allogeneic approaches but not *in vivo* CAR T approaches), as described in Pereira Chilima (2019) and Jenkins et al. (2018). It can also be used to identify the most suitable manufacturing strategy i.e. exploring the investment & profitability of scenarios beyond those analysed in this thesis e.g. CMO versus hotel manufacturing model versus academic institution manufacturing model. Furthermore, it can be used for exploring different routes to lowering COG/dose as well as modelling different process types such as gene-modified HSC cell therapy processes and others.

In terms of limitations, this tool does not include a model for determining the cost of drug development. Moreover, it is not suitable for performing extensive capacity planning analyses. For example, the model does not exploit fully the advantages of modular manufacturing over those of the integrated manufacturing approach from a manufacturing capacity point of view.

8.2.3 Lentiviral vector process economics: an upstream processing appraisal

Chapter 5 addressed a specific component of the autologous *ex vivo* gene therapies supply chain, the viral vector manufacture component. A decisional tool was created so as to compare multiple GMP-grade cell culture technologies used in lentiviral vector manufacture, either run in adherent or suspension mode, from a cost of goods (COG_{LV}/dose) perspective, in a range of product scenarios. Cost breakdowns were discussed so as to provide explanation to the rankings achieved. Sensitivity analyses were run to capture impact of fluctuations in parameter values. Target harvest titre values were generated and discussed in the context of minimising lentiviral vector contributions to autologous *ex vivo* gene therapies. A brief impact analysis of switching away from transient transfection to a stable producer cell line was also given.

The deterministic analysis of the COG_{LV}/dose revealed that the single-use stirred tank bioreactor (STR) run in suspension mode provided the highest cost reduction, followed by the fixed bed bioreactor and rocking motion bioreactor run with microcarriers. Switching to any of these technologies predicted ~90% cost reductions when compared to the 10-layer vessel process. COG_{LV}/dose breakdown in terms of raw materials, labour, indirect and QC costs were generated so as to explain the ranking achieved between cell culture options. Labour and indirect costs were found to dominate at low manufacturing scales and raw material costs prevailed with increase in manufacturing scale. This exercise revealed the cost drivers, one of which being plasmid DNA cost, and, a sensitivity analysis was performed to assess the impact of assumption changes on COG_{LV}/dose. Furthermore, a range of product types associated with different dose size and process performance was investigated in terms of identifying the most cost-effective cell culture option. Whilst this confirmed the previous ranking achieved in the deterministic exercise, it also informed on the COG_{LV}/dose levels for each scenario, the

manufacturing scales required as well as scenarios where existing cell culture technologies would not be feasible to meet demand.

The tool was then tasked to identify the target harvest titre values which enabled substantial cost reductions of lentiviral vector in the case of three different product types. This exercise revealed that 10-fold to 100-fold increases harvest titre were required to reduce the COG_{LV}/dose to under $1,000 and $10,000, respectively, depending on LV dose and cell culture technology.

The impact of changing core assumptions on productivity achieved with the fixed-bed bioreactor was captured by assessing the ranking when the productivity of the fixed-bed was as high as that of the STR run in suspension mode. This was found to favour the fixed bed bioreactor route. The constraints of transient transfection in a fixed bed bioreactor were raised and a discussion of the impact of switching to a stable producer cell line on COG_{LV}/dose was provided. In the context of a producer cell line scenario, given that plasmid DNA has a high cost contribution to the STR process, when removing this cost, the latter was found to be as attractive as the fixed bed route, despite matched productivity levels.

This work demonstrated the superior cost-benefit of adopting scalable processes for lentiviral vector manufacture. Further to this, it represents an example of a decisional tool application which analyses technology trade-offs and generates useful data to serve as input to designing process development and manufacturing strategies.

8.2.4 Gene therapy process change evaluation framework: transient transfection and stable producer cell line comparison

Since **Chapter 5** identified plasmid DNA cost to have a high contribution to large scale viral vector manufacturing costs, **Chapter 6** provided an analysis of the trade-offs associated with switching from transient transfection to a stable producer cell line system

at different stages in the viral vector drug development pathway. While transient transfection is associated with a relatively short process development time frame assuming that a GMP-grade cell bank is in place, the running costs are high due to costly GMP-grade plasmid DNA requirement. On the other hand, developing a SPCL system is time consuming and costly and could lead to delays to market, but once established, it leads to lower running costs due to removal of the plasmid DNA requirement. This trade-off was characterised in the context of four gene therapy products, by capturing the ranking between the transient transfection and process change scenarios from a cost of drug development, project lifecycle cost and profitability perspectives. Critical plasmid DNA price levels that altered the profitability ranking were identified and conditions favouring switching early to SPCL were characterised.

From a cost of drug development and project lifecycle cost perspective, switching to SPCL early was found to be the most favourable option, more favourable than transient transfection, while switching late was found to be the least favourable for most gene therapy product types. For products with very low plasmid DNA cost contribution to $COG_{overall}$/dose (e.g. CAR T), no significant differences were identified between transient transfection and the SPCL scenarios.

From a profitability perspective, however, no significant differences between transient transfection and switching early to SPCL scenarios were identified when assuming that the early switch to SPCL did not lead to delays to market. Furthermore, if a delay to market was associated with the early switch to SPCL scenario, the tool predicted that the transient transfection was the most attractive, and as attractive as switching to SPCL post-approval for most product types. However, for products with very high plasmid DNA cost contribution to $COG_{overall}$/dose (e.g. $LV_{\textit{in vivo}}$), switching early to SPCL was significantly

more attractive than transient transfection in a no delay to market scenario, and as attractive, in a delay to market scenario.

The impact of various price levels of GMP-grade plasmid DNA was also assessed and critical price values which changed the ranking between transient transfection and switching to SPCL early were identified. For products such as HSC_{LV} or AAV products, this exercise revealed that price points within the industry reported plasmid DNA price range can significantly favour the early switch to SPCL, even when delays to market would be experienced with this route. However, for products associated with even larger plasmid DNA cost contributions (e.g. $LV_{in\ vivo}$), a significant drop in plasmid DNA price levels would be required, lower than the currently lowest reported price point.

Apart from lower running costs due to absence of plasmid DNA, another potential advantage of SPCL was captured here, that of achieving higher harvest titre levels relative to transient transfection. The tool was tasked to compare transient transfection where pDNA cost increased from $60,000 to $600,000/g to switching to SPCL early, where up to 50-fold higher titres and decreases in delay to market were assumed to be possible. As such, the conditions favouring switching to SPCL early over sticking to transient transfection were mapped out from COG_{VV}/dose, cost of viral vector drug development savings as well as profitability perspectives.

This work demonstrated the application of a comprehensive gene therapy process change framework which included cost of goods, cost of drug development, project lifecycle and profitability metrics assessments. This was used to analyse holistically the financial consequences of changing from transient transfection to a stable producer cell line system, and it can be used to address other industry-relevant process change questions.

8.2.5 Overall models' contributions

The decisional tools employed in this work were an autologous CAR T-cell therapy tool, and a novel gene therapy process change evaluation tool, developed as part of this work. The autologous CAR T-cell therapy decisional tool, previously described, consisting of a whole bioprocess economics model computing COG and fixed capital investment (FCI) and a project valuation model, was used to generate new insights on the supply chain economics of alternative options to centralised manufacture (**Chapter 4**). On the other hand, the novel gene therapy process evaluation tool, described in **Chapter 3**, consisted of a whole bioprocess economics model computing viral vector COG and FCI, a cost of drug development model and a process valuation model. This tool enabled the identification of the optimal cell culture technology and target process performance (**Chapter 5**) for viral vector manufacture and it facilitated the impact analysis of process changes on financial metrics for a variety of cell and gene therapy product types (**Chapter 6**).

8.3 Future work

8.3.1 CAR T therapy supply chain economics and decision-making at the enterprise level

Chapter 4 presented a feasibility study of the manufacturing strategy associated with a range of decentralised models from the perspective of profitability levels relative to the centralised model and that of shop-floor logistics. However, this study assumed a steady flow of demand and hence maximised resource utilisation levels, regardless of model type (centralised or decentralised), which is not realistic for autologous CAR T-cell therapies. Instead, since the starting material in the autologous CAR T process belongs to the patient, fluctuations in patient demands will affect capacity utilisation and hence advanced resource planning is paramount to avoid facility underutilisation levels. A tool

which is employed typically in addressing capacity planning problems, and could be employed here, is the discrete event simulation methodology (DES). DES platforms contain libraries of predefined codes assembled in blocks so as to reproduce simple operations within a dynamic environment such as time delays, uncertainty and mathematical calculations modules. Complex models with input parameters under uncertainty can be built using activity, queuing and resource blocks making this tool highly versatile. Historically, DES models were developed for case studies on portfolio selection, facility capacity optimisation, facility fit of legacy facilities, process synthesis and facility design for existing technologies. As such, DES models can be used to create in silico replicas of operational manufacturing facilities allowing modelling of fluctuating patient demands, impact of delays, resource constraints or batch and equipment failures. The key outputs are resource requirements under patient demand uncertainty and needle-to-needle durations (turn-around time) in a variety of scenarios which can help decision-makers design optimal manufacturing strategies. The development of such tool was initiated as part of this project with the aim of exploring the capacity planning problems associated with centralised autologous CAR T-like product manufacture. The objectives were to investigate the impact of modular versus integrated end-to-end manufacturing, fresh-versus-frozen logistics and scheduling impact on resource utilisation. The following paragraphs will describe the work done on this topic throughout this project as well as indicate the future work that should be employed to consolidate it.

Initially, a DES model (V.1) was built to explore the impact of modular versus integrated end-to-end manufacturing, where two flowsheets were analysed in the context of fresh-in logistics and ball-room manufacture. The integrated end-to-end manufacturing flowsheet employed one single system similar to the Prodigy® (Miltenyi). On the other hand, the modular manufacturing flowsheet assumed the utilisation of 2 systems: one similar to the Prodigy (Miltenyi) for all steps other than the expansion step and a rocking

motion cell culture solution such as the Wave® (Cytiva) for the expansion step. An overview of this initial model using the modular flowsheet can be seen in **Figure 8.1**. The key question addressed here was how many equipment units were required for each flowsheet in a fixed demand context. The results of this initial analysis predicted that the modular flowsheet required approximately a three-fold lower number of Prodigy-like units than the integrated flowsheet (data not shown). The reason behind this result is that in the modular scenario, the Prodigy-like instruments were utilised for performing relatively quick steps, hence these instruments were released quickly to enable processing of new batches. On the other hand, in the case of the integrated end-to-end flowsheet, the Prodigy-like instruments were 'locked in' for extensive periods of time due to the lengthy expansion step, requiring additional instruments to process new batches. Furthermore and in line with the point raised above, the tool predicted that if the expansion duration decreased, significant reductions in the Prodigy-like equipment numbers could be achieved in the case of the integrated end-to-end flowsheet (data not shown).

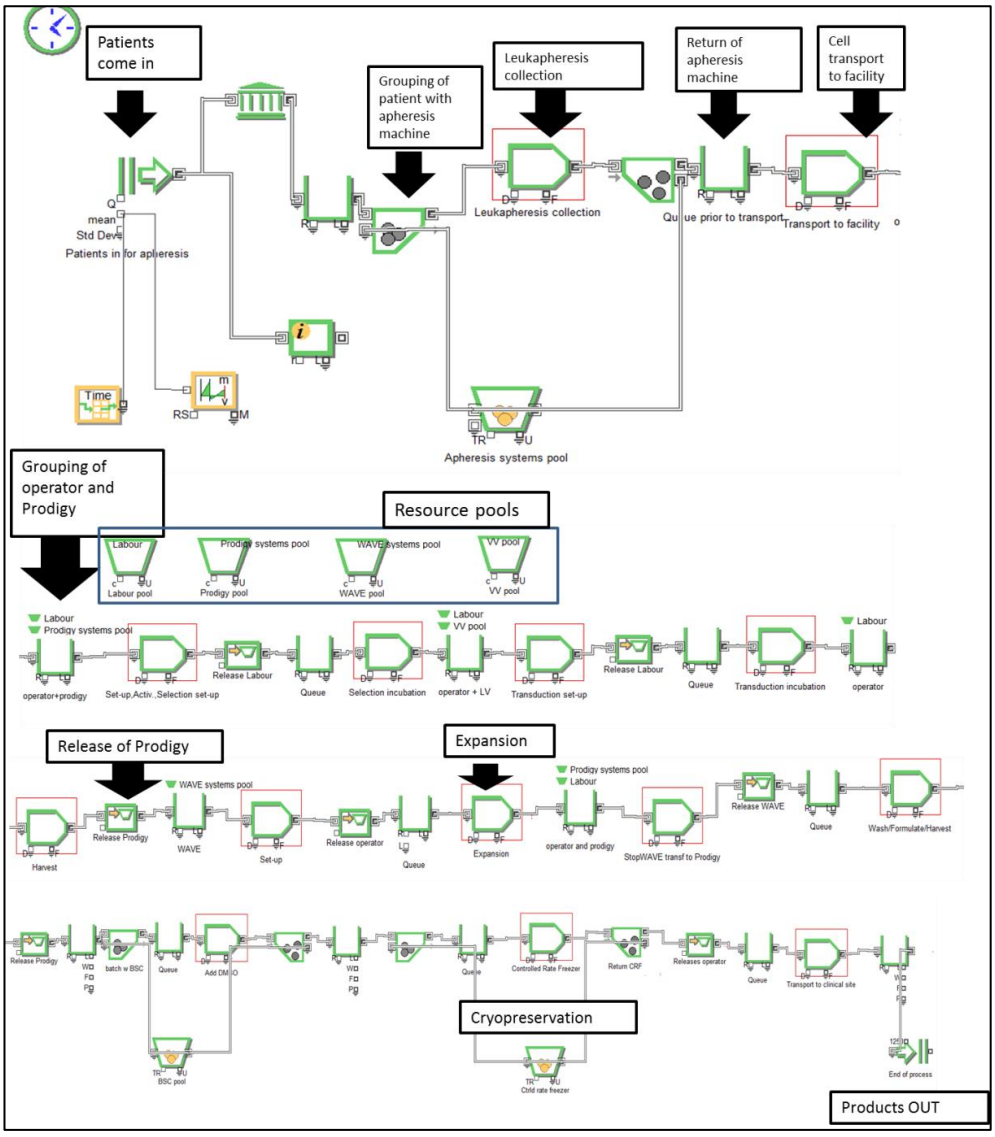

Figure 8.1 Overview of the initial V.1 DES model employing a modular flowsheet using the rocking-motion bioreactor (e.g. Wave-like) for the expansion stage and the integrated USP/DSP equipment (e.g. Prodigy-like) for all the other steps other than the cryopreservation step. This model was built in a linear fashion, by connecting processing blocks in the sequence dictated by the flowsheet.

This model, however, was crude in the sense of not capturing key activities such as operator gowning activities or any in process control and release testing. Furthermore, the model was constrained to "fresh in" logistics, including leukapheresis activities.

As such, a version 2 model was built based on an updated integrated end-to-end flowsheet which excluded leukapheresis activities, assumed "frozen in" logistics and comprised production and QC labour requirements, in process control and release testing activities.

The key question addressed here was how to best schedule manufacturing so as to maximise labour and equipment utilisation while minimising needle-to-needle (turnaround) time. Specifically, the questions addressed here were: what is the impact of staggering the batch start times versus grouping batches and starting them at the same time on resource requirements and what is the impact of batching versus not batching QC tests on resource requirements.

To enable modelling the impact of grouping batches during processing in a scenario in which batches would be started at different time points (staggered approach), the need to departure from the linear modelling approach adopted in V.1 became obvious. The V.2 model was built by connecting a number of different block sequences. Each block sequence represented either one processing step or multiple processing steps which had the same resource and time requirements (**Figure 8.2**). As such, one batch would pass through all the block sequences of the model, and in certain situations multiple times through the same block sequence, as dictated by the flowsheet, in order to reach drug product status. To implement this system, each batch was assigned a parameter at the beginning of the process. As the batch progressed from one processing step (block sequence) to the next, this parameter's value was increased by one unit. To ensure that each batch followed the established flowsheet, logic gates were implemented which directed each batch to the appropriate block sequence of the model depending on the batch's parameter value. Checkpoints were introduced at various points of the model to verify that all batches followed the steps as dictated by the flowsheet. Furthermore, each batch was assigned another parameter which counted the total time spent during processing i.e. the turn-around time (from thaw to the point after the drug product gets cryopreserved). The fluctuation in this value was assessed in the context of grouping batches, varying resource availability and changing schedules.

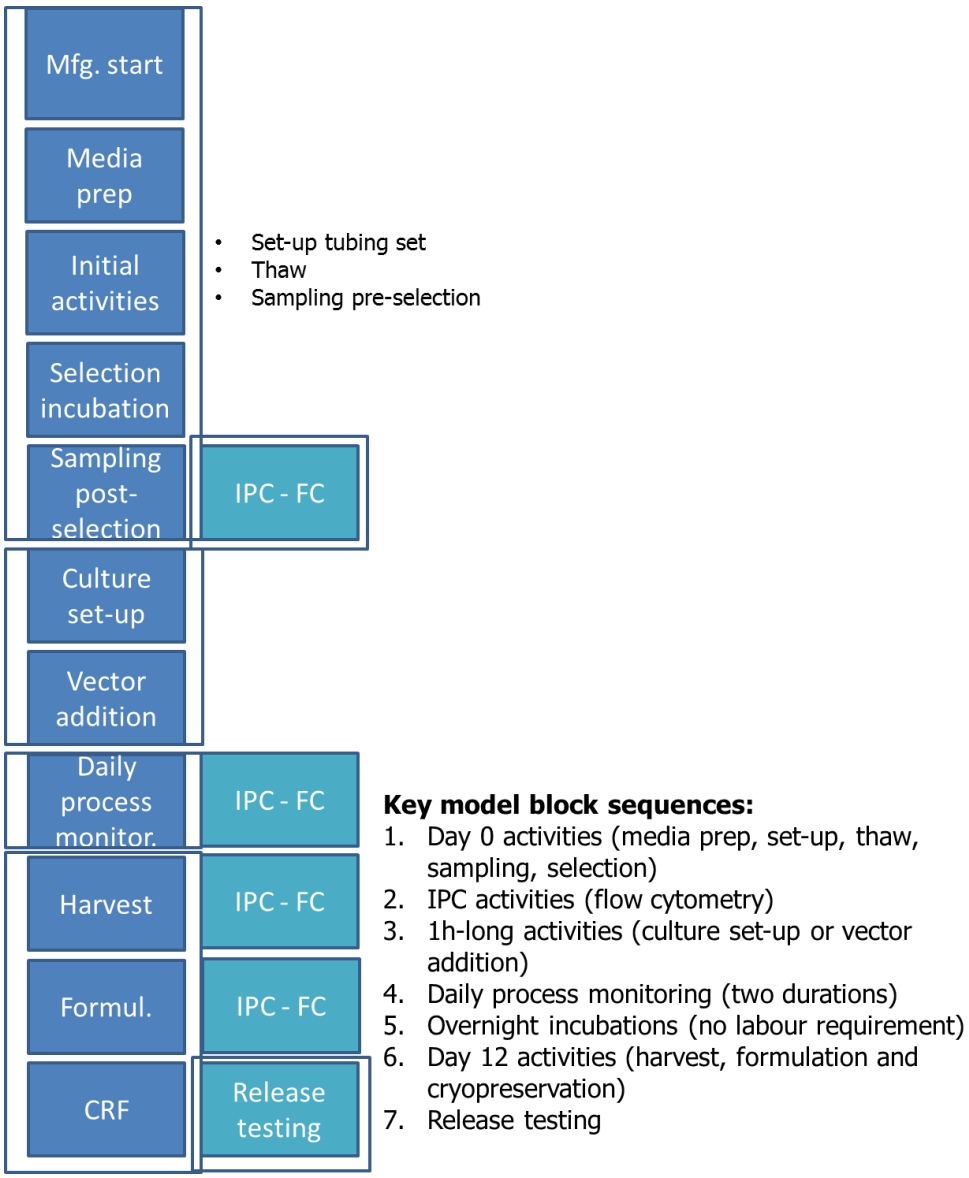

Figure 8.2 Flowsheet modelled in version 2 DES model showing the steps requiring labour intervention in blue and the QC steps in turquoise. The key model block sequences created are listed on the right hand side. Mfg = manufacturing, IPC = in-process control, FC = flow cytometry, CRF = control rate freezer.

In terms of the impact of batch manufacture scheduling on resource requirement, **Figure 8.3** shows the resource requirements outputs when the model was run using a range of different schedules. Furthermore, it shows how the number of flow cytometer equipment units changes upon assuming that multiple tests can occur at the same time. No resource constraints were applied here.

This exercise confirms that spreading out manufacturing evenly across each day leads to the lowest resource requirements, as opposed to starting batches every other day and close

together rather than evenly apart. Starting manufacture every eight hours was found to lead to the lowest resource requirements with only 7 operators being needed for activities in the cleanroom, 39 INT units, 9 QC operators and 11 or 10 flow cytometer units depending on QC batching strategy (**Figure 8.3**). On the other hand, the QC batching strategy was found to have a limited effect on decreasing the number of flow cytometer requirement in this schedule scenario, but enabled significant decreases in the case of the other schedules tested (**Figure 8.3**).

	Starting mfg every	One QC sample at a time				QC batching *,**			
		#Op.	#INT.	#QCs	#Cyto.	#Op.	#INT.	#QCs	#Cyto.
1.1	2h daily (3/day) [1]	12	39	10	20	12	39	10	13
1.2	8h daily (3/day) [1]	7	39	9	11	7	39	9	10
2	3 at once daily [1]	15	39	13	20	15	39	9	10
3.1	Other day, 2 at once, every 2h [2]	16	42	15	32	16	42	10	17
3.2	Other day, 2 at once, every 8h [2]	10	42	14	16	10	42	8	10

Figure 8.3 Impact of scheduling and QC test batching (in process control, flow cytometry assays) on resource requirements at a demand of 1,000 patients/year. The orange rows indicate starting batches a couple of hours apart rather than starting them all at once while the yellow row indicates grouping batches and starting them all at the same time. The number of operators indicates how many people should be available to perform manufacturing activities at any time. Mfg = manufacturing, # = number, Op.= operator, INT = integrated USP/DSP system, QCs = QC operators, Cyto. = flow cytometer, PCR = PCR machine e.g. Quantum studio, Bact. = Bactec slots (automated sterility testing equipment).[1] assumes that 2-3 samples can be grouped and tested at the same time, [2] assumes that 4-6 samples can be grouped for testing (above 4, two different flow cytometer runs were assumed as up to four samples were allowed to be processed per test run). *No additional time has been associated with handling multiple samples at the same time in terms of sample prep and read out time; **Only the cytometry tests occurring in parallel to process flow were grouped.

To put these results into perspective, the decisional tool used in **Chapter 4** outputs similar results in terms of resource requirements to the DES V.2 model, however it slightly under-

estimates the number of INT units since it assumes maximised utilisation (i.e. 31 units predicted by the static model, data not shown, versus 39 units selected by the DES model).

As it currently stands, the DES tool can be used to capture the impact of resource constraints or fluctuating patient demand on batch turn-around time and resource requirements. Furthermore, it can be adapted to study extensively the impact of "fresh in" versus "frozen in" logistics, provide input towards capacity ramp-up strategies and can be expanded to study decentralised manufacturing options in relation to the centralised paradigm.

This tool could be developed further to have a user interface. For instance, the current dashboard (not shown) with key inputs and outputs can be further improved to enable new users to utilise the model. However, more complex updates are required to optimise the model for a faster execution time. This methodology is particularly powerful when it comes to modelling autologous cell therapy process where demand uncertainty is in the picture; it is less useful when it comes to modelling allogeneic processes.

Another topic that **Chapter 4** tackled was automation of QC activities as an avenue towards enabling bedside manufacturing options. The strategy adopted here was to test the impact of higher QC equipment cost and higher associated tubing set costs on COG/dose assuming a range of labour reduction levels achieved by implementing this QC automation. This relied on the sector to make such equipment available rather than the sponsor company investing in developing a bespoke automated equipment solution. Another strategy that could be explored to assess the impact of automation implementation would be assuming that the Sponsor company could develop a bespoke equipment solution in house. In such scenario, a range of development costs and timelines could be tested to assess the impact on COG/dose and profitability if the bespoke system

could lead to pre-defined cost reductions at labour as well as raw material or equipment level.

8.3.2 Lentiviral vector process economics: an upstream processing appraisal

Chapter 5 compared a range of cell culture technologies including the suspension STR option, used in the manufacture of LV products, from a cost of goods perspective. However, the STR option was assumed to be run in batch mode. Since perfusion processes offer advantages in terms of throughput and cost reductions in the case of biopharma products manufacture, it may represent an attractive candidate for viral vector manufacture. However, lentiviral vectors manufacture is associated with stark declines in cell viability levels post-transfection. Furthermore, challenges in finding scalable cell retention system solutions which do not compromise LV yields were flagged. On the other hand, since LV stability levels are poor at room temperature, systems which could quickly transfer it into more favourable conditions and quickly push it through to further processing would be ideal. Therefore, analyses of the trade-offs associated with slightly longer production windows, yield losses over the cell retention device and larger media consumption versus higher total number of transducing units (TU) achieved per run are proposed. To further aid process development strategy decision-makers, the tool could be adapted to identify the minimum TU output gains that would justify investing in a change from batch to semi-continuous cell culture process.

Chapter 5 only focused on capturing the cost differences between cell culture options. However, another analysis that could be run so as to provide operational metrics in addition to the financial metrics, would be assessing the performance of the cell culture technologies from a process robustness perspective. As such, Monte Carlo analysis could be performed to analyse which technologies would be associated with the lowest impact on COG_{LV}/dose upon applying fluctuations in harvest titre. In this context, the ranking

between technologies could then be analysed holistically from both financial and operational parameter perspectives using multi-attribute-decision making (MADM) methodology.

The focus of **Chapter 5** was purely on upstream processing trade-offs. Downstream processing trade-offs should also be explored, especially since the LV process yields are known to be particularly low in comparison to other viral vector manufacturing processes. High step yields were reported using new chromatographic technologies (e.g. nanofibers), however these likely come at a premium price. As such, the cost metrics achieved when adopting a new more expensive chromatography technology which leads to higher step yields should be compared to the cost metrics achieved with the current process. Target step yield improvements could be identified to justify utilisation of a more expensive chromatography solution. Furthermore, the impact of developing a bespoke chromatography solution for LV, in house, which could deliver significant yield increases, could be explored.

This tool, as well as the CAR T decisional tool used in this work, can be turned into an user-friendly tool by building a user interface. With further work, the viral vector tool can be adapted to model mRNA/LNP manufacturing processes since the manufacturing flowsheet of these therapeutics shares some key unit operations with the flowsheet of viral vectors (i.e. UF/DF and chromatography steps). An example of a change required to adapt the model would be that the cell culture step would be replaced by a cell-free unit operation where in vitro transcription (IVT) takes place using a processed pDNA template and enzymes in a similar vessel to a bioreactor.

On the other hand, an adaptation to model DNA synthesis approaches such as aptamers manufacture (known as chemical antibodies) as biomolecular therapeutics would require more effort as the manufacturing process is very different from that of viral vectors

(Daniels et al. 2021). Even so, the tool provides a comprehensive framework that can be implemented by industry players for a wide range of applications in whichever formats they feel most comfortable. The structure, composition and application of the viral vector decisional tool is described in **Chapter 3** and **Chapter 5 & 6.**

8.3.3 Gene therapy process change evaluation framework: transient transfection and stable producer cell line comparison

Chapter 6 focused on two advantages of moving away from transient transfection and towards stable producer cell line systems, namely the removal of the plasmid DNA requirement and the possibility of achieving higher harvest titres. Another advantage of the SPCL system that could be captured in future work is superior process robustness. Monte Carlo analysis could be performed to assess the impact of differences in process robustness levels between the two expression systems. The resulting operational metrics as well as the financial metrics generated in **Chapter 6** could be used to provide an even more holistic comparison between the two systems by running a MADM analysis.

Other scenarios could be tested using the decisional tool and compared to those addressed in the work described in **Chapter 6.** An example of such scenario could be that in which both a transient transfection process and a stable producer cell line were developed in parallel. The intention here would be to start Phase 1 clinical trial with the transient transfection process to ensure speed to clinic, and then switch to the SPCL process for Phase 2 clinical trial manufacture. Such scenario could be associated with robust comparability chances and could eliminate delays to market.

An alternative to the stable producer cell line system that could be explored in future work is the stable packaging cell line system. The advantages of such system are the potential to use the same cell line to produce multiple viral vector products, and the reduced plasmid DNA requirement relative to the transient transfection route. Whilst **Chapter 6**

briefly touches on this topic, a thorough assessment of the packaging route is proposed. Some of the topics that should be investigated to enable this assessment would be the development timelines and efforts to develop a packaging cell line as well as the realistic number of products that could be produced using one such cell line. Furthermore, the impact of switching from one product to another on development timelines and costs, as well as the realistic plasmid DNA cost reduction should be characterised.

This thesis revealed new insights on the supply chain economics of autologous CAR T-cell therapies at an enterprise-level, building on previous work published in this space. It described the first account of bioprocess economics analysis for lentiviral vectors and the first exhaustive process change analysis for cell and gene therapy products. The future work proposed herein will help decision-makers to better plan their manufacturing strategies so as to maximise resource utilisation when operating under demand uncertainty and optimise process performance in the context of low yielding viral vector manufacture. Furthermore, it will help decision-makers confidently reach ‘go/no go’ decision points in a timely fashion with regards to introducing process changes so as to minimise financial losses. The development of more complex yet user-friendly cell and gene therapy decisional tools will support the industry navigate the translation journey more efficiently from a financial and timelines perspective. As a result, this will increase the chances of commercial viability and enable highly efficacious products to reach patients.

References

Abina, S. H.-B., et al. 2015. Outcomes following gene therapy in patients with severe wiskott-aldrich syndrome. *JAMA,* 313**,** pp. 1550-1563.

Abou-El-Enein, M., et al. 2013. Good manufacturing practices (gmp) manufacturing of advanced therapy medicinal products: A novel tailored model for optimizing performance and estimating costs. *Cytotherapy,* 15**,** pp. 362-383.

Adair, J. E., et al. 2016. Semi-automated closed system manufacturing of lentivirus gene-modified haematopoietic stem cells for gene therapy. *Nature communications,* 7**,** pp. 1-10.

Adams, B., et al. 2020. Moving from the bench towards a large scale, industrial platform process for adeno-associated viral vector purification. *Biotechnology and bioengineering,* 117**,** pp. 3199-3211.

Ahmed, N., et al. 2015. Human epidermal growth factor receptor 2 (her2)–specific chimeric antigen receptor–modified t cells for the immunotherapy of her2-positive sarcoma. *Journal of clinical oncology,* 33**,** pp. 1688.

Aiuti, A., et al. 2013. Lentiviral hematopoietic stem cell gene therapy in patients with wiskott-aldrich syndrome. *Science,* 341**,** pp. 1233151.

Aiuti, A., et al. 2009a. Hematopoietic stem cell gene therapy for adenosine deaminase deficient-scid. *Immunol Res,* 44**,** pp. 150-159.

Aiuti, A., et al. 2009b. Gene therapy for immunodeficiency due to adenosine deaminase deficiency. *N Engl J Med,* 360**,** pp. 447-458.

Aiuti, A., et al. 2017. Gene therapy for ada-scid, the first marketing approval of an ex vivo gene therapy in europe: Paving the road for the next generation of advanced therapy medicinal products. *EMBO Molecular Medicine,* 9**,** pp. 737-740.

Aleksandrova, K., et al. 2019. Functionality and cell senescence of cd4/cd8-selected cd20 car t cells manufactured using the automated clinimacs prodigy® platform. *Transfusion Medicine and Hemotherapy,* 46**,** pp. 47-54.

Alhakamy, N. A., et al. 2021. The era of gene therapy: From preclinical development to clinical application. *Drug discovery today***,** pp.

Allay, J. A., et al. 2011. Good manufacturing practice production of self-complementary serotype 8 adeno-associated viral vector for a hemophilia b clinical trial. *Human gene therapy,* 22**,** pp. 595-604.

Allen, E. S., et al. 2017. Autologous lymphapheresis for the production of chimeric antigen receptor t cells. *Transfusion,* 57**,** pp. 1133-1141.

Alton, E. W., et al. 2017. Preparation for a first-in-man lentivirus trial in patients with cystic fibrosis. *Thorax,* 72**,** pp. 137-147.

Alton, E. W. F. W., et al. 2020. Lentiviral vectors. Google Patents.

Alzubi, J., et al. 2021. Automated generation of gene-edited car t cells at clinical scale. *Molecular Therapy-Methods & Clinical Development,* 20**,** pp. 379-388.

Ansorge, S. 2010. *Development of a scalable process for lentiviral vector mass production by transient transfection.* École Polytechnique de Montréal.

Ansorge, S., et al. 2010. Recent progress in lentiviral vector mass production. *Biochemical Engineering Journal,* 48**,** pp. 362-377.

Aponte-Ubillus, J. J., et al. 2018. Molecular design for recombinant adeno-associated virus (raav) vector production. *Appl Microbiol Biotechnol,* 102**,** pp. 1045-1054.

Aranda, F., et al. 2015. Trial watch: Adoptive cell transfer for oncological indications. *Oncoimmunology,* 4**,** pp. e1046673.

Ardeshna, K., et al. 2018. Study of auto3, the first bicistronic chimeric antigen receptor (car) targeting cd19 and cd22, followed by anti-pd1 consolidation in patients with relapsed/refractory (r/r) diffuse large b cell lymphoma (dlbcl): Alexander study. *Blood,* 132**,** pp. 1679-1679.

Arm. 2020. *2020: Growth & resilience in regenerative medicine annual report* [Online]. Alliance for Regenerative Medicine. Available: https://alliancerm.org/sector-report/2020-annual-report/.

Arm. 2021. *Regenerative medicine in 2021: A year of firsts and records* [Online]. Alliance for Regenerative Medicine. Available: http://alliancerm.org/wp-content/uploads/2021/08/ARM-H1-2021-Report.pdf.

Atchison, R. W., et al. 1965. Adenovirus-associated defective virus particles. *Science,* 149**,** pp. 754-756.

Ausubel, L. J., et al. 2012a. Production of cGMP-grade lentiviral vectors. *BioProcess International,* 10**,** pp. 32-43.

Avramescu, A., et al. A multi-objective multi-type facility location problem for the delivery of personalised medicine. EvoApplications: International Conference on the Applications of Evolutionary Computation, 2021.

Ball, O., et al. 2018. Bioprocessing automation in cell therapy manufacturing: Outcomes of special interest group automation workshop. *Cytotherapy,* 20**,** pp. 592-599.

Bandeira, V., et al. 2012. Downstream processing of lentiviral vectors: Releasing bottlenecks. *Hum Gene Ther Methods,* 23**,** pp. 255-263.

Barczak, W., et al. 2015. Universal real-time pcr-based assay for lentiviral titration. *Molecular biotechnology,* 57**,** pp. 195-200.

Basu, P., et al. 2008. Analysis of manufacturing costs in pharmaceutical companies. *Journal of Pharmaceutical Innovation,* 3**,** pp. 30-40.

Baudequin, T., et al. 2021. Objectives, benefits and challenges of bioreactor systems for the clinical-scale expansion of t lymphocyte cells. *Biotechnology Advances***,** pp. 107735.

Bauler, M., et al. 2020. Production of lentiviral vectors using suspension cells grown in serum-free media. *Molecular Therapy-Methods & Clinical Development,* 17**,** pp. 58-68.

Beatty, G. L., et al. 2014. Mesothelin-specific chimeric antigen receptor mrna-engineered t cells induce antitumor activity in solid malignancies. *Cancer immunology research,* 2**,** pp. 112-120.

Bicudo, E., Brass, I., Carmichael, P. and Farid, S., 2021. The UK's emerging regulatory framework for point-of-care manufacture: insights from a workshop on advanced therapies. *Cell and Gene Therapy Insights, 7*(9), pp.1005-1015.

Biffi, A., et al. 2013. Lentiviral hematopoietic stem cell gene therapy benefits metachromatic leukodystrophy. *Science,* 341**,** pp. 1233158.

Bio, B. 2016. Bluebird bio provides update on lentiglobin™ programs and research and development strategy at gene therapy day. *In:* Bio, B. (ed.). bluebird bio.

Blaeschke, F., et al. 2018. Induction of a central memory and stem cell memory phenotype in functionally active cd4(+) and cd8(+) car t cells produced in an automated good manufacturing practice system for the treatment of cd19(+) acute lymphoblastic leukemia. *Cancer Immunol Immunother,* 67**,** pp. 1053-1066.

Blanche, F., et al. 2005. Method for purifying plasmid dna. Google Patents.

Bogdan, B., et al. 2010. Valuation in life sciences. *Valuation in life sciences.* Springer.

Booth, C., et al. 2016. Treating immunodeficiency through hsc gene therapy. *Trends in molecular medicine,* 22**,** pp. 317-327.

Boudeffa, D., et al. 2019. Towards a scalable purification protocol of galv-tr pseudotyped lentiviral vectors. *Human gene therapy***,** pp.

Brennan, Z. 2021. *Ema begins safety review of bluebird gene therapy following aml case in related therapy* [Online]. Endpoints News. Available: https://endpts.com/ema-begins-safety-review-of-bluebird-gene-therapy-following-aml-case-in-therapy/ [Accessed 19 June 2021 2021].

Brentjens, R. J., et al. 2012. Novel cellular therapies for leukemia: Car-modified t cells targeted to the cd19 antigen. *Hematology Am Soc Hematol Educ Program,* 2012**,** pp. 143-151.

Britten, C. M., et al. 2021. Industrializing engineered autologous t cells as medicines for solid tumours. *Nature reviews Drug discovery***,** pp. 1-13.

Brudno, J. N., et al. 2016. Allogeneic t cells that express an anti-cd19 chimeric antigen receptor induce remissions of b-cell malignancies that progress after allogeneic hematopoietic stem-cell transplantation without causing graft-versus-host disease. *Journal of clinical oncology,* 34**,** pp. 1112.

Bryant, L. M., et al. 2013. Lessons learned from the clinical development and market authorization of glybera. *Human gene therapy Clinical development,* 24**,** pp. 55-64.

Bulcha, J. T., et al. 2021. Viral vector platforms within the gene therapy landscape. *Signal Transduction and Targeted Therapy,* 6**,** pp. 53.

Burnham M, M. A., Wuxi Apptec 2017. Accelerating viral vector manufacturing - introducing the wuxi hyper-pro platform.

Bussow, K. 2015. Stable mammalian producer cell lines for structural biology. *Curr Opin Struct Biol,* 32**,** pp. 81-90.

Cai, Y., et al. 2009. DNA vaccine manufacture: Scale and quality. *Expert Rev Vaccines,* 8**,** pp. 1277-1291.

Cai, Y., et al. 2010. Production of pharmaceutical-grade plasmids at high concentration and high supercoiled percentage. *Vaccine,* 28**,** pp. 2046-2052.

Cameau, E., et al. 2019. Cost modelling comparison of adherent multitrays with suspension and fixed-bed bioreactors for the manufacturing of gene therapy products. *Cell and Gene Therapy Insights,* 5**,** pp. 1663-1674.

Campbell, A., et al. 2015. Concise review: Process development considerations for cell therapy. *Stem cells translational medicine,* 4**,** pp. 1155-1163.

Campochiaro, P. A., et al. 2017. Lentiviral vector gene transfer of endostatin/angiostatin for macular degeneration (gem) study. *Human gene therapy,* 28**,** pp. 99-111.

Carmo, M., et al. 2009. Stabilization of gammaretroviral and lentiviral vectors: From production to gene transfer. *The Journal of Gene Medicine: A cross-disciplinary journal for research on the science of gene transfer and its clinical applications,* 11**,** pp. 670-678.

Carmo, M., et al. 2008. From retroviral vector production to gene transfer: Spontaneous inactivation is caused by loss of reverse transcription capacity. *J Gene Med,* 10**,** pp. 383-391.

Carnes, A. E., et al. 2011. Plasmid DNA fermentation strain and process-specific effects on vector yield, quality, and transgene expression. *Biotechnol Bioeng,* 108**,** pp. 354-363.

Cartier, N., et al. 2009a. Hematopoietic stem cell gene therapy with a lentiviral vector in x-linked adrenoleukodystrophy. *Science,* 326**,** pp. 818-823.

Casucci, M., et al. 2011. Suicide gene therapy to increase the safety of chimeric antigen receptor-redirected t lymphocytes. *J Cancer,* 2**,** pp. 378-382.

Cattoglio, C., et al. 2010. High-definition mapping of retroviral integration sites defines the fate of allogeneic t cells after donor lymphocyte infusion. *PLoS One,* 5**,** pp. e15688.

Cavazzana-Calvo, M., et al. 2010a. Transfusion independence and hmga2 activation after gene therapy of human β-thalassaemia. *Nature,* 467**,** pp. 318.

Cavazzana, M., et al. 2017. Gene therapy for β-hemoglobinopathies. *Molecular Therapy***,** pp.

Cesari M., L. P., Pedregal A. 2017. Cost modeling of upstream production process of lentiviral vectors in hek-293 cells comparing multi-tray 10 stacks and fixed-bed bioreactor. *In:* Sciences, P. L. (ed.). Poster Content as Presented at ESACT 2017.

Chahal, P. S., et al. 2014. Production of adeno-associated virus (aav) serotypes by transient transfection of hek293 cell suspension cultures for gene delivery. *Journal of virological methods,* 196**,** pp. 163-173.

Challener, C. A. 2019. Seeking solutions for large-scale gmp viral vector manufacturing. 32. Available: http://www.biopharminternational.com/seeking-solutions-large-scale-gmp-viral-vector-manufacturing?pageID=3 [Accessed 15 October 2019].

Chen, Y. H., et al. 2020. Rapid lentiviral vector producer cell line generation using a single DNA construct. *Molecular Therapy-Methods & Clinical Development,* 19**,** pp. 47-57.

Chicaybam, L., et al. 2013. An efficient low cost method for gene transfer to t lymphocytes. *PLoS One,* 8**,** pp. e60298.

Chilima, T. D. P., et al. 2018. Impact of allogeneic stem cell manufacturing decisions on cost of goods, process robustness and reimbursement. *Biochemical Engineering Journal,* 137**,** pp. 132-151.

Chilima, T. D. P., et al. 2020. Estimating capital investment and facility footprint in cell therapy facilities. *Biochemical Engineering Journal,* 155**,** pp. 107439.

Chmielewski, M., et al. 2015. Trucks: The fourth generation of cars. *Expert opinion on biological therapy,* 15**,** pp. 1145-1154.

Ciceri, F., et al. 2009. Infusion of suicide-gene-engineered donor lymphocytes after family haploidentical haemopoietic stem-cell transplantation for leukaemia (the tk007 trial): A non-randomised phase i-ii study. *Lancet Oncol,* 10**,** pp. 489-500.

Clarner, P., et al. 2021. Development of a one-step rt-ddpcr method to determine the expression and potency of aav vectors. *Molecular Therapy-Methods & Clinical Development***,** pp.

Cockrell, A. S., et al. 2007. Gene delivery by lentivirus vectors. *Mol Biotechnol,* 36**,** pp. 184-204.

Collaud, F., et al. 2019. Preclinical development of an aav8-hugt1a1 vector for the treatment of crigler-najjar syndrome. *Molecular Therapy-Methods & Clinical Development,* 12**,** pp. 157-174.

Comisel, R.-M., et al. 2021. Lentiviral vector bioprocess economics for cell and gene therapy commercialization. *Biochemical Engineering Journal,* 167**,** pp. 107868.

Costariol, E., et al. 2020. Demonstrating the manufacture of human car-t cells in an automated stirred-tank bioreactor. *Biotechnology Journal,* 15**,** pp. 2000177.

Croyle, M. A., et al. 2004. Pegylation of a vesicular stomatitis virus g pseudotyped lentivirus vector prevents inactivation in serum. *Journal of virology,* 78**,** pp. 912-921.

Cruz, C. R., et al. 2013. Infusion of donor-derived cd19-redirected virus-specific t cells for b-cell malignancies relapsed after allogeneic stem cell transplant: A phase 1 study. *Blood,* 122**,** pp. 2965-2973.

Cytovance. 2020. *An integrated single-use platform for manufacturing plasmid DNA (pdna)* [Online]. Bioprocess online. Available: https://www.bioprocessonline.com/doc/an-integrated-single-use-platform-for-manufacturing-plasmid-dna-pdna-0001 23 June 2021].

Da Silva, J. M., et al. 2021. Decisional tool for cost of goods analysis of bioartificial liver devices for routine clinical use. *Cytotherapy***,** pp.

Daniels, M. and Sanches-Kuiper, R., 2021. Synthetic DNA in Drug Discovery and Development: Evonetix describes DNA synthesizer technology that will speed development across multiple therapeutic modalities. Genetic Engineering & Biotechnology News, 41(9), pp.28-29.

De Ravin, S. S., et al. 2016a. Targeted gene addition in human cd34+ hematopoietic cells for correction of x-linked chronic granulomatous disease. *Nat Biotech,* advance online publication**,** pp.

De Ravin, S. S., et al. 2016b. Lentiviral hematopoietic stem cell gene therapy for x-linked severe combined immunodeficiency. *Sci Transl Med,* 8**,** pp. 335ra357.

De Rooij, J., et al. 2019. Upstream and downstream solutions for aav manufacturing. *Cell Gene Ther Insights,* 5**,** pp. 1017-1029.

De Wilde, S., et al. 2018. Eu decision-making for marketing authorization of advanced therapy medicinal products: A case study. *Drug discovery today,* 23**,** pp. 1328-1333.

Derniame, S., et al. 2014. Multiplex genome editing as a platform for "off-the-shelf" adoptive car t-cell immunotherapies. American Society of Hematology Washington, DC.

Di Stasi, A., et al. 2011. Inducible apoptosis as a safety switch for adoptive cell therapy. *N Engl J Med,* 365**,** pp. 1673-1683.

Digiusto, D. L., et al. 2016. Preclinical development and qualification of zfn-mediated ccr5 disruption in human hematopoietic stem/progenitor cells. *Mol Ther Methods Clin Dev,* 3**,** pp. 16067.

Digiusto, D. L., et al. 2012. Current translational and clinical practices in hematopoietic cell and gene therapy. *Cytotherapy,* 14**,** pp. 775-790.

Digiusto, D. L., et al. 2013. Development of hematopoietic stem cell based gene therapy for hiv-1 infection: Considerations for proof of concept studies and translation to standard medical practice. *Viruses,* 5**,** pp. 2898-2919.

Dull, T., et al. 1998. A third-generation lentivirus vector with a conditional packaging system. *Journal of virology,* 72**,** pp. 8463-8471.

Elsallab, M., et al. 2020. Mitigating deficiencies in evidence during regulatory assessments of advanced therapies: A comparative study with other biologicals. *Molecular Therapy-Methods & Clinical Development,* 18**,** pp. 269-279.

Eon-Duval, A., et al. 2004. Purification of pharmaceutical-grade plasmid DNA by anion-exchange chromatography in an rnase-free process. *Journal of chromatography B,* 804**,** pp. 327-335.

Escors, D., et al. 2010. Lentiviral vectors in gene therapy: Their current status and future potential. *Arch Immunol Ther Exp (Warsz),* 58**,** pp. 107-119.

Esrick, E. B., et al. 2018. Successful hematopoietic stem cell mobilization and apheresis collection using plerixafor alone in sickle cell patients. *Blood advances,* 2**,** pp. 2505-2512.

Farid, S. S. 2012. Evaluating and visualizing the cost-effectiveness and robustness of biopharmaceutical manufacturing strategies. *Biopharmaceutical Production Technology,* 1**,** pp. 717-741.

Farid, S. S., et al. Benchmarking biopharmaceutical process development and manufacturing cost contributions to r&d. Mabs, 2020. Taylor & Francis, 1754999.

Farid, S. S., et al. 2000. A tool for modeling strategic decisions in cell culture manufacturing. *Biotechnology progress,* 16**,** pp. 829-836.

Farid, S. S., et al. 2005. Decision-support tool for assessing biomanufacturing strategies under uncertainty: Stainless steel versus disposable equipment for clinical trial material preparation. *Biotechnology progress,* 21**,** pp. 486-497.

Farsi, M., et al. 2019. A modular hybrid simulation framework for complex manufacturing system design. *Simulation Modelling Practice and Theory,* 94**,** pp. 14-30.
Fda 2017a. Luxturna (voretigene neparvovec-rzyl) intraocular suspension for subretinal injection, package insert.
Fda 2017b. Luxturna package insert. FDA.
Fda 2018a. Kymriah package insert. FDA.
Fda 2018b. Package insert kymriah. FDA.gov: FDA.
Fda 2019a. Packaging insert for zolgensma. FDA.
Fellows, M. R., et al. 2012. Local search: Is brute-force avoidable? *Journal of Computer and System Sciences,* 78**,** pp. 707-719.
Ferreira, M. M. 2018. Cell therapy production moves to factory floor. *Genetic Engineering & Biotechnology News,* 38**,** pp. 1, 16-17.
Ferreira, M. V., et al. 2020. Progress and perspectives in the development of lentiviral vector producer cells. *Biotechnology Journal***,** pp. 2000017.
Ferrua, F., et al. 2019. Lentiviral haemopoietic stem/progenitor cell gene therapy for treatment of wiskott-aldrich syndrome: Interim results of a non-randomised, open-label, phase 1/2 clinical study. *The Lancet Haematology,* 6**,** pp. e239-e253.
Fesnak, A., et al. 2016a. Car-t cell therapies from the transfusion medicine perspective. *Transfusion medicine reviews,* 30**,** pp. 139-145.
Fesnak, A. D., et al. 2016b. Engineered t cells: The promise and challenges of cancer immunotherapy. *Nat Rev Cancer,* 16**,** pp. 566-581.
Fesnak, A. and O'Doherty, U., 2017. Clinical development and manufacture of chimeric antigen receptor t cells and the role of leukapheresis. *Eur. Oncol. Haematol,* 13**,** pp. 28-34.
Fesnak, A. D., et al. 2017. Considerations in t cell therapy product development for b cell leukemia and lymphoma immunotherapy. *Current hematologic malignancy reports,* 12**,** pp. 335-343.
Field, A. C., et al. 2015. Engineered t cell therapies. *Expert Rev Mol Med,* 17**,** pp. e19.
Fischer, S., et al. 2012. Transient recombinant protein expression in a human amniocyte cell line: The cap-t® cell system. *Biotechnology and bioengineering,* 109**,** pp. 2250-2261.
Forsberg N., G. C., Hughes J.V., P. Jaluria, D. King, J. Madsen, A. Moore, J. Nilsson, S. Pettit, S. Pincus, B. Sargent, C. Schwartz, T.L. Tredenick 2018. Key considerations in gene therapy manufacturing for commercialization. *In:* Dish, C. C. (ed.). Cell Culture Dish.
Gao, G., et al. 2004. Clades of adeno-associated viruses are widely disseminated in human tissues. *Journal of virology,* 78**,** pp. 6381.
Garfall, A. L., et al. 2015. Chimeric antigen receptor t cells against cd19 for multiple myeloma. *N Engl J Med,* 373**,** pp. 1040-1047.
Geethakumari, P. R., et al. 2021. Balancing quality, cost, and access during delivery of newer cellular and immunotherapy treatments. *Current hematologic malignancy reports***,** pp. 1-12.
George, E. D., et al. 2008. Strategic biopharmaceutical portfolio development: An analysis of constraint-induced implications. *Biotechnology progress,* 24**,** pp. 698-713.
Geraerts, M., et al. 2005b. Upscaling of lentiviral vector production by tangential flow filtration. *J Gene Med,* 7**,** pp. 1299-1310.
Geraerts, M., et al. 2006. Comparison of lentiviral vector titration methods. *BMC Biotechnol,* 6**,** pp. 34.
Gill, S., et al. 2015. Going viral: Chimeric antigen receptor t-cell therapy for hematological malignancies. *Immunol Rev,* 263**,** pp. 68-89.

Glimm, H., et al. 2000. Human hematopoietic stem cells stimulated to proliferate in vitro lose engraftment potential during their s/g(2)/m transit and do not reenter g(0). *Blood,* 96**,** pp. 4185-4193.
Greene, M. R., et al. 2012. Transduction of human cd34+ repopulating cells with a self-inactivating lentiviral vector for scid-x1 produced at clinical scale by a stable cell line. *Hum Gene Ther Methods,* 23**,** pp. 297-308.
Grieger, J. C., et al. 2016. Production of recombinant adeno-associated virus vectors using suspension hek293 cells and continuous harvest of vector from the culture media for gmp fix and flt1 clinical vector. *Molecular Therapy,* 24**,** pp. 287-297.
Grimm, D., et al. 1998. Novel tools for production and purification of recombinant adenoassociated virus vectors. *Human gene therapy,* 9**,** pp. 2745-2760.
Gruntman, A. M., et al. 2015. Stability and compatibility of recombinant adeno-associated virus under conditions commonly encountered in human gene therapy trials. *Hum Gene Ther Methods,* 26**,** pp. 71-76.
Gutierrez-Guerrero, A., et al. 2020. Lentiviral vector pseudotypes: Precious tools to improve gene modification of hematopoietic cells for research and gene therapy. *Viruses,* 12**,** pp. 1016.
Hacein-Bey-Abina, S., et al. 2008. Insertional oncogenesis in 4 patients after retrovirus-mediated gene therapy of scid-x1. *The Journal of clinical investigation,* 118**,** pp. 3132-3142.
Harrison, C. 2019. First gene therapy for [beta]-thalassemia approved. *Nature Biotechnology,* 37**,** pp. 1102-1104.
Harrison, R., et al. 2016. Au-tomating decentralized manufacturing of cell and gene therapy products. *Cell & Gene Therapy Insights,* 2**,** pp. 115-120.
Harrison, R. P., et al. 2018a. Cell therapy-processing economics: Small-scale microfactories as a stepping stone toward large-scale macrofactories. *Regenerative medicine,* 13**,** pp. 159-173.
Harrison, R. P., et al. 2018b. Centralised versus decentralised manufacturing and the delivery of healthcare products: A united kingdom exemplar. *Cytotherapy,* 20**,** pp. 873-890.
Harrison, R. P., et al. 2017. Decentralized manufacturing of cell and gene therapies: Overcoming challenges and identifying opportunities. *Cytotherapy,* 19**,** pp. 1140-1151.
Harrison, R. P., et al. 2018c. Decentralised manufacturing of cell and gene therapy products: Learning from other healthcare sectors. *Biotechnology Advances,* 36**,** pp. 345-357.
Harrison, R. P., et al. 2019. Chimeric antigen receptor–t cell therapy manufacturing: Modelling the effect of offshore production on aggregate cost of goods. *Cytotherapy,* 21**,** pp. 224-233.
Hartmann, J., et al. 2017. Clinical development of car t cells-challenges and opportunities in translating innovative treatment concepts. *EMBO Mol Med,* 9**,** pp. 1183-1197.
Hassan, N., et al. 2013. *The t cell promise.(2013) european biopharmaceutical review (summer 2013)* [Online]. PDF. Available: http://www.immuno.myzen.co.uk/technology/publications/.
Hassan, S., et al. 2016. Process change evaluation framework for allogeneic cell therapies: Impact on drug development and commercialization. *Regenerative medicine,* 11**,** pp. 287-305.
Hassan, S., et al. 2015. Allogeneic cell therapy bioprocess economics and optimization: Downstream processing decisions. *Regen Med,* 10**,** pp. 591-609.
Haworth, K. G., et al. 2017. Ccr5-edited gene therapies for hiv cure: Closing the door to viral entry. *Cytotherapy***,** pp.

Hebben, M. Pre-industrial manufacturing of lentiviral vectors by transient transfection in single use systems. Spring Meeting of ISBiotech, 2015.
Hein, K., et al. 2020. Inducible aav rep genes. Google Patents.
Hein, K., et al. 2018. Generation of helper virus-free adeno-associated viral vector packaging/producer cell lines based on a human suspension cell line. pp.
Hematti, P., et al. 2004. Distinct genomic integration of mlv and siv vectors in primate hematopoietic stem and progenitor cells. *PLoS Biol,* 2**,** pp. e423.
Higashikawa, F., et al. 2001a. Kinetic analyses of stability of simple and complex retroviral vectors. *Virology,* 280**,** pp. 124-131.
Higashikawa, F., et al. 2001b. Kinetic analyses of stability of simple and complex retroviral vectors. *Virology,* 280**,** pp. 124-131.
Hitchcock, A., et al. 2010. Scale-up of a plasmid DNA purification process. *BioProcess International,* 8**,** pp. 46-54.
Holzinger, A., et al. 2016. The growing world of car t cell trials: A systematic review. *Cancer Immunol Immunother,* 65**,** pp. 1433-1450.
Hu, C., et al. 2016. Gram-scale production of plasmid pudk-hgf with current good manufacturing practices for gene therapy of critical limb ischemia. *Preparative Biochemistry and Biotechnology,* 46**,** pp. 844-849.
Huber, H., et al. 2008. Industrial manufacturing of plasmid DNA: Boehringer's new cgmp production system employs prudent vector design as a backbone. *Genet Eng Biotechnol News,* 28**,** pp. 4-6.
Hudecek, M., et al. 2017. Going non-viral: The sleeping beauty transposon system breaks on through to the clinical side. *Crit Rev Biochem Mol Biol,* 52**,** pp. 355-380.
Humbert, O., et al. 2016. Development of third-generation cocal envelope producer cell lines for robust lentiviral gene transfer into hematopoietic stem cells and t-cells. *Mol Ther,* 24**,** pp. 1237-1246.
Inc., G. B. 2018. Lentivirus production protocol.
Jackson, Z., et al. 2020a. Automated manufacture of autologous cd19 car-t cells for treatment of non-hodgkin lymphoma. *Frontiers in Immunology,* 11**,** pp. 1941.
Jackson, Z., et al. 2020b. Automated manufacture of autologous cd19 car-t cells for treatment of non-hodgkin lymphoma. *Frontiers in immunology,* 11**,** pp.
Jaklevic, M. C. 2021. Car-t therapy is approved for non-hodgkin lymphoma. *JAMA,* 325**,** pp. 1032-1032.
Jankauskas, K., et al. 2019. Fast genetic algorithm approaches to solving discrete-time mixed integer linear programming problems of capacity planning and scheduling of biopharmaceutical manufacture. *Computers & Chemical Engineering,* 121**,** pp. 212-223.
Jenkins, M., et al. 2016. Patient-specific hipsc bioprocessing for drug screening: Bioprocess economics and optimisation. *Biochemical Engineering Journal,* 108**,** pp. 84-97.
Jenkins, M. J., et al. 2015. Human pluripotent stem cell-derived products: Advances towards robust, scalable and cost-effective manufacturing strategies. *Biotechnol J,* 10**,** pp. 83-95.
Jenkins, M. J., et al. 2018. Cost-effective bioprocess design for the manufacture of allogeneic car-t cell therapies using a decisional tool with multi-attribute decision-making analysis. *Biochemical Engineering Journal,* 137**,** pp. 192-204.
Jørgensen, J., et al. 2020. Outcomes-based reimbursement for gene therapies in practice: The experience of recently launched car-t cell therapies in major european countries. *Journal of Market Access & Health Policy,* 8**,** pp. 1715536.

Jung, S., et al. 2018. Highly modular and generic control software for adaptive cell processing on automated production platforms. *Procedia CIRP,* 72**,** pp. 1245-1250.
Kabi, F. 2019. Lovo®automated cell processing system, the easy-to-use, flexible, filtered way to wash and volume-reduce cell products. pp.
Kaiser, A. 2017. The evolving role of automation in car-t cell commercialization. *In:* Insights, C. G. T. (ed.). CELL & GENE THERAPY INSIGHTS.
Kalos, M., et al. 2012. Prolonged t cell persistence, homing to marrow and selective targeting of antigen positive tumor in multiple myeloma patients following adoptive transfer of t cells genetically engineered to express an affinity-enhanced t cell receptor against the cancer testis antigens ny-eso-1 and lage-1. American Society of Hematology.
Kansteiner, F. 2021. Bluebird's zynteglo trials set to resume, putting gene therapy back on flight path to fda filing. Available: https://www.fiercepharma.com/pharma/bluebird-s-zynteglo-trial-cleared-to-resume-putting-gene-therapy-back-flight-path-to-fda.
Katz, M. G., et al. 2019. Targeted gene delivery through the respiratory system: Rationale for intratracheal gene transfer. *J Cardiovasc Dev Dis,* 6**,** pp.
Kebriaei, P., et al. 2016. Phase i trials using sleeping beauty to generate cd19-specific car t cells. *The Journal of clinical investigation,* 126**,** pp. 3363-3376.
Keeler, A. M., et al. 2019. Recombinant adeno-associated virus gene therapy in light of luxturna (and zolgensma and glybera): Where are we, and how did we get here? *Annual review of virology,* 6**,** pp. 601-621.
Kili, S., et al. 2020. Development and deployment of gene therapies: An ada-scid case study. *Second generation cell and gene-based therapies.* Elsevier.
Kimura, T., et al. 2019. Production of adeno-associated virus vectors for in vitro and in vivo applications. *Scientific reports,* 9**,** pp. 1-13.
Kochenderfer, J. N., et al. 2013. Donor-derived cd19-targeted t cells cause regression of malignancy persisting after allogeneic hematopoietic stem cell transplantation. *Blood,* 122**,** pp. 4129-4139.
Kolata, G. 2017. Gene therapy hits a peculiar roadblock: A virus shortage. *The New York Times* [Online]. Available: https://www.nytimes.com/2017/11/27/health/gene-therapy-virus-shortage.html [Accessed 3 September 2019].
Kong, J., et al. 2008. Correction of the disease phenotype in the mouse model of stargardt disease by lentiviral gene therapy. *Gene therapy,* 15**,** pp. 1311.
Kumar, S. R., et al. 2016. Clinical development of gene therapy: Results and lessons from recent successes. *Molecular Therapy-Methods & Clinical Development,* 3**,** pp. 16034.
Kutner, R. H., et al. 2009a. Simplified production and concentration of hiv-1-based lentiviral vectors using hyperflask vessels and anion exchange membrane chromatography. *BMC Biotechnol,* 9**,** pp. 10.
Kutner, R. H., et al. 2009b. Simplified production and concentration of hiv-1-based lentiviral vectors using hyperflask vessels and anion exchange membrane chromatography. *BMC biotechnology,* 9**,** pp. 10.
Lakhdar, K., et al. 2007. Multiobjective long-term planning of biopharmaceutical manufacturing facilities. *Biotechnology progress,* 23**,** pp. 1383-1393.
Lam, C., et al. 2018. Decision support tools for regenerative medicine: Systematic review. *Journal of medical Internet research,* 20**,** pp. e12448.
Lam, C., et al. 2021. Comparison between centralized and decentralized supply chains of autologous chimeric antigen receptor t-cell therapies: A uk case study based on discrete event simulation. *Cytotherapy***,** pp.

Legmann, R., et al. 2020. Transient transfection at large scale for clinical aav9 vector manufacturing. *Cytotherapy,* 22**,** pp. S151.
Leinonen, H. M., et al. 2020. Benchmarking of scale-x bioreactor system in lentiviral and adenoviral vector production. *Human gene therapy,* 31**,** pp. 376-384.
Leinonen, H. M., et al. 2019. Preclinical proof-of-concept, analytical development, and commercial scale production of lentiviral vector in adherent cells. *Mol Ther Methods Clin Dev,* 15**,** pp. 63-71.
Lesch, H. P., et al. 2015. Process development of adenoviral vector production in fixed bed bioreactor: From bench to commercial scale. *Hum Gene Ther,* 26**,** pp. 560-571.
Lesch, H. P., et al. 2021. Evaluation of the single-use fixed-bed bioreactors in scalable virus production. *Biotechnology Journal,* 16**,** pp. 2000020.
Levine, B. 2015. Performance-enhancing drugs: Design and production of redirected chimeric antigen receptor (car) t cells. *Cancer gene therapy,* 22**,** pp. 79-84.
Levinson, Y., et al. 2018. Bespoke cell therapy manufacturing platforms. *Biochemical Engineering Journal,* 132**,** pp. 262-269.
Li, A., et al. 2021. Advances in automated cell washing and concentration. *Cytotherapy***,** pp.
Li, T., et al. Determination of full, partial and empty capsid ratios for adeno-associated virus (aav) analysis. pp.
Lim, A. C., et al. 2005. Application of a decision-support tool to assess pooling strategies in perfusion culture processes under uncertainty. *Biotechnology progress,* 21**,** pp. 1231-1242.
Limonta, M., et al. 2010. The purification of plasmid DNA for clinical trials using membrane chromatography. *BioPharm International,* 23**,** pp.
Lipsitz, Y. Y., et al. 2016. Quality cell therapy manufacturing by design. *Nature Biotechnology,* 34**,** pp. 393-400.
Liu, A. 2022. *Johnson & Johnson, Legend's CAR-T Carvykti enters myeloma ring with FDA nod* [Online]. Fierce Pharma: Fierce Pharma. Available: https://www.fiercepharma.com/pharma/johnson-johnson-legend-car-t-cilta-cel-myeloma-ring-fda-approval-rivaling-bristol-myers [Accessed 25 May 2022].
Liu, A. 2021. *Bluebird bio lays off staffers in europe as zynteglo rollout hits an early reimbursement snag* [Online]. Fierce Pharma: Fierce Pharma. Available: https://www.fiercepharma.com/marketing/bluebird-bio-lays-off-staffers-europe-as-zynteglo-rollout-hits-a-snag-from-start [Accessed 23 June 2021].
Liu, B., et al. 2019. Target selection of car t cell therapy in accordance with the tme for solid tumors. *American journal of cancer research,* 9**,** pp. 228.
Liu, R., et al. 1996. Homozygous defect in hiv-1 coreceptor accounts for resistance of some multiply-exposed individuals to hiv-1 infection. *Cell,* 86**,** pp. 367-377.
Lock, D., et al. 2017. Automated manufacturing of potent cd20-directed chimeric antigen receptor t cells for clinical use. *Human gene therapy,* 28**,** pp. 914-925.
Lock, M., et al. 2010. Characterization of a recombinant adeno-associated virus type 2 reference standard material. *Human gene therapy,* 21**,** pp. 1273-1285.
Lopes, A. G., et al. 2020. Cost analysis of vein-to-vein car t-cell therapy: Automated manufacturing and supply chain. *Cell & Gene Therapy Insights***,** pp.
Macarthur, C., et al. 2019. Superior expansion of long-term hematopoietic stem cells using stempro™ hsc medium kit. pp.
Macleod, D. T., et al. 2017. Integration of a cd19 car into the tcr alpha chain locus streamlines production of allogeneic gene-edited car t cells. *Molecular Therapy,* 25**,** pp. 949-961.
Mamcarz, E., et al. 2019. Lentiviral gene therapy combined with low-dose busulfan in infants with scid-x1. *N Engl J Med,* 380**,** pp. 1525-1534.

Manceur, A. P., et al. 2017. Scalable lentiviral vector production using stable hek293sf producer cell lines. *Human gene therapy methods,* 28**,** pp. 330-339.
Manfredi, F., et al. 2020. Tcr redirected t cells for cancer treatment: Achievements, hurdles, and goals. *Frontiers in Immunology,* 11**,** pp.
Marceau, N., et al. 2014. Scalable lentiviral vector production system compatible with industrial pharmaceutical applications. Google Patents.
Marceau, N., et al. 2019. Scalable lentiviral vector production system compatible with industrial pharmaceutical applications. Google Patents.
Marín Morales, J. M., et al. 2019. Automated clinical grade expansion of regulatory t cells in a fully closed system. *Frontiers in immunology,* 10**,** pp.
Marin, V., et al. 2016. Rd-molpack technology for the constitutive production of self-inactivating lentiviral vectors pseudotyped with the nontoxic rd114-tr envelope. *Mol Ther Methods Clin Dev,* 3**,** pp. 16033.
Marquez Loza, L. I., et al. 2019. Lentiviral vectors for the treatment and prevention of cystic fibrosis lung disease. *Genes (Basel).*
Masri, F., et al. 2019. Viral vector manufacturing: How to address current and future demands. *Cell Gene Ther. Insights,* 5**,** pp. 949-970.
Mccarron, A., et al. 2016. Challenges of up-scaling lentivirus production and processing. *J Biotechnol,* 240**,** pp. 23-30.
Mccoy, R., et al. 2020. The necessity of automated manufacture for cell-based immunotherapies: A cost-based analysis. *Cell Gene Ther. Insights,* 6**,** pp. 673-690.
Mcguire, R. 2013. Impact of clinical development on oncology drug prices. *Pharmaphorum* [Online]. Available: www.pharmaphorum.com/articles [Accessed 04/12/2020].
Medcalf, N. 2016. Centralized or decentralized manufacturing? Key business model considerations for cell therapies. pp.
Meehan, K. R., et al. 2000. Mobilization, collection, and processing of autologous peripheral blood stem cells: Development of a clinical process with associated costs. *Journal of hematotherapy & stem cell research,* 9**,** pp. 767-771.
Merten, O.-W. 2016. Aav vector production: State of the art developments and remaining challenges. *Cell Gene Ther Insights,* 2**,** pp. 521-551.
Merten, O.-W., et al. 2014a. Manufacturing of viral vectors: Part ii. Downstream processing and safety aspects. *Pharmaceutical Bioprocessing,* 2**,** pp. 237-251.
Merten, O.-W., et al. 2014b. Manufacturing of viral vectors for gene therapy: Part i. Upstream processing. *Pharmaceutical Bioprocessing,* 2**,** pp. 183-203.
Merten, O. W., et al. 2011. Large-scale manufacture and characterization of a lentiviral vector produced for clinical ex vivo gene therapy application. *Hum Gene Ther,* 22**,** pp. 343-356.
Merten, O. W., et al. 2016. Production of lentiviral vectors. *Mol Ther Methods Clin Dev,* 3**,** pp. 16017.
Milani, M., et al. 2019. Phagocytosis-shielded lentiviral vectors improve liver gene therapy in nonhuman primates. *Science Translational Medicine,* 11**,** pp. eaav7325.
Milone, M. C., et al. 2009. Chimeric receptors containing cd137 signal transduction domains mediate enhanced survival of t cells and increased antileukemic efficacy in vivo. *Molecular Therapy,* 17**,** pp. 1453-1464.
Miltenyi. 2021. *Clinimacs® electroporator for fully automated cell electroporation* [Online]. https://www.miltenyibiotec.com. Available: https://www.miltenyibiotec.com/GB-en/products/cell-manufacturing-platform/clinimacs-prodigy-platform/CliniMACS-Electroporator.html [Accessed 21 June 2021.

Miskin, J. 2015. Production strategies for lentiviral vectors. 12th Annual bioProcessUK Conference, 25-26 November 2015 2015 Cambridge, United Kingdom. Oxford Biomedica.
Miskin, J. 2016. Lentiviral vector manufacturing strategies to supply the market. *In:* Biomedica, O. (ed.) *Annual bioProcessUK Conference.*
Mock, U., et al. 2016. Automated manufacturing of chimeric antigen receptor t cells for adoptive immunotherapy using clinimacs prodigy. *Cytotherapy,* 18**,** pp. 1002-1011.
Modlich, U., et al. 2009. Insertional transformation of hematopoietic cells by self-inactivating lentiviral and gammaretroviral vectors. *Mol Ther,* 17**,** pp. 1919-1928.
Monjezi, R., et al. 2017. Enhanced car t-cell engineering using non-viral sleeping beauty transposition from minicircle vectors. *Leukemia,* 31**,** pp. 186-194.
Montini, E., et al. 2009. The genotoxic potential of retroviral vectors is strongly modulated by vector design and integration site selection in a mouse model of hsc gene therapy. *The Journal of clinical investigation,* 119**,** pp. 964-975.
Morgan, R. A., et al. 2010. Case report of a serious adverse event following the administration of t cells transduced with a chimeric antigen receptor recognizing erbb2. *Mol Ther,* 18**,** pp. 843-851.
Morrissey, J. B., et al. 2017. End-to-end cell therapy automation: An immunotherapy case study. *BioProcess International***,** pp. 10-18.
Moutsatsou, P., et al. 2019. Automation in cell and gene therapy manufacturing: From past to future. *Biotechnology letters,* 41**,** pp. 1245-1253.
Mukherjee, S., et al. 2021. Establishment of a cell processing laboratory to support hematopoietic stem cell transplantation and chimeric antigen receptor (car)-t cell therapy. *Transfusion and Apheresis Science,* 60**,** pp. 103066.
Munshi, N. C., et al. 2021. Idecabtagene vicleucel in relapsed and refractory multiple myeloma. *New England Journal of Medicine,* 384**,** pp. 705-716.
Naldini, L. 2011. Ex vivo gene transfer and correction for cell-based therapies. *Nat Rev Genet,* 12**,** pp. 301-315.
Nam, S., et al. 2019. Driving the next wave of innovation in car t-cell therapies Available: https://www.mckinsey.com/industries/pharmaceuticals-and-medical-products/our-insights/driving-the-next-wave-of-innovation-in-car-t-cell-therapies#.
National Academies of Sciences, E., et al. 2018. Navigating the manufacturing process and ensuring the quality of regenerative medicine therapies: Proceedings of a workshop. pp.
Nature 2019. Gene therapy's next installment. *Nat. Biotechnol,* 37**,** pp. 697.
Negre, O., et al. 2016. Gene therapy of the β-hemoglobinopathies by lentiviral transfer of the βa (t87q)-globin gene. *Human gene therapy,* 27**,** pp. 148-165.
Nelson, J., et al. 2013. Antibiotic-free production of a herpes simplex virus 2 DNA vaccine in a high yield cgmp process. *Human vaccines & immunotherapeutics,* 9**,** pp. 2211-2215.
Neo, B. H., et al. 2020. The cocoon® platform combined with the 4d-nucleofector™ lv unit. pp.
Nicholson, I. C., et al. 1997. Construction and characterisation of a functional cd19 specific single chain fv fragment for immunotherapy of b lineage leukaemia and lymphoma. *Molecular immunology,* 34**,** pp. 1157-1165.
Nilsson, S. M. 2016. *Process development of lentiviral vector expression, purification and formulation for gene therapy applications.* UCL (University College London).

O'donnell, D. 2015. The cell therapy supply chain: Logistical considerations for autologous immunotherapies. *BioProcess International,* 13**,** pp. 39-44.
Ongkudon, C. M., et al. 2011. Mitigating the looming vaccine crisis: Production and delivery of plasmid-based vaccines. *Crit Rev Biotechnol,* 31**,** pp. 32-52.
Orphanet 2020. The portal for rare diseases and orphan drugs. https://www.orpha.net.
Ostrowska, A., et al. 2009. Hypothermic storage of isolated human hepatocytes: A comparison between university of wisconsin solution and a hypothermosol platform. *Archives of toxicology,* 83**,** pp. 493-502.
Pagliarulo, N. 2019. Novartis still hasn't solved its car-t manufacturing issues. *BIOPHARMADIVE*. https://www.biopharmadive.com: BIOPHARMADIVE.
Palfi, S., et al. 2018. Long-term follow-up of a phase i/ii study of prosavin, a lentiviral vector gene therapy for parkinson's disease. *Human gene therapy Clinical development,* 29**,** pp. 148-155.
Papathanasiou, M. M., et al. 2020. Autologous car t-cell therapies supply chain: Challenges and opportunities? *Cancer gene therapy,* 27**,** pp. 799-809.
Pasi, K. J., et al. 2020. Multiyear follow-up of aav5-hfviii-sq gene therapy for hemophilia a. *New England Journal of Medicine,* 382**,** pp. 29-40.
Penaud-Budloo, M., et al. 2018. Pharmacology of recombinant adeno-associated virus production. *Molecular Therapy-Methods & Clinical Development,* 8**,** pp. 166-180.
Pereira Chilima, T. D. 2019. *Decisional tools for enabling successful manufacture and commercialisation of cell therapy products.* UCL (University College London).
Pernet, O., et al. 2016. Stem cell-based therapies for hiv/aids. *Advanced drug delivery reviews,* 103**,** pp. 187-201.
Perry, C., et al. 2021. Lentiviral vector bioprocessing. *Viruses,* 13**,** pp. 268.
Pesando, J. M., et al. 1989. Cd19 is functionally and physically associated with surface immunoglobulin. *The Journal of experimental medicine,* 170**,** pp. 2159-2164.
Peterson, C. W., et al. 2016. Multilineage polyclonal engraftment of cal-1 gene-modified cells and in vivo selection after shiv infection in a nonhuman primate model of aids. *Mol Ther Methods Clin Dev,* 3**,** pp. 16007.
Pillai, V. B., et al. 2008. Comparative studies on in vitro expression and in vivo immunogenicity of supercoiled and open circular forms of plasmid DNA vaccines. *Vaccine,* 26**,** pp. 1136-1141.
Poirot, L., et al. 2015. Multiplex genome-edited t-cell manufacturing platform for "off-the-shelf" adoptive t-cell immunotherapies. *Cancer Res,* 75**,** pp. 3853-3864.
Pollock, J., et al. 2013. Fed-batch and perfusion culture processes: Economic, environmental, and operational feasibility under uncertainty. *Biotechnology and bioengineering,* 110**,** pp. 206-219.
Pollock, J., et al. Fed-batch and perfusion culture processes: Operational, economic and environmental feasibility under uncertainty. 2011.
Porter, D. L., et al. 2015. Chimeric antigen receptor t cells persist and induce sustained remissions in relapsed refractory chronic lymphocytic leukemia. *Sci Transl Med,* 7**,** pp. 303ra139.
Priesner, C., et al. 2016. Automated enrichment, transduction, and expansion of clinical-scale cd62l+ t cells for manufacturing of gene therapy medicinal products. *Human gene therapy,* 27**,** pp. 860-869.
Prommersberger, S., et al. 2021. Caramba: A first-in-human clinical trial with slamf7 car-t cells prepared by virus-free sleeping beauty gene transfer to treat multiple myeloma. *Gene therapy***,** pp. 1-12.
Qasim, W., et al. 2017. Molecular remission of infant b-all after infusion of universal talen gene-edited car t cells. *Science Translational Medicine,* 9**,** pp.

Qiu, T., Wang, Y., Liang, S., Han, R. and Toumi, M., 2021. The impact of COVID-19 on the cell and gene therapies industry: disruptions, opportunities, and future prospects. Drug discovery today, 26(10), pp.2269-2281.
Qu, W., et al. 2015. Scalable downstream strategies for purification of recombinant adeno-associated virus vectors in light of the properties. *Current pharmaceutical biotechnology,* 16**,** pp. 684-695.
Quinonez, R., et al. 2002. Lentiviral vectors for gene delivery into cells. *DNA and cell biology,* 21**,** pp. 937-951.
Raghavan, B., et al. 2019. Optimizing the clarification of industrial scale viral vector culture for gene therapy. *Cell Gene Ther. Insights,* 5**,** pp. 1311-1322.
Rai, P., et al. 2016. Gene therapy for hemoglobin disorders - a mini-review. *J Rare Dis Res Treat,* 1**,** pp. 25-31.
Ran, T., et al. 2020. Cost of decentralized car t-cell production in an academic nonprofit setting. *International Journal of Cancer,* 147**,** pp. 3438-3445.
Raper, V. 2020. Precision medicines that are tailored and off-the-rack: Manufacturing efficiency and point-of-care access are making precision medicine more accessible while ensuring genetic, environmental, and lifestyle fits. *Genetic Engineering & Biotechnology News,* 40**,** pp. 40-43.
Rapoport, A. P., et al. 2015. Ny-eso-1-specific tcr-engineered t cells mediate sustained antigen-specific antitumor effects in myeloma. *Nat Med,* 21**,** pp. 914-921.
Ribeil, J. A., et al. 2017. Gene therapy in a patient with sickle cell disease. *N Engl J Med,* 376**,** pp. 848-855.
Rinaldi, M., et al. 2014. *DNA vaccines: Methods and protocols,* Springer.
Rio, P., et al. 2017. Engraftment and in vivo proliferation advantage of gene corrected mobilized cd34+ cells from fanconi anemia patients. *Blood***,** pp.
Roddie, C., et al. 2019. Manufacturing chimeric antigen receptor t cells: Issues and challenges. *Cytotherapy,* 21**,** pp. 327-340.
Rodrigues, T., et al. 2007a. Purification of retroviral vectors for clinical application: Biological implications and technological challenges. *J Biotechnol,* 127**,** pp. 520-541.
Rodrigues, T., et al. 2007b. Scaleable purification process for gene therapy retroviral vectors. *J Gene Med,* 9**,** pp. 233-243.
Rosenberg, S. A. 2012a. Raising the bar: The curative potential of human cancer immunotherapy. *Science Translational Medicine,* 4**,** pp. 127ps128-127ps128.
Rosenberg, S. A. 2012b. Raising the bar: The curative potential of human cancer immunotherapy. *Sci Transl Med,* 4**,** pp. 127ps128.
Rotondi, M., et al. 2019. Development of a novel bioreactor platform for car t-cells expansion. *Cytotherapy,* 21**,** pp. S43-S44.
Ruiz, O., et al. 2011. Scalable technology to produce pharmaceutical grade plasmid DNA for gene therapy. *Gene therapy-developments and future perspectives.* InTech.
Ruscic, J., et al. 2019. Lentiviral vector purification using nanofiber ion exchange chromatography. *Molecular Therapy-Methods & Clinical Development***,** pp.
Sanber, K. S., et al. 2015. Construction of stable packaging cell lines for clinical lentiviral vector production. *Sci Rep,* 5**,** pp. 9021.
Sarkis, M., et al. 2021. Decision support tools for next-generation vaccines and advanced therapy medicinal products: Present and future. *Current Opinion in Chemical Engineering,* 32**,** pp. 100689.
Sautto, G. A., et al. 2016. Chimeric antigen receptor (car)-engineered t cells redirected against hepatitis c virus (hcv) e2 glycoprotein. *Gut,* 65**,** pp. 512-523.
Scherr, M., et al. 2002. Efficient gene transfer into the cns by lentiviral vectors purified by anion exchange chromatography. *Gene therapy,* 9**,** pp. 1708.

Schmeer, M., et al. 2017. Plasmid DNA manufacturing for indirect and direct clinical applications. *Hum Gene Ther***,** pp.
Scholler, J., et al. 2012. Decade-long safety and function of retroviral-modified chimeric antigen receptor t cells. *Science Translational Medicine,* 4**,** pp. 132ra153-132ra153.
Schwarze, L. I., et al. 2021. Automated production of ccr5-negative cd4+-t cells in a gmp-compatible, clinical scale for treatment of hiv-positive patients. *Gene therapy***,** pp. 1-16.
Schweizer, M., et al. 2010. Large-scale production means for the manufacturing of lentiviral vectors. *Curr Gene Ther,* 10**,** pp. 474-486.
Scott, C. T., et al. 2016. Gene therapy's out-of-body experience. *Nature Biotechnology,* 34**,** pp. 600-607.
Segura, M. M., et al. 2013. New developments in lentiviral vector design, production and purification. *Expert Opin Biol Ther,* 13**,** pp. 987-1011.
Seimetz, D., et al. 2019. Approval of first car-ts: Have we solved all hurdles for atmps? *Cell Medicine,* 11**,** pp. 2155179018822781.
Senior, M. 2018. Rollout of high-priced cell and gene therapies forces payer rethink. *Nature Biotechnology,* 36**,** pp. 291-292.
Sharma, N., et al. 2013. Efficient sleeping beauty DNA transposition from DNA minicircles. *Mol Ther Nucleic Acids,* 2**,** pp. e74.
Sheridan, C. 2011. Gene therapy finds its niche. *Nature Biotechnology,* 29**,** pp. 121-128.
Sheu, J., et al. 2015. Large-scale production of lentiviral vector in a closed system hollow fiber bioreactor. *Mol Ther Methods Clin Dev,* 2**,** pp. 15020.
Shi, Y., et al. 2019. End-to-end cell therapy automation. Google Patents.
Silva, D., et al. 2020. High efficiency protocol for lymphocytes gene modification by lentiviral vector within an automated closed system. *Cytotherapy,* 22**,** pp. S202.
Simaria, A. S., et al. 2011. Designing multi-product biopharmaceutical facilities using evolutionary algorithms. *Computer aided chemical engineering.* Elsevier.
Simaria, A. S., et al. 2014. Allogeneic cell therapy bioprocess economics and optimization: Single-use cell expansion technologies. *Biotechnol Bioeng,* 111**,** pp. 69-83.
Singh, H., et al. 2013. Manufacture of clinical-grade cd19-specific t cells stably expressing chimeric antigen receptor using sleeping beauty system and artificial antigen presenting cells. *PLoS One,* 8**,** pp. e64138.
Singh, H., et al. 2014. A new approach to gene therapy using sleeping beauty to genetically modify clinical-grade t cells to target cd19. *Immunol Rev,* 257**,** pp. 181-190.
Singh, H., et al. 2015. Manufacture of t cells using the sleeping beauty system to enforce expression of a cd19-specific chimeric antigen receptor. *Cancer Gene Therapy,* 22**,** pp. 95-100.
Singh, S. R., et al. 2012. Hospital financial management: What is the link between revenue cycle management, profitability, and not-for-profit hospitals' ability to grow equity? *Journal of Healthcare Management,* 57**,** pp. 325-341.
Slauson, S., et al. 2016. 458. Development of a stable producer cell line for scalable lentiviral vector production for gene therapy of hemoglobinopathie. *Molecular Therapy,* 24**,** pp. S182.
Slepushkin, V., et al. 2003. Large-scale purification of a lentiviral vector by size exclusion chromatography or mustang q ion exchange capsule. Bioproc. J. September. October.
Spink, K., et al. 2018. The long road to affordability: A cost of goods analysis for an autologous car-t process. *Cell Gene Therapy Insights,* 4**,** pp. 1105-1116.

Stamatis, C. 2019. *Integrating high-throughput experimentation with advanced decision-support tools for chromatography process development.* UCL (University College London).
Stan, R., et al. 2014. Practical considerations in gene therapy for hiv cure. *Current HIV/AIDS Reports,* 11**,** pp. 11-19.
Stevens, D., et al. 2020. Onasemnogene abeparvovec-xioi: Gene therapy for spinal muscular atrophy. *Annals of Pharmacotherapy,* 54**,** pp. 1001-1009.
Stewart, H. J., et al. 2011. A stable producer cell line for the manufacture of a lentiviral vector for gene therapy of parkinson's disease. *Hum Gene Ther,* 22**,** pp. 357-369.
Stonier, A., et al. 2013. Integration of stochastic simulation with multivariate analysis: Short-term facility fit prediction. *Biotechnol Prog,* 29**,** pp. 368-377.
Strachan, J. 2019. *In the land of the living logistics* [Online]. The Medicine Maker: The Medicine Maker. Available: https://themedicinemaker.com/business-regulation/in-the-land-of-the-living-logistics [Accessed 26 June 2021.
Stroncek, D. F., et al. 2014. Counter-flow elutriation of clinical peripheral blood mononuclear cell concentrates for the production of dendritic and t cell therapies. *Journal of translational medicine,* 12**,** pp. 1-8.
Stroncek, D. F., et al. 2016. Preliminary evaluation of a highly automated instrument for the selection of cd34+ cells from mobilized peripheral blood stem cell concentrates. *Transfusion,* 56**,** pp. 511-517.
Sui, Z. 2007. *Simulation-based meta-optimization in vendor managed inventory systems,* State University of New York at Buffalo.
Takeda, S.-I., et al. 2004. Successful gene transfer using adeno-associated virus vectors into the kidney: Comparison among adeno-associated virus serotype 1–5 vectors in vitro and in vivo. *Nephron Experimental nephrology,* 96**,** pp. e119-e126.
Tang, C., et al. 2019. Resveratrol improves ex vivo expansion of cb-cd34+ cells via downregulating intracellular reactive oxygen species level. *Journal of cellular biochemistry,* 120**,** pp. 7778-7787.
Tebas, P., et al. 2013. Antiviral effects of autologous cd4 t cells genetically modified with a conditionally replicating lentiviral vector expressing long antisense to hiv. *Blood,* 121**,** pp. 1524-1533.
Tebas, P., et al. 2014. Gene editing of ccr5 in autologous cd4 t cells of persons infected with hiv. *N Engl J Med,* 370**,** pp. 901-910.
Technology, P. 2019. Catalent and thermo fisher scientific's high-stakes investment in viral vector capabilities. Available: https://www.pharmaceutical-technology.com/comment/biologic-drugs-2019/ [Accessed 15 October 2019].
Terova, O., et al. 2018. Overcoming downstream purification challenges for viral vector manufacturing: Enabling advancement of gene therapies in the clinic. *Cell Gene Ther Insights,* 4**,** pp. 101-111.
Terumo Bct, L. T. White paper: Paper enrichment of lymphocytes from apheresis residues. *In:* Bct, T. (ed.). TERUMO BCT.
Tipanee, J., et al. 2017. Preclinical and clinical advances in transposon-based gene therapy. *Bioscience reports,* 37**,** pp.
Tiwari, N., et al. 2015. 675. High quality plasmid DNA manufacturing for ex-vivo protein synthesis and viral vector production for gene therapy. *Molecular Therapy,* 23**,** pp. S268.
Todd Upton, V. G. 2021. How fixed bed bioreactors are changing the game for adherent cell culture-based vector production. *In:* Spotlight, B. (ed.). Cell & Gene Therapy insights: Bioinsights.
Torikai, H., et al. 2012. A foundation for universal t-cell based immunotherapy: T cells engineered to express a cd19-specific chimeric-antigen-receptor and eliminate expression of endogenous tcr. *Blood,* 119**,** pp. 5697-5705.

Tostoes, R., et al. 2020. Acoustic affinity cell selection: A non-paramagnetic scalable technology for t cell selection from unprocessed apheresis products. *Cytotherapy,* 22**,** pp. S16.
Toueille, M., et al. 2018. Development of purification steps for several aav serotypes using poros™ captureselect™ aavx affinity chromatography. *Cell & Gene Therapy Insights,* 4**,** pp. 637-645.
Trainor, N., et al. 2014. Rethinking clinical delivery of adult stem cell therapies. *Nature Biotechnology,* 32**,** pp. 729-735.
Transfiguracion, J., et al. 2020. Rapid in-process monitoring of lentiviral vector particles by high-performance liquid chromatography. *Molecular Therapy-Methods & Clinical Development,* 18**,** pp. 803-810.
Truran, R., et al. 2009. Virus purification. *US patent US,* 12**,** pp.
Tyagarajan, S., et al. 2020. Optimizing car-t cell manufacturing processes during pivotal clinical trials. *Molecular Therapy-Methods & Clinical Development,* 16**,** pp. 136-144.
Uchida, N., et al. 2019. Development of a forward-oriented therapeutic lentiviral vector for hemoglobin disorders. *Nature Communications,* 10**,** pp. 4479.
Urthaler, J., et al. 2005. Improved downstream process for the production of plasmid DNA for gene therapy. *Acta Biochimica Polonica,* 52**,** pp. 703-711.
Valkama, A. J., et al. 2018. Optimization of lentiviral vector production for scale-up in fixed-bed bioreactor. *Gene Ther,* 25**,** pp. 39-46.
Vantourout, P., et al. 2013. Six-of-the-best: Unique contributions of γδ t cells to immunology. *Nature Reviews Immunology,* 13**,** pp. 88-100.
Venditti, C. P. 2021. Safety questions for aav gene therapy. *Nature Biotechnology,* 39**,** pp. 24-26.
Voelker, R. 2020. Car-t therapy is approved for mantle cell lymphoma. *JAMA,* 324**,** pp. 832-832.
Voelker, R. 2021. Cell-based gene therapy is new option for multiple myeloma. *JAMA,* 325**,** pp. 1713-1713.
Vormittag, P., et al. 2018. A guide to manufacturing car t cell therapies. *Current opinion in biotechnology,* 53**,** pp. 164-181.
Waehler, R., et al. 2007. Engineering targeted viral vectors for gene therapy. *Nat Rev Genet,* 8**,** pp. 573-587.
Wagner, E. K., et al. 2009. *Basic virology,* Wiley.
Wakap, S. N., et al. 2020. Estimating cumulative point prevalence of rare diseases: Analysis of the orphanet database. *European Journal of Human Genetics,* 28**,** pp. 165-173.
Wang, K., et al. 2019. A multiscale simulation framework for the manufacturing facility and supply chain of autologous cell therapies. *Cytotherapy,* 21**,** pp. 1081-1093.
Wang, X., et al. 2017. Genetic engineering and manufacturing of hematopoietic stem cells. *Mol Ther Methods Clin Dev,* 5**,** pp. 96-105.
Wang, X., et al. 2016. Clinical manufacturing of car t cells: Foundation of a promising therapy. *Molecular Therapy-Oncolytics,* 3**,** pp. 16015.
Wang, X., et al. 2017. Genetic engineering and manufacturing of hematopoietic stem cells. *Molecular Therapy-Methods & Clinical Development,* 5**,** pp. 96-105.
Ward, A. 2018. Exploring a new enzymatic tool for aav production: Balancing optimal nuclease activity with effective DNA digestion. *Genetic Engineering & Biotechnology News,* 38**,** pp. 22-22.
Watson, D. J., et al. 2002. Targeted transduction patterns in the mouse brain by lentivirus vectors pseudotyped with vsv, ebola, mokola, lcmv, or mulv envelope proteins. *Molecular Therapy,* 5**,** pp. 528-537.

Watts, M. J., et al. 2016. Optimisation and quality control of cell processing for autologous stem cell transplantation. *British journal of haematology,* 175**,** pp. 771-783.
Weist, M., et al. 2020. Development of a new semi-automated closed modular system for car-t cell therapy manufacturing. *Cytotherapy,* 22**,** pp. S201.
Willasch, A., et al. 2010. Enrichment of cell subpopulations applying automated macs technique: Purity, recovery and applicability for pcr-based chimerism analysis. *Bone marrow transplantation,* 45**,** pp. 181.
Williams, J. A., et al. 2009. Generic plasmid DNA production platform incorporating low metabolic burden seed-stock and fed-batch fermentation processes. *Biotechnology and bioengineering,* 103**,** pp. 1129-1143.
Williams, T., et al. 2020. Lentiviral vector manufacturing process enhancement utilizing tfdf™ technology. *Cell Gene Ther. Insights,* 6**,** pp. 455-467.
Wolstein, O., et al. 2014. Preclinical safety and efficacy of an anti–hiv-1 lentiviral vector containing a short hairpin rna to ccr5 and the c46 fusion inhibitor. *Molecular Therapy-Methods & Clinical Development,* 1**,** pp. 11.
Wright, J. F. 2020. Quality control testing, characterization and critical quality attributes of aav vectors used for human gene therapy. *Biotechnology Journal***,** pp. 2000022.
Wright, J. F. 2021. Quality control testing, characterization and critical quality attributes of adeno-associated virus vectors used for human gene therapy. *Biotechnology Journal,* 16**,** pp. 2000022.
Wu, Y. Y., et al. 2018. Automated cell expansion: Trends & outlook of critical technologies. *Cell & Gene Therapy Insights***,** pp.
Xenopoulos, A., et al. 2014. Production and purification of plasmid DNA vaccines: Is there scope for further innovation? *Expert Rev Vaccines,* 13**,** pp. 1537-1551.
Yip, A., et al. 2018. The market for chimeric antigen receptor t cell therapies. *Nature reviews Drug discovery,* 17**,** pp. 161.
Ylä-Herttuala, S. 2012. Endgame: Glybera finally recommended for approval as the first gene therapy drug in the european union. *Mol Ther,* 20**,** pp. 1831-1832.
Zallocchi, M., et al. 2014. Eiav-based retinal gene therapy in the shaker1 mouse model for usher syndrome type 1b: Development of ushstat. *PLoS One,* 9**,** pp. e94272.
Zeh, N., et al. 2019. Human cap cells represent a novel source for functional, mirna-loaded exosome production. *PLoS One,* 14**,** pp. e0221679.
Zemmar, A., et al. 2015. 474. A new cgmp facility to produce clinical grade batches of lentiviral vectors and car-t cell in europe. *Molecular Therapy,* 23**,** pp. S188.
Zhang, W., et al. 2018. Characterization of clinical grade cd19 chimeric antigen receptor t cells produced using automated clinimacs prodigy system. *Drug design, development and therapy,* 12**,** pp. 3343.
Zhang, Y., et al. 2010. Transduction of human t cells with a novel t-cell receptor confers anti-hcv reactivity. *PLoS Pathog,* 6**,** pp. e1001018.
Zhao, Q., et al. 2021. Engineered tcr-t cell immunotherapy in anticancer precision medicine: Pros and cons. *Frontiers in immunology,* 12**,** pp. 812.
Zhao, Y., et al. 2017. Development of the first world health organization lentiviral vector standard: Toward the production control and standardization of lentivirus-based gene therapy products. *Human gene therapy methods,* 28**,** pp. 205-214.
Zhou, X., et al. 2015. Inducible caspase-9 suicide gene controls adverse effects from alloreplete t cells after haploidentical stem cell transplantation. *Blood,* 125**,** pp. 4103-4113.
Zhao, H., Lee, K.J., Daris, M., Lin, Y., Wolfe, T., Sheng, J., Plewa, C., Wang, S. and Meisen, W.H., 2020. Creation of a high-yield AAV vector production platform

in suspension cells using a design-of-experiment approach. Molecular Therapy-Methods & Clinical Development, 18, pp.312-320.
Zhu, F., et al. 2018. Closed-system manufacturing of cd19 and dual-targeted cd20/19 chimeric antigen receptor t cells using the clinimacs prodigy device at an academic medical center. *Cytotherapy,* 20**,** pp. 394-406.
Zonari, E., et al. 2017. Efficient ex vivo engineering and expansion of highly purified human hematopoietic stem and progenitor cell populations for gene therapy. *Stem Cell Reports,* 8**,** pp. 977-990.
Zufferey, R., et al. 1999. Woodchuck hepatitis virus posttranscriptional regulatory element enhances expression of transgenes delivered by retroviral vectors. *J Virol,* 73**,** pp. 2886-2892.
Zufferey, R., et al. 1998. Self-inactivating lentivirus vector for safe and efficient in vivo gene delivery. *J Virol,* 72**,** pp. 9873-9880.

Appendix

Table A1 Cryovials sizes and costs.

Cryovial sizes (total volume, ml)	Cost per nest of 54	Max volume (ml)
50	772	52.1
20	535	21.8
10	405	11.7
6	331	7.6
2	213	2.25
1	161	1.35

Note: It was assumed that filling can take place over a period of maximum three days. Each day assumed 3 shifts of 8 hours and 2 operators per shift. Tubing set costs for the filling machines were assumed to be $900 USD per batch. Caps costs were also accounted for at $60/100 caps.

Table A2 Automated vialling machines throughput and costs.

Automated vialling machines	Max. no. cryovials/h	Cost USD (including isolator cost)
1	600	1,226,500
2	180	595,000

Table A3 Key equipment cost and footprint.

Equipment	Cost (USD)	Footprint (m^2)
Incubator	20,000	0.46
BSC	20,000	1
Sterile tube welder	20,000	0.5
Controlled rate freezer	30,000	1
Freezer	30,000	1
Automated vialling machine 1 (includ. Isolator)	1,226,500	1
Automated vialling machine 2 (includ. Isolator)	595,000	0.8
Controlled rate freezer	30,000	0.5
Fixed bed bioreactor (e.g. iCELLis 500 series)	325,000	3.2
Hollow fibre bioreactor	$150,000	0.3

Table A4 Single-use stirred tank bioreactor costs and footprint.

Size	Consumable cost (USD)	Control system cost (USD	Footprint (m^2)
SUB2000	18,750	250,000	4.2
SUB1000	13,750	275,000	3.9
SUB500	11,875	275,000	3.75
SUB300	9,000	300,000	3.7
SUB200	7,500	300,000	3.66
SUB100	7,000	375,000	3.66
SUB50	6,250	437,500	2

Table A5 Rocking motion bioreactor equipment costs and footprint.

Size	Consumable cost (USD)	Control system cost (USD)	Footprint (m^2)
RMmc10	300	80,000	0.22
RMmc24	350	80,000	0.22
RMmc60	420	80,000	0.44
RMmc120	650	180,000	0.8
RMmc240	800	180,000	1.6
RMmc600	1,386	325,000	3.2

Table A6 Rocking motion bioreactor run in adherent mode using microcarriers: surface area and mass of microcarrier requirements.

Size	Surface area in microcarrier (cm^2)	Mass of microcarrier required (g)
RMmc10	120,000	100
RMmc24	240,000	200
RMmc60	600,000	500
RMmc120	1,200,000	1,000
RMmc240	2,400,000	2,000
RMmc600	6,000,000	5,000

Table A7 AAV chromatography media cost and dynamic binding capacity (DBC).

AAV data	Chromatography media cost/L (USD)	DBC (vg/ml)
Affinity chromatography step (e.g. AVB sepharose)	22,000	3×10^{12}
Polish chromatography step (AEX, e.g. POROS HQ)	2,000	1×10^{13}

.

Table A8 Assumptions used in the FCI calculation.

Parameter	Value	Unit and comments
Material airlock footprint	6	m^2
Personnel airlock footprint	6	m^2
Number of samples/QC lab	400	
Process support equipment costs	2,389	$/$m^2$ of cleanroom
Logistics equipment costs	548	$/ m^2 of cleanroom
EMS central unit	108,800	$
Probe costs	1,920	$/sampling point
Equipment installation costs	1,920	$/unit
Building shell costs	548	$/$m^2$
Fit-out costs (Grade B)	8,320	$/$m^2$
Fit-out costs (Grade C)	6,106	$/$m^2$
Fit-out costs (Grade D)	5,082	$/$m^2$
Fit-out costs (CNC)	1,741	$/$m^2$
Fit-out costs (unclassified)	64	$/$m^2$
Contractor's fees	0.12	of fitout costs
Land costs	0.06	of shell costs
Yard improvement costs	0.10	of shell costs
Engineering, management and consultants fees	0.20	of direct costs
Contingency costs	0.20	of (direct costs + Engineering, management and consultants fees)
Cold room cost per m2	5,000	relevant for CF10 process, harvest storage area

Table A9 Gowning costs and gowning requirements assumptions.

Parameter	Value	Unit
Gown for grade B	60	$/gown
Gown for grade C	45	$/gown
Number of gowns/day	4	/operator

Table A10 Key ratios and costs assumptions used in the indirect cost calculations.

Parameter	Value	Unit
Equipment maintenance	0.10	*TEPC (total equipment purchase cost)
Facility maintenance costs	0.10	*facility costs
Equipment to cleanroom footprint ratio	0.16	
Cleanroom to facility footprint ratio	0.15	
Cold room to equipment footprint ratio	0.50	
Class B monitoring	7,232	$/$m^2$/year
Class C monitoring	1,012	$/$m^2$/year
Energy costs	637	$/$m^2$/year

TEPC = total equipment purchase cost.

Table A11 Key ratios used in the calculation of the total facility footprint.

Area	Area/Product manufacture area	Classification
Product manufacture	1	Cleanroom
Clean change 1	0.105	Grade C/B
Clean change 2	0.147	Grade C/B
Clean corridors	0.322	Grade C/B
Clean Janitor	0.042	Grade C/B
QC labs	0.65	Grade D
Microbiology lab	0.301	GradeD
Labs corridor	0.273	Grade D
PCR room	0.294	Grade D
Janitor	0.042	Grade D
Waste corridor	0.804	Unclassified
Waste change	0.042	Unclassified
Waste treatment	0.168	Unclassified
Logistics	1.077	Unclassified
Offices	3.147	Unclassified
Meeting rooms	0.105	Unclassified
Stairs	0.231	Unclassified
Cold rooms	0.168	Unclassified
Janitor	0.042	Unclassified
General corridor	0.399	Unclassified
Lorry/Van loading docks	0.224	Unclassified
Reception	0.538	Unclassified
WC	0.392	Unclassified
Plant level	4.755	CNC area

Table A12 Clarification filter capacity associated with each cell culture technology.

Technology	Clarification filter capacity (L/m^2)
CF10	60
HF	60
FB	60
RM	60
SUB	20

The equations used for determining the annual harvest volume for LV ($V_{h,annual,LV}$) and AAV ($V_{h,annual,AAV}$) used in generating **Figure 6.4, Chapter 6,** are shown below:

$$V_{h,annual,LV} = \frac{N_{dose,annual} \times m_{dose} \times (1+F)}{Y_{overall} \times T_{harvest}} + \frac{N_{batch,annual} \times (V_{QC,DP} \times \frac{c_{DP}}{Y_{overall}} + V_{QC,DS} \times \frac{c_{DS}}{Y_{DSP}})}{T_h}$$

$$V_{h,annual,AAV} = \frac{N_{dose,annual} \times m_{dose} \times (1+F)}{Y_{overall} \times T_h} + \frac{N_{batch,annual} \times \left(V_{QC,DP} \times \frac{c_{DP}}{Y_{overall}}\right)}{T_h}$$

Where

$N_{dose,annual}$ = peak annual demand in number of doses

m_{dose} = dose size in TU/dose (LV) or vg/dose (AAV)

F = fill overage %

Y_{DSP}= DSP yield

$Y_{overall}$ = overall process yield (DSP and fill-finish) (without accounting for losses to release testing QC)

T_h= viral vector titre at harvest (TU/ml for LV and vg/ml for AAV)

$N_{batch,annual}$= number of batches required per year to satisfy demand

$V_{QC,DS}$= volume of DS (drug substance) required per batch for QC release testing as well as reference samples and retains (ml)

$V_{QC,DP}$= volume of DP (drug product) required per batch for QC release testing as well as reference samples and retains (ml)

c_{DP} = drug product concentration (TU/ml for LV and vg/ml for AAV)

c_{DP} = drug substance concentration (TU/ml for LV and vg/ml for AAV)

Papers by the author

Comisel, R. M., Kara, B., Fiesser, F.H. and Farid, S.S. (2021): **Lentiviral vector bioprocess economics for cell and gene therapy commercialization**. *Biochemical Engineering Journal*, 167, p.107868.

Comisel, R. M., Kara, B., Fiesser, F.H. and Farid, S.S. (2021): **Gene therapy process change evaluation framework: transient transfection and stable producer cell line comparison**. *Biochemical Engineering Journal*, doi:https://doi.org/10.1016/j.bej.2021.108202.